University of Sheffield

Elucidating the Role of Novel Proteins in Plasma Cell Differentiation and Antibody Secretion

Ola Shehata

A thesis submitted in partial fulfilment of the requirements for the degree of Doctor of Philosophy

The University of Sheffield

School of Biosciences – Molecular and Cellular Biology

March 2023

Acknowledgments

Firstly, I would like to thank my supervisor Professor Andrew Peden. I am extremely grateful for the opportunities that Andrew has given me within and beyond my project. In addition to being a remarkable scientist and supervisor, Andrew's mentorship throughout the years has significantly enhanced my PhD experience and growth as a scientist. I have never felt not supported by Andrew, thank you for all the guidance that you have provided me throughout my PhD.

I would also like to thank Dr Mark Collins for all his support with mass spectrometry experiments and for always greeting me with smiles whenever I popped in for questions. I would like to extend my gratitude regarding mass spectrometry to Dr Khoa Pham for his help. I would love to thank Dr Mohamed Nassar and Dr Mark Collins for all their support, advice and for our pleasant advisory meetings during the past three years. I would like to thank Susan Clark and Kay Hopkinson from the flow cytometry facility and Nicholas Van Hateren from the light microscopy facility for providing me with training.

I would love to express my gratitude to all members of the Peden Lab who have supported me and made my PhD experience enjoyable. Dr Daniel Williams, Dr Amber SM Shun Shion, Samuel Lewin, Polly Rouse and Miguela Min. A big thank you to Dan who has massively helped me throughout my PhD by transferring to me so many lab skills. Thank you for always being willing to share your experience and help. Sam, thank you for always bringing energy to the office and for all the enthusiastic science discussions. Polly, thank you for being the only person I can trust to check that the freezers and incubators are shut for the fifth time. I would also love to extend my gratitude to my friends Mohamed ElGhazaly and Salma Srour for always being there and for their endless words of encouragement. To all the members of the Erdmann and the King lab, thank you for companionship and for being a great bunch to share a working space with. I would like to acknowledge all the friendly faces of Florey, especially Jorge Ferreira, Ana Paula, Nadia Baseer and Weronika Buczek. You have all contributed so much to my PhD experience, thank you.

I wish to thank my friends and all the special people in my life who mean the world to me and make my days. Last but not least, I would love to express my deepest gratitude and love to my family. Without their support and selflessness, I wouldn't have been able to be where I am today. I dedicate this thesis to them.

Abstract

Antibodies play an essential role in the humoral component of the immune system. They are produced by Antibody Secreting Cells (ASCs) which are capable of secreting thousands of antibody molecules per second. To facilitate this function, ASCs undergo a dramatic upregulation of their biosynthetic pathway, and therefore represent a unique physiological model of constitutive secretion.

In a previous study performed in the lab, a large number of poorly characterised genes were identified as highly upregulated in ASCs compared to naïve B-cells, suggesting that they may be novel factors involved in intracellular trafficking and antibody secretion. To investigate the role of these genes in ASC physiology we have first established a model of B cell differentiation and antibody secretion based on I.29 cells. These cells respond to LPS treatment, expand their biosynthetic capacity, and secrete antibodies. Importantly, they also upregulate the expression of many genes which were identified in the previous proteogenomic work (e.g., FNDC3B, SEC24D, CREB3L2, RRBP1, CRELD2 and TMEM214). To determine the function of these genes, we have developed a CRISPR/Cas9 based platform in I.29 cells and have demonstrated the feasibility of this approach by disrupting the expression of several genes including the R-SNARE VAMP3, the transcription factor CREB3L2 and the coat protein SEC24D. SEC24D, a component of the COPII coat, is one of the most differentially expressed genes in ASC and its expression is thought to be regulated by CREB3L2. Loss of SEC24D did not impact IgM secretion two days post LPS induction. However, its loss leads to a significant reduction in the levels of other COPII components. Surprisingly, the levels of FNDC3B are also perturbed in these cells. FNDC3B is an ER localised protein recently shown to have a role in ER proteostasis suggesting that ER proteostasis in cells with disrupted SEC24D function may be perturbed. Loss of CREB3L2 did not impact the production of antibodies or the expression levels of SEC24D suggesting that other members of this transcription factor family may regulate the levels of SEC24D expression. Finally, we investigated the role of the OASIS family of transcription factors including CREB3L2 in regulating the expression of SEC24D. We have observed that these transcription factors resulted in increased expression of SEC24D, increased cell size and an expanded staining of SEC24D structures in HeLa cells, making them interesting targets for secretory pathway engineering in non-professional secretory cells.

Abbreviations

AID activation-induced cytidine deaminase

ASC antibody secreting cell

β2m B2-microglobulin

BSA bovine serum albumin

Cas9 CRIRP-associated system 9

CHO chinese hamster ovary

COPII coat protein complex II

CRISPR clustered, regulatory interspaced, short palindromic repeats

DMEM dublecco's modified Eagle medium

ECL enhanced chemiluminescence substrate

ECM extra cellular matrix

ELISA enzyme-linked immunosorbent assay

ER endoplasmic reticulum

ERAD ER associated degradation

ERES ER exit sites

ERGIC ER Golgi intermediate compartment

ERQC ER quality control compartment

FACS fluorescence-activated cell sorting

FBS fetal bovine serum

GC germinal centre

GEF guanine exchange factor

GFP green fluorescent protein

GO gene ontology

GTP guanosine triphosphate

Ig immunoglobulin

ISRE interferon sequence response element

KO knockout

LLPC long lived plasma cell

LPS lipopolysaccharide

MEF mouse embryonic fibroblast

MM multiple myeloma

mTOR mammalian/mechanistic target of rapamycin

OASIS old astrocyte specifically induced substance

PAMP pathogen associated molecular pattern

PDI protein disulphide isomerase

PI proteasome inhibitor

QCV quality control vesicle

RER rough endoplasmic reticulum

RIDD regulated IRE1 dependent decay

RPMI roswell park memorial institute medium 1640

SFFV spleen focus-forming virus

TD T-cell dependent

TI T-cell independent

UGGT UDP-glycose:glycoprotein glucosyltransferase

UPR unfolded protein response

UPS ubiquitin proteasome system

Table of Contents

Chapter 1: Introduction

1.1 Antibody Secreting Cells

1.1.1 A Special Model of Constitutive Secretion

Antibodies play crucial roles in immune protection. Their protective functions vary and include neutralisation of antigens, antibody-dependent cellular cytotoxicity, and lysis of pathogens via activation of complement (Forthal, 2015). It is estimated that humans can make 10^{18} (one million trillion) of unique antibodies (Briney et al., 2019). These antibodies are synthesised and secreted by plasma cells or plasma blasts, both referred to as Antibody Secreting Cells (ASCs), which are terminally differentiated B cells. It has been proposed that plasma cells are capable of secreting thousands of antibody molecules per second (Hibi & Dosch, 1986)(Bromage et al., 2009), while utilising the constitutive secretory pathway (Zagury et al., 1970). To achieve such high levels of secretion, activated B-cells undergo an impressive transformation during differentiation which includes a large expansion of their biosynthetic apparatus.

1.1.2 TI and TD Antigens

B-cells differentiate into ASCs upon encountering an antigen. Antigens are broadly defined as T-cell independent (TI) or T-cell dependent (TD) (Fairfax et al., 2008). TI antigens stimulate B-cells directly, without the need to be co-stimulated by helper T cells and typically include bacterial carbohydrate-based components such as polysaccharides (LPS). TD antigens include soluble proteins which become processed and presented by the B-cell, and the B cell's activation depends on its interaction with CD4+ helper T cells.

1.1.3 B-Cell Types

There are three types of mature B-cells which can respond to antigen, and they have distinct specialisation and anatomical location (Allman & Pillai, 2008) (**Table 1.1**). The localization of B1 and MZ B cells enable them to quickly respond to TI antigens, while follicular B cells, the most common subset, are more specialised for TD protein antigens.

Table 1.1: Mature B-Cell Subsets

Cell Type	B1 B Cells	MZ B Cells	Follicular Cells
Location	Peritoneal and pleural cavities and mucosal sites	Marginal sinus of the spleen	Lymphoid follicles of the spleen and lymph nodes.
Location Specialisation	Surveillance of tissues that are prone to pathogens.	Encounter blood-borne pathogens	Undergo maturation and are more specialised for responding to protein antigens that also prompt CD4+ T helper cell activation.

B1 B Cells & Marginal Zone B Cells

B1 cells predominate during early development and produce poly-specific antibodies which can recognise multiple antigens (Baumgarth, 2010). Antibodies secreted by B1 cells tend to be of low affinity and broad specificity, and the cells can clear apoptotic/damaged cells and contribute to tissue homeostasis. B1 cells are a major source of natural IgM and IgA, mostly encoded by germline genes. Natural IgM plays multiple roles from protection from infections to regulating autoimmunity (Ehrenstein & Notley, 2010).

Marginal Zone (MZ) B cells are predominantly present in the marginal zone of the spleen, which is a site of blood flow, and are therefore recognized to play an important role for mounting rapid defence against blood-borne pathogens. In addition to TI responses, they can also contribute to TD responses (Allman & Pillai, 2008).

Both B1 cells and MZ B cells can quickly become ASCs and provide fast protection without T-cell help and their similarity in functional characteristics have been previously described (Martin et al., 2001). Expression of the ASC transcription factor BLIMP1 is higher in these cells than follicular B-cells. In addition, the levels of the B-cell transcription factors PAX5 and BCL6 are lower. This suggests that these cells are primed to allow them to rapidly differentiate and produce antibodies (Fairfax et al., 2007).

Follicular B Cells

Follicular B cells are the most common type of B-cells residing in the spleen and lymph nodes. Despite being able to respond to TI antigens, they are mainly specialised to respond to TD antigens. Stimulation of follicular B cells through Toll Like Receptor ligands such as LPS (TI antigen), is less potent in inducing their differentiation unlike B1 and MZ B cells (Genestier et al., 2007).

TD antigen responses occur in two steps. The first step is referred to as the extrafollicular response, where the B-cells recognize antigen and differentiate into plasmablasts that secrete antibodies for

early protection. The second step involves some of these activated cells to re-enter the follicle and with the help of T follicular helper cells form a Germinal Centre (GC) (Nutt & Tarlinton, 2011). The B cells in the GC activate a site directed hypermutation mechanism through activation-induced cytidine deaminase (AID) which introduces mutations in the rearranged variable regions of immunoglobulin (Bannard & Cyster, 2017). In the GC, B-cells with highest binding affinity to antigen are positively selected by CD4+ T cells and also follicular dendritic cells. This selection ultimately yields B-cells with high affinity antibodies. Some of the GC derived plasma cells migrate into the bone marrow and become long lived.

1.2 The ASC Transcriptional Program

ASCs have a distinct transcriptional profile compared to their B cell precursor (Trezise & Nutt, 2021). Its acquisition terminates the B cell specific program and allows the remodelling of the cell which includes a dramatic expansion of the endoplasmic reticulum (ER). The expression of ASC signature genes is shared between both plasmablasts and plasma cells, with 70% of their transcripts encoding for immunoglobulin (Ig) (Shi et al., 2015). Although many transcription factors participate in the differentiation process of ASCs, three major factors largely drive the differentiation program and have received most focus relating to their functions in ASC. These are IRF4, BLIMP1 and XBP1 (**Figure 1.1**).

IRF4 is a transcription factor expressed in both B and ASCs, whose expression increases during differentiation (Ochiai et al., 2013). Varying concentrations of IRF4 allows it to regulate the mutually exclusive programs of B and ASCs. At low concentrations IRF4 binds, as a heterodimer with other transcription factors such as PU.1, to motifs of genes involved in B cell activation and functions. As the concentration of IRF4 increases during differentiation, it binds as a homodimer to interferon sequence response element (ISRE) motifs in plasma cell target genes. These include genes encoding for proteins involved in secretory functions and importantly for BLIMP1, a master regulator of ASCs' development (Sciammas et al., 2006). The role of IRF4 is essential for initiating the differentiation of ASCs from B-cells.

Unlike IRF4, BLIMP1 is not required for the initial stages of differentiation of B cells, however, is required for the formation of ASCs and antibody secretion. It represses B cell specific genes such as BCL6 and PAX5 and upregulates the expression of ATF6 and indirectly of XBP1 (Lin et al., 2002)(Shaffer et al., 2002)(Tellier et al., 2016). BLIMP1 upregulates immunoglobulin gene expression and also promotes the transition of membrane bound antibody into its secreted form by activating expression of ELL2, a transcription elongation factor which directs this process (Minnich et al., 2016)(Tellier et al., 2016).

Although not required for generation of ASCs, XBP1 is essential for enhancing the biosynthetic capacity in ASCs and enabling high levels of antibody secretion by inducing the expression of genes encoding a wide range of components involved in the secretory pathway (Shaffer et al., 2004) (**see 1.4.2**).

In addition, other transcription factors include the antiapoptotic factors BCL-2 and MCL-1. Expression of MCL-1 is mediated by signalling through the BCMA receptor and is required for the survival of ASCs in the bone marrow (Peperzak et al., 2013). Notably, the BCMA pathway is of therapeutic interest for the treatment of multiple myeloma and an immune-conjugate against it is currently in clinical trials (Trudel et al., 2019) (GSK, 2022).

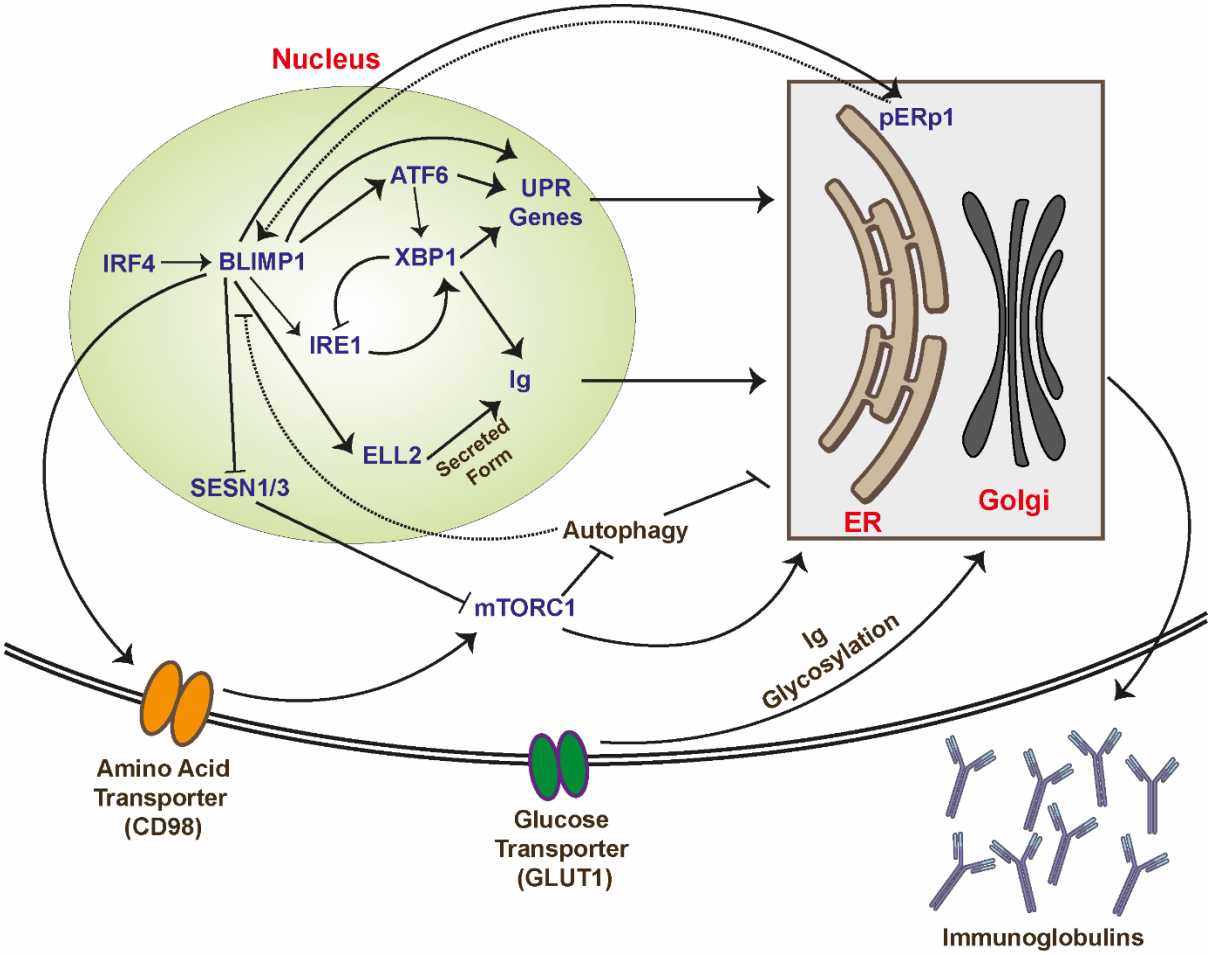

Figure 1.1: The regulatory network of ASCs. Adapted from (Tellier & Nutt, 2019). Illustration of the regulatory network between BLIMP1 and components of the unfolded protein response (UPR), mTORC1 and autophagy. Expression of BLIMP1 is induced by IRF4 during differentiation which enables the necessary expansion of the secretory machinery and antibody secretion. To modulate the UPR, BLIMP1 activates the expression of many genes including ATF6 and IRE1, which both lead to the expression and activation of XBP1. Active XBP1 then upregulates the expression of a wide range of proteins spanning the secretory pathway and coordinates the expansion of the ER. BLIMP1 also upregulates immunoglobulin gene expression and promotes its secreted form by upregulating ELL2, an elongation factor which drives the generation of the secreted form of immunoglobulin transcripts. pERp1, a co-chaperone for immunoglobulin folding, is directly transcriptionally upregulated by BLIMP1. A positive feedback loop between both proteins has been suggested. The proteosynthetic activity of mTORC1 in ASCs is sustained by BLIMP1 which directly enhances expression of the amino acid transporter CD98.

BLIMP1 also indirectly enhances mTORC1 activity by inhibiting Sestrin-1 and -3 which are negative regulators of mTORC1. Subsequently, the activity of mTORC1 supports the biosynthetic expansion and limits autophagy. Autophagy plays an important role in the cells' homeostasis by negatively regulating BLIMP1 and the secretory apparatus expansion. Plasma cells have increased expression of GLUT1, a glucose transporter. Most of the glucose utilised by these cells is used for glycosylation of immunoglobulins.

1.3 Antibody Folding at the ER

Antibodies consist of two heavy and two light chains which are linked by disulphide bonds. The folding of antibodies happens co-translationally when the polypeptide is translocated into the ER lumen (Bergman & Kuehl, 1979). Nascent polypeptides are bound by BiP which facilitates their correct folding and prevents immature disulphide bond formation (Lee et al., 1999)(Vanhove et al., 2001)(Feige et al., 2010). The interaction of the correctly folded light chain with the heavy chain releases BiP and allows the full folding and assembly of the antibody.

Many proteins have been identified to assist the folding of antibody molecules (Feige et al., 2010). These include chaperones such as GRP94, co-chaperones of BiP such as ERdj3, and PDI which in addition to assisting folding acts as a disulphide isomerase. Expression of folding chaperones in ASCs may play more roles than just aiding antibody folding and secretion. *Mzb1*, encoding the ER localised co-chaperone pERp1, is transcriptionally activated by BLIMP1 (Minnich et al., 2016). pERp1 is a co-chaperone for GRP94 and is required for high levels of antibody secretion. It acts through aiding immunoglobulin (Ig) folding by increasing the interactions of Ig with GRP94 (Van Anken et al., 2009)(Rosenbaum et al., 2014). In addition to its requirement for antibody folding and secretion, it has been identified to be important for plasma cell differentiation where pERp1 deficient mice exhibit impaired generation of plasma cells post TI antigen induction (Andreani et al., 2018). Interestingly, loss of pERp1 results in the deregulation of some of BLIMP1's target genes suggesting that it is a key effector in BLIMP1's functions and/or the presence of a potential positive feedback loop between these proteins.

During protein folding, a core glycan precursor is added to Asn297 of the heavy chain (Jennewein & Alter, 2017). Post folding, the antibody is transported to the Golgi in COPII vesicles. In the Golgi, this glycan is processed by glycosidases and modified by glycosyltransferases to generate the final glycan structure on the antibody to be secreted. The variable addition of monosaccharides by glycosyltransferases can yield up to 36 unique glycans. The glycan content of the antibodies can influence their effector function by modulating their interactions with Fc receptors on other immune cells. For example, afucosylation of antibodies enhance antibody mediated cellular cytotoxicity by improving the carbohydrate-based interaction between the antibody which is coating a target cell and

the Fc receptor on the effector cell (e.g., natural killer cells) (Ferrara et al., 2011)(Nigro et al., 2019). These properties are useful and have been harnessed for the development of antibody therapeutics.

Following the folding and assembling of antibodies, they are trafficked through the constitutive secretory pathway (Zagury et al., 1970), which is enhanced in ASCs. How these cells adapt to high biosynthetic load is discussed next.

1.4 Protein Homeostasis in ASCs

It is estimated that ~30% of newly synthesised proteins are defective and are rapidly degraded to prevent their toxic accumulation (Schubert et al., 2000). Enhanced folding capacity and clearance of unfolded protein is especially important for ASCs which synthesise and secrete large amounts of antibodies. To maintain the homeostasis of ASCs, the cells are dependent on a range of ER stress responses. Therefore, it is not surprising that many of the genes involved in the ER Associated Degradation (ERAD) and Unfolded Protein Response (UPR) are upregulated in ASCs (Shaffer et al., 2004)(Shi et al., 2015)(Tellier et al., 2016)(Rahman, 2019). Previous Gene Ontology (GO) enrichment analysis of upregulated proteins in ASCs indicated that ER stress was highly enriched which included components of both the UPR and ERAD (Rahman, 2019).

1.4.1 ERAD

The ERAD system works to eliminate misfolded proteins from the ER and mark their degradation (Tannous et al., 2015)(Qi et al., 2017)(Shenkman & Lederkremer, 2019) (Ninagawa et al., 2021) (**Figure 1.2**). To recognise unfolded proteins, the glycan group added to the asparagine serves to indicate maturation of the folding of the protein. Removing the terminal glucose happens right after the glycan is added and this state is short lived, however is recognised and bound by malectin. Malectin is a carbohydrate binding protein able to detect and mark misfolded proteins early shortly after their expression (Schallus et al., 2008). Removing the second glucose enables the binding of calnexin and calreticulin which can engage with oxidoreductases and isomerases to promote the correct folding of the protein (Tannous et al., 2015)(Shenkman & Lederkremer, 2019). This monoglucosylated state persists for a longer time to allow for the folding process. When the final glucose is removed, binding of these chaperons is terminated. However, if the protein is misfolded, UGGT1 senses it through the recognition of an exposed hydrophobic moiety and transfers a glucose back to it. The misfolded protein is monoglucosylated again and re-enters the calnexin binding cycle. Folded proteins are not a substrate of UGGT1 and concentrate at ER exit sites where they are trafficked to the Golgi through the secretory pathway.

During the calnexin binding cycle, misfolded or slow-to-fold proteins cycle between the ER and the ER-derived quality control compartment (ERQC) (Shenkman & Lederkremer, 2019). The ERQC is referred to as the "staging ground" for targeting misfolded proteins to ERAD. If the protein fails to fold, it is subjected to extensive mannose trimming by mannosidases which are compartmentalised in quality control vesicles. Proteins whose mannoses have been extensively trimmed (to Man6GlcNAc2 or Man5GlcNAc2) due to slow cycling or misfolding are then bound by the lectin OS-9 at the ERQC which targets the unfolded protein to the ERAD complex. The complex, containing the E3 ligase HRD1, is responsible for ubiquitinating and retro-translocating the misfolded protein to the cytoplasm where it is degraded by the proteasome machinery. Independent of glycosylation, proteins can still be targeted to the ERAD through binding of chaperones, for example BiP (Ushioda et al., 2013)(Ninagawa et al., 2015)(Ninagawa et al., 2021).

When the biosynthetic load is too high and the accumulation of misfolded protein cannot be avoided through the ERAD, the UPR is typically activated.

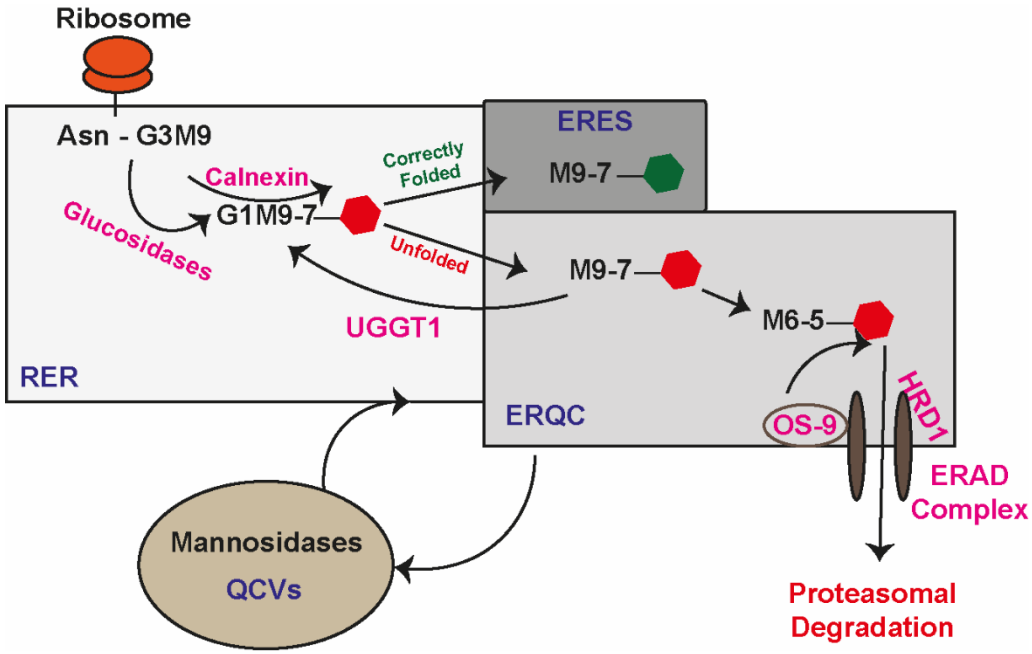

Figure 1.2: Schematic of the major steps of targeting misfolded glycosylated protein to ERAD. Adapted from (Shenkman & Lederkremer, 2019). N-linked glycosylation occurs at the rough endoplasmic reticulum (RER) co-translationally. Glucosidases remove two glucoses from the glycan, which allows calnexin and calreticulin to bind the protein and promote its correct folding. Binding of the chaperones is terminated when the final glucose is removed. During the folding cycle, up to two mannose residues can be removed. UGGT senses misfolded proteins and therefore re-glucosylate the protein so that it can re-enter the calnexin folding cycle. Correctly folded protein concentrates at ER exit sites (ERES) to be trafficked. For misfolded proteins, during the calnexin folding rounds, the protein cycles between the RER and the ER-derived quality control compartment (ERQC). During these cycles it becomes exposed to mannosidases sequestered in quality control vesicles (QCVs). Extensive mannose trimming (up to four mannose residues) releases the misfolded protein from the calnexin cycle, and it is then bound by the lectin OS-9 at the ERQC to target it to ERAD for degradation by the proteasomal machinery in the cytosol.

1.4.2 The Unfolded Protein Response in ASCs

The Unfolded Protein Response (UPR) is a complex program which is initiated in response to physiological and pathological triggers (Ricci et al., 2021). The latter is mostly caused by an accumulation of unfolded protein which activates the three stress sensors involved in the UPR, while the former occurs as a normal part of the development of some cells. Initially, it was mostly thought that the UPR is activated in response to unfolded protein stress hence the term UPR. However, it is now appreciated that components of the UPR can become upregulated as part of normal differentiation of cells prior to any secretory stress, such as during the differentiation of B-cells into ASCs.

1.4.2.1 The Conventional UPR

The UPR can be activated in three parallel pathways by the following transmembrane ER stress transducers: IRE1, PERK and ATF6 which are all normally inhibited by binding of BiP (Bertolotti et al., 2000). BiP preferentially binds nascent or unfolded proteins, therefore in ER stress conditions the inhibition on the three transmembrane sensors is relieved.

Activated IRE1 has RNase activity which cleaves 26 internal nucleotides from Xbp1 transcripts that are then spliced into an active form (XBP1s) (Yoshida et al., 2001). XBP1s behaves as a transcription factor which activates the transcription a large number of genes encoding proteins along the secretory pathway and components of the UPR and ERAD, drives the expansion of the ER and results in increased protein synthesis (Yoshida et al., 2001)(Shaffer et al., 2004). ATF6, in addition to being controlled by BiP binding, also has another layer of regulation where it is proteolytically cleaved at the Golgi (Haze et al., 1999)(**see section 1.8.5**). The released cytosolic domain then translocates to the nucleus where it acts as a transcription factor that promotes expression of XBP1, ER chaperones and ERAD proteins (Yoshida et al., 2001)(Yamamoto et al., 2007). Finally, activated PERK contributes to the UPR by reducing the ER's biosynthetic load through phosphorylating eIF2α which results in global inhibition of protein translation. Phosphorylated EIF2α can also selectively upregulates ATF4 and later on CHOP which is pro-apoptotic (Harding et al., 2000).

Overall, the outcomes of the signalling from each branch are varied, except for ATF6 whose regulation is mainly pro-survival. Even though signalling by IRE1 via XBP1 splicing is generally viewed as positive to the cells through upregulation of genes to manage ER stress, it is also implicated to induce JNK signalling which is pro-apoptotic (Urano et al., 2000). IRE1 dependent decay (RIDD) is another mechanism that IRE1 performs to lower the load of nascent ER proteins by cleaving their RNAs reducing ER burden (Hollien & Weissman, 2006). However, high levels of RIDD have been shown to be pro-apoptotic (Ghosh et al., 2014). PERK can also lead to pro-apoptotic responses through activation

of CHOP or through prolonged inhibition of protein translation. In summary, the three branches of UPR work to maintain the homeostasis in the cell in response to ER stress. If the stress persists and is not reversed, apoptosis is induced (Walter & Ron, 2011).

1.4.2.2 The Physiological UPR

Activation of the proteins involved in UPR can be triggered by signals beyond unfolded proteins (Rutkowski & Hegde, 2010). For example, IRE1 can be activated by Toll-like receptors in macrophages which subsequently activates XBP1. TLR activated XBP1 drives the production of inflammatory cytokines without inducing chaperone expression or ER expansion (Martinon et al., 2010), indicating that UPR signalling in response to different stimuli can vary. Moreover, the UPR has been shown to be strongly implicated in liver development (Reimold et al., 2000) and neurogenesis (Godin et al., 2016). Physiological functions and involvements of the UPR components in organ development are reviewed here (Cornejo et al., 2013). Therefore, it is evident that components of the UPR can be tailored to different cell types with specific biological processes. The UPR in ASCs is an example of this and is described next.

1.4.2.3 ASCs May Undergo a Two-Step UPR

ASCs benefit from a physiological UPR which enhances their secretory capacity and ensures the production, folding, and secretion of Immunoglobulin (Ig). The first hallmark of this specialised UPR is that it is anticipatory and occurs prior to increased synthetic load (Van Anken et al., 2003). Before increased Ig production, the ER expands, expression of ER chaperones such as BiP and GRP94 is increased and the activation of XBP1 and ATF6 into their active forms occurs (Gass et al., 2002)(Van Anken et al., 2003).

As accumulated antibodies are not the trigger for the initial UPR in ASCs, alternative stimuli have been suggested (Ricci et al., 2021)(Trezise & Nutt, 2021). In response to induction by LPS, B-cells lacking XBP1, or BLIMP-1 do not upregulate the genes involved in the expansion of the secretory pathway (Shaffer et al., 2004). BLIMP1 acts upstream of XBP1 to increase its expression and activation, and is also able to directly activate components of the UPR (Tellier et al., 2016). Therefore, BLIMP1 has been proposed to drive the special UPR that happens during ASCs' differentiation.

Upregulation of the biosynthetic machinery enables the biosynthesis and secretion of large quantities of antibodies. Once antibodies reach a level where they may start accumulating, a more common UPR is suggested to be triggered which drives further expansion of the ER that eventually leads to cell death (Van Anken et al., 2003).

1.4.2.4 Only XBP1 is Required

Another hallmark of the UPR in ASCs is its partial nature. It is mainly driven by the IRE1 branch which results in XBP1's activation. ASCs lacking XBP1 exhibit reduction in antibody expression and secretion as their ER is not remodelled appropriately (Taubenheim et al., 2012). In addition to activating the expression of a plethora of proteins involved in the secretory process, XBP1 also plays an important role in the expansion of the ER through the regulation of lipid biosynthesis (Shaffer et al., 2004)(Sriburi et al., 2007). Finally, XBP1 helps maintain Ig mRNA levels by regulating the RIDD function of IRE1 and reduction of Ig is partially rescued in IRE1/XBP1 double knockout cells. Taken together, the requirement for XBP1 to achieve high antibody synthesis and secretion relies on its transcriptional activation role and also its regulatory function on IRE1.

In contrast to XBP1, ATF6 and PERK are not essential for biosynthetic pathway remodelling and antibody secretion. ATF6 does become activated early in ASCs differentiation (Gass et al., 2002)(Aragon et al., 2012) and is able to drive ER expansion independently of XBP1 (Bommiasamy et al., 2009)(Maiuolo et al., 2011). However, the loss of ATF6 does not impact the formation of ASCs and antibody secretion (Aragon et al., 2012). ATF6's dispensable role in ASCs has been suggested to be due to compensatory mechanisms with other proteins performing its functions, such as XBP1 (which co-regulates some genes with ATF6) and CREB3L2 (Ricci et al., 2021). Compensatory mechanisms relating to ATF6 can be exemplified here, where acute knockdown of ATF6 in pancreatic cells results in significantly reduced downstream gene expression while chronic knockdown had minor impacts possibly due to compensation (Sharma et al., 2020). PERK is not required for antibody secretion and is selectively inhibited during differentiation through ufmylation by Ufbp1 (Gass et al., 2008)(Ma et al., 2010)(H. Zhu et al., 2019)

In summary, ASCs benefit from a physiological UPR likely driven by BLIMP1, that precedes synthetic load and the functional adaptations of this UPR rely mostly on the IRE1 branch.

1.5 Autophagy in ASCs and Multiple Myeloma

In addition to ERAD, autophagy plays a key role in the homeostasis of ASCs by safeguarding ER expansion and antibody synthesis to sustainable levels (**Figure 1.1**)(Pengo et al., 2013). Several autophagy genes are upregulated in ASCs and the loss of ATG5 results in elevated levels of BLIMP1, an expanded ER, and higher levels of antibody synthesis which ultimately results in lower ATP levels and increased cell death. In vivo work suggested that autophagy is also important for mounting effective immune responses and generating long lived immunity. The ER particularly seems to be a specific target of autophagy in ASCs, as ER proteins were significantly enriched in ATG5 deficient ASCs while mitochondrial and ribosomal proteins were not impacted.

The autophagic receptor, p62, has been recognised for its ability to yield resistance to proteasome inhibitor based therapies in multiple myeloma (MM)(Milan et al., 2015)(Milan et al., 2016). Due to the high load of unfolded proteins on the ubiquitin-proteasome system (UPS) during Ig production, MM cells are very sensitive to proteasome inhibitors (PIs). However, MM cells can compensate for proteasome insufficiency in response to PI by increasing the de novo expression of P62 and by diverting the interaction of P62 from cellular signalling partners to ubiquitinated proteins. This enhances p62 dependent autophagy, thereby relieving the proteostatic load during proteasome inhibition. Consequently, P62 dependent autophagy poses an important therapeutic target to help overcome PI resistance (Marino et al., 2019). Combinatory treatment with an autophagic inhibitor and bortezomib (PI) was shown to be effective in bortezomib resistant cells (Hideshima et al., 2016), indicating that inhibition of autophagy can alleviate its protective role in MM cells in response to proteasome insufficiency.

1.6 Metabolic Adaptations in ASCs

In addition to enhancing the biosynthetic pathway and equipping ASCs with the necessary machinery for high rates of antibody production, metabolic adaptations enable the cells to cope with the energetic and metabolic demands of producing large amounts of Ig. Mitochondrial and cytosolic chaperons are highly upregulated during early differentiation in anticipation of bulk secretion of antibodies (Van Anken et al., 2003). Long lived plasma cells (LLPCs) have higher energetic needs due to prolonged antibody production. Mice lacking Ennp1, a nucleotide recycling enzyme whose expression is promoted by BLIMP1, have significantly reduced numbers of LLPCs (H. Wang et al., 2017). Cells lacking Ennp1 also show reduced glucose uptake and glycolysis.

Glucose uptake is enhanced in plasma cells, and they have higher expression of the surface GLUT1 glucose transporter compared to plasmablasts (Lam et al., 2016). 90% of glucose usage is directed to

antibody glycosylation through the hexosamine biosynthesis pathway which generates glycosylation precursors. XBP1 promotes the expression of several key enzymes of this pathway (Z. V. Wang et al., 2014). The increased expression of glucose transporters is suggested to be due to post-transcriptional regulation, as the mRNA levels of the transporter between the plasma cells and plasmablasts are similar (Lam et al., 2016). Therefore, in addition to transcriptional level contributions, post-transcriptional modifications likely play important roles in maintaining the metabolic networks of ASCs.

The mTOR pathway which regulates protein synthesis and cell survival, is upregulated in ASCs. BLIMP1 promotes mTOR activity by upregulating the amino acid transporter, CD98, an important modulator of mTOR (**Figure 1.1**). The suppression of Sestrin proteins which are negative regulators of mTOR is carried out by BLIMP1 thereby also indirectly promoting its activity (Tellier et al., 2016). Inhibition of mTORC1 results in decreased Ig synthesis and secretion (Jones et al., 2016). Activity of mTORC1 was also shown to be required for the upregulation of UPR genes anticipatory of antibody secretion independently of XBP1 and therefore contributes to the "physiological" UPR (Gaudette et al., 2020). Some functional overlap between XBP1 and mTOR has been reported (Benhamron et al., 2015). Activation of mTOR in XBP1 deficient mice helps to partially rescue the phenotype and enhances Ig synthesis. Following the increase in protein synthesis, mTOR signalling is downregulated at later stages of LPS activation in response to ER stress (Goldfinger et al., 2011). Therefore, it seems that the UPR and mTOR work closely together to enable a sustainable level of protein synthesis and antibody secretion without impacting cellular viability.

1.7 Proteogenomic Identification of Membrane Trafficking Components in ASCs

1.7.1 Why Study ASCs

ASCs play a crucial role in the humoral component of the immune system by providing protection against infections. They are also the basis of vaccination strategies, with vaccines' protection being mainly dependent on neutralising antibodies produced by plasma cells against the antigen (Zinkernagel & Hengartner, 2006). Beyond antibody secretion, they have been implicated in other functional processes such as regulating haematopoiesis and gut homeostasis (Pioli, 2019). ASCs are also the origin of several cancers including multiple myeloma which remains incurable. Therefore, studying and gaining a better understanding of the biology of ASCs can provide important therapeutic insights. To carry out their protective function, ASCs have an impressive biosynthetic ability and are able to secrete thousands of antibodies per second (Hibi & Dosch, 1986). Importantly, the cells utilise the classical secretory pathway and secrete antibodies constitutively (Zagury et al., 1970), which makes them a good model to understand the molecular processes which underpin the biosynthetic pathway.

1.7.2 Previous Proteogenomic Project

To gain better understanding of ASCs, the lab has previously set out to identify novel factors involved in antibody secretion and ASCs' physiology by looking at transcriptomic and proteomic data between naïve B cells and differentiated antibody secreting cells (Rahman, 2019). Mass spectrometry analysis was performed on purified splenic mouse B cells which were used to generate antibody secreting plasmablasts sorted by using either CD138 or CD93 magnetic beads. In addition to the in-house generated proteomics data, the project also utilised published microarray and RNAseq datasets to generate a multi-omics and multi-species analysis of ASCs. The expression of mRNA/protein in ASCs across the cell types was analysed and compared to the levels in the naïve B-cell cells. The cell types used in the study are summarised in **Table 1.2**. Results from this multi-omics project have been made available through this user-friendly web resource (https://plasmacytomics.shinyapps.io/home/). As confirmation of the robustness of the analysis carried out by this project, we looked at a series of well-characterised markers of naïve B cells and ASCs to confirm that their expression is as would be predicted (**Figure 1.3**). The B-cell identity transcription factors PAX5, BACH2, BCL-6 and IRF8 are consistently downregulated in ASCs. In contrast, IRF4, PRDM1 (BLIMP1) and XBP1 are all upregulated in ASCs verifying the integrity of the results. Data obtained from this project will be used throughout the thesis as plots generated through our web resource; PlasmacytOMICs.

Table 1.2: Brief Description of the Sources of ASC Types Used in the Proteogenomic Project

Cell Type	Description	Source
mSpIPC.array	RNA extracted from in vivo generated mouse splenic plasma cells and hybridised to MG430.2A array	(Kaji et al., 2012) (Luckey et al., 2006)
mBMPC.array	RNA extracted from in vivo generated mouse bone marrow plasma cells and hybridised to MG430.2A	(Benson et al., 2012)
hPB.array hPC.array hBMPC.array	RNA extracted from human plasmablasts, and plasma cells generated in vitro from memory B-cells and RNA extracted from bone marrow plasma cells hybridised to the HG133A array.	(Jourdan et al., 2009) (Jourdan et al., 2011) (Kassambara et al., 2015)
mPB.rSeq	RNA extracted from in vitro generated plasmablasts from mouse splenic B cells and sequencing carried out using Illumina HiSeq 2500	(W. Shi et al., 2015)
mSpIPC.rSeq mBMPC.rSeq	RNA extracted from mouse spleen and bone marrow plasma cells and sequencing carried out using Illumina HiSeq 2500	
hPB.rSeq hBMPC.rSeq	RNA extracted from patient human plasma blasts and bone marrow plasma cells and sequencing performed using Illumina HiSeq 2500	(Lam et al., 2016)
mPBCD93.protein mPBCD138.protein	Lysates from in vitro generated plasmablasts isolated using either CD93 or CD138 magnetic beads were fractionated and analysed using the Orbitrap system (Thermofisher)	In-house generated data

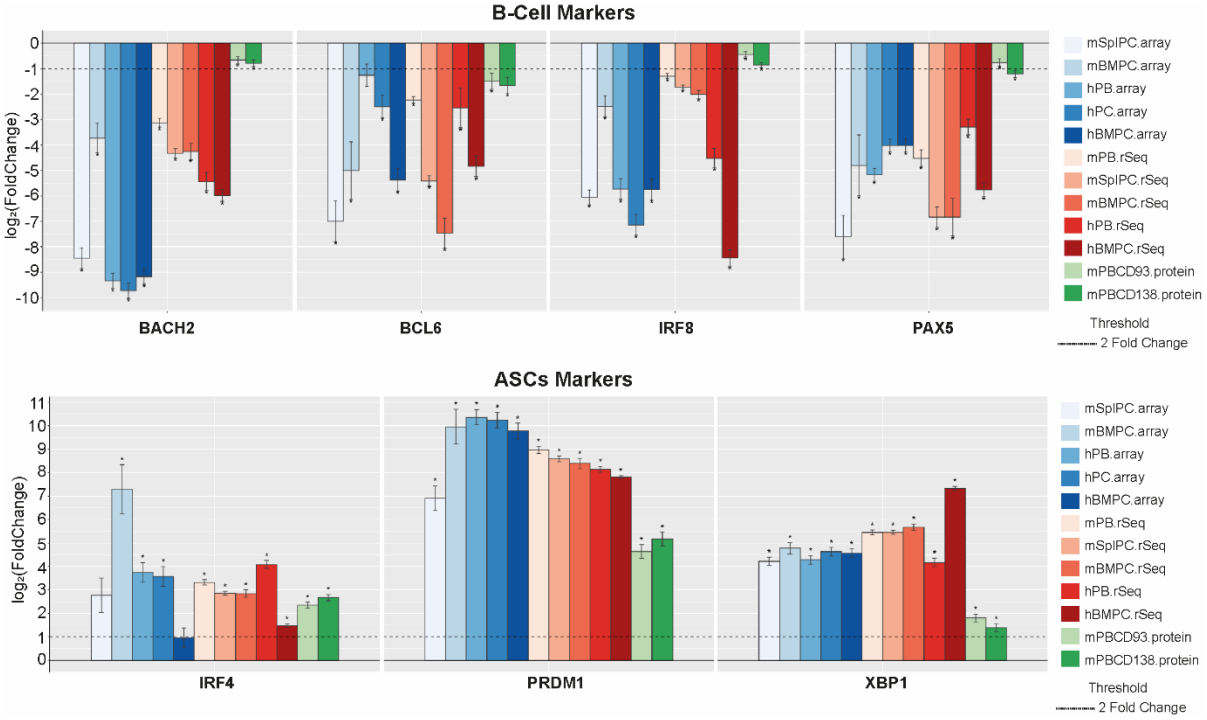

Figure 1.3: Differential regulation results of markers of naïve B cells and ASCs from the proteogenomic project. Fold change in mRNA and protein expression were plotted using the PlasmacytOMICs web resource which shows differential regulation of indicated markers between naïve B cells and ASCs. Literature shows that genes in the top panel of the figure are markers of naïve B cells and need to be downregulated when the cells differentiate to become ASCs, while the genes in the bottom panel are positive regulators of the ASC phenotype. In accordance with the literature, the results from the proteogenomic project show that the top genes are consistently downregulated in ASC and the bottom genes are upregulated compared to naïve B cells. **Error bars indicate standard error of mean.**

1.8 Identification of SEC24D as a Protein of Interest in ASCs

Gene Ontology (GO) enrichment analysis of the upregulated ASCs components showed that membrane trafficking and ER stress were the most enriched biological processes (Rahman, 2019). The expansion of membrane trafficking components and apparatus that respond to ER stress is predicted to enhance the secretory capacity of the cells, therefore, these enrichment results are expected in accordance with the cells' functions. Within the membrane trafficking category, transport between the ER and Golgi was the most significantly enriched. Enrichment of GO cellular compartments showed that the upregulated proteins in ASCs were mostly localised to the ER. We were particularly interested in protein candidates early in the membrane trafficking pathway which have not been previously characterised in ASCs, specifically components of the COPII complex.

1.8.1 COPII Vesicle Formation

The first step in the secretory pathway involves the packaging of correctly folded cargo into vesicles which bud from the ER. The formation of these vesicles is mediated by the Coat Protein Complex II (COPII) which consists of a highly conserved set of proteins that form two structural layers of the coat (Zanetti et al., 2011). The layers constitute Sar1 GTPase, Sec23/24 heterodimer (forming the inner vesicle coat) and Sec13/31 heterotetramers (forming the outer vesicle coat).

COPII subunits assemble on ribosome-free locations on the ER membrane called ER-exit sites (ERES) (Barlowe et al., 1994). The assembly of the coat starts with the recruitment of SAR1 GTPase. As with other small G- proteins, SAR1 cycles between an active and inactive state regulated by GTP hydrolysis. When SAR1 is GDP bound, it is cytosolic and inactive. SAR1 is activated and recruited to ER membranes by the action of SEC12, a guanine nucleotide exchange factor (GEF) which loads the protein with GTP (Weissman et al., 2001). More precisely, this occurs at specialised ER subdomains defined by the scaffolding protein, SEC16 and TFG (Watson et al., 2006)(Johnson et al., 2015). Through its carboxy-terminal domain, SEC16 binds SEC12 and enriches SAR1-GTP at these sites initiating COPII coat formation (Montegna et al., 2012). TFG interacts with SEC23, a component of the inner layer of the COPII coat, in addition to SEC16 (Witte et al., 2011)(Hanna et al., 2017)(Hanna et al., 2018).

Activated SAR1 exposes an N-terminal amphipathic alpha-helix that embeds into the ER membrane and initiates coat assembly (Lee et al., 2005) which was recently visualised utilising cryo-tomography (Hutchings et al., 2018). The membrane bound SAR1 can now recruit other COPII components and the SEC23-SEC24 heterodimer is recruited via direct binding between SAR1 and SEC23 (Bi et al., 2002). The recruitment of SEC23-SEC24 to SAR1 not only serves a structural function but also a catalytic function (Bi et al., 2002). Structurally, the SEC23-24 lattice has a positively charged surface which may

act to stabilise the curvature of the membrane. Catalytically, SEC23 plays a GTPase-activating role for SAR1 by providing a catalytic arginine to its active site. The SAR1-SEC23/24 complex can now be referred to as a pre-budding complex.

The full GTPase activity of SAR1 is not reached until the complete assembly of COPII coat, and this is achieved by the recruitment of the outer coat made from SEC13-SEC31 (Bi et al., 2007). SEC31 directly interacts with SAR1 and SEC23. The SEC13-SEC31 heterotetramers polymerize, shaping the membrane to form a bud. Activated SAR1 shows enhanced affinity for bent membranes and highly curved membranes have been shown to enhance the GTPase activity of SAR1 further (Hanna et al., 2016). Therefore, as membrane bending increases throughout the formation of the vesicle, SAR1 binding is increased and concentrated facilitating rapid fission upon GTP hydrolysis. There is also evidence that SEC31 promotes SEC23's GTPase activating role by direct interaction (Bi et al., 2007), further increasing GTP hydrolysis by SAR1, which is needed for vesicle uncoating after fission (Sato & Nakano, 2005). Therefore, in the current model, the outer coat is the main driver of membrane curvature. However recently, using N-terminal deletions of SEC31, it has been shown that the inner coat on its own can induce membrane remodelling in settings where membranes have less resistance to deform, such as lack of cargo (Hutchings et al., 2021).

Multiple mechanisms have been proposed to aid COPII's ability to accommodate a diverse plethora of cargo (McCaughey & Stephens, 2018) (Hutchings & Zanetti, 2019)(Peotter et al., 2019). These include posttranslational modifications such as ubiquitination, COPII organising factors such as SEC16 and TFG, and the use of receptors including TANGO1. The existence of COPII isoforms with distinct specialisations has also been proposed to aid in cargo selectivity.

1.8.2 COPII Paralogues and Their Roles

COPII cargoes are quite diverse and include a range of proteins from small cytokines to collagen and extracellular matrix proteins. One of the properties of COPII components which enables adaptation to this complexity is the existence of COPII paralogues (Zanetti et al., 2012). Even the GTPase involved in the budding process exist as two paralogues (A and B) which both need to be depleted to block secretion (Winslow et al., 2010)(Cutrona et al., 2013). Despite their apparent redundancy, they have been shown to exhibit different affinities to other COPII subunits (Fromme et al., 2007)(Fromme et al., 2008) and Sar1B seems to be specifically required for formation of large COPII vesicles (Jones et al., 2003). The inner coat complex which is most proximal to the ER membrane and acts as the cargo capture platform consists of SEC23 and SEC24. SEC23 acts as a GTPase activating protein for SAR1 while SEC24 acts as the cargo selector. There are two paralogues (A/B) for SEC23 and four for SEC24 (A/B/C/D).

SEC23A/B

Mammals encode two SEC23 paralogues, SEC23A and SEC23B, which are ~85% identical and are reported to have similar functions (Khoriaty et al., 2018). However, their deficiencies cause different diseases. SEC23B is required for erythrocyte development with mutations in humans resulting in anaemia and hyperglycosylated proteins in erythrocytes (Bianchi et al., 2009). It is also suggested to be involved in the transport of the EGF-R from the ER to the Golgi (Scharaw et al., 2016). Mutations in SEC23A cause Cranio-lenticulo-sutural dysplasia and results in collagen accumulation in fibroblast cultures (Boyadjiev et al., 2006).

The levels of SEC23A are regulated by the transcription factor, CREB3L2 and its disruption in mice leads to a similar phenotype as observed with SEC23A deficiency where collagen accumulates in the ER and chondrogenesis is impaired (Saito et al., 2009). This phenotype can be completely restored when SEC23A is re-introduced in the CREB3L2 KO chondrocytes suggesting that the loss of SEC23A is the main cause of the observed defect. The expression levels of SEC23B in chondrocytes is low, therefore it is possible that in other cell types which have higher levels of SEC23B, the loss of CREB3L2 wouldn't cause a significant phenotype. In CREB3L2 KO fibroblasts which have high expression levels of SEC23B, the distention in the ER is only slight. Therefore, it seems that the presence of either of paralogue may enable normal SEC23 function. Moreover, low levels of SEC23B expression in calvarial osteoblasts has been suggested to cause the phenotype seen in patients with SEC23A mutations (Fromme et al., 2007). SEC23A has also been recently reported to rescue phenotypes of erythroid defects in SEC23B deficient cells (King et al., 2021).

Different phenotypes observed due to differential tissue expression can also be exemplified here where SEC23B deficient mice exhibit prenatal lethality due to pancreatic degeneration (Tao et al., 2012), while humans exhibit anaemia (Bianchi et al., 2009). This could be explained by SEC23B being predominantly expressed in the mouse pancreas while in humans it is in the bone marrow (Khoriaty et al., 2018). The functional redundancy between both paralogues has been further investigated, where SEC23A could functionally replace SEC23B in mice (Khoriaty et al., 2018).

Finally, to identify cytoskeletal related functional interactors with both paralogues, a study was carried out using a double siRNA screen of several cytoskeleton and Extracellular Matrix (ECM) proteins with either SEC23A or B and assaying for VSVG secretion (Jung et al., 2021)(Jung et al., 2022). The knockdown of either SEC23A or B individually results in no transport defect in VSVG supporting the idea that the paralogues are functionally redundant for its transport in this experimental context. Interestingly, knocking down a selection of SEC23 interactors which are involved in focal adhesions and plating cells on ECM resulted in downregulation of SEC23A. Given that SEC23A has been previously

implicated in collagen secretion and is suggested here to be regulated at a transcriptional level by ECM and adhesion signalling, a feedback mechanism hypothesis is presented.

Taken together, the phenotypes and diseases associated with SEC23 components may be due to differences in their transcriptional regulation. However, the need of both SEC23A and SEC23B in zebrafish craniofacial development has been previously reported which suggested that they may not be able to compensate for each other in zebrafish (Lang et al., 2006). SEC23B deficiency in mice has also been reported not to cause defects in collagen secretion, while SEC23A deficiency does even in the presence of SEC23B (M. Zhu et al., 2015). It may be that sufficient SEC23 is needed regardless of the paralogue, and that in these tested conditions, not enough SEC23 was available to allow proper COPII formation in the absence of just one. Moreover, whether SEC23B can replace SEC23A is yet to be tested to determine if in fact SEC23A has a specific role for collagen secretion.

SEC24 – The Cargo Selector Component for COPII

SEC24 is the cargo selector subunit of the COPII, and its paralogues are generally defined into groups of SEC24A/B and SEC24C/D based on their sequence homology which is ~60% within a group and ~25% across them (Tang et al., 1999) (Mancias & Goldberg, 2008). The selection of cargo between the different paralogues is broadly defined as exclusive, preferential, and redundant (Chatterjee et al., 2021). The ability of SEC24 to select and bind cargo is mediated by direct interactions between binding sites present on SEC24 and sorting signals on the cargo proteins. Proteins without the signal sequence can still be included in the COPII vesicle by interacting with cargo receptors/adaptor proteins (Baines & Zhang, 2007) or by passive diffusion (Thor et al., 2009).

14 sequence motifs have been identified so far to be involved in ER export of mammalian proteins (Chatterjee et al., 2021). These signal motifs can have exclusive binding abilities depending on the SEC24 paralogue. For example, the IxM signal motif found in Syntaxin 5 and membrin can bind to SEC24C/D but not A/B as the IxM binding site is obstructed by a polypeptide in SEC24A/B as shown by x-crystallography (Mancias & Goldberg, 2008). Other cargo examples include the GABA1 transporter which exhibits specificity to SEC24D (Farhan et al., 2007) and autoaxin which selectively utilises SEC24C (Lyu et al., 2017). In addition to short peptide sequences directing ER export, some recognition sites are conformational. For example, the export motif of SEC22 is created by the folding of two elements of SEC22 to enable binding with SEC24A/B (Mancias & Goldberg, 2007), and Syntaxin 5 binds SEC24C in its open conformation where the N-terminal domain is not folded back onto the SNARE motif (Adolf et al., 2016). SILAC-based proteomics revealed heterogeneity and differences in compositions of COPII vesicles depending on which SEC24 paralogue was used which further illustrated the specificity in protein sorting depending on the SEC24 paralogue (Adolf et al., 2019).

When comparing the profile of SEC24A and C vesicles, the authors reported two types of proteins. The first type showed no preferential sorting with the tested paralogue, for example ERGIC53. The second type were proteins enriched with a specific paralogue. For example, CNHI4 with SEC24A and SURF4 with SEC24C, however in general more proteins were enriched with SEC24C.

The cargo specificity and selection by SEC24 paralogues may also be different among different cell types. For example, PCSK9's secretion was found to be mediated by overexpressing SEC24A and B but not C/D in 293T cells which express no endogenous PCSK9 (X. W. Chen et al., 2013), while knockdown of SEC24A/B and also C but not D in Huh7 cells significantly reduced the secretion of endogenous PCSK9 (Deng et al., 2020).

In the case of mutations in the SEC24 paralogues, a number of diseases have been identified. This can be expected when a protein important for a certain function confers sorting specificity for a paralogue that has been mutated. For example, a loss of function mutation in SEC24B was reported to impact neural tube closure and cause embryonic lethality (Merte et al., 2010). Vangl2, a protein important for the process was discovered to be preferentially sorted by SEC24B using a vesicle budding assay. Therefore, in SEC24B mutant mice, Vangl2 is not trafficked from the ER to the plasma membrane. Another example is the hypocholesteraemia observed in SEC24A deficient mice due to impaired PCSK9 secretion which is important for LDL receptor degradation (X. W. Chen et al., 2013).

The distinct functions of SEC24 can also be strongly highlighted by the unique abnormalities in mouse embryonic development. SEC24D deficiency results in early embryonic lethality that cannot be rescued by any other paralogue (Baines et al., 2013) while SEC24C deficiency results in later embryonic lethality (Adams et al., 2014). Interestingly, knocking in the coding sequence of SEC24D into the SEC24C locus in SEC24C deficient mice rescues embryonic lethality however they do not survive after birth (Adams et al., 2021), indicating partial functional overlap, however that they can't fully compensate for each other in this context.

In humans, mutations in Sec24D have been reported to cause skeletal disorders and severe forms of osteogenesis imperfecta (Garbes et al., 2015). Fibroblasts of patients suffering from these mutations show a retention of procollagen in the ER and the dilation of the ER cisternae. Similar skeletal defects were also observed in medaka (Ohisa et al., 2010) and zebrafish mutants (Sarmah et al., 2010). These results suggest that SEC24D plays an important role in the trafficking of collagen and extracellular matrix proteins. However, SEC24D deficient mice show very early embryonic lethality which may suggest differences amongst species and/or differential tissue expression profiles.

In summary, SEC23 paralogues seem to largely be able to compensate for each other with major differences potentially being exhibited due to differential tissue expression while SEC24 paralogues exhibit more functional differences.

1.8.3 SEC24D is Highly Upregulated in ASCs

In a previous study looking at human B cell differentiation and COPII coat components as part of ER exit sites expansion, the authors reported an increase in the levels of SEC24C and SEC31A using qRT-PCR (Kirk et al., 2010). Utilising our proteogenomic study which has RNA and protein data across human and mouse, we take a closer look at COPII vesicle components in ASCs (Rahman, 2019)(**Figure 1.4**). Even though these genes do show upregulation in our data, the increase is relatively weaker compared to other components in the inner coat. Of note are SEC23B, SEC24A and SEC24D which have the most consistently upregulated data. SEC24D clearly stood out compared to the other components with significance and extent of the upregulation. Therefore, we hypothesised that our data may suggest that SEC24D plays an important role in IgM cargo selection at the ER.

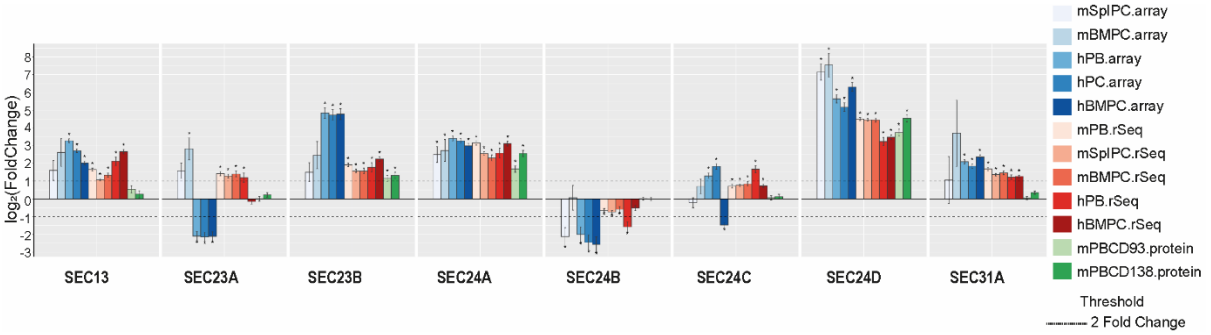

Figure 1.4: SEC24D is highly upregulated in ASCs. Fold changes in mRNA and protein expression were plotted using the PlasmacytOMICs web resource which shows differential regulation of indicated markers between naïve B cells and ASCs. Plots are showing differential regulation of COPII components in ASCs. **Error bars indicate standard error of mean.**

1.8.4 CREB3L2 Activates SEC24D

Similarly to ASCs, hepatic stellate cells (HSCs) upregulate their ER and Golgi apparatus during their activation into myofibroblasts in response to liver injury and inflammatory cytokines (Tomoishi et al., 2017). This biosynthetic enlargement enhances the synthesis and deposition of extracellular matrix components which includes collagen I. The expression of early secretory genes was analysed between precursor and activated states in HSCs, and SEC23A and SEC24D were shown to be upregulated by the transcription factor CREB3L2. The authors also showed using luciferase reporter assays that CREB3L2 binds and activates the Sec24d promoter between 525bp and 205bp upstream of its transcription start

site. Importantly, CREB3L2 is highly upregulated in ASCs according to our proteogenomic data and has also been identified by others (Shi et al., 2015).

CREB3L2 is a member of the basic leucine zipper (bZIP) transcription factor family and is upregulated in response to ER stress mildly at the transcriptional level and strongly at the translational level (Shinichi Kondo et al., 2007). In addition to its role in HSCs, CREB3L2 was previously implicated in chondrogenesis and identified as a transcriptional factor for SEC23A in chondrocytes (Saito et al., 2009). Mouse chondrocytes lacking CREB3L2 show ER retention of collagen II indicating that its secretion was prevented in CREB3L2 deficient chondrocytes, a phenotype completely restored by introduction of SEC23A. In fish, CREB3L2 mutants also exhibit defects in collagen secretion (Melville et al., 2011)(Ishikawa et al., 2017).

1.8.5 The OASIS Protein Family

CREB3L2 is part of a protein group with other ER localised transcription factors referred to as the OASIS (old astrocyte specifically induced substance) family. These include CREB3L1, CREB-H, CREB4 and Luman in addition to CREB3L2, with CREB3L2 being most similar to CREB3L1 (51% amino acid identity) (Shinichi Kondo et al., 2007) (Shinichi Kondo et al., 2011). They exhibit tissue specific expression, for example CREB3L2 is predominantly expressed in chondrocytes (Saito et al., 2009), while CREB3L1 is mainly expressed in osteoblasts and astrocytes (Murakami et al., 2009) (Shinichi Kondo et al., 2005) and CREBH in liver cells (Omori et al., 2001). These proteins reside in the ER through their alpha helical transmembrane domain and have a transcriptional activation and bZIP motif in their cytoplasmic portion (Shinichi Kondo et al., 2011) (**Figure 1.5**). In their luminal portion, they contain consensus sequences for S1P and S2P cleavage which can undergo intramembrane proteolysis. The activated cleaved cytoplasmic domain then translocates into the nucleus where it activates transcription of target genes containing ER stress and cyclic AMP-responsive elements (Shinichi Kondo et al., 2005)(Murakami et al., 2006).

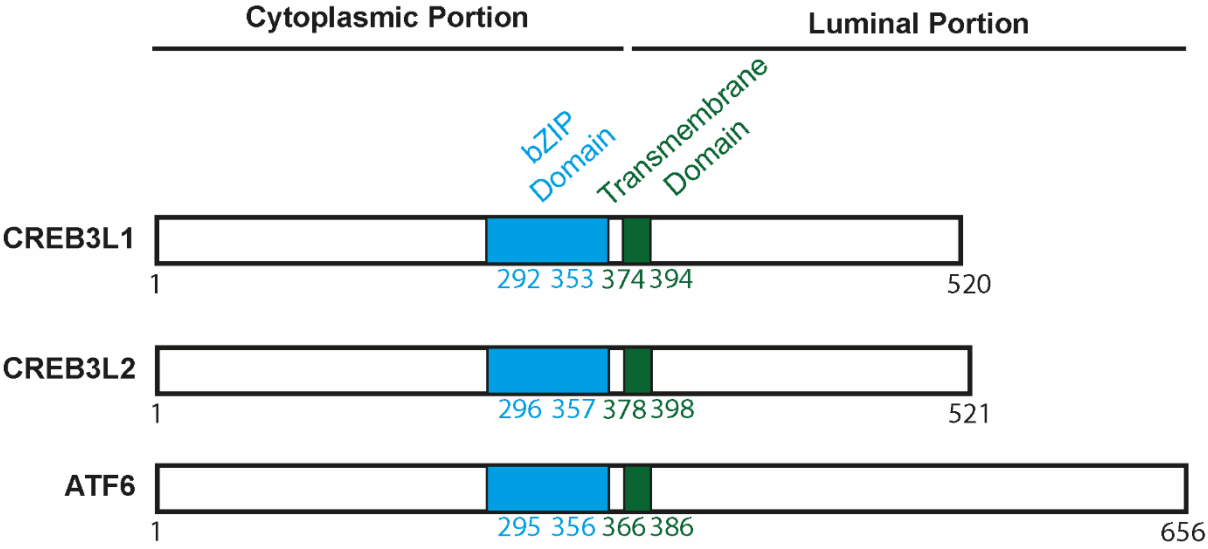

Figure 1.5: Schematic showing domain structures of CREB3L1, CREB3L2 (OASIS family members) and ATF6 – Figure adapted from (Shinichi Kondo et al., 2011). All three proteins have a transmembrane domain which enables their ER localization. Their cytoplasmic portion contains a transcriptional activating and bZIP domain. The luminal domains contain consensus sequences for cleavage by S1P and S2P proteases. The luminal domain is distinct between CREB3L1/2 and ATF6.

Even though OASIS family members have a similar overall domain structure to ATF6 and a high sequence identity at the transmembrane domain (31%), they are distinguishable due to distinct luminal portions and activation in response to stimuli. For example, ATF6 is normally bound to BiP at the ER via its luminal domain. BiP binds misfolded proteins during ER stress allowing ATF6 to translocate to the Golgi apparatus for cleavage by the S1P and S2P proteases due to the presence of Golgi localization signals in its luminal portion (Shen et al., 2002)(X. Chen et al., 2002). This is unlike OASIS members which can translocate to the Golgi apparatus in absence of those signals (Murakami et al., 2006) and also that CREB3L1/2 do not bind BiP (S. Kondo et al., 2012), indicating the presence of a separate ER stress transduction and ER-Golgi apparatus translocation mechanism. In terms of ER stress transduction, it has been proposed that ER stress stabilises CREB3L1/2's full length and activated protein forms (S. Kondo et al., 2012). These forms are otherwise sensitive to ubiquitin degradation through interaction at the transmembrane region with the E3 ubiquitin ligase HRD1. This interaction is not detected under ER stress conditions therefore during ER stress the degradation of CREB3L1/2 is prevented, enhancing their activation.

1.8.6 Potential Cargo Proteins of SEC24D Relevant to ASCs

We have previously carried out transcription factor co-expression analysis on our multi-omics data to predict which transcription factors co-regulate with genes upregulated in ASCs. Of the analysed transcription factors, CREB3L2 stood out as having the highest number of co-expressed proteins related with membrane trafficking (Rahman, 2019). Of these is the cargo protein, CD59, which is a GPI anchored membrane protein. Interestingly, it has been found to be selectively exported from the ER by the SEC24 isoforms SEC24C and SEC24D (Bonnon et al., 2010). This study links a CREB3L2 co-expressed cargo protein with SEC24D, a cargo selector which itself is regulated by CREB3L2.

Another co-expressed protein with CREB3L2 and is of particular interest to us is FNDC3B. In a study focusing on FNDC3B as a poor prognostic marker of cervical cancer potentially via involvements with ER stress and the UPR, the authors report a list of the co-expressed genes with FNDC3B, which of noteworthy includes SEC24D (Han et al., 2020). This list contained 79 genes co-expressed positively with FNDC3B, 16 of which are also co-expressed with CREB3L2 in ASCs according to our analysis (**Figure 1.6**). Taken together, this data may suggest a possible link between CREB3L2 regulated proteins and proteins co-expressed with FNDC3B. As exemplified by CD59 which is co-expressed with CREB3L2 and selectively exported by SEC24D (highly upregulated in ASCs), we predict that more proteins co-expressed with CREB3L2 could be selectively trafficked by SEC24D in ASCs. Of these proteins, we pay special interest to FNDC3B which is a potential biomarker of ASCs with a co-expression profile that shares ~20% of its proteins with CREB3L2 co-expressed proteins in ASCs.

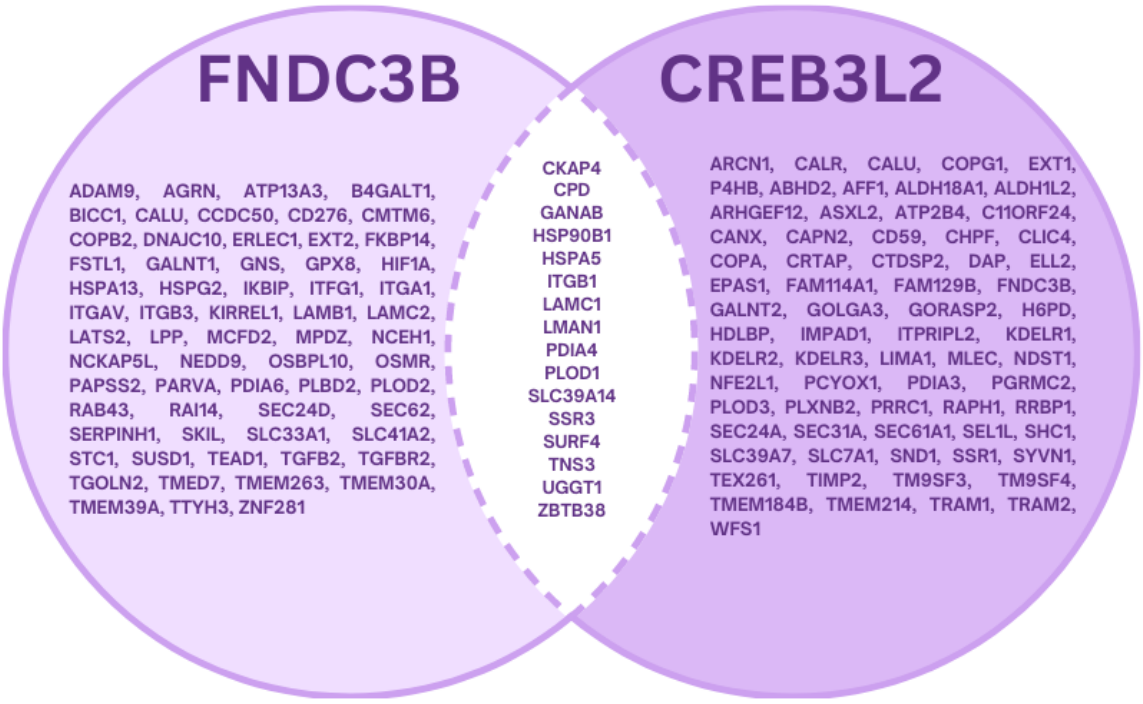

Figure 1.6: Positively co-expressed genes with FNDC3B (Source: Han et al., 2020) and CREB3L2's predicted co-expressed genes which are upregulated in ASCs (Source: (Rahman, 2019)) – Venn Diagram Created on Canva. FNDC3B is an upregulated ASCs marker that is co-expressed with CREB3L2. ~20% of the co-expression profile of FNDC3B is shared with CREB3L2's predicted co-expressed genes which are upregulated in ASCs. Gene names arranged in alphabetical order.

1.9 Aims of Thesis

ASCs have remarkable biosynthetic and secretory capacity, and therefore present a unique model for studying constitutive secretion. A previous project in the lab identified a large number of genes which are differentially expressed when naïve B cells differentiate into ASCs using a multi species proteogenomic study (Rahman, 2019). As predicted, many of these proteins were involved in trafficking suggesting that this approach will be useful for identifying novel players which act on this pathway. We hypothesised that proteins which were consistently and significantly upregulated in ASCs likely play an important role in ASC physiology (e.g., differentiation, antibody synthesis/secretion, proteostasis). To investigate this, this thesis aims to:

I. Characterise the I.29 B cell line to determine whether it is a suitable ASC model.
II. Validate the upregulation of our identified proteins of interest in the I.29s cells.
III. Develop a useful experimental platform in the I.29s to study the roles of our proteins of interest in ASCs through CRISPR/Cas9 and proximity labelling systems.
IV. Investigate the role of SEC24D in ASCs by assessing antibody secretion and the regulation of differentiation markers.
V. Explore the regulation of SEC24D by transcription factors of the OASIS family.

Chapter 2: Materials & Methods

2.1 Molecular Biology

2.1.1 sgRNA Cloning

gRNAs against a gene of interest targeting the first exon were chosen using CHOPCHOP. The oligonucleotides comprising the gRNA and sticky ends compatible with a BbsI cut site were ordered from Sigma-Aldrich (**Table 2.3**). 8.5µl of each complementary oligonucleotide (100µM) were mixed with 2µl of ligase buffer in a 20µl reaction and annealed by heating at 95°C for 5 minutes then cooling down to room temperature (RT). The annealed oligos were then ligated into the gRNA expression plasmid overnight using 1µl of T4 ligase at 4°C. The modified gRNA expression vector (Addgene #50946, deposited by Dr.Kosuke Yusa) was obtained from Paul Lehner's group. To prepare this vector for cloning, 5µg of plasmid was cut with 1.5µl of BbsI enzyme (NEB) in a 30µl digestion reaction for 3 hours at 37°C.

2.1.2 Genomic DNA Extraction, TOPO Cloning and Sequencing

To purify genomic DNA, approximately $5x10^6$ cells were lysed following the manufacturer's protocol (Quick-DNA isolation kit, Zymo Research, Cat #: D3024). To amplify the genomic region of interest, PCR was performed using primers designed to flank SEC24D's targeted exon (**Table 2.2**). Taq polymerase (Promega, Cat #: M3001) was used and the reaction is described below:

DNA	~100ng
5x Colorless GoTaq Flexi Buffer	10µl
dNTPs (50mM)	0.5µl
SEC24D Forward primer (10µM)	2.5µl
SEC24D Reverse primer (10µM)	2.5µl
$MgCl_2$ (25mM)	4µl
ddH_2O	To 49.75µl
GoTaq	0.25µl

Typical cycling parameters were used (35 cycles, annealing temperature at 60°C), however a 30-minute extension step at 72°C was added to ensure 3' adenylation. 10µl of the PCR product was ran on 1% agarose DNA gel to confirm the specificity of the amplified PCR product. The remaining product was purified using QIAquick PCR purification kit (Qiagen, Cat #:28104) and ligated using a TOPO cloning kit following the manufacturer's protocol (Invitrogen, Cat #: 11533127). The ligated plasmids were

transformed into bacteria, purified and then sent for Sanger sequencing (Genewiz) using the M13R primer.

2.1.3 Q5 Site-Directed Mutagenesis

A mouse SEC24D expression construct was obtained from Sino Biological (MG5A4182-U). To make the construct resistant to Cas9 endonuclease, site directed mutagenesis was performed using the Q5 site-directed mutagenesis kit (NEB, Cat #: E0554) (**Figure 4.15**) following the manufacturer's protocol. Primers were designed using NEBaseChanger (**Table 2.2)**. Post mutagenesis, the plasmid was transformed, purified, and sent for Sanger sequencing using the M13F primer.

2.1.4 Generating Lentiviral Expression Constructs

The lentiviral vectors pLVX-IRES-Neo (Takara Bio, Cat #: 632181) was used for the expression of the following genes:

SEC24D

CRISPR/Cas9 resistant SEC24D sequence was cloned into the PLVX-IRES-NEO vector using EcoRI and NotI. Post digestion, the reactions were run on a 1% agarose gel and the appropriate fragments were purified (Omega Bio-Tek: Cat #: D2500-01) then ligated overnight using 1µl of T4 ligase at 4°C.

ER Membrane Tagged Ascorbate Peroxidase 2 (ERM-APEX2)

Blunt-end cloning was performed to express ERM-APEX2 using the pLVX-IRES-Neo vector. Plasmids were linearised (BtsbI for the ERM APEX2 and EcoRI for the pLVX-IRES-Neo) then blunt ends generated using the Klenow polymerase. Blunt-ended linear DNA was then column purified (Qiagen: Cat #: 28104). ERM-APEX2 was digested using NheI and the pLVX-IRES-Neo using SpeI. Post digestion, the reactions were run on a 1% agarose gel and the appropriate fragments were purified (Omega Bio-Tek: Cat #: D2500-01) then ligated overnight using 1µl of T4 ligase at 4°C.

2.1.5 Transformations and Bacterial Culture

All lentiviral plasmids were transformed into STBL3 cells, and any other type of plasmid were transformed into DH5alpha cells. Competent cells were thawed on ice and between 1-5µl of chilled DNA was added to the bacteria. The bacteria and DNA were gently mixed by taping and incubated on ice for 30 minutes. The bacteria were heat-shocked at 42 °C for 45 seconds and incubated on ice for 2 minutes. 250µl of SOC media was then added to the bacteria and they were incubated at 37°C at 220rpm for 1 hour. The bacteria were plated onto pre-warmed agar plates containing the appropriate antibiotic for selection (100µg/ml of ampicillin for all described plasmids in this thesis) and incubated

overnight at 37°C. Bacterial colonies were picked into 3ml of LB media containing antibiotics. For mini-prep plasmid isolation, they were grown for 12-16 hours at 37°C (220rpm) and harvested. For maxi-prep plasmid isolation, bacteria were initially incubated for 8 hours 37°C (220rpm). They were then diluted at 1:1000 in 250ml of LB media, incubated overnight at 37°C (220rpm) and harvested.

2.1.5 Plasmid Isolation

Plasmid DNA was isolated using GeneJet mini (Thermo Scientific, Cat #: K0502) or maxi prep (Thermo Scientific, Cat #: K0491) kits following the manufacturer's protocol. DNA yield was then determined using a nanodrop spectrophotometer and stored at -20°C.

2.2 Mammalian Cell Culture

2.2.1 Cell lines and Antibiotic Selection

HeLa, HEK293T and MEF cells were grown in DMEM media supplemented with 10% Fetal Bovine Serum (FBS) and 1% Penicillin/Streptomycin (P/S). When cells reached 80-90% confluency they were passaged by aspirating the media, washing with PBS, and incubating at 37°C for 5 minutes with 1ml of trypsin. The cells were then resuspended in fresh media and routinely maintained by splitting at a ratio between 1:10 to 1:20 of cells to media. I.29 cells were grown in RMPI 1640 media (Gibco, Cat #: 12004997) supplemented with 10% FBS (Gibco, Cat #: 16140071), 1% Penicillin/Streptomycin and 50µM β-mercaptoethanol. The cells were split every two days between 0.2-0.4x10^6 cells/ml (approximately a 1:10 dilution).

For antibiotic selection of cells post transduction, HeLa cells were selected with 1µg/ml Puromycin, 6µg/ml Blasticidin and 400µg/ml G418. MEF cells were selected with 1µg/ml puromycin. I.29 cells were selected with 1µg/ml Puromycin, 12µg/ml Blasticidin and 1mg/ml G418. When indicated, cells were treated with 2µg/ml tunicamycin and 1µM MG132 for the specified times. For induction of tet-inducible shRNAs, cells were incubated with 1µg/ml of doxycycline typically for 2 days before characterisation.

2.2.2 Transient Transfection of Cells

HeLa or HEK293T cells were seeded in 6 well, 12 well or 10cm plates depending on the scale of the transfection. The following transfection reagents were routinely used during this work: PEI, FuGENE HD (Promega, Cat #: E2311) and ViaFect (Promega, Cat #: E4981) at a 3:1 ratio of reagent to DNA. Transfection conditions and details used in this thesis are summarised below:

Table 2.1: Summary of Transfection Conditions and Purposes

Culture Plate	Culture Volume	Transfection Reagent	Optimem volume	[DNA]	Purpose of experiments
10cm	6ml	PEI	800 µl	11µg	Transfecting HEK293T cells as packaging cells for viral transductions (**Figure 2.1**)
6 well	2 ml	ViaFect	200 µl	2µg	Transfection of HeLa cells
12-well	1 ml	ViaFect	100 µl	1µg	

For all transfections, media was replaced at least an hour before transfection with antibiotic free media. For PEI transfections, PEI was added to a tube of 400µl of OPTIMEM, and DNA was added to a second tube of 400µl OPTIMEM. They were incubated separately for 5 minutes, then mixed and incubated for 20 minutes at room temperature before being added drop wise to cells. For transfections using Fugene and ViaFect, the manufacturer's protocol was followed (Promega). After transfection the cells were incubated at 37°C overnight.

2.2.3 Viral Transduction of Cells

To produce lentivirus, a triple transfection of HEK293T cells was performed (**Figure 2.1**). Cells were seeded in a 10cm dish at 60-70% confluency and transfected with a total of 11µg DNA using PEI. The next day, cells were washed, and media was replaced with the media of the cells to be transduced (e.g., RPMI for I.29s). The collected media was inactivated before discarding. 48 hours post changing media, viral-containing media was harvested and filtered through a 0.45µm syringe filter. The viral supernatant was then applied to the cells to be transduced (at 50% confluency) and centrifuged at 2000rpm for 90 minutes. Post transduction, the cells were grown overnight at 37°C. The following day, cells were centrifuged and resuspended in fresh media. Discarded media is inactivated first. Cells were left in fresh media overnight and then antibiotic selection was started the next day.

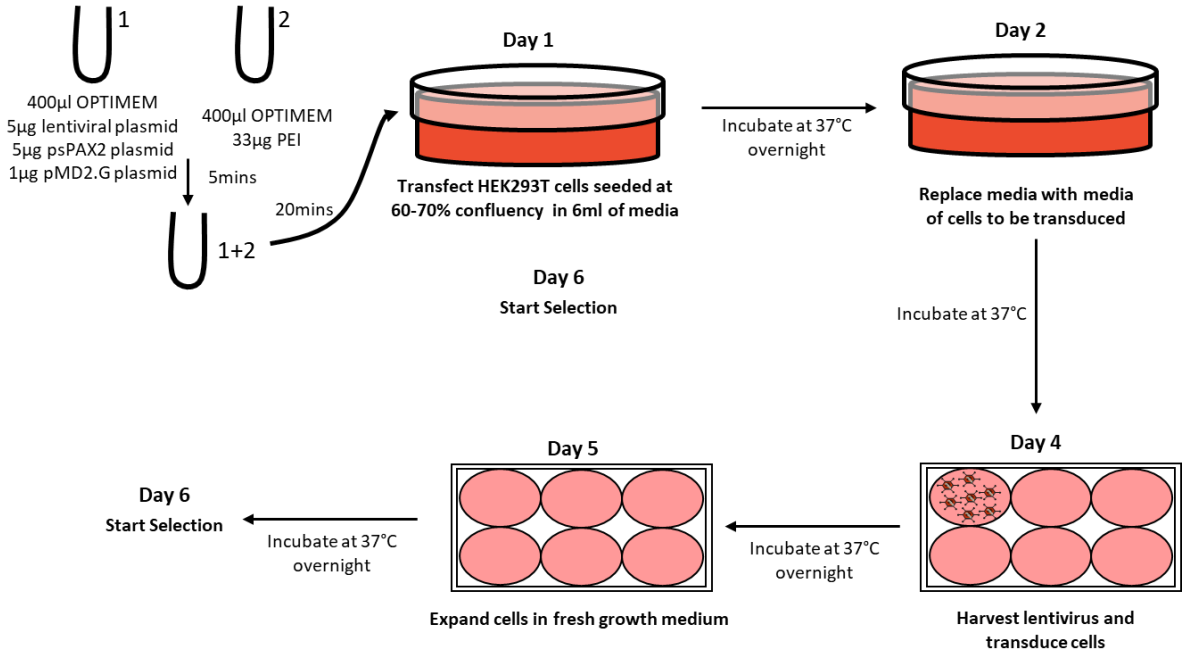

Figure 2.1: Schematic showing steps followed for viral transduction of cells

2.2.4 LPS differentiation of I.29 cells

To initiate differentiation in I.29 cells, $0.6x10^6$ cells were seeded in 2ml of RPMI media containing LPS at 20µg/ml (Sigma, Cat #L2630) in a 6 well plate. Two days post induction, the cells were split to $0.3x10^6$ cells/ml while maintaining the LPS concentration at 20µg/ml.

To measure IgM secretion, cells were collected (typically $2x10^6$ cells) on the specified days, washed and resuspended in fresh media. 5 hours post incubation in fresh media, the supernatant was harvested by removing the cells with centrifugation at 1500rpm for 5 minutes, followed by filtering the supernatant using a 0.45µm syringe filter.

2.3 Cell Biology

2.3.1 Immunofluorescence Microscope

HeLa or MEF cells were seeded on glass coverslips at approximately 70,000-100,000 cells per ml and grown overnight. To perform immunostaining on I.29 cells, cells were spun down onto coverslips pre-coated with fibronectin (Sigma Aldrich, Cat #: F2006). To precoat the coverslips, they were incubated with 10µg/ml of fibronectin in media overnight at 37°C. The next day, fibronectin containing media was aspirated, and the coverslips were air dried in the hood for at least 45 minutes. $1x10^6$ (for one well of a 24 well plate) or $2x10^6$ I.29 cells (for one well of a 12 well plate) were collected and spun down onto the dried coverslips at 2000rpm for 15 minutes.

Depending on the protein to be stained, cells were either fixed using 4% PFA (10 minutes at RT) or 100% methanol for 5 minutes at -20°C (methanol had been prechilled for at least 1 hour at -20°C). If fixed by PFA, the reaction was quenched using 0.1M glycine (5 minutes at RT). Cells were permeabilized using 0.1% saponin or 0.1% triton (10 minutes), then blocked using 1% BSA for 30 minutes. Primary antibodies were diluted in 1% BSA and incubated with the coverslips for 1 hour at RT. The unbound antibodies were removed by washing with 1% BSA. Cells were incubated with the secondary antibodies diluted in 1% BSA for one hour. The cells were then washed two times using the blocking solution and once using PBS. The coverslips were mounted onto glass slides using ProLong Gold Antifade Mounting Media (Invitrogen, Cat #: 11539306). Imaging was then performed using the Nikon Widefield Live-Cell system and the images processed using ImageJ. All solutions used were made up in PBS.

2.3.2 Flow cytometry

2.3.2.1 Intracellular Protein Labelling for HeLa Cells

For the of OASIS proteins overexpression experiments, HeLa cells were harvested by trypsinization, washed and fixed using pre-chilled methanol (-20°C for 5 minutes). The cells were washed and resuspended in 0.1% Triton in PBS (10 minutes) and then blocked in 1% BSA for 30 minutes. The primary antibody was diluted in 1% BSA and incubated with the cells for 1 hour at RT. The cells were washed using 1% BSA and then resuspended with the secondary antibody diluted in 1% BSA for a further hour at RT. Cells were then washed twice using blocking solution and once using PBS. The fluorescent intensity of the cells was then measured using the BD LRSII flow cytometer. All solutions used were made up in PBS. Cells were spun down at 2000rpm between each step to resuspend in the described solutions.

2.3.2.2 Cell Surface Staining

For cell surface staining of MHC1 in HeLa cells, cells were harvested using the Gibco Cell Dissociation Buffer (Cat: 13151014) and resuspended in fresh media with the primary antibody for 1 hour on ice. Cells were then washed using ice cold media and resuspended in media with the secondary antibody for 1 hour on ice. To remove unbound antibodies, cells were washed three times using ice cold media and their fluorescent intensity measured using the BD FACSCalibur flow cytometer.

2.3.2.3 Assaying GFP Expression in I.29 Cells

I.29 cells were harvested, washed using media and resuspended in ~300µl of fresh media. Resuspended cells were then run on the BD FACSCalibur flow cytometer to measure GFP intensity.

2.3.2.4 Sample Acquisition and Data Analysis

Live cells were manually gated using forward and side scatter and approximately 10,000 cells were collected. Analysis of the data acquired was performed using FlowJo software. For quantification, the geometric mean fluorescent intensity for the described channel and population was measured using FlowJo.

2.3.2.5 Single Cell Sorting

The population of cells to be sorted was collected in growth media, passed through a cell strainer and then sorted using the BD FACSMelody cell sorter into 96 well plates containing 200µl of media. The media used contained 20-30% of condition media which was collected from cells at sub-confluency and filtered through a 0.45µm filter.

2.4 Protein Chemistry

2.4.1 Cell lysis and Sample Preparation

For ECL based immunoblotting, equal number of cells (typically ~$2x10^6$ of I.29s) were collected by centrifugation, washed in PBS, lysed in Laemmli sample buffer (BioRad, Cat #: 1610747) supplemented with 5% β-mercaptoethanol and boiled for 10 minutes at 95°C. Lysates were then stored at -20°C.

For immunoblotting which utilised secondary fluorescent antibodies, equal number of cells (typically ~$2x10^6$ of I.29s) were collected, washed, and lysed on ice using 1ml of RIPA buffer (1% Triton, 0.1% SDS, 150mM NaCl and 50mM Tris Base) for 30 minutes. Lysates were then centrifuged at full speed at 4°C and the supernatant was retained. Protein concentrations were determined using the Pierce Micro BCA kit (Thermo Scientific, Cat #: 23235). Laemmli buffer was added to the sample to a final concentration of 1x (supplemented with 5% β-mercaptoethanol) and then the samples boiled at 95°C for 10 minutes before storing at -20°C.

For streptavidin pull down experiments, cells were lysed on ice for 30 minutes in 1ml of lysis buffer comprising 50 mM Tris-HCL at pH 8.0, 150mM NaCl, 1% Triton-X100, 0.1% SDS and 0.5% sodium deoxycholate. Lysates were then centrifuged at full speed at 4°C and the supernatant retained. Protein concentrations were determined using the Pierce Micro BCA kit (Thermo Scientific, Cat #: 23235).

2.4.2 SDS PAGE

Cell lysates were separated using SDS-PAGE. Depending on the protein of interest 8%, 10% or 12% tris-glycine acrylamide gels were used. In general, for proteins above 100kDa, 8% gels were used and for proteins below 25kDa, 12% gels were used. For streptactin-HRP blots and medium sized proteins, 10% gels were used. To separate the proteins, the lysates were run at 75V for 30 minutes then at 150V for 45 minutes to 1 hour in a gel running buffer (0.3% Tris base, 1.44% glycine and 0.1% SDS in H20).

The recipe to make 2x of each gel is described below:

Solutions	**Gels**			
	8%	**10%**	**12%**	**Stacking**
ddH_20	9.4ml	8.2ml	6.8ml	5.7ml
Tris pH 8.8 (resolving) /6.8(stacking)	5.0ml	5.0ml	5.0ml	2.5ml
30% Acrylamide	5.4ml	6.6ml	8.0ml	1.7ml
10% SDS	200µl	200µl	200µl	100µl
10% APS	100µl	100µl	100µl	50µl
TEMED	10µl	10µl	10µl	10µl

2.4.3 Immunoblotting

Proteins separated by SDS-PAGE were transferred onto Polyvinylidene fluoride (PVDF) membrane (pre-activated by soaking in methanol) at 0.1 amps for 18 hours at 4°C in transfer buffer (0.6% Tris base, 0.3% glycine and 20% methanol). Post transfer, membranes were blocked in blocking solution (5% skimmed milk in PBS-T (PBS with 0.1% Tween-20)) for 1 hour at RT then probed with the primary antibody in fresh block solution overnight at 4°C. Membranes were washed 3 times for 5 minutes in PBS-T then probed with secondary antibodies in block solution for 1 hour at RT. Post 3 x 5 minutes washes with PBS-T, bands were visualised using Clarity ECL (Biorad, Cat #: 1705061) for secondary antibodies conjugated with horseradish peroxidase (HRP) and imaged using Licor C-DiGit scanner. When fluorescent secondary antibodies were used, the signal was visualised using the Licor Odyssey Sa. Quantification was performed using Image Studio Lite software.

2.4.5 Enzyme-Linked Immunosorbent Assay (ELISA) for Measuring Secreted IgM

ELISA plates (Corning, Cat #: 3590) were coated overnight at 4°C with 100µl of anti-mouse IgM antibody (Southern Biotech, Cat #: 1021-01) at 1:1000 dilution in PBS. Coated wells were then washed 4 times using wash buffer (0.05% Tween-20 in PBS) then blocked for 1 hour at RT using 100µl of blocking buffer (5% BSA and 0.1% Tween-20 in PBS). The wells were washed a further 4 times before

being incubated with 50µl of the following material: the samples (diluted 1:20 with blocking solution), IgM standards (Invitrogen: Cat #: 39-50470-65) and negative controls (blocking buffer and media). IgM standards were used from 1 to 1:64 of standard to blocking buffer. The samples were incubated for 2 hours at RT. The wells were washed 4 times, and 100µl of detection antibody (anti-mouse IgM conjugated to HRP at 1:2000) (Southern Biotech, Cat #: 1021-05) was added to the wells and incubated for 1 hour at RT. The wells were washed 4x with wash buffer and 1x with PBS, then 100µl of substrate solution (ThermoFisher Scientific, Cat #: 34028) was added for 20 minutes at RT in the dark. The Reaction was quenched using 50µl of 2M sulphuric acid. The plate was then read at 492nm using the FLUOstar Omega microplate reader.

2.5 Proteomics

2.5.1 Biotin Labelling of Proteins using TurboID

I.29 cells were typically seeded at ~$1x10^6$ cells/ml in and incubated with 0.5mM of biotin (Sigma, Cat #: B4501) for 30 minutes at 37°C. Cells were washed 3x with cold PBS and the cell pellets collected for downstream processing.

2.5.2 Biotin-Phenol Labelling of Proteins using APEX2

I.29 cells were seeded at ~$1x10^6$ cells/ml in 3 wells of a 6-well plate and incubated with 2.5mM of biotin phenol (Sigma, Cat #: SML2135) for 2 hours and 15 minutes at 37°C. The labelling was initiated by adding 1mM of H_2O_2 for 1 minute and the reaction quenched by adding equal volume of 2x quenching solution (10mM Trolox, 20mM sodium azide and 20mM sodium ascorbate). The cells were washed 2 times using 1x quenching solution and 2 times using PBS. They were then collected by centrifugation for lysis and downstream processing.

2.5.3 Streptavidin Magnetic Beads Pull Down

50µl of streptavidin magnetic beads were washed 3 times with 0.5ml of cold lysis buffer. The cell lysate, whose protein content was pre-quantified using Micro BCA and normalised among samples, was added to the beads, and incubated overnight with end over end rotation at 4°C. The unbound protein was removed and retained for immunoblotting. The beads were then washed for 5 minutes with the following solutions with end over end rotation:

1. 2% SDS and 50mM Tris pH7.4 in H20 (2ml per tube).
2. 2% SDS in H20 (2ml per tube).
3. 2M Urea and 50mM ammonium bicarbonate in H20 (2ml per tube).
4. 50mM ammonium bicarbonate in H20 (2ml per tube).

All wash steps using the magnetic beads were performed by inserting the tubes in the magnetic rack holder, waiting till all the beads were collected at the bottom of the tubes then aspirating the solutions.

Following the washes, the beads were finally resuspended in 100µl of 50mM ammonium bicarbonate. For immunoblotting, the proteins were collected by removing the ammonium bicarbonate and boiling the beads with sample buffer for 10 minutes at 95°C. For mass spectrometry the beads were processed as outlined below. If the samples were to be used for both immunoblotting and mass spectrometry, 10ul of beads were aliquoted for immunoblotting and the remainder for mass spectrometry.

2.6 Statistical Analysis

Graphs and statistical analysis were performed using GraphPad Prism. Statistical comparisons used unpaired t-testing.

2.7 Materials

2.7.1 Primer and Guide Sequences

Table 2.2 Primers Sequences

Primer	Sequence
SEC24DF	GTCTTAAGCCATATTCAGGGGA
SEC24DR	GAGATAAGTGCGTGTTTTGCTG
M13R	CAGGAAACAGCTATGAC
M13F	GTAAAACGACGGCCAG
SEC24D_Q5_MutF	gggcatttcccctCCTCACTACGGACACTATG
SEC24D_Q5_MutR	ataccgggttgtgaCTGAGAATAAGGGGGTGTC

Table 2.3 Guide Sequences

Target Gene	gRNA sequence
B2M (Human)	GGCCGAGATGTCTCGCTCCG
VAMP3 1	CACCGCAGCGCGTCACTCACATTT
VAMP3 2	CACCGCGCGTCACTCACATTTTGG
VAMP3 3	CACCGTTTATACCTTTCAGGTCTAC
SEC24D 1	CACCGCATGAGCCAACAAGGCTATG
SEC24D 2	CACCGAGAGATACCCATTCCAGGC
SEC24D 3	CACCGCCCCTCACTACGGACACTAT
SEC24D 4	CACCGCCCCCTCACTACGGACACTA
CREB3L2	CACCGCTGACAGCTCGCTCAGCTTG

The guide against human B2M was already cloned into the pKLV vector and provided by Paul Lehner's group. The remaining guide sequences were designed against mouse sequences. When designing the oligos, CACC was added at the 5' of the forward oligo and AAAC was added at the 5' of the reverse oligo so that they can ligate with the BbsI cut guide vector. If the guide sequence did not naturally start with a G, a G was added to promote high expression from the human U6 promoter.

2.7.2 Enzymes

Enzymes used for any described DNA work are from New England Biolabs (NEB) unless otherwise stated.

2.7.3 Constructs

The lentiCas9-Blast vector was a gift from Feng Zhang (Addgene plasmid #52962). The TurboID and the APEX2 expressing vectors were a gift from Alice Ting (Addgene plasmid #107175, #79055).

2.7.4 Antibodies

Primary Antibodies

The following antibodies were used for immunoblotting and immunofluorescence microscopy.

Target	Host	Source
ATF6	Rabbit	Cell Signalling Technology (CST), 65880S
BIP	Rabbit	CST, 3177
CREB3L2	Rabbit	Novus Biologicals, NBP1-88697
CRELD2	Rabbit	Santa Cruz, SC-86110
ERp72	Rabbit	CST, D70D12
FLAG-tag	Mouse	CST, 8146S
FNDC3A	Rabbit	Atlas Antibodies, HPA008927
FNDC3B	Rabbit	Santa Cruz, SC-99895
HA-tag	Rabbit	Biolegend, 901502
IRE1alpha	Rabbit	CST, 3294
IgM	Goat	Southern Biotech, 1021-05
MHC1	Mouse	BD Bioscience, 560169
MIST1	Rabbit	CST, 14896
NBAS	Rabbit	Atlas Antibodies, HPA036817
P62	Rabbit	CST, 5114
P-P62	Rabbit	CST, 13121
RRBP1	Rabbit	Atlas Antibodies, HPA009026
SEC23A	Rabbit	Kind gift from David Stephens
SEC24D	Rabbit	CST, 14687
SEC31A	Rabbit	CST, 13466
TMEM214	Rabbit	Origene, TA360932
TUBULIN	Mouse	Proteintech, 66240
Ubiquitin	Rabbit	CST, 3933
V5-tag	Rabbit	CST, 13202S
XBP1s	Rabbit	CST, 12782

Secondary Antibodies

Immunoblotting: Horseradish Peroxidase (HRP)-conjugated antibodies against mouse (115-035-008) and rabbit (111-035-008) antibody were obtained from Jackson ImmunoResearch. Streptactin-HRP (161-0380) was obtained from BioRad. Fluorescent secondary antibodies used are anti-rabbit AF 680 (Invitrogen, Cat #: A21109) and anti-mouse IRDye 800CW (Licor, Cat #: 926-32212)

Immunofluorescence Microscopy and Flow Cytometry: Alexa Fluor 488 and Alexa Fluor 594 conjugated antibodies against rabbit (Invitrogen, Cat #: A32731, A32740). Alexa Fluor 488 and Alexa Fluor 594 conjugated antibodies against mouse (Invitrogen, Cat #: A32723, A32742). StrepTactin XT Conjugate DY-488 (IBA, Cat #: 2-1562-050)

Chapter 3: Characterisation of the I.29 Cell Model

3.1 Introduction

3.1.1 Background

Previous work in the lab to attempt knockdown and overexpression of protein in primary cells proved to be problematic with inconsistent results. From detailed literature searches it became apparent that primary B-cells are difficult to transduce and not very well-suited for generating stable cell lines. The biggest potential caveat of using primary B cells for relevant tools such as CRISPR/Cas9 is the need to activate the B-cells to achieve high transduction efficiencies with the most common application being screening, not generation of stable lines (Chu et al., 2016)(Pinter et al., 2022)(Xiong et al., 2023).

In addition to primary generated cells, B-cell lymphoma lines can be used as a differentiation model. A previous student from the group looked at B cell differentiation by LPS in the B cell lymphoma lines BCL1, WEHI 231 and I.29. His work showed that the I.29 cell model had the most efficient differentiation in which they increased in size and began expressing the ASC differentiation marker, CD138 (Simon Gilbert, Unpublished Data).

3.1.2 I.29 Cell Model

I.29μ+ is a monoclonal B cell lymphoma line that expresses IgM on the cell surface and differentiate in response to LPS to become IgM secreting cells (Alberini et al., 1987). The cell line was initially derived from the I.29 B cell mouse lymphoma which consisted of cells that express either membrane bound IgM or IgA, with a smaller proportion of cells expressing both at the surface (J Stavnezer et al., 1982). The IgM subline (I.29μ+) was purified from the I.29 lymphoma line by fluorescent-activating cell sorting and adapted for in vitro growth (Janet Stavnezer et al., 1985). This cell line has been used since in many studies as a B-cell model that can differentiate into plasmablasts (Qiu & Stavnezer, 1998) (M. J. Shi & Stavnezer, 1998)(J Stavnezer et al., 1999) (Romijn et al., 2005) and (Ma et al., 2010). For example, to study the potential immune dampening effect of the Kaposi's sarcoma-associated herpesvirus' K4.2 protein. K4.2 was shown to cause reduction in IgM secretion in differentiated I.29 cells potentially due to its inhibitory interaction with pERP1, a chaperone that enables efficient IgM folding, a discovery also made using the I.29s (Van Anken et al., 2009) (Wong et al., 2013). Notably, this cell line was also used in one of the first studies which suggested that activation of the Unfolded Protein Response (UPR) in ASCs preceded biosynthetic load (Van Anken et al., 2003)(**section 1.4.2.3**). Taken together, we decided to utilise the I.29 cell line for this project as they have been previously used to model ASCs' differentiation according to the literature and are amenable to viral transductions.

3.1.3 Chapter Aims:

We have previously carried out a proteogenomic project on ASCs and identified novel differentially expressed genes (Rahman, 2019)(**section 1.7-1.8**). We hypothesised that genes that are consistently highly upregulated in ASCs are likely to be key factors required for ASCs physiology and/or antibody secretion. To directly test this hypothesis, we intend to specifically perturb proteins of interest in the I.29 cell model to investigate their potential functions.

In this chapter, we aim to assess and characterise the I.29 cells as a model of B cell differentiation. We next aim to build the experimental platform needed to investigate the function of upregulated proteins in ASCs' biology. In particular we will: **a)** determine whether the I.29 cells appropriately upregulate and secrete IgM, and upregulate cellular markers known to be expressed in other models of B-cell differentiation by utilising our web-resource PlasmacytOMICs; **b)** optimise techniques to genetically manipulate these cells to develop approaches to deplete (shRNA) or disrupt (CRISPR/Cas9) protein functions, and introduce reporter systems which can be used for proximity based proteomic approaches (APEX and BiRA).

3.2 Results

3.2.1 Validation of the I.29 Cell Model

Before setting out to study protein functions in the context of ASCs, we first aimed to validate the chosen cell line as a suitable model for ASC biology by inducing the differentiation of the cells and assessing whether they appropriately upregulate previously identified plasma cell machinery and secrete antibodies.

3.2.1.1 LPS Can be Used to Induce Secretion of IgM

Innate immune receptors are germline encoded and allow recognition of several molecules that are common among multiple infectious agents, commonly known as pathogen associated molecular patterns (PAMPs). One of the best characterised PAMPs is lipopolysaccharides (LPS), a structurally integral component of the outer membrane of gram-negative bacteria (Farhana & Khan, 2022). The main receptor of LPS in immune cells is Toll Like Receptor 4 (TL4), as initially shown by a mouse strain with a missense mutation in TL4 that exhibited resistance to endotoxin shock by LPS injection (Poltorak et al., 1998) (Hoshino et al., 1999). B cells have TL4 receptors and the use of LPS to induce differentiation of B-cells to ASCs in vitro is a well-established system that is commonly used (Gass et al., 2002(Shaffer et al., 2004).

To induce the I.29 cells to differentiate, the cells were seeded in a 6-well plate at a density of ~0.3x10^6 cells/ml and incubated with 20µg/ml of LPS. To collect differentiated cells up to 4 days post induction, cells were subcultured back to the seeding density two days post induction to reduce cell death (**Figure 3.1A**). Typically, standard differentiation induced by LPS of mouse B-cells result in significant cell death at day 3 post induction due to proteostatic stress. Subculturing the cells at day 2, enabled us to have ~60% viable cells by day 4 post induction. To assay the levels of secreted IgM, 2x10^6 differentiated cells were collected, washed, and resuspended in fresh media. The cells were then incubated for a further 5 hours and the media and cells were collected for downstream immunoblotting processing. Following LPS induction, we observe that the cells increase in size (**Figure 3.1B**) and upregulate the expression and secretion of IgM (**Figure 3.1C**).

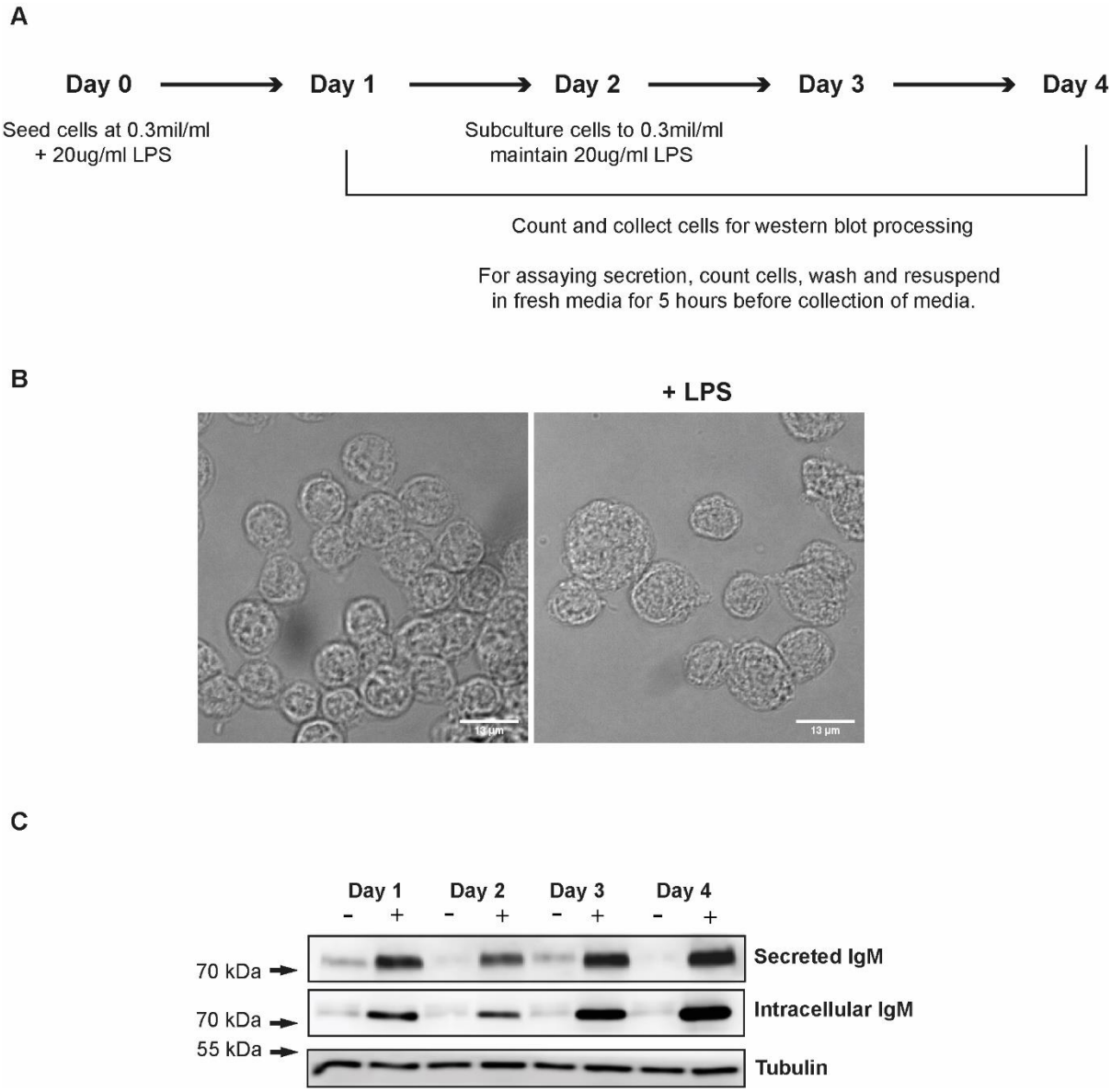

Figure 3.1: I.29 cells can be induced to synthesise and secrete IgM using LPS A) Diagram outlining the steps followed for differentiating I.29 cells. I.29 cells were seeded ($0.3x10^6$ cells/ml) in a 6 well plate and induced to differentiate using 20µg/ml of LPS (+). Two days post induction, the cells were sub-cultured while maintaining the concentration of LPS. **B)** Brightfield images showing I.29 cells two days post LPS induction (Nikon WideField System). Cells were induced to differentiate, collected on day 2 post induction, centrifuged on fibronectin coated coverslips and fixed with methanol. **C)** Immunoblots of intracellular and secreted IgM in un/differentiated I.29 cells. $2x10^6$ cells were washed and transferred into fresh media. Post 5 hours, cells were collected by centrifugation for lysis and media collected was filtered using a 0.45µm syringe filter.

3.2.1.2 Expression of Transcription Factors in Response to Differentiation

ASCs have a distinct transcriptional profile compared to their precursor B-cells (W. Shi et al., 2015) and the acquisition of ASCs' specific transcription factors (TFs) terminates the B-cell specific transcriptional program. Importantly, differentiation of B-cells to either plasmablasts or plasma cells are driven by the same set of transcription factors (Nutt et al., 2015). Therefore, assessing the upregulation of some of these ASCs identity factors in differentiated I.29s can indicate their validity as an ASC model as these TFs modulate key pathways in ASC development.

Following LPS induction in the I.29 cells, we assessed the levels of transcription factors known to be upregulated during differentiation by immunoblotting. These are XBP1, a key TF required for ER expansion and secretion of antibodies in ASCs (**see 1.4.2.4**) and has been previously shown to be upregulated in differentiated I.29s (Ma et al., 2010). We also look at another mediator of the UPR, ATF6, and the ER stress transducer CREB3L2 (**see 1.8.5**). Finally, we look at MIST1, a specific marker of plasma cells that is induced during differentiation, which has recently been implicated in playing a regulatory role in ASCs through in vivo studies (Wöhner et al., 2022). **Figure 3.2A** shows the PlasmacytOMICs differential regulation of the described transcription factors. Following LPS induction in I.29 cells, these TFs show upregulation suggesting that the transcriptional program of the I.29s adopt the expected profile of ASCs (**Figure 3.2B**).

3.2.1.3 Expression of Endoplasmic Reticulum Proteins in Response to Differentiation

To determine if I.29 cells expand their ER and upregulate ER localised proteins when they differentiate, we used immunofluorescence microscopy and immunoblotting to analyse the expression of a selection of ER proteins. As predicted, proteins involved in protein folding such as BIP and ERP72 (protein disulphide isomerase) are dramatically upregulated (**Figure 3.3-3.4)**. BiP has previously been shown to be upregulated in differentiated I.29s (Van Anken et al., 2003)(Romijn et al., 2005)(Ma et al., 2010). Immunofluorescence staining of ERP72 also suggests that most of the cytoplasmic portion of the cell is occupied by the ER compartment which is expected of a professional secretory cell type (**Figure 3.3**). In addition, NBAS, RBP1, TMEM214 and CRELD2 were confirmed to be upregulated in

differentiated I.29s as we have predicted (Rahman, 2019) (**Figure 3.4B**). Other ER localised proteins upregulated in I.29s are FNDC3B and FNDC3A, which have recently been implicated in ER proteostasis (Fucci et al., 2020). Finally, we confirmed the upregulation of IRE1alpha, a well characterised sensor of unfolded proteins which activates XBP1 (Chen & Brandizzi, 2013), and P115, a Golgi tethering factor whose upregulation may indicate enhanced vesicle transport to the Golgi. The PlasmacytOMICs profiles of these proteins are shown in **Figure 3.4A** and their upregulation during LPS induction in the I.29 model is shown in **Figure 3.4B**.

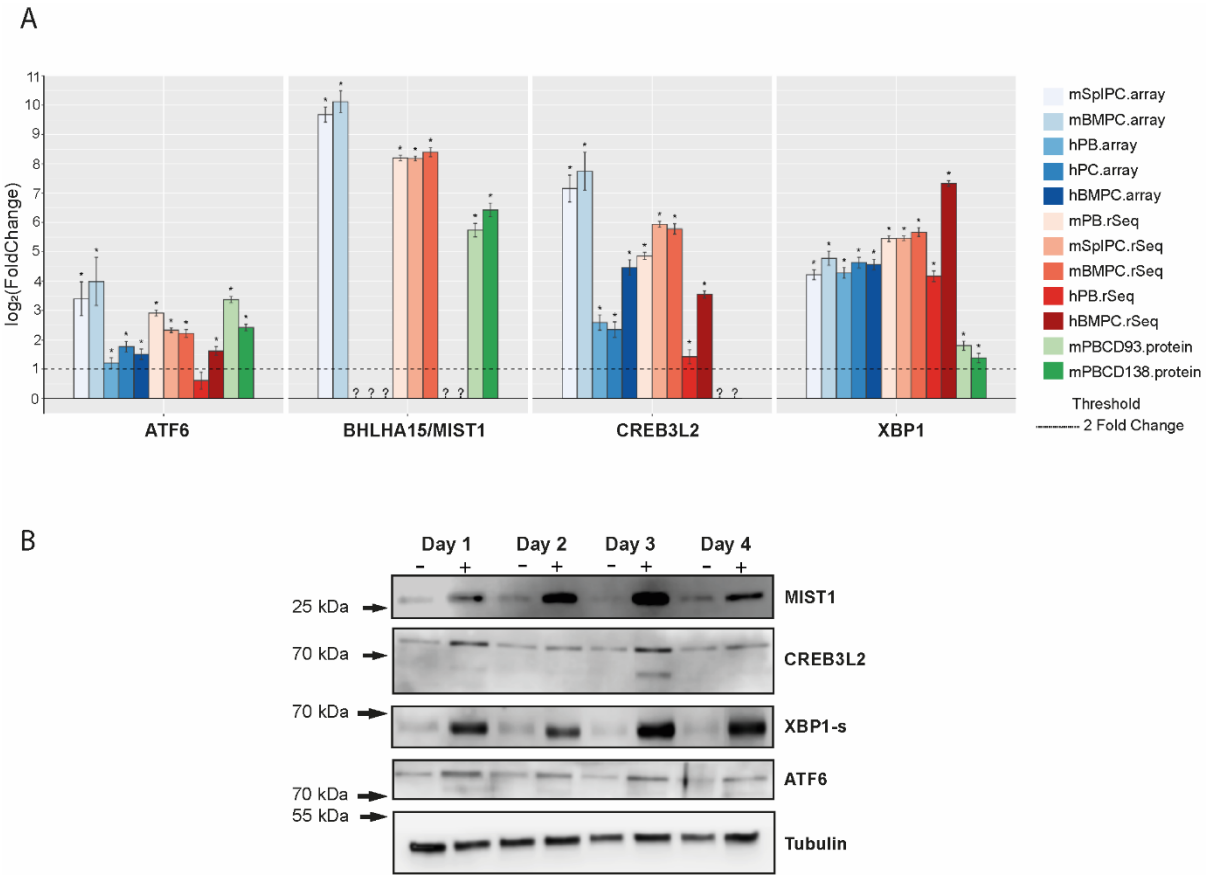

Figure 3.2: The transcriptional profile of differentiated I.29s is similar to in vitro generated plasmablasts. To investigate whether I.29 cells behave in an expected manner as differentiating ASCs, we assessed the protein levels of transcription factor markers in un/differentiated cells. **A)** Fold change in mRNA and protein expression were plotted using the PlasmacytOMICs web resource which shows differential regulation of indicated markers between naïve B cells and ASCs. ATF6 and XBP1 are known mediators of the UPR which plays important roles in the development of ASCs. The fold changes in XBP1 in the mouse protein levels (green bars) are underestimated as the protein was not detected in the naïve B-cells samples and values were imputed. CREB3L2 is another regulator of the secretory apparatus that is consistently upregulated in ASCs. MIST1 is highly upregulated in ASCs which may play a regulatory role. The human gene chip used did not have a probe for this gene and the RNA-sequencing depth for human data was lower than mouse hence the missing human microarray and RNA Seq data. **Error bars indicate standard error of mean. B)** Immunoblots probed for the indicated transcription factors using lysates of un/differentiated I.29 cells. I.29 B-cells were induced to differentiate using 20µg/ml of LPS (+) and collected for immunoblotting processing on the indicated days.

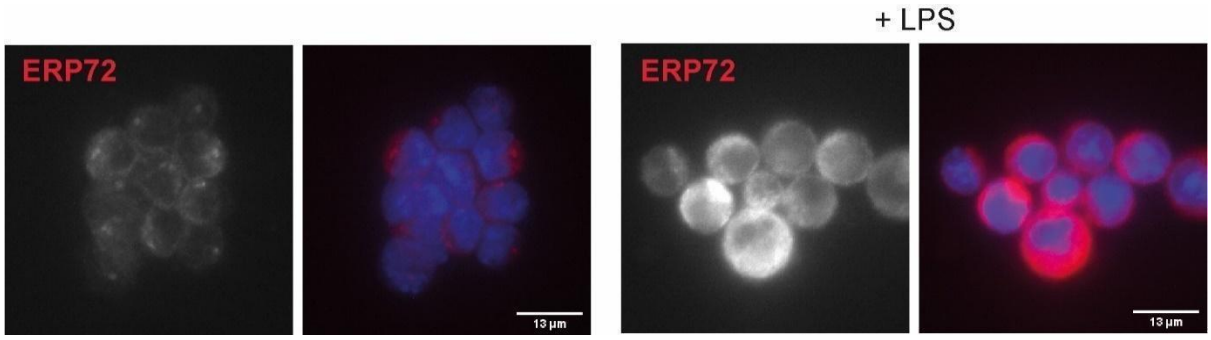

Figure 3.3: Upregulation of ER localised ERP72 in differentiated I.29 cells. I.29 cells were induced to differentiate using 20µg/ml of LPS. 2 days post induction, cells were collected, centrifuged on fibronectin coated coverslips, fixed by methanol, and processed for immunofluorescence staining of ERP72. Results show that undifferentiated B-cells have minimal staining of the ER localised protein which becomes dramatically upregulated in the differentiated cells.

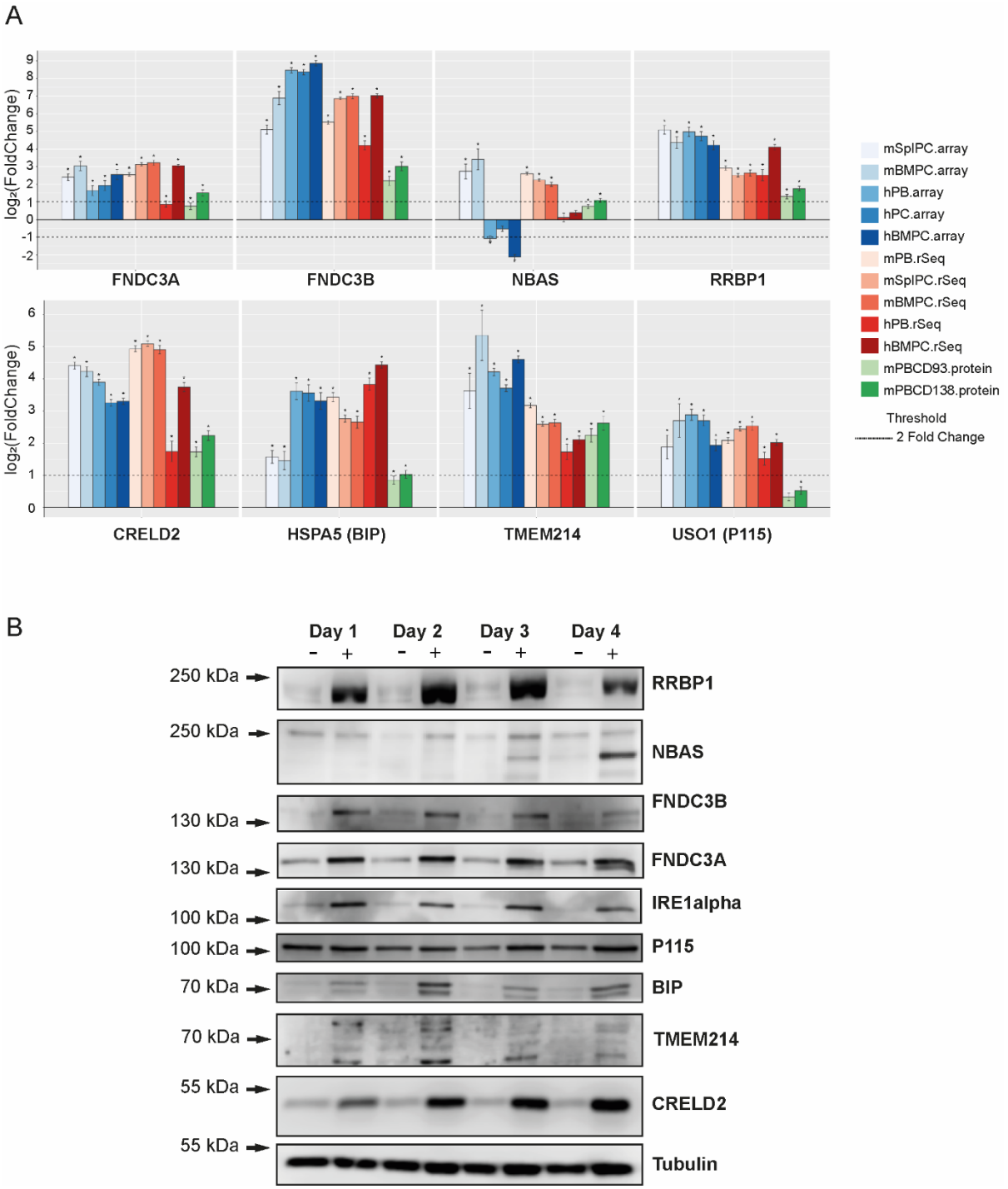

Figure 3.4: I.29 cells upregulate a range of ER localised proteins during differentiation. To investigate whether I.29 cells behave in an expected manner as differentiating ASCs, we assessed the protein levels of ER localised markers in un/differentiated cells. **A)** Fold changes in mRNA and protein expression were plotted using the PlasmacytOMICs web resource which shows differential regulation of indicated markers between naïve B cells and ASCs. Proteins shown are ER localised (except P115 which resides in the Golgi). Plots show that FNDC3A, FNDC3B, NBAS, RRBP1, CRELD2, BIP, TMEM214 and P115 are upregulated in ASCs. **Error bars indicate standard error of mean. B)** Immunoblots probed for the indicated ER markers using lysates of un/differentiated I.29 cells. I.29 B-cells were induced to differentiate using 20µg/ml LPS (+) and collected for immunoblotting processing on the indicated days.

3.2.1.4 Expression of SNAREs and COPII Components in Response to Differentiation

We have previously observed an upregulation in COPII components in ASCs (Rahman, 2019)(**3.5A**). To determine whether I.29s upregulate these components in response to differentiation, we assessed the levels of SEC24D, SEC31A, SEC23A and SEC13 (**Figure 3.5C**). Differentiated I.29 cells show upregulation in all the mentioned components compared to undifferentiated samples, except for SEC13 whose levels seem to be comparable in both samples at days 3 and 4.

SNAREs are key players in the fusion of transport vesicles with target compartments and, in accordance with upregulation of both COPII and trafficking components in ASCs, are expected to be upregulated. To determine if SNARE proteins are upregulated in ASCs, we assessed the levels of YKT6, SEC22B, STX5 and VAMP3. We observe a consistent upregulation in YKT6 and SEC22B according to the proteogenomic data (**Figure 3.5B**). They act as v-SNARES involved in anterograde transport of COPII vesicles (Daste et al., 2015). Both v-SNAREs are also involved in retrograde transport at the Golgi. The NRZ complex, whose components are upregulated in ASCs (Rahman, 2019), captures COPI vesicles at the ER via association with the ER SNARE SEC22B (Tagaya et al., 2014), while YKT6 mediates intra-Golgi retrograde transport (Daste et al., 2015). The upregulation of these SNAREs was confirmed in differentiated I.29s (**Figure 3.5D**). Finally, we also look at STX5, a t-SNARE which captures COPII vesicles at the Golgi and participates in intra-Golgi transport (Wang et al., 2017), which are both processes predicted to be enhanced in ASCs (Rahman, 2019), and VAMP3 which has been implicated in constitutive secretion (Gordon et al., 2010). These two SNAREs show less consistent upregulation according to the proteogenomic data (**Figure 3.5B**), however do seem to show an upregulation in the differentiated I.29 cells validating their upregulation in ASCs (**Figure 3.5D**).

The data presented so far shows that the I.29 cells become bigger and upregulate and secrete IgM in response to LPS induction. They also appropriately upregulated markers of primary ASCs and components of membrane trafficking (chaperones, COPII and SNAREs), suggesting that they are correctly reflecting the differentiation process of primary cells in these aspects.

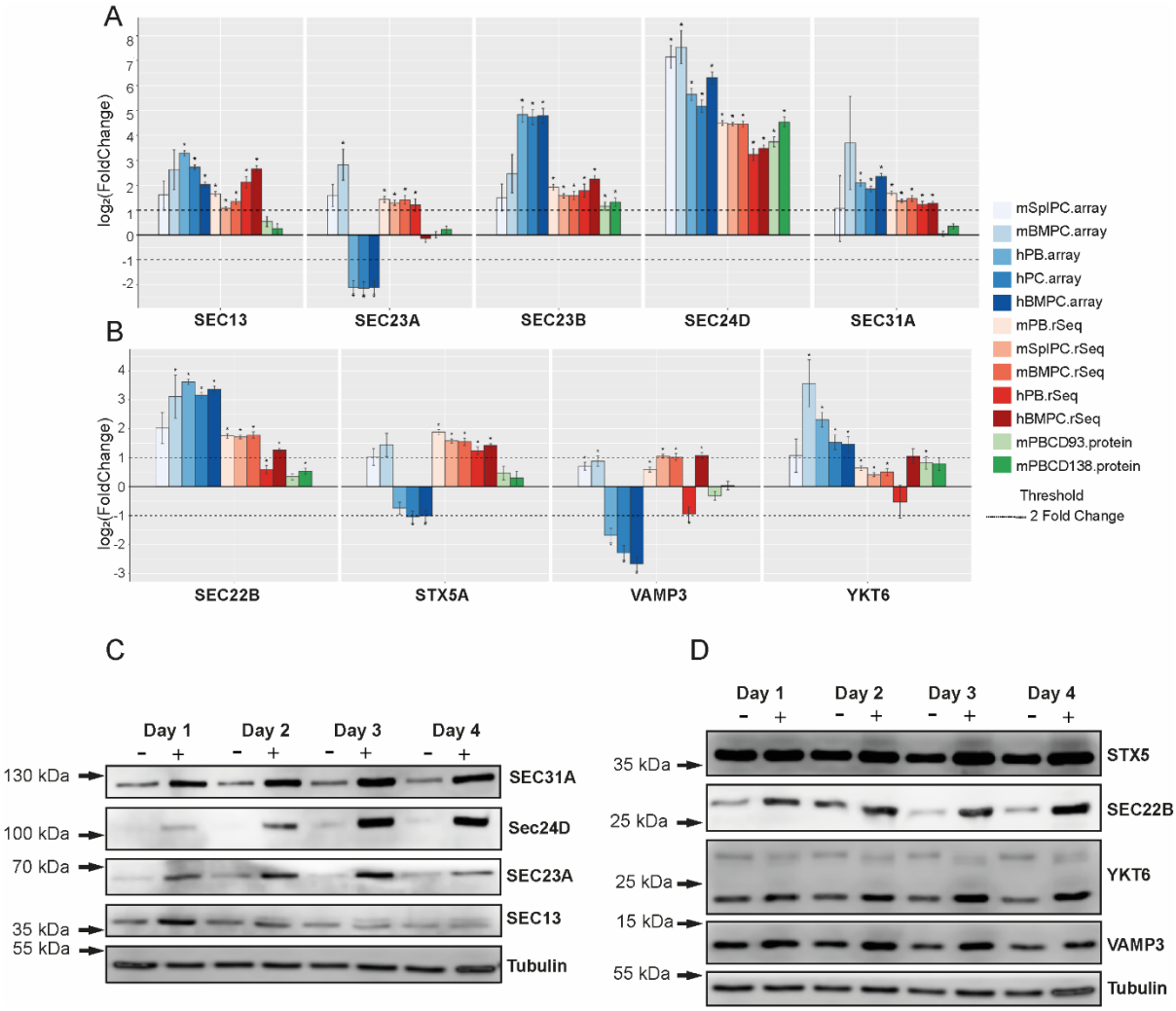

Figure 3.5: Upregulation of COPII proteins and SNAREs in differentiated I.29 cells. To investigate whether I.29 cells behave in an expected manner as differentiating ASCs, we assessed the protein levels of COPII components and SNAREs in un/differentiated cells. **A)** Fold changes in mRNA and protein expression were plotted using the PlasmacytOMICs web resource which shows differential regulation of indicated markers between naïve B cells and ASCs. Plots show that COPII inner coat components SEC24D and SEC23B are consistently upregulated in ASCs compared to their precursor naïve B-cells. Components of the outer coat, SEC31A and SEC13 also show upregulation albeit to a lesser extent compared to inner coat components. **Error bars indicate standard error of mean. B)** The R-SNAREs YKT6 and SEC22B show consistent upregulation in ASC types tested. STX5 also shows considerable upregulation importantly at the tested protein levels (green bars). VAMP3 generally shows inconsistent data. **C)** Immunoblots probed for the indicated COPII proteins and SNAREs **(D)** using lysates of un/differentiated I.29 cells. I.29 B-cells were induced to differentiate using 20µg/ml of LPS (+) and collected for processing on the indicated days.

3.2.2 Developing Tools to Genetically Manipulate I.29 Cells

We have assessed and confirmed that differentiated I.29 cells show predicted behaviours of primary ASCs which suggests that they are a good model of B-cell differentiation and antibody secretion. We moved on next to building the experimental platform needed to assess the roles of consistently upregulated protein in ASCs' biology.

3.2.2.2 Creating an I.29 Cell Line Stably Expressing Cas9

To study the function of genes in the I.29 cell model we decided to take a CRISPR/Cas9 based approach. I.29 cells have previously been shown to be amenable to viral transduction (Van Anken et al., 2009)(Simon Gilbert, Unpublished Data), therefore they were transduced with a lentiviral construct encoding the Ca9 nuclease (**Figure 3.6A**). Two days post transduction, the cells were selected with blasticidin at 12µg/ml. By day 6, the non-transduced cells were dead, and the viability of the transduced cells was recovering indicating a successful transduction (**Figure 3.6B**). However, the Cas9 protein was not detected by either immunoblotting or immunofluorescence microscopy even after weeks of selection (data not shown). The ability of the cells to survive Blasticidin selection suggested that they were expressing the Blasticidin S Deaminase (BSD). Given that the BSD and Cas9 endonuclease genes were driven by two separate promoters, we suspected that the cells were silencing the promoter upstream of the Cas9 gene. A similar phenomenon was reported in embryonic stem cells (Xia et al., 2007). We hypothesised then that the SFFV (Spleen Focus-Forming Virus) promoter was being silenced in the cells, possibly via methylation (Herbst et al., 2012), and that PGK promoter was resisting this silencing resulting in BSD gene expression. To investigate this, I.29 cells were transduced with a lentiviral plasmid that expresses GFP and puromycin resistance from a PGK promoter (**Figure 3.6C**) and their fluorescence measured using flow cytometry 5 days post selection (**Figure 3.6D**). As predicted GFP fluorescence could be observed in these cells suggesting that we needed to obtain another viral vector that expresses both the antibiotic resistance and the Cas9 from the same promoter (**Figure 3.7A**). I.29 cells were transduced with the new vector and after one week of selection, the Cas9 protein expression was detected and the stable cell line expressing the endonuclease was generated (**Figure 3.7B**). This cell line was then tested for its ability to be induced by LPS for differentiation compared to the parental line (**Figure 3.7C**). No difference in upregulation and secretion of IgM could be detected between transduced and non-transduced cell lines, suggesting that Cas9 expression has no effect on the differentiation of I.29 cells.

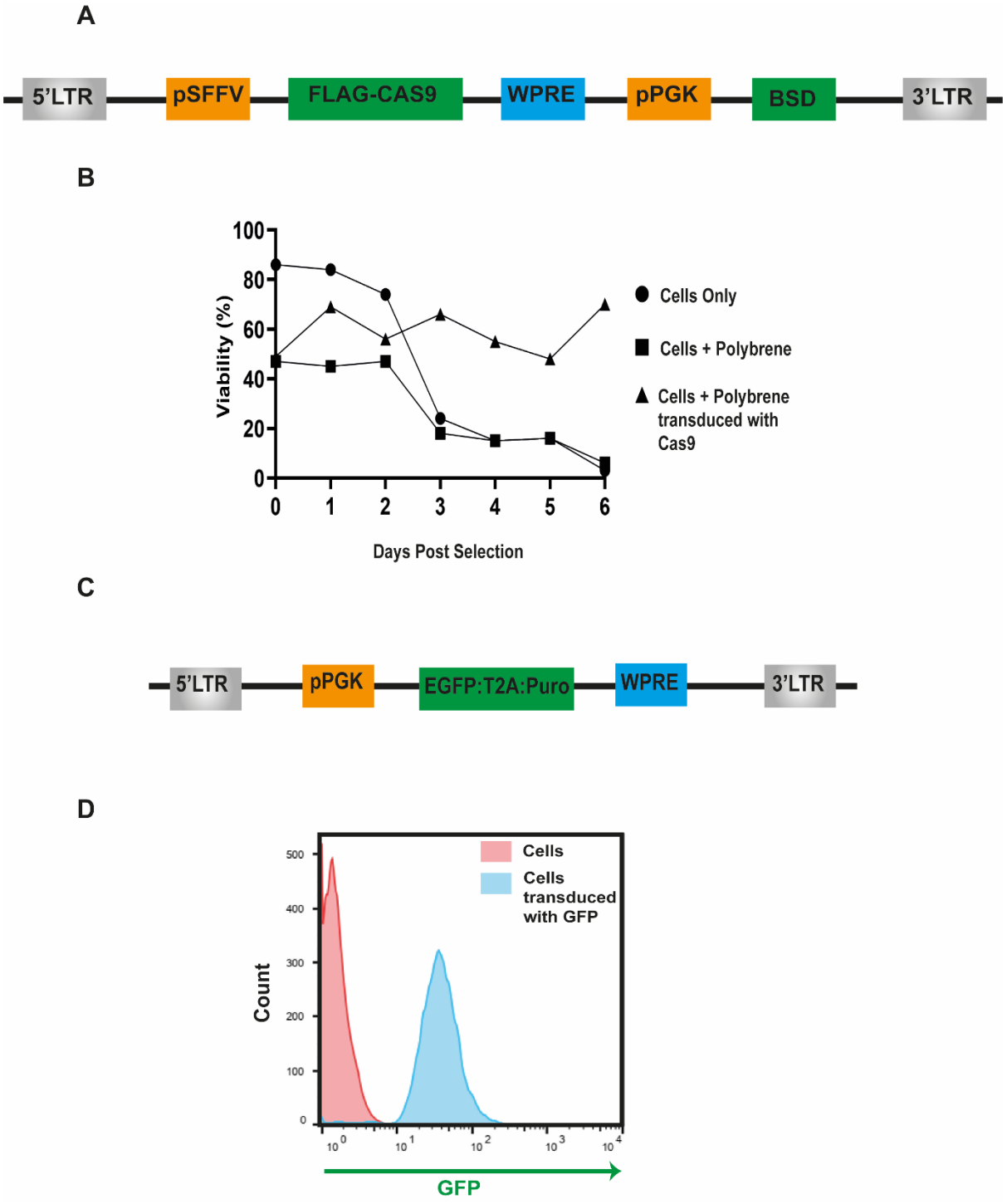

Figure 3.6: Transduction of the I.29 cells. **A)** Schematic of the initial lentiviral construct used for expressing Cas9. Expression of the Cas9 (SFFV) and the BSD (PGK) are driven by different promoters (LTR: Long-Terminal Repeat, WRPE: Woodchuck hepatitis virus posttranscriptional regulatory element). **B)** I.29 cells were transduced with the Cas9 construct. Two days post transduction, cells were selected using 12µg/ml of Blasticidin for at least 10 days. Transduced cells survived and recovered post Blasticidin selection, however, did not show expression of the Cas9 possibly due to silencing of the SFFV promoter. **C)** Schematic of the lentiviral construct expressing eGFP and puromycin resistance from the same PGK promoter. **D)** I.29 cells were transduced with the eGFP construct. Two days post transduction, cells were selected using 1µg/ml of Puromycin. After 5 days of selection, cells were analysed on the BDFACsCalibur flow cytometer to assay for eGFP expression using the FL1 channel. Shift in signal intensities shows GFP protein expression.

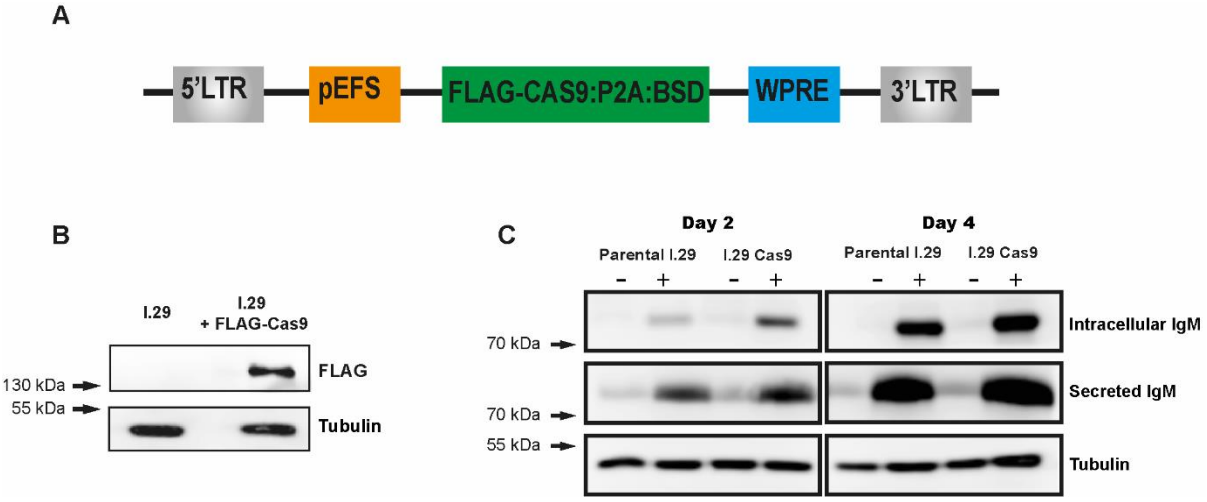

Figure 3.7: Creating a Cas9 stable expressing I.29 cell line. A) Schematic of the lentiviral construct expressing FLAG-Cas9 and Blasticidin resistance from the same EFS promoter. **B)** I.29 cells were transduced with the new Cas9 construct. Two days post transduction, cells were selected using 12µg/ml of Blasticidin for at least 10 days. Post selection, cell lysates were processed for immunoblotting with an anti-FLAG antibody. Immunoblot results indicated FLAG-Cas9 expression in the transduced cell line. **C)** The Cas9 expressing cell line differentiates in response to LPS**.** Cells were taken out of selection for 2 days before induction for differentiation using 20µg/ml of LPS (+). On the specified days, $2x10^6$ cells were pelleted for processing for immunoblotting of intracellular IgM. To measure IgM secretion, cells were washed and transferred into fresh media and incubated for 5 hours. The media was then collected by pelleting the cells, keeping the media, and filtering it using a 0.45µm syringe filter.

3.2.2.3 Functional validation of Cas9

In parallel to generating the Cas9 I.29 cells we also generated a Cas9 expressing HeLa cell line as it would allow this approach to be validated relatively easily. HeLa cells were transduced with a well characterised guide which targets β2M, a component of MHC-1 (**Figure 3.8A**). This guide was previously used by Paul Lehner's group and reported to result in ~90% reduction of MHC-1. As predicted, a similar reduction of MHC-1 levels was achieved indicating that the Cas9 was active (**Figure 3.8B-C**). To test its functionality in the I.29 system, we needed to choose another target to knock out as we lacked a good antibody against mouse MHC-1. Our lab is largely focused on studying membrane trafficking, so we have a good collection of SNARE antibodies and decided to proceed with VAMP3 as a target. VAMP3 is expressed at high levels in B-cells (**Figure 3.5D**), therefore assaying for its reduction would not require the induction/differentiation of the cells. CHOPCHOP was used to choose 3 guides against mouse VAMP3, and they were cloned into the lentiviral guide vector. Out of the three tested guides, only one guide resulted in a significant reduction in VAMP3 (**Figure 3.9A-B**). Our results indicated that the Cas9 is active and highlighted the importance of testing multiple guides for activity when targeting a protein.

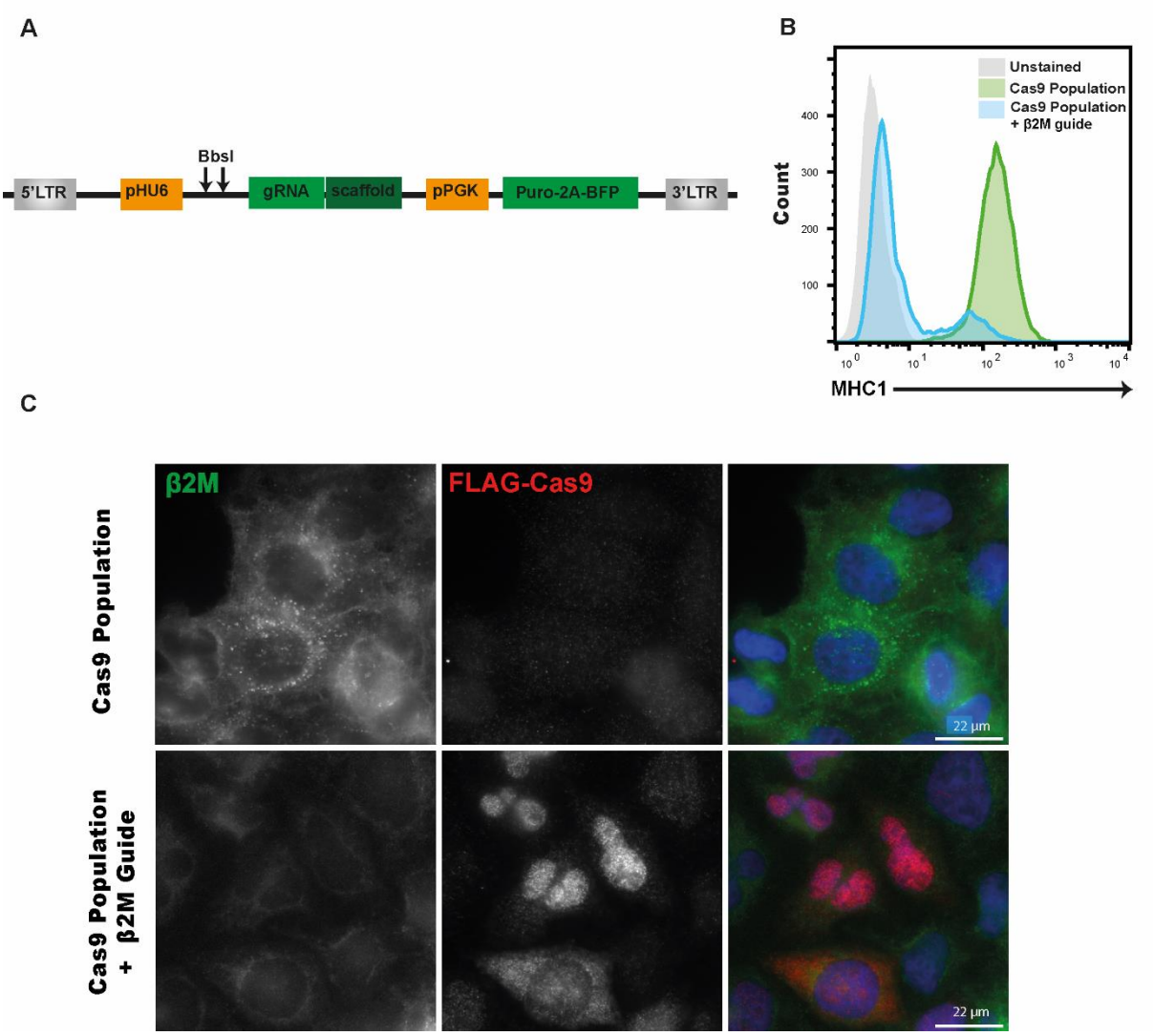

Figure 3.8: Validating the Cas9 endonuclease functionally in HeLa cells. A) Schematic of the lentiviral construct encoding the gRNA**.** The construct encodes a gRNA scaffold downstream the BbsI cloning site and also encodes puromycin resistance linked to blue fluorescent protein (BFP). Guides against the proteins of interest are designed to have compatible sticky ends with BbsI to allow for its cloning into the cut vector. HeLa cells expressing Cas9 were transduced with the construct encoding a gRNA against β2M. Two days post transduction, cells were selected with 1µg/ml of Puromycin for at least 7 days. Post selection, flow cytometry was performed by staining MHC-1. The Cas9 population transduced with the guide against β2m showed ~90% reduction in the surface levels of the protein **(B)**. **C)** Immunofluorescence (IF) imaging was also performed to stain for MHCI in the parent cells and the population transduced with the β2m guide showing a marked reduction in MHC1 staining.

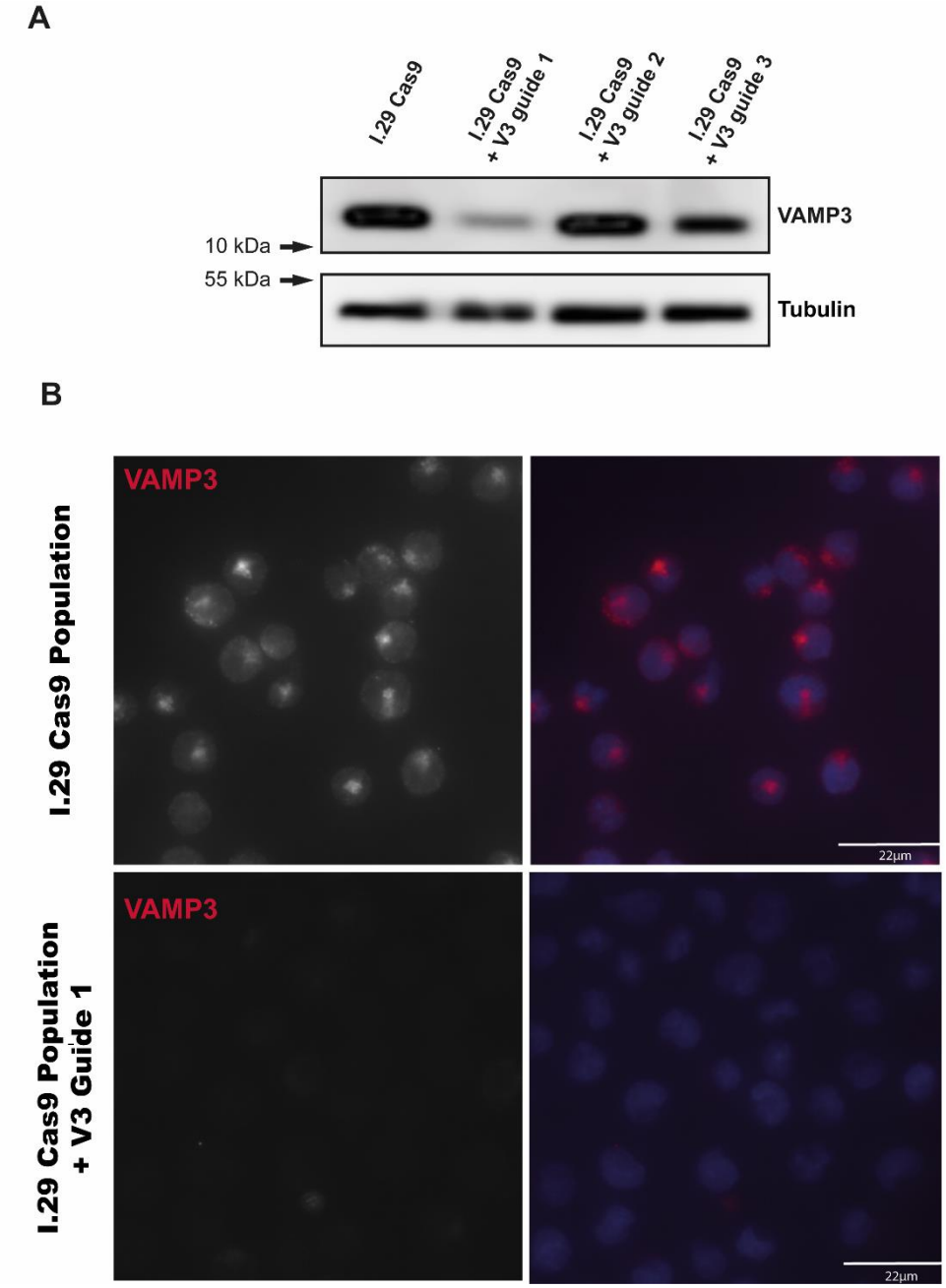

Figure 3.9: Validating the Cas9 endonuclease functionally in I.29 cells. A) I.29 cells expressing Cas9 were transduced with three different guides against VAMP3 chosen using CHOPCHOP. 2 days post transduction, cells were selected using 1µg/ml of puromycin for at least 7 days. 9 days post selection, cells were collected for immunoblotting and probed with anti-VAMP3 antibody. The population transduced with guide 1 showed the greatest reduction in VAMP3 levels. **B)** Cells transduced with guide 1 were centrifuged on fibronectin coated coverslips for immunofluorescence staining with anti-VAMP3 antibody.

3.2.2.4 Investigating the Feasibility of Tet-Inducible shRNA System as a Backup Platform

As a backup platform to CRISPR/Cas9 gene disruption, we decided to investigate the feasibility of using a tet-inducible shRNA lentiviral system to deplete the proteins of interest (**Figure 3.10A**). This system would make it possible to study the function of essential genes and without the issues of compensation. The described work was carried out in both the I.29 cells and Mouse Embryonic Fibroblasts (MEFs) with the latter used as an easier model. Both cell lines were successfully transduced with 3 plasmids expressing shRNAs against Syntaxin 5 (STX5). As expected, cells incubated with doxycycline expressed GFP (**Figure 3.10B**) suggesting that the shRNA was also being expressed. In the I.29s, the transduced cells' viability was significantly impacted even in the absence of doxycycline (**Figure 3.10C**) making the results inconclusive. In the MEFs, the cells were tested for STX5 reduction using immunofluorescence microscopy (**Figure 3.11**). Only one population of cells showed reduced levels of STX5 after doxycycline incubation suggesting that this approach could potentially work. At that stage during the project, the CRISPR/Cas9 platform established in the I.29s already showed good efficacy. Therefore, we decided not to go ahead with further optimisations of the tet-inducible shRNA system and to proceed with the project utilising CRISPR. If we were to continue with this system, another set of plasmids with different shRNA targets would have needed to be tested in the I.29s. Doxycycline concentrations and incubation times would have also been needed to be optimised to potentially achieve stronger protein depletions.

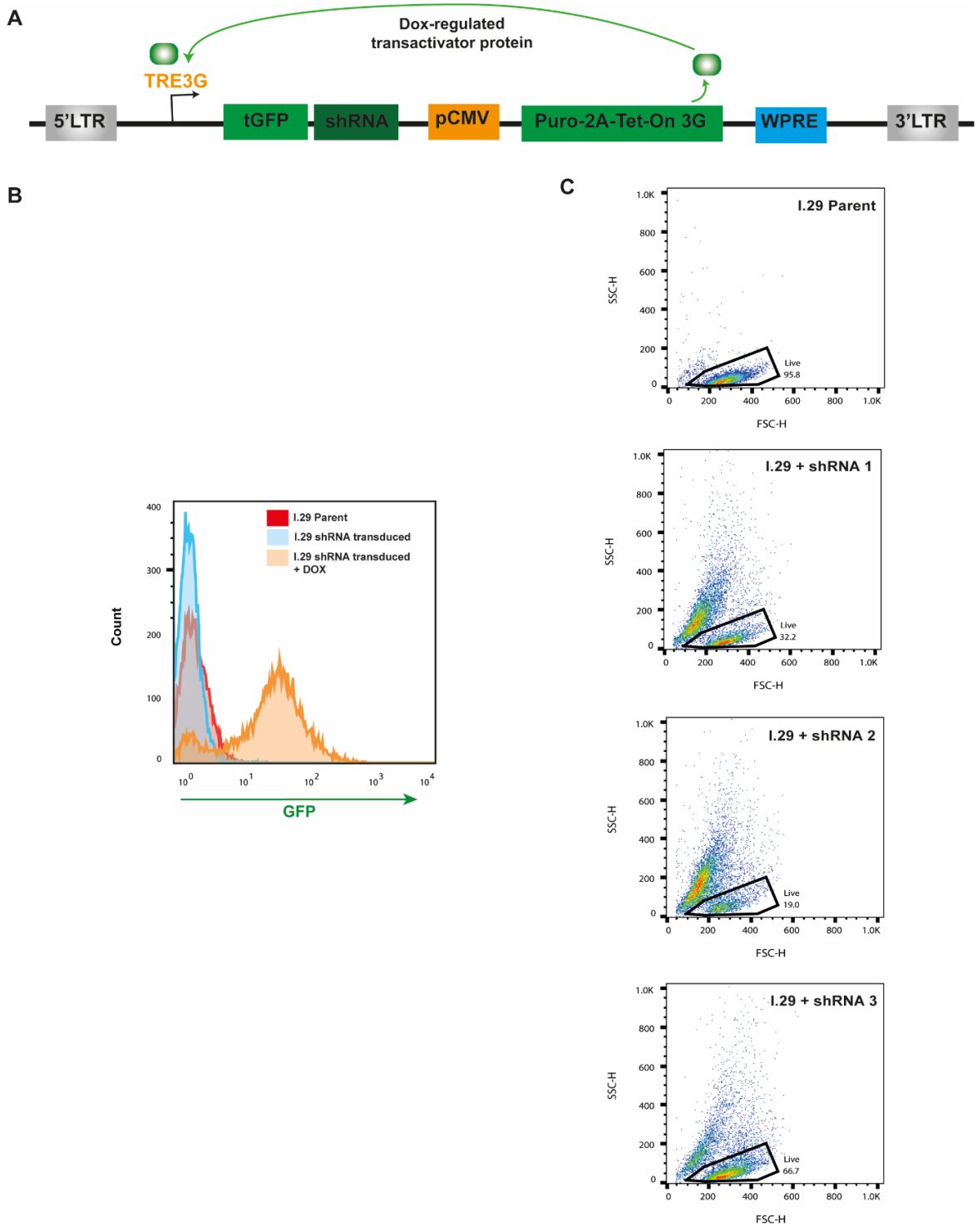

Figure 3.10: Investigating utilisation of tet-inducible shRNA for protein studies in the I.29 cells. A) Schematic of the tet-inducible shRNA plasmid. Expression of the Tet-On 3G transactivator protein and puromycin resistance are under the control of the constitutive CMV promoter. In the presence of doxycycline, the Tet 3G promoter (TRE3G) is bound by the transactivator protein that is constitutively expressed, promoting the expression of the turboGFP (tGFP) and the shRNA in a controlled manner. **(B)** I.29 cells transduced with empty shRNA plasmid were incubated with doxycycline at 1µg/ml and were analysed for GFP expression by flow cytometry 2 days post incubation **(C)** I.29 cells transduced with tet-inducible shRNA plasmids against Syntaxin 5 were successfully selected however shortly after had significant viability reductions measured by looking at the cells' forward and side scatter.

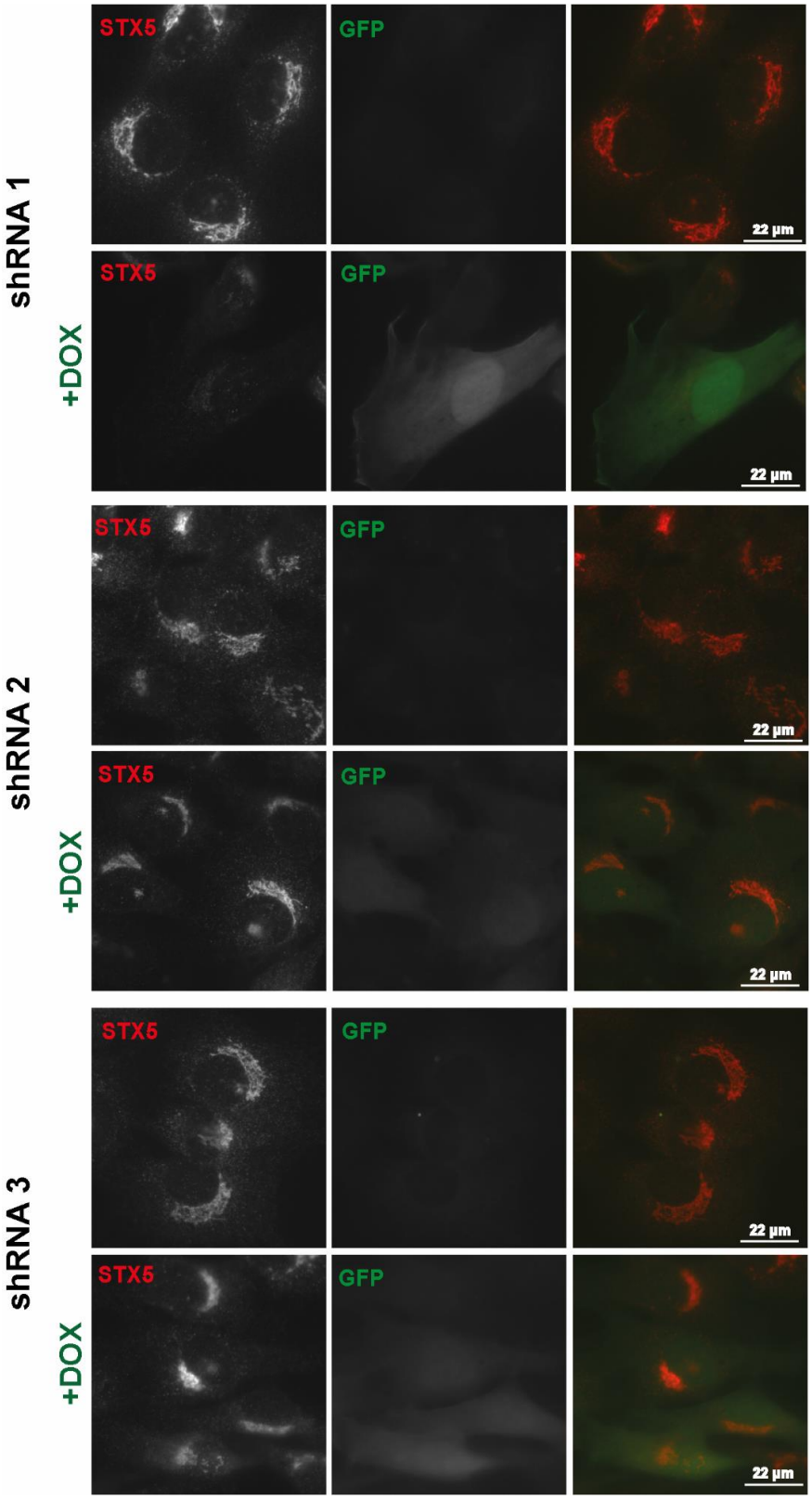

Figure 3.11: MEF cells were transduced with three different shRNAs against STX5 and selected with 1µg/ml of puromycin for at least 7 days. They were then seeded on coverslips in 12 well plates. Expression of the turboGFP and the shRNAs was induced by incubation with doxycycline (1µg/ml). Two days post doxycycline incubation, cells were assessed for STX5 expression by immunofluorescence microscopy. All three populations responded to doxycycline treatment by expressing GFP. Cells transduced with shRNA 1 showed reduction in STX5 staining in response to doxycycline.

3.2.2.5 Generating an I.29 Reporter Line for Studying Changes in the Proteome of the ER

BioID is a well-recognised proximity labelling technique that is used to identify protein-protein interactions. It is based on fusing a protein of interest with the promiscuous E.coli protein ligase BirA and was first used to identify protein interactors with human lamin A protein (Roux et al., 2012). It was later developed to BioID2 which has better biotin sensitivity (Kim et al., 2016). These techniques amongst other proximity labelling methods are reviewed here (Li et al., 2017). One of the limitations of BioID2 is the biotin labelling time which is conventionally between 12-24 hours. Utilising yeast display directed evolution, TurboID was then developed which is capable of significantly faster proximity labelling of just 10 minutes (Branon et al., 2018)

To study how the ER changes during B-cell differentiation post protein perturbation we decided it would be useful to look at the proteomic profile of the ER. One way to do this is to utilise the biotin ligase, Turbo-ID localised to the ER Membrane (ERM). We transduced the I.29 cells with a plasmid which expresses a V5-tagged Turbo-ID protein containing an ER localisation signal (amino acids 1-29 of cytochrome P450). Post selection, the Turbo-ID expression was validated using immunofluorescence microscopy which showed that the construct was expressed and gave a labelling pattern consistent with its localisation at the ER (**Figure 3.12A**). Cells were then treated with biotin and the biotinylated proteins pulled down using magnetic streptavidin beads (**Figure 3.12B**). Streptavidin blot analysis was performed and surprisingly we detected a significant amount of biotinylation in the absence of added biotin. Unfortunately, RPMI media contains 0.2mg/ml biotin (Thermofisher website) and therefore the BiRA was constitutively biotinylating proteins. To validate this observation, the experiment was repeated, and the cells were stained with Streptactin DY-488 and analysed by flow cytometry (**Figure 3.12C**). As expected, cells expressing the Turbo ID were constitutively biotinylating their proteins. This result highlights the importance of checking media formulation before performing these studies. To try and resolve this problem, we moved to another labelling technique referred to as APEX (**3.2.2.6**).

We observed a large upregulation of ER proteins being biotinylated in the differentiated compared to undifferentiated cells (**Figure 3.12B).** Surprisingly, TurboID-V5 was also shown to be upregulated. As an exogenous protein, this was not expected. We investigated this further by looking if another exogenous protein (Cas9) showed a similar upregulation in response to differentiation which will be discussed later in section **3.2.2.7**.

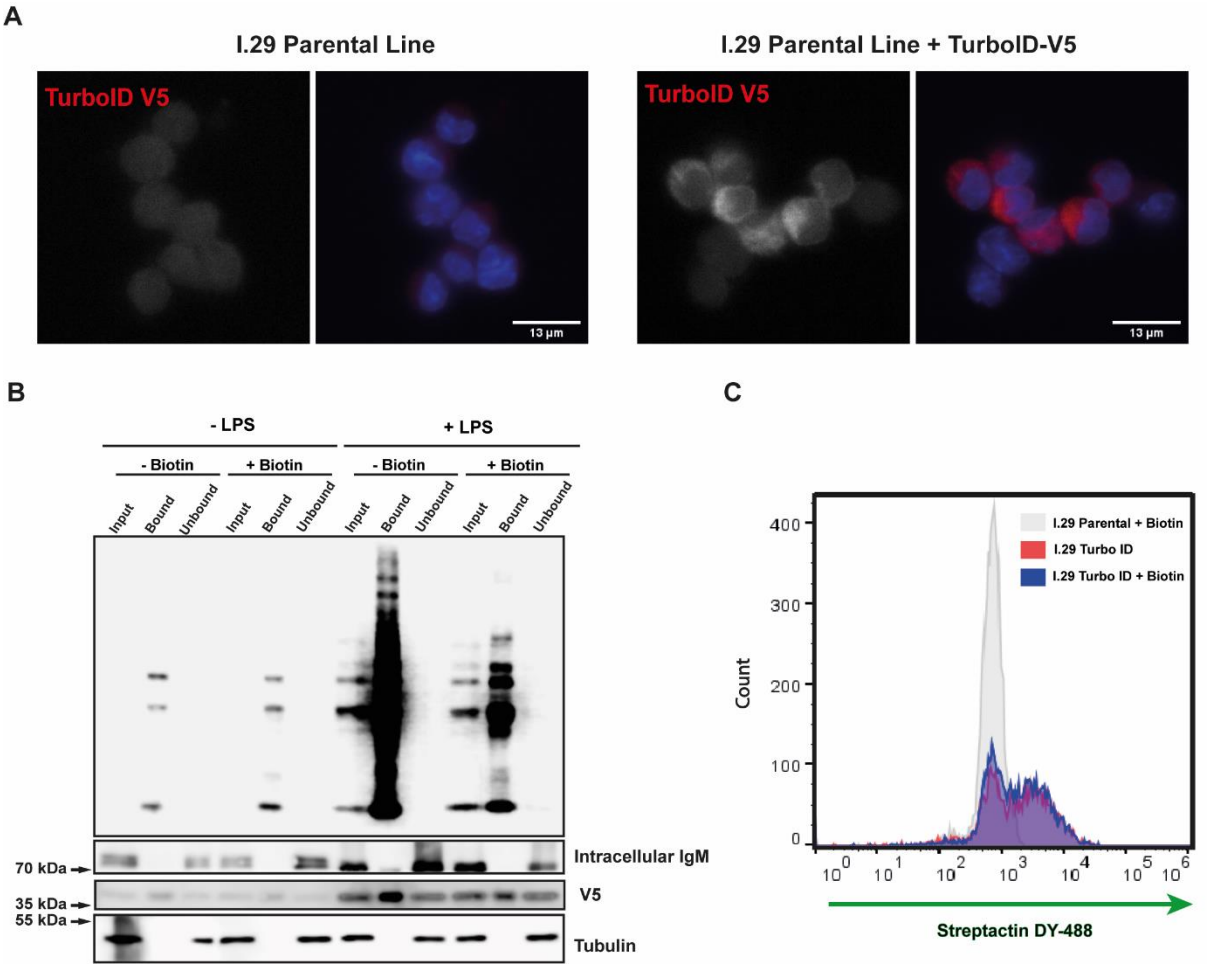

Figure 3.12: Proteins in I.29 cells expressing TurboID are constantly biotinylated. A) I.29 cells transduced with the TurboID construct were selected and centrifuged on fibronectin coated coverslips. The cells were fixed and stained with anti-V5 antibody and immunofluorescence microscopy performed. **B)** I.29 cells expressing TurboID were incubated with 0.5mM biotin for 30 minutes at 37°C. Cells were washed, lysed and the biotinylated proteins enriched using streptavidin beads. The input, elute and unbound samples were analysed by immunoblotting with streptavidin HRP. Results show biotinylation in absence of added biotin due to its presence in the RPMI media. Surprisingly, the V5-TurboID also showed upregulation in response to LPS. **C)** I.29 cells expressing Turbo-ID were incubated with or without biotin then fixed, permeabilized and stained with streptactin DY-488. Samples were run on the Attune flow cytometer to measure the amount of streptactin staining. As predicted from the immunoblotting data, TurboID biotinylates the proteins in the absence of exogenous biotin due to its presence in culturing media.

3.2.2.6 APEX2 Labelling of the Endoplasmic Reticulum

APEX is a 28kDa monomeric ascorbate peroxidase engineered from APX which is a class I cytosolic plant peroxidase (Martell et al., 2012), which was initially used in Electron Microscopy (EM). It was then shortly used for proteomic mapping to identify mitochondrial matrix proteins and their topology (Rhee et al., 2013). Using yeast-display directed evolution, APEX2 was developed which has enhanced ability for proximal protein labelling and enrichment (Lam et al., 2014). To utilise APEX2 for proximal mapping, APEX2 is genetically targeted to the cellular organelle/protein of interest. Cells expressing the construct are then pre-incubated with Biotin Phenol (BP) and treated with H_2O_2 for 1 minute resulting in the oxidation of biotin phenol into short-lived biotin-phenol radicals. The radicals covalently biotinylate proximal proteins which allows their pull-down for enrichment with streptavidin beads and their analysis by mass spectrometry.

APEX's reliance on biotin-phenol and not biotin made it an excellent alternative for performing the proximity based biotinylation in I.29s which grow in biotin-containing media. We therefore obtained a plasmid encoding a V5 tagged APEX2 targeted to the cytosolic face of the ER via a localization sequence (amino acids 1-29 of cytochrome P450). Cells were transduced with the construct and its expression was validated post selection using immunofluorescence microscopy (**Figure 3.13**). Surprisingly, similarly to the TurboID construct, the levels of V5-APEX2 were dramatically upregulated in differentiated I.29 cells (**Figure 3.13**). This unexpected upregulation of exogenous proteins will be discussed in section **3.2.2.8**.

APEX2 is utilised by pre-incubating the cells with 0.5mM of BP for 30 minutes at 37ºC, treating the cells with H_2O_2 for 1 minute and then quenching the reaction (Lam et al., 2014) (Lee et al., 2016) (Hung et al., 2016). These conditions were initially followed for the I.29s, however they did not yield biotinylation. We note through the literature reports of poor membrane permeability of biotin phenol in some cells (Hwang & Espenshade, 2016)(Mannix et al., 2019)(Tan et al., 2020). To enable biotin phenol labelling in the I.29s, BP concentrations and incubation times were optimised (**Figure 3.14A**). Surprisingly, incubating with the suggested 0.5mM of BP up to 135 minutes still resulted in no apparent biotinylation. 2.5mM of BP resulted in better biotinylation at all tested time points with significantly higher levels at 135 minutes. We also tested 4mM and 5mM which were better than 2.5mM in terms of biotinylation signal. The maximum solubility of biotin phenol in DMSO to make a stock solution is 250mM which means that a working concentration of 2.5mM results in 1% DMSO in solution. Therefore, we decided to look at the morphology of the cells (data not shown) and viability (**Figure 3.14B**) at each time point to check any obvious detrimental effects of DMSO for the tested period. Even though there was no significant reduction in the cells' viabilities at all concentrations for

the tested times, 2.5mM was used for 135 minutes moving forward to keep the DMSO concentration at a maximum of 1%.

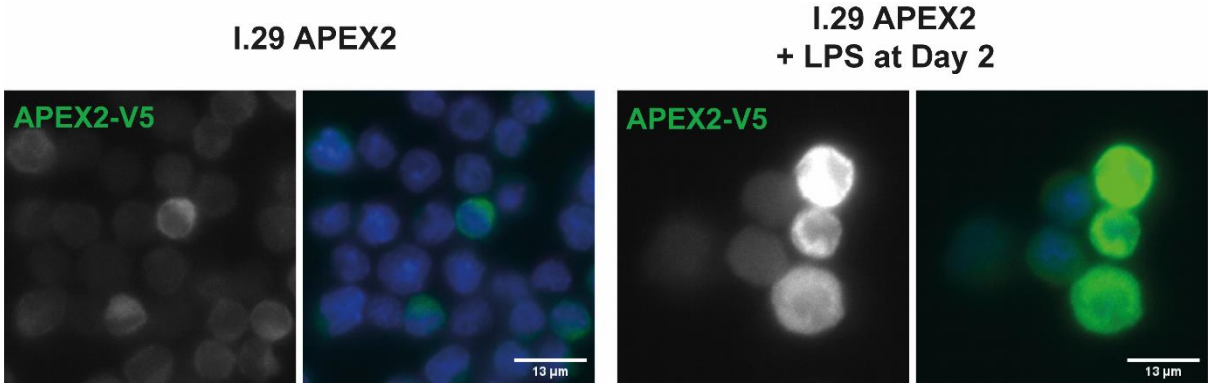

Figure 3.13: The APEX2 construct is upregulated in response to B cell differentiation. I.29 cells transduced with APEX2-V5 were induced to differentiate with 20µg/ml of LPS. Two days post inductions, cells were fixed and stained for immunofluorescence microscopy with an anti V5 antibody.

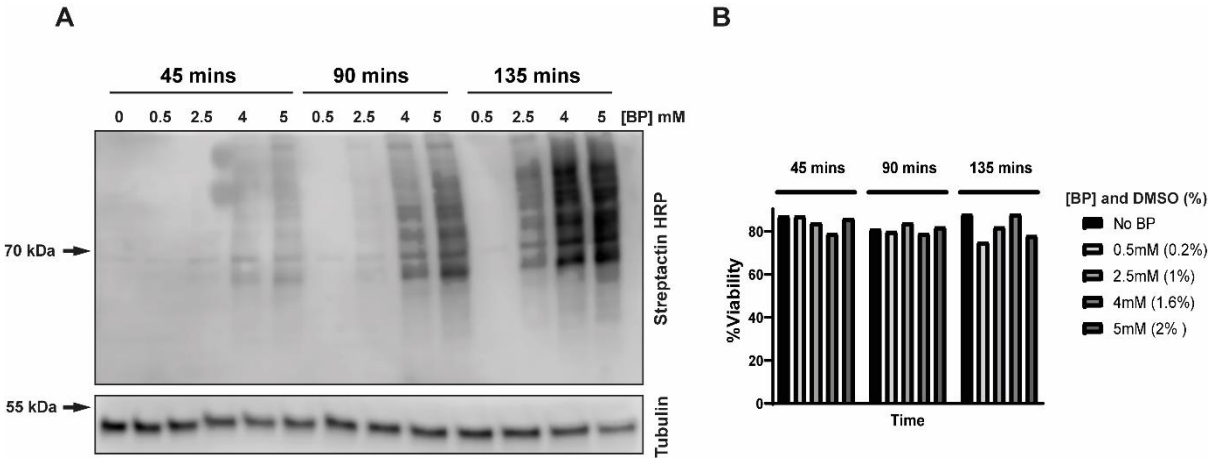

Figure 3.14: Optimization of biotinylation in I.29 cells with biotin phenol. I.29 cells expressing APEX2 were incubated with biotin phenol at the described concentrations and times. At each time point, cells were treated with 1mM H_2O_2 for 1 minute and the reaction quenched. The cells were collected, washed and processed for immunoblotting. **A)** Streptactin immunoblotting show that increasing BP concentration increases efficiency of biotinylation. **B)** Trypan blue cell counting was performed using the BioRad TC20 automated cell counter at each tested time point.

3.2.2.7 Upregulation of Exogenous Proteins in Differentiated I.29s

Following the transduction of TurboID and APEX2 in the I.29s, we were surprised to observe significant upregulation of the reporter proteins in differentiated cells. This is unexpected because the expression of these proteins is driven by exogenous promoters. To determine if this was a more general phenomena, we also looked at the expression of the Flag-Cas9 in our Cas9 expressing cell line to assess whether it also becomes upregulated during differentiation (day 2 post LPS treatment). We observed an approximate ~5-fold increase in protein level at day 2 post induction (**Figure 3.15**) (n1).

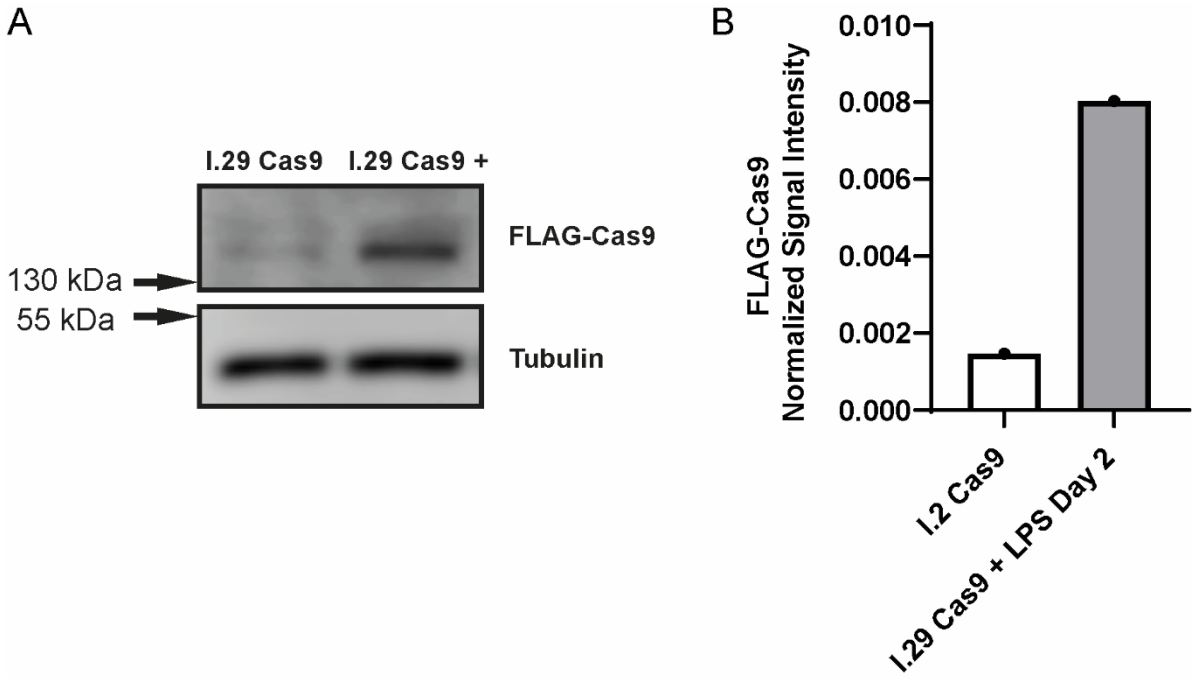

Figure 3.15: Upregulation of Cas9 in transduced I.29 cells during differentiation. To examine whether the expression of the exogenous Cas9 was upregulated upon differentiation in the I.29 cells, cells were induced with 20µg/ml of LPS (+) and collected on day 2 post induction. Collected lysates were processed for immunoblotting and probed with anti-FLAG antibody. **A)** Immunoblot results show an upregulation of the Cas9 expression in the differentiated cells. **B)** Western blot bands were quantified and normalised against tubulin showing a potential ~5 fold at days 2 post LPS induction **(n=1)**.

3.2.2.8 Are Changes in Exogenous Proteins Expression due to Changes in Transcription Factor Expression During I.29 Differentiation?

We and others have shown that as B-cells differentiate there are significant changes in transcription factor expression (**Figure 3.2**)(Rahman, 2019)(W. Shi et al., 2015). We speculate that this could potentially lead to changes in the transcription of exogenous promoters. For example, some upregulated transcription factors could be binding to regulatory elements in the promoter regions. A transcription factor that we know is significantly upregulated in ASCs and has a defined conserved promoter element is CREB3L2. This TF binds to the cAMP response element which has the conserved sequence of 5'-TGACGTCA-3' (Carlezon et al., 2005). Both the TurboID and APEX2 constructs are driven by the CMV promoters, so as a very crude way to find out whether this hypothesis could stand, we search for the conserved regulatory sequence in the promoter's region (**Figure 3.16A**). We find that the sequence is matched 4 times, 3 of which are within the CMV enhancer region and 1 time within the CMV promoter region. These results suggest that the increased levels of CREB3L2 in differentiated I.29s can potentially bind to these sequences enhancing expression from the CMV promoter. If the binding site of a transcription factor is not readily available, JASPAR 2022 can be used to predict the binding sites of transcription factors (**Figure 3.16B**) (Castro-Mondragon et al., 2022).

To enable further investigations of this phenomenon, we searched for a tool which can output which transcription factors are predicted to bind to an inputted DNA sequence, and found Ciiider (Castro-Mondragon et al., 2022). We used this software to input the sequence of CMV, and it returned 280 transcription factors predicted to bind sequences in the enhancer and promoter region. Exporting the results also importantly showed the sequence of the binding site and the number of times it is predicted to bind (**Figure 3.17A-B**). This list of transcription factors can then be inputted in PlasmacytOMICs to analyse whether they are upregulated/downregulated during differentiation. For example, MIST1, which is highly upregulated in ASCs and differentiated I.29 cells, was identified as a potential binding transcription factor for the CMV promoter. Taken together, the observed changes in reporter protein expression are likely to be driven by changes in the transcriptional profile of differentiated ASCs.

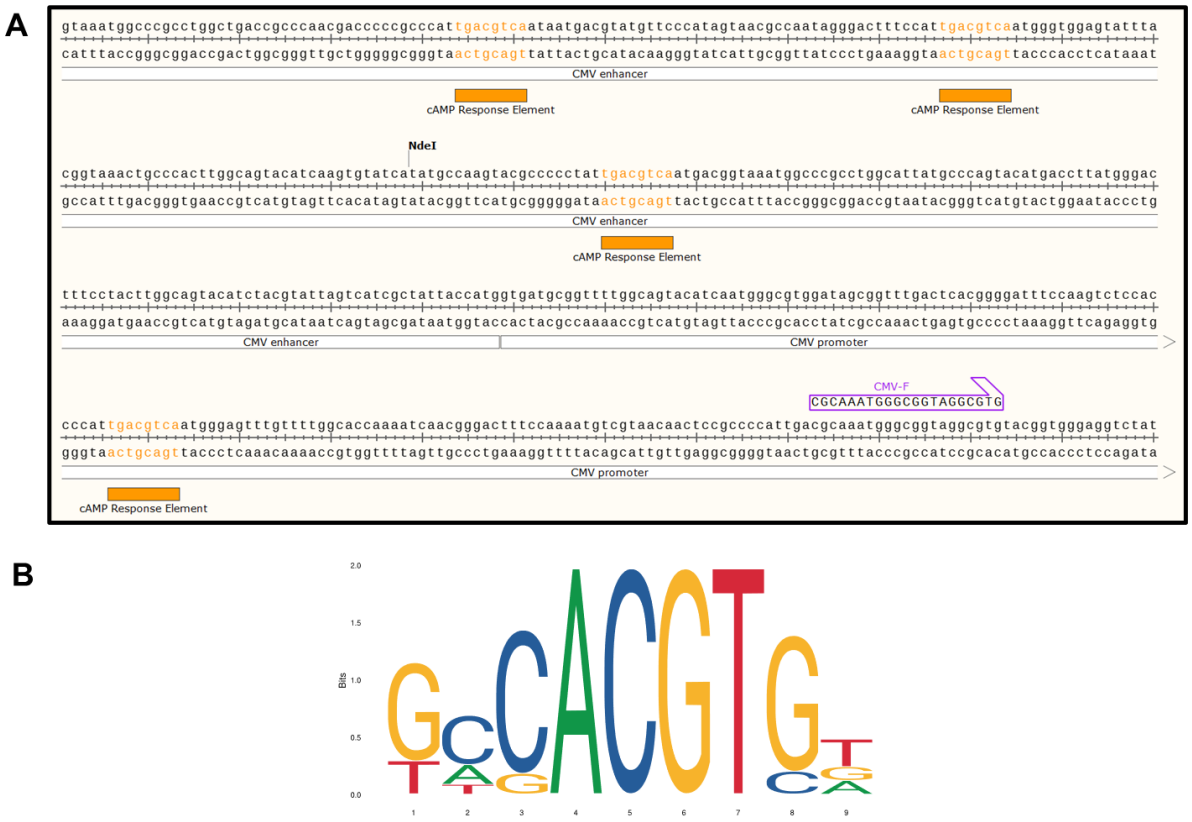

Figure 3.16: Investigating cAMP response elements in CMV enhancer and promoter regions and predicting CREB3L2's binding sequence using JASPER. A) Screenshot is showing part of the CMV enhancer and promoter sequence from the APEX2 plasmid (Addgene #79055). To crudely assess whether CREB3L2, as an upregulated transcription factor in ASCs, could potentially bind the CMV region, we searched for the cAMP response element sequence 5'-TGACGTCA-3' and noted that it was matched 4 times within the CMV region. **B)** In addition to well characterised and conserved binding sites easily available to find such as the cAMP response element, we also report that the JASPAR 2022 database can be used to predict potential binding sequences of transcription factors. The output is a position-specific sorting matrix which uses experimentally validated data of transcription factors binding to these sequences. The screenshot is showing the predicted nucleotide sequence binding site for CREB3L2.

A

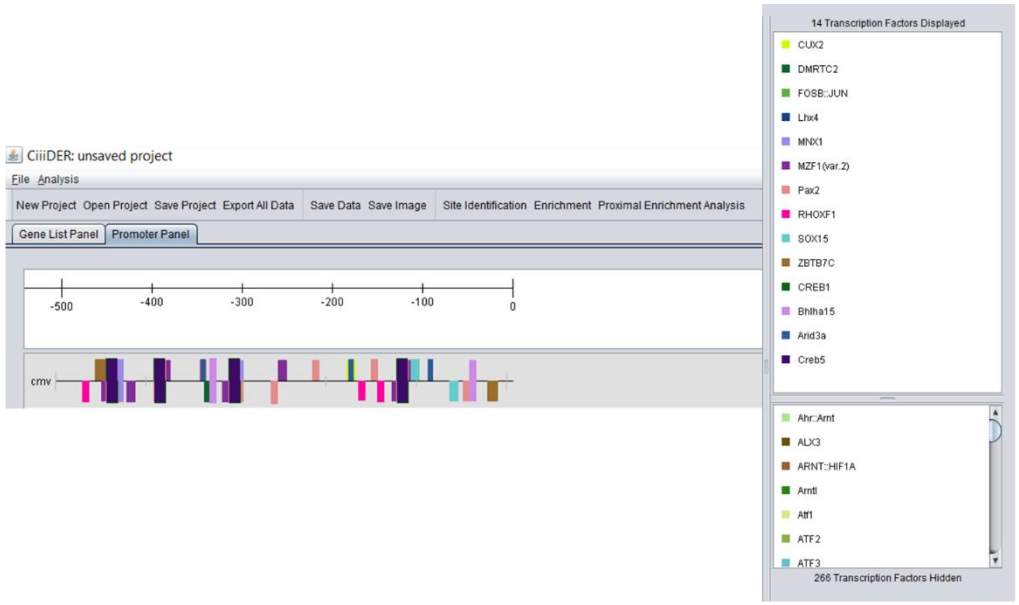

B

Gene Name	Gene ID	Transcription Factor Name	Transcription Factor ID	Start Position	End Position	Strand	Core Match Score	Matrix Match Score	Sequence
cmv	2	Creb5	MA0840.1	57	68	1	1	0.897	ATTGACGTCAAT
cmv	2	Creb5	MA0840.1	110	121	1	1	0.897	ATTGACGTCAAT
cmv	2	Creb5	MA0840.1	193	204	1	1	0.897	ATTGACGTCAAT
cmv	2	Creb5	MA0840.1	379	390	1	1	0.897	ATTGACGTCAAT
cmv	2	Creb5	MA0840.1	379	390	-1	1	0.897	ATTGACGTCAAT
cmv	2	Creb5	MA0840.1	193	204	-1	1	0.897	ATTGACGTCAAT
cmv	2	Creb5	MA0840.1	110	121	-1	1	0.897	ATTGACGTCAAT
cmv	2	Creb5	MA0840.1	57	68	-1	1	0.897	ATTGACGTCAAT

Figure 3.17: Using CiiiDER to predict transcription factor binding sites in CMV promoter. To identify all transcription factors predicted to bind to the CMV region, CiiiDER software was used. **A)** The CMV sequence was inputted into the software and the output is a promoter panel showing visually the predicted binding sites of the transcription factors along the sequence. On the right side is the list of all predicted transcription factors. Hidden TFs can be dragged into the displayed window to visualize. **B)** Results can be exported as an excel worksheet. Excel sheet shows the predicted position of each TF binding site, a core match score (core region of most conserved 5 bases is matched against the model) and a matrix match score (full length of the transcription factor binding site is matched against the model). These scores must be below the selected deficit cut-off. Figure is only showing, as an example, the top 8 rows out of 983 rows of the excel sheet exported from the CMV region analysis.

3.3 Chapter Discussion & Summary

The main aims of this chapter were to determine whether I.29 cells are a good model for: a) studying B-cell differentiation and antibody secretion and b) gene disruption studies.

I.29 Cells Appropriately Express Genes Implicated in B-cell Differentiation and Antibody secretion

I.29 cells have been previously used as a B-cell model that can differentiate into ASCs and showed expression of well-known ASCs markers such as XBP1 and BLIMP1 (Ma et al., 2010). They have proved a useful tool for the study of antibody secretion, class switching and CD138 expression (Qiu & Stavnezer, 1998)(Stavnezer et al., 1999)(Van Anken et al., 2003)(Romijn et al., 2005)(Van Anken et al., 2009)(Ma et al., 2010a)(Wong et al., 2013). Their proteome has been profiled during differentiation (Van Anken et al., 2003)(Romijn et al., 2005), however the number of proteins detected was very small and most of the ASCs' markers that we have described throughout this chapter were not identified in those studies.

We have utilised what we know from the literature and the previously generated PlasmacytOMICs resource to directly assess the expression of proteins known to be upregulated in primary immune cells during I.29 differentiation (**Figures 3.2-3.5**). Most of the proteins that we looked at behave in a manner that one would expect based on the PlasmacytOMICs data confirming that I.29 cells are able to recapitulate many aspects of B-cell biology. In summary, we have shown that the I.29 cells express key ASCs transcription factors such as XBP1 which is necessary for development of antibody secretion and others; CREB3L2, ATF6 and MIST1. We have also shown the upregulation of biosynthetic pathway proteins which may be associated with functions of ASCs that include ER localised proteins, COPII components and SNAREs.

We have previously hypothesised that ASCs mainly upregulate the v-SNAREs rather than the t-SNAREs in the early secretory pathway based on their differential regulation profile (Rahman, 2019). Upregulation of SEC22B and YKT6 in differentiated I.29s supports this hypothesis (**Figure 3.5D**). SEC22B shows the clearest upregulation in differentiated I.29s cells, which is interesting as it has been recently reported to be required for plasma cell maintenance, survival, and antibody secretion through more functions than just vesicular transport (Bonaud et al., 2023). This exemplifies how upregulated proteins in ASCs likely reflect the cells' requirement for them to carry out important biological processes in the differentiation process/state.

One limitation of the work presented is that only one biological repeat was performed for the immunoblotting time course experiments. To address this, we had initially planned to use mass-spectrometry data. However, due to issues with the instrument this data has not been included here in the thesis. In the longer term it would be helpful to include the I.29 data in the PlasmacytOMICs resource so a more comprehensive comparison to primary cells can be performed.

An initially unexpected observation made during the time course experiments was that some proteins' upregulation was not always linear. Expression of COPII components seemed to follow a linear trend, with the upregulation being linear until day 3 then dropping at day 4 (**Figure 3.5C**). This is with the exception of SEC13 whose reduction was earlier at day 2, showing similar levels to undifferentiated cells at day 3 and 4. In addition to being a COPII component, SEC13 is also a part of the nuclear pore complex which enables trafficking of molecules between the nucleus and cytoplasm (Enninga et al., 2003). The presence of SEC13 in a distinct complex other than COPII, unlike the remaining tested components, may potentially mask differences in its protein levels during differentiation. The dynamics of expression for some proteins were distinct. For example, the levels of CREB3L2 and XBP1s in differentiated cells seemed to rise at day 1, drop on day 2 and then peak at day 3 (**Figure 3.2B**). Even though initially unexpected, different expression kinetics of proteins during B-cell differentiation has been reported previously through proteomic profiling in I.29 cells (Romijn et al., 2005). Intriguingly, some proteins within a functionally similar group (i.e., ER-resident proteins), displayed different expression kinetics along the days post LPS induction. It would be interesting to confirm the dynamic changes in expression of the proteins examined here with further repeats, as these differences may reflect the fine tuning of some proteins' functions over the time course of B cell differentiation. For example, the drop in XBP1s levels at day 2 may be reflecting the transition of the proposed two-step UPR model where it is initially upregulated as part of the early differentiation process and then as a response to accumulated immunoglobulins (**see section 1.4.2.3**) (Van Anken et al., 2003). Indeed, while studying the UPR in I.29 cells, slower dynamics of differentiation were observed compared with primary splenic B cells which the authors suggested as an advantage that may provide clearer observations of UPR activation (Ma et al., 2010).

Challenges Faced While Genetically Manipulating the I.29 Cells

We have faced several challenges while developing the I.29 cell model for this project including promoter silencing, unpredictable gene expression and issues impacting proximity based proteomic approaches. One of the most surprising observations which we have made during this work is the upregulation of exogenous proteins during differentiation.

During the differentiation process of I.29 cells there is a change in the cells' transcriptional profile which is clearly impacting the expression of exogenous promoters. We have observed an upregulation of TurboID, APEX2 and Cas9 expression in differentiated cells (**Figure 3.12B, 3.13, 3.15**). Even though we have described in this thesis a few tools which can aid in exploring this hypothesis, this kind of analysis is not straightforward and outside the scope of this project. For example, to predict whether a promoter's expression may be enhanced during differentiation we would need to consider aspects such as a) the number of potential binding sites; b) the upregulation or actual expression level of the transcription factor in the differentiated vs the undifferentiated states; c) importantly the fact that these predictions do not necessary indicate that the transcription factors will actively bind these sites. Experimentally these observations could be confirmed by techniques such as chromatin immunoprecipitation and luciferase reporter assays in the specific biological context tested i.e., differentiated I.29 cells.

This phenomenon presents us with two opportunities. The first is screening the effect of differentiation on different promoters through an easily assayable protein such as GFP by flow cytometry. This can provide important information to ourselves and researchers on what to expect when introducing exogenous proteins in B-cells during differentiation especially when the levels of the protein may influence a readout. For example, when using proximity labelling techniques, the levels of TurboID/APEX2 directly impact the amounts of labelled proteins. This would make comparing the labelled proteome of differentiated vs undifferentiated cell states challenging. However, it may potentially not be a problem when comparing just one state between different cell lines, assuming no significant difference in their differentiation ability (for example comparing a differentiated I.29 parent line versus a differentiated I.29 line where a protein of interest has been knocked out). The second exciting opportunity is exploiting this phenomenon to develop a tool which indicates the differentiation state of the cell. For example, creating a stable cell line expressing GFP and using the changes of GFP expression in response to induction as a simple readout of differentiation.

Other challenges faced during this work included potential promoter silencing which has been previously reported during use of viral transductions (Xia et al., 2007)(Herbst et al., 2012)(Zúñiga et al., 2019)(Cabrera et al., 2022). For future work it may be beneficial to screen the activity of different promoters in our system and have the selection marker and protein of interest expressed from the same promoter. More methods can be used in the design of constructs to prevent transgene silencing such as targeting the transgene in genomic "safe harbours", such as the Rosa26 locus (Cabrera et al., 2022). Later in the project we discovered that the expression of exogenous proteins is upregulated during differentiation. As we have assayed for FLAG-Cas9 expression of the initial plasmid in undifferentiated cells, it may be useful to rule out the possibility that the cell line was expressing the

protein at a very low level at the B-cell stage by inducing the cells to differentiate and assaying again for its expression.

Summary

We have validated the I.29 cell line as a useful model of ASCs which in response to a differentiation stimulus, upregulates and secretes IgM, expresses ASCs' transcription identity markers, and expands its ER and secretory apparatus to aid antibody secretion. We have also generated and validated a Cas9 based gene disruption platform which will be useful not only for our research, but other groups interested in plasma cell biology. In addition, the ER localised APEX2 expressing line could provide useful characterisation of the ER profile in response to protein perturbation. Finally, we have described a phenomenon where exogenous proteins are upregulated during differentiation of I.29s that needs to be considered during experimental design and provides an exciting potential opportunity for development of a tool to assay differentiation.

Chapter 4: Perturbing and Characterising SEC24D in I.29 Cells

4.1 Chapter Aims

According to our previous data, SEC24D is the most highly upregulated COPII component in ASCs compared to precursor B cells (Rahman, 2019) (**Figure 1.4**), and we hypothesise that it may be playing an important role in the functions of ASCs. To test this hypothesis, we intend to **a)** use CRISPR/Cas9 to perturb SEC24D in I.29 cells and **b)** investigate the effect of SEC24D's loss on the synthesis and secretion of IgM utilising immunoblotting and ELISA.

Additionally, SEC24D has been previously shown to be regulated by the transcription factor CREB3L2 in hepatic stellate cells (Tomoishi et al., 2017). We aim to explore the regulation of SEC24D by CREB3L2 by **a)** overexpressing OASIS transcription factor family members in HeLa cells and assessing the protein levels of SEC24D; **b)** knocking out CREB3L2 in I.29s and assessing the level of SEC24D post differentiation and **c)** investigating the protein levels of other proteins predicted to be regulated by CREB3L2 in the absence of SEC24D such as FNDC3B, SEC31A and SEC23A.

4.2 Results

4.2.1 Transduction of I.29s with guides against SEC24D

The mRNA and protein levels of SEC24D are highly upregulated when naive B-cells differentiate into ASCs (**Figure 1.4**). Thus, to investigate its role in antibody secretion, four guides against SEC24D were chosen using CHOPCHOP and cloned into the guide plasmid. The four guides target the earliest conserved exon between all validated and predicted mouse sec24d transcripts (**Figure 4.1**). I.29 cells expressing Cas9 were then transduced with the guides and selected. Post selection, the generated four populations were differentiated using LPS and SEC24D levels were assayed by western blots. All populations showed significant levels of SEC24D, and it was unclear whether we had successfully disrupted the gene (data not shown). To investigate this, genomic DNA was obtained and purified from the parent population and the guides-transduced populations. The DNA was PCR amplified using primers that flanked the targeted SEC24D exon and TOPO-TA cloned for sequencing. The sequencing results showed that the populations did indeed have mutations near the guides' PAM site. However, many of the clones had the wild type sequence suggesting that the population was genotypically heterogeneous (**Figure 4.2**).

4.2.2 Single-Cell Cloning to Screen for SEC24D

The genomic PCR indicated that our CRISPR/Cas9 approach was resulting in successful gene editing. However, at a population level, no significant reduction in SEC24D was being achieved. To address this,

we proceeded to perform single cell cloning of the population transduced with the guide that resulted in the highest frequency of frameshift mutations. 11 clones were picked at random and induced to differentiate with 20µg/ml of LPS and SEC24D levels were screened by immunofluorescence microscopy (**Figure 4.3**). Clone 41 (C41) was chosen for further analysis as it showed a significant reduction in levels of SEC24D two days post LPS induction by immunofluorescence microscopy.

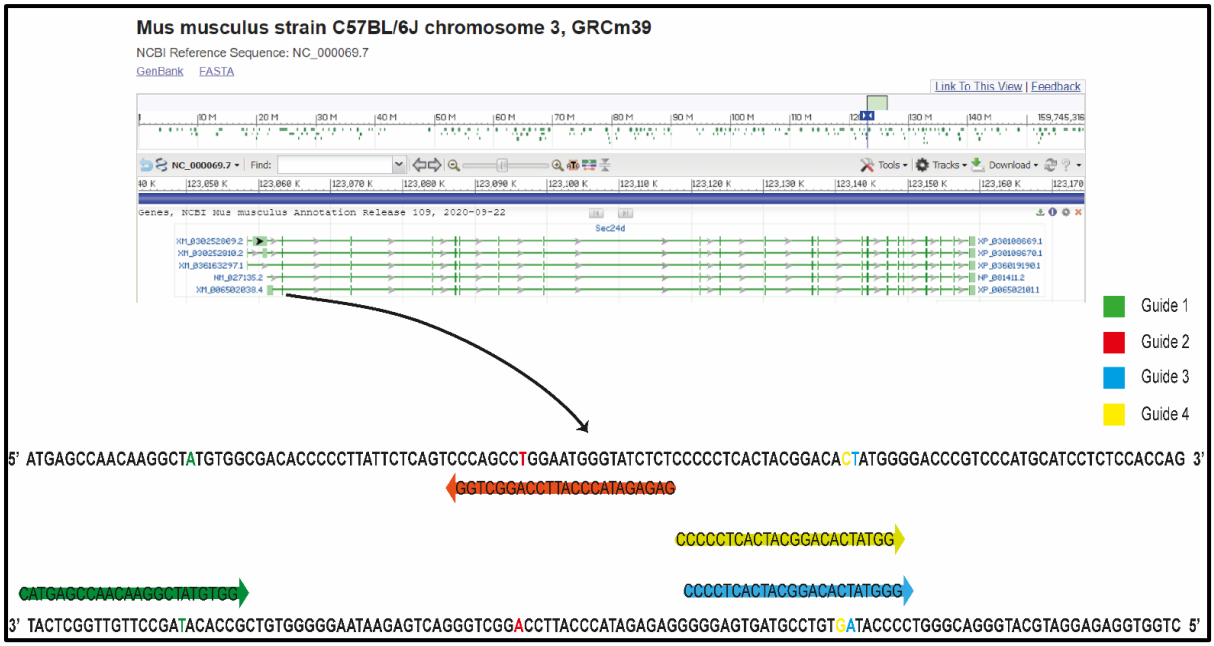

Figure 4.1: The four guides against mouse SEC24D. Four guides against SEC24D were chosen using the web tool CHOPCHOP. They were chosen to target the earliest conserved exon between sec24d transcripts as predicted by NCBI. The guides are predicted to cut 3-4 base pairs upstream of the PAM sequences which are canonically 5'-NGG-3'. The predicted cut nucleotide is coloured in the same colour that the guide sequence is highlighted with.

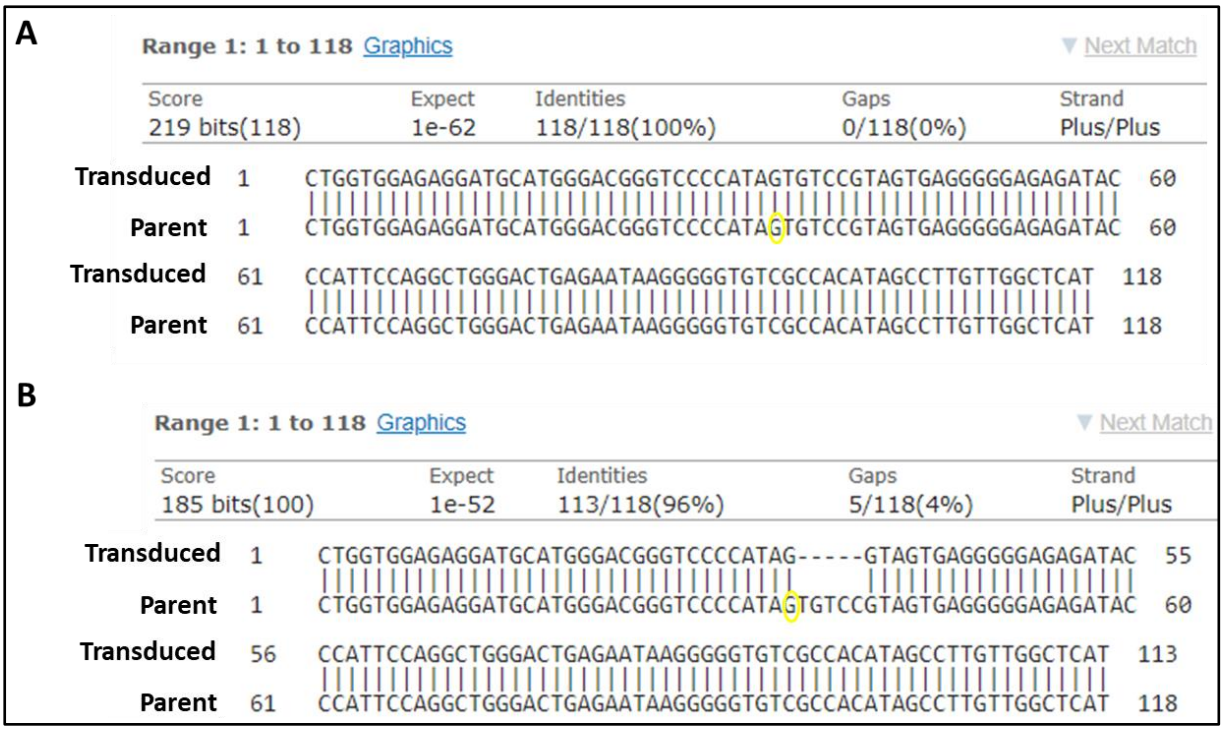

Figure 4.2: Populations transduced with guides are genotypically heterogeneous. Sequencing results from genomic PCR TOPO clones show that transduced and selected cell populations are heterogeneous. This example is showing SEC24D's targeted region sequences of two clones picked from the population transduced with guide 4. Nucleotide circled in yellow is the predicted cut site. **A)** Sequence showing an unedited clone compared to the parent's sequence. **B)** Sequence showing a frameshift-resulting mutation of 5 nucleotide deletions compared to the parent sequence.

4.2.3 SEC24D Levels are Significantly Reduced in Clone 41 up to 4 Days Post LPS Induction

Clone 41 was induced by 20µg/ml LPS and collected at day 2 and 4 post induction to test SEC24D levels by IF and immunoblotting (**Figure 4.4**). Results show significant reduction in protein signal by both techniques.

4.2.4 Genotyping Clone 41

To investigate whether C41 is a SEC24D null, genomic PCR and sequencing from TOPO clones was performed. 15 colonies were picked, the plasmid isolated and prepped for sequencing. All sequencing results came back showing two types of edits, which would result in frameshift mutations indicating a potential successful creation of a knock out line (**Figure 4.5**). However, as the karyotype of I.29 cells is not known, C41 may be hypomorphic and will not be referred to as a null.

4.2.5 Does the Loss of SEC24D Impact IgM Secretion?

Having confirmed that SEC24D is significantly reduced in clone C41, we proceeded to characterise the cell line. IgM secretion was the first aspect of ASCs biology to be looked at to determine whether SEC24D has an important role in IgM trafficking and/or secretion. Cells were induced by LPS for two days and anti-IgM ELISA performed on media collected from the cells (**Figure 4.6C**). In addition, the levels of intracellular IgM were determined by immunoblotting to determine whether disrupting the function of SEC24D could impact the levels of its synthesis (**Figure 4.6A-B**). Surprisingly, we observed no significant reduction in the amount of intracellular or secreted IgM suggesting that SEC24D is not required for its secretion, despite its upregulation in ASCs.

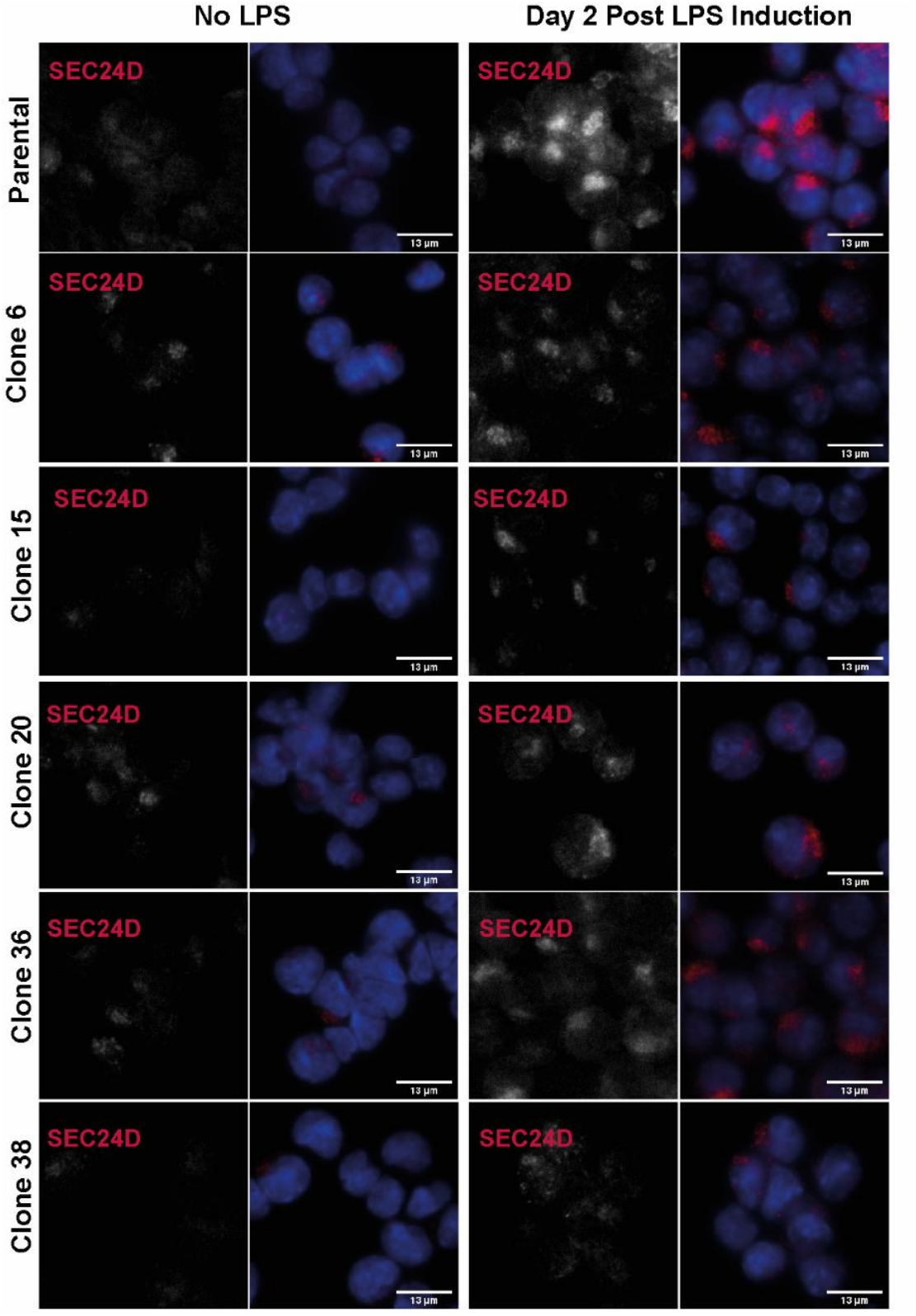
No LPS
Day 2 Post LPS Induction
Parental
Clone 6
Clone 15
Clone 20
Clone 36
Clone 38
SEC24D
13 µm

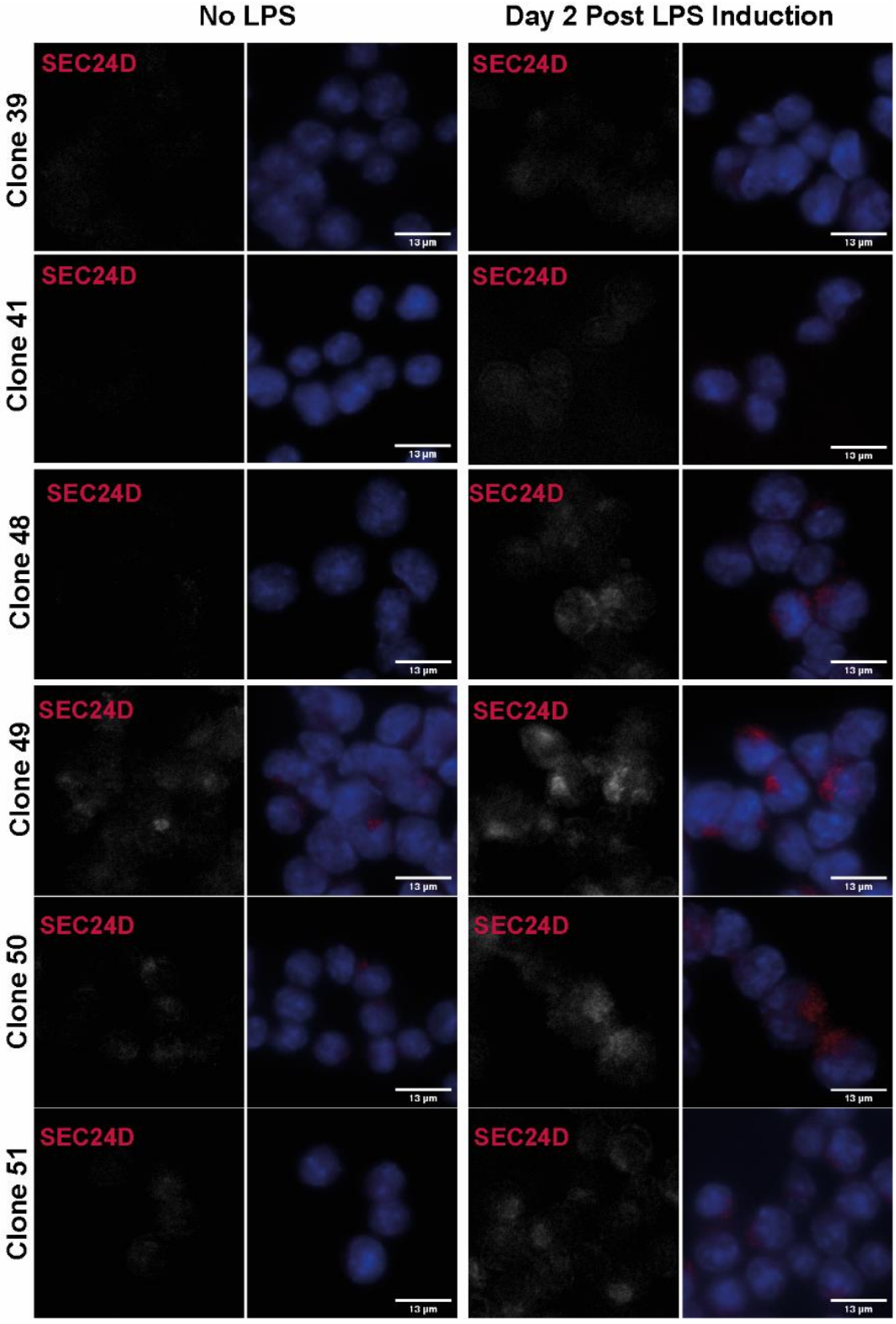

Figure 4.3: Screening clones for a SEC24D KO line: I.29 cell population transduced with guide 2 against SEC24D was sorted on the Melody FACs machine to deposit single cell clones into 96 well plates. Clones were then grown and cultured for 2 to 3 weeks. 11 clones were then picked at random and induced by LPS to assay for SEC24D levels. Cells were collected at day 2 LPS induction, centrifuged on fibronectin coated coverslips, fixed by methanol and immunofluorescence staining was performed for SEC24D. Most clones seemed to have reduced levels of SEC24D compared to the parental population (not transduced with the guide). Clone 41 showed no clear SEC24D signal. **Scale bar: 13µm**

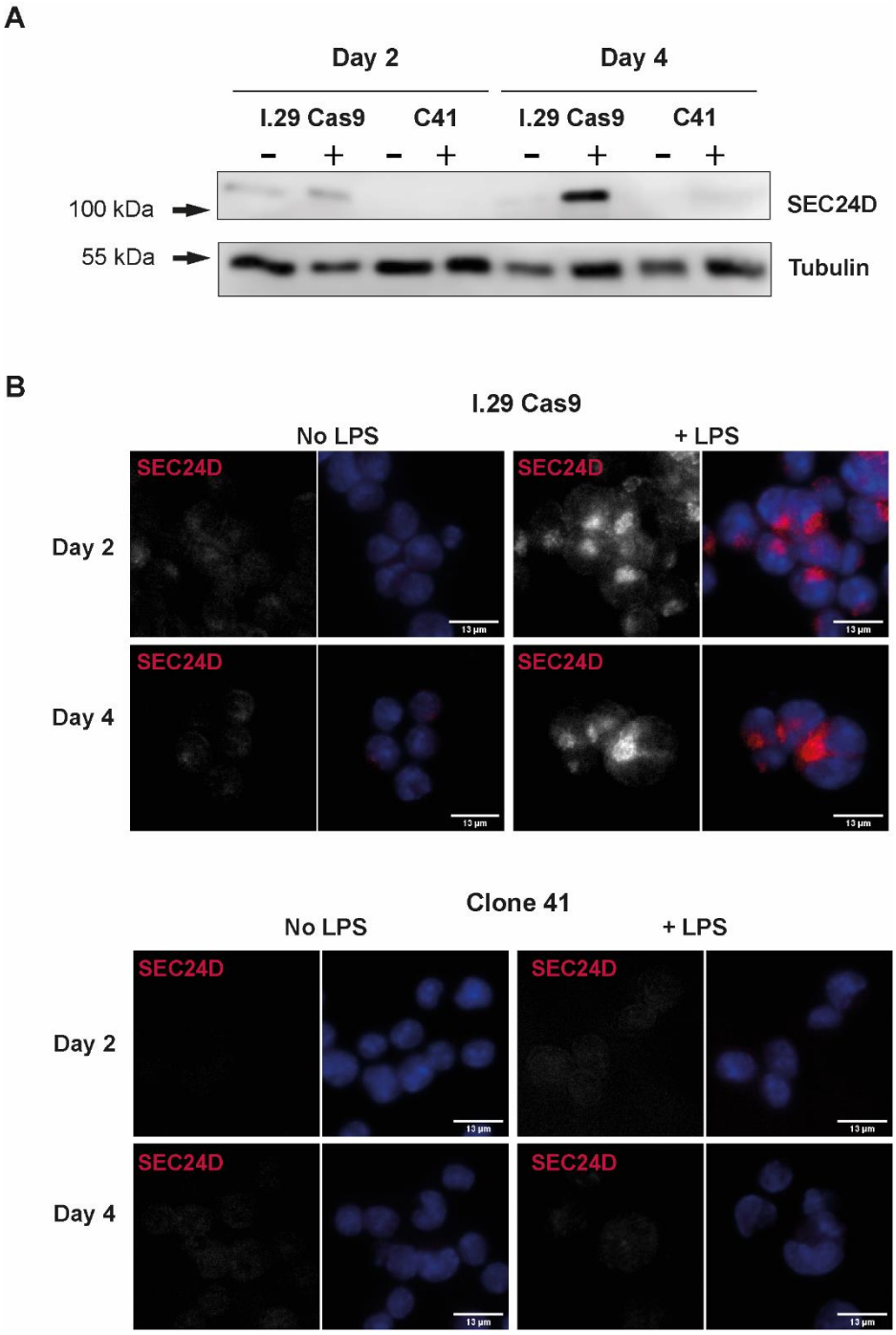

Figure 4.4: Clone 41 has dramatically reduced levels of SEC24D at day 4 post LPS induction. (A) Cells were collected at day 2 and 4 post LPS induction (+) and cell lysates were processed for immunoblotting and probed with anti-SEC24D antibody. Immunoblots show dramatic reduction of SEC24D for clone 41 at day 2 or 4 post differentiation. **(B)** Cells were collected at day 2 and 4 post LPS induction, centrifuged on fibronectin coated coverslips, fixed by methanol and immunofluorescence staining was performed for SEC24D. Results show induction of SEC24D in the parent line at day 2 and 4, with no clear staining observed for clone 41.

A

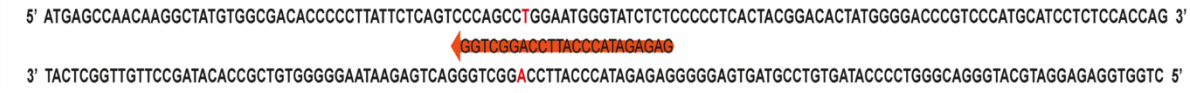

B

Figure 4.5: Genomic sequencing of C41. A) Genomic DNA sequence of the SEC24D exon targeted by the guide. Guide sequence is shown in the red arrow and the nucleotide predicted to be cut by the endonuclease is highlighted in red. **(B)** Sequencing results from 15 genomic PCR TOPO colonies show one of the two described frameshift causing edits: deletion at the predicted cut site (circled in red) and one base pair downstream it (top) and a mismatch mutation one base pair downstream the predicted cut site and an insertion (bottom).

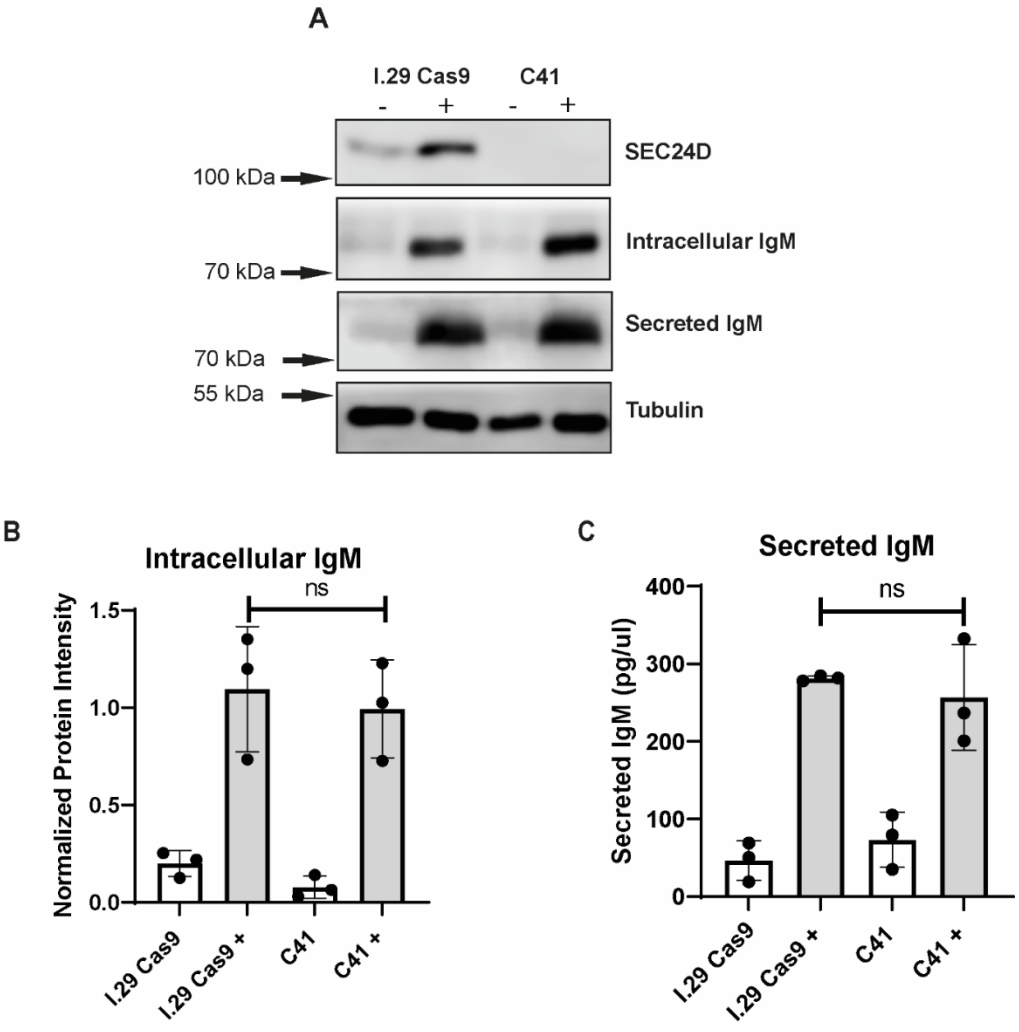

Figure 4.6: SEC24D is not required for IgM secretion in differentiated I.29s at day 2 post induction. I.29 cells were differentiated using 20µg/ml of LPS (+) and collected 2 days post induction. They were washed and resuspended in fresh media for 5 hours to assess IgM secretion. **A)** Media and cells were collected post the 5 hours and processed for immunoblotting. Lysates were probed for SEC24D and intracellular IgM, and media probed for secreted IgM. **B)** Immunoblots quantification of intracellular IgM normalised to tubulin. **C)** ELISA was performed on collected media and values were normalised against an IgM standard. **Unpaired t-test performed on data from three biological replicates (n=3). ns; not significant. Error bar indicates standard deviation of the mean.**

4.2.6 Is CREB3L2 Required for the Expression of SEC24D in I.29 Cells?

Despite having identified SEC24D as a highly upregulated marker in ASCs, we did not observe significant perturbations in IgM biosynthesis and secretion in the SEC24D mutant clone (C41). Beyond antibody synthesis and secretion, we wondered if SEC24D has other roles in the functions of ASCs. We first wanted to investigate whether the knockout of CREB3L2, a transcription factor which has been shown to upregulate SEC24D, would impact the expression of SEC24D in I.29s. I.29 cells expressing the Cas9 were transduced with a guide RNA against CREB3L2. Post selection, single cell cloning was performed and screened using immunoblotting. Clones 36 and 38 showed the highest reduction of CREB3L2. These clones were induced to differentiate using LPS and collected four days post induction. No noticeable reductions in the levels of SEC24D were observed (**Figure 4.7**). We reasoned that this lack of effect is potentially due to redundancy with other OASIS family members expressed in I.29 cells. In parallel to this study, we were also investigating whether expression of other OASIS family members could induce the expression of SEC24D in HeLa cells.

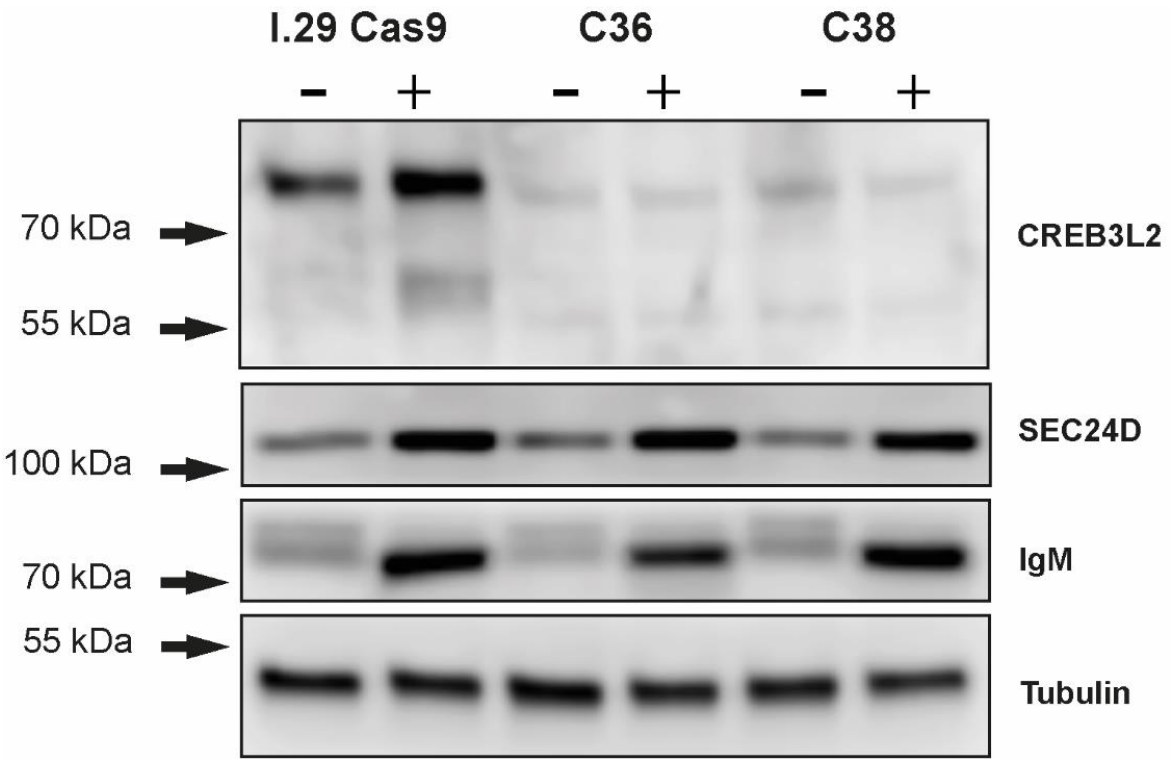

Figure 4.7: CREB3L2 mutant clones do not show reduced SEC24D protein levels. I.29 cells were differentiated using 20µg/ml of LPS (+) and collected 3 days post induction. Cell lysates were processed for immunoblotting and probed with anti-CREB3L2, SEC24D and IgM antibodies. Results showed no reduction in SEC24D protein for CREB3L2 mutant clones.

4.2.7 Validation of New CREB3L2 Antibody

Due to the ability of OASIS family members to potentially manipulate the secretory capacity of cells, the lab has previously generated cDNA constructs encoding the activated cytosolic domains of CREB3L1, CREB3L2, CREBH and Luman with the purpose of transfection into Chinese Hamster Ovary (CHO) cells to assess whether they increase antibody production. For my project, we utilise these constructs in HeLa cells to assess whether they can drive the expression of SEC24D, which may explain why reduction of CREB3L2 alone in the I.29s results in no significant effect on SEC24D levels.

To validate the CREB3L2 antibody for microscopy, we transfected the CREB3L2 construct in HeLa cells using ViaFect. ER stress was induced by treating the cells with 2µg/ml of tunicamycin one day post transfection and 16-18 hours before fixation to stabilise CREB3L2's expression. Transfected cells showed nuclear staining which is the expected localization (**Figure 4.8**). Cells with higher expression levels predominantly showed nuclear expression with some staining in the cytoplasm. The tested antibody has previously shown bands at the right size using western blots that became enhanced in response to LPS induction in I.29 cells (**Figures 3.2, 4.7**) and has now shown expected localization of the activated protein in the nucleus using immunofluorescence microscopy, indicating that it is specific to CREB3L2. Finally, we note that cells expressing CREB3L2 may be exhibiting a larger nucleus or cell size compared to un-transfected cells.

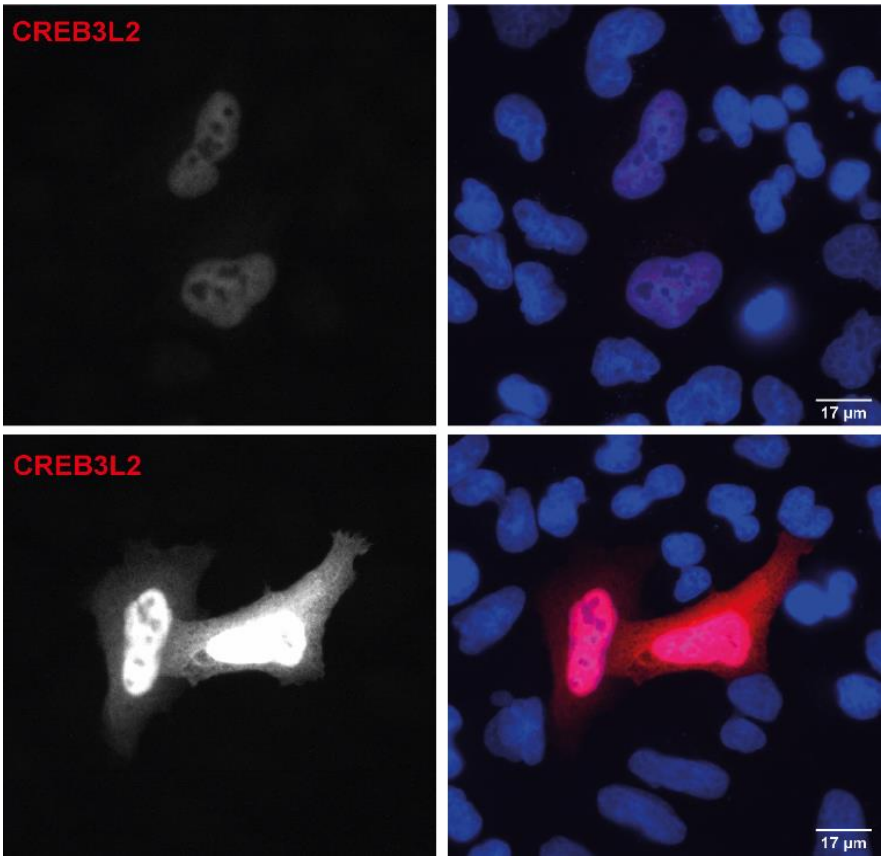

Figure 4.8: The activated form of CREB3L2 is localised predominantly to the nucleus. HeLa cells were transfected with the activated form of CREB3L2 and left overnight. The next day the media was replaced with fresh media containing 2µg/ml of tunicamycin for 16-18 hours. The cells were fixed with methanol and stained with an anti-CREB3L2 antibody. Transfected cells show expression of the protein in the nucleus, with higher expressing cells showing some cytoplasmic expression.

4.2.8 CREB3L2 and Tunicamycin Treatment Increase Expression of SEC24D

We next wanted to investigate whether CREB3L2 and tunicamycin increase the levels of SEC24D by immunofluorescence microscopy. HeLa cells were transfected with the CREB3L2 construct and treated with tunicamycin one day post-transfection and 16-18 hours before fixation. We observed that HeLa cells show a perinuclear staining pattern for SEC24D (**Figure 4.9**). When the cells are transfected with CREB3L2, cells show more dispersed, enlarged, and brighter SEC24D staining. We also note that untransfected cells treated with tunicamycin show brighter SEC24D staining compared to untreated cells which haven't been transfected, however the staining is still compact and not expanded like in the transfected cells. Cells which have been transfected with CREB3L2 and treated with tunicamycin show brighter SEC24D staining which is more spread out than the transfected untreated cells. Therefore, the enlargement of the SEC24D structures seem to either depend on higher expression levels of SEC24D or on the expression CREB3L2, and not the ER stress caused by tunicamycin. Images were quantified and the data suggests a significant increase in SEC24D expression between untransfected and transfected cells (**Figure 4.9B**). However, as this data is from one biological replicate (n=1), further conclusions cannot be drawn. This increase is less significant with tunicamycin treatment where the untransfected cells already have increased SEC24D staining. The level of SEC24D in the transfected groups is not significant whether treated or untreated with tunicamycin suggesting that the level of SEC24D reached with CREB3L2 transfection is not further increased in response to further ER stress possibly as a regulatory mechanism in HeLa cells. Finally, as observed previously in **Figure 4.8**, the transfected cells appear larger.

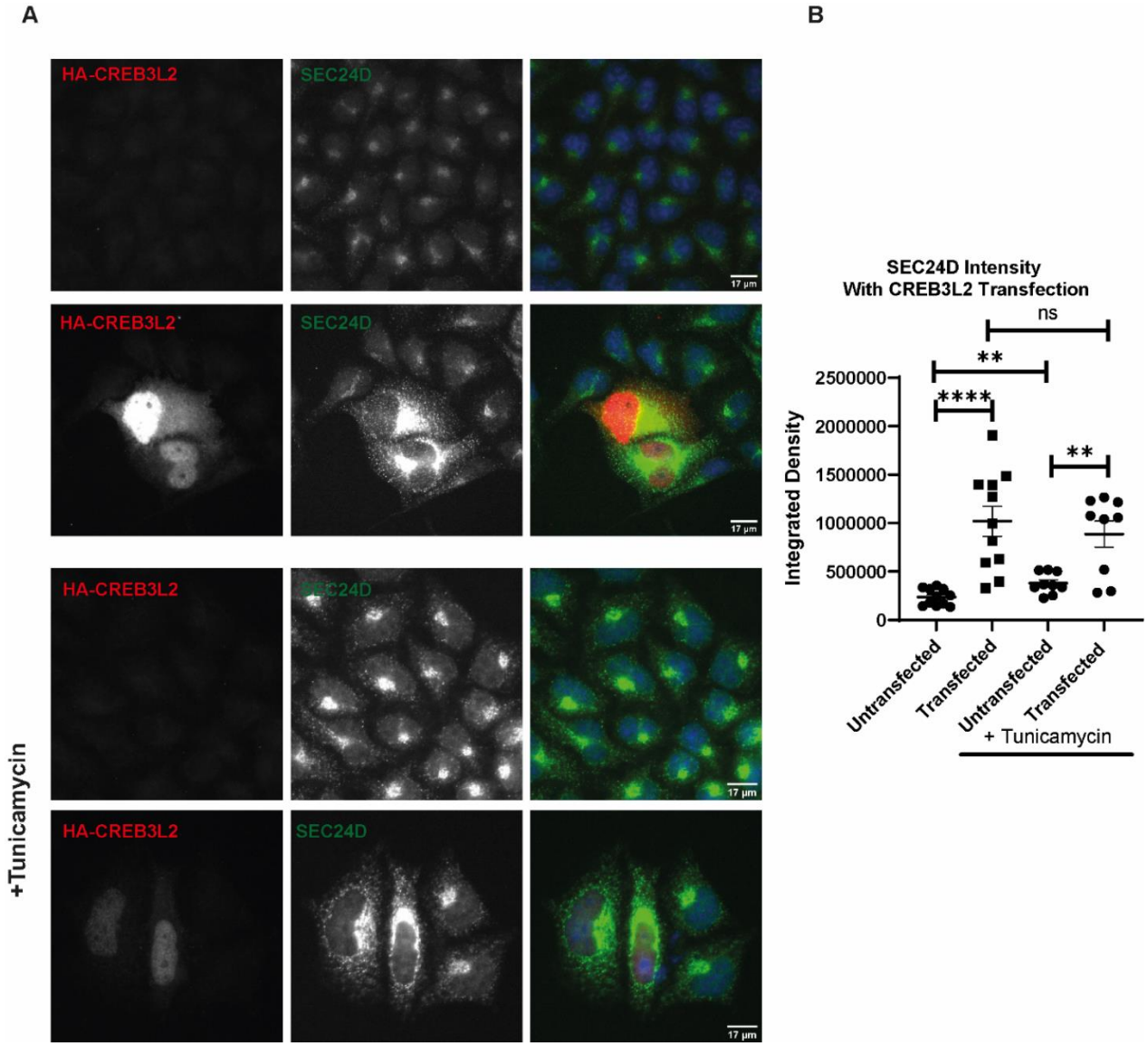

Figure 4.9: Activated CREB3L2 and tunicamycin treatment increase SEC24D levels in HeLa cells. HeLa cells were transfected with active CREB3L2 using ViaFect. The next day, media was replaced with or without 2µg/ml of tunicamycin. 16-18 hours post treatment, cells were fixed using methanol for immunostaining using anti-HA and anti-SEC24D antibodies. **A)** HeLa cells show perinuclear like SEC24D staining while transfected cells with CREB3L2 show more enlarged and dispersed staining. Cells treated with tunicamycin show brighter SEC24D staining in response to treatment. Cells transfected with CREB3L2 prior to tunicamycin treatment show more dispersed staining however do not show significantly more SEC24D staining compared to transfected but untreated cells. **Scale bar: 17µm**. **B)** Quantification **(n=1)** of SEC24D signal in untransfected and transfected cells using integrated density signals. **Unpaired t-testing performed between the described groups. ns; not significant. **; p-value ≤ 0.01. ****; p-value ≤ 0.0001. Error bars indicate standard error of mean.**

4.2.9 Investigating Regulation of Other OASIS Protein Members on SEC24D in HeLa

We have observed that loss of CREB3L2 alone does not impact levels of SEC24D in I.29 cells and that overexpressing CREB3L2 in HeLa cells results in upregulation of SEC24D. We next wanted to investigate whether this effect is shared by other OASIS family members which may support a hypothesis of possible redundancy. Cells were transfected with the activated forms of CREB3L1, CREB4 and Luman in addition to CREB3L2. They were fixed one day post transfection for immunostaining with anti-HA and anti-SEC24D antibodies (**Figure 4.10**). As before, cells transfected with CREB3L2 showed increased expression levels of SEC24D. A similar phenotype was also observed in cells overexpressing activated CREB3L1, and Luman. Cells transfected with CREB4 seemed to have the brightest and most enlarged SEC24D staining from the constructs tested in this experiment. To more easily investigate this, we developed a flow cytometry-based assay to measure the expression levels of SEC24D.

4.2.10 Flow Cytometry Assay to Assess Impact on OASIS Family Members on SEC24D and Cell Size

To quantify the impact of OASIS family members more effectively on SEC24D and cell size we performed intracellular staining and flow cytometry. Cells were transfected as previously described and fixed using methanol (**Figure 4.11**). Cells with CREB3L2 expression show higher SEC24D expression levels compared to untransfected cells (~2.6-fold increase). As previously observed, CREB4 is more effective at driving SEC24D expression possibly due to its greater stability (~4.2-fold increase). We then gated for HA-positive and HA-negative cells in the transfected population to quantify changes in cell size. As expected, cells expressing CREB3L2 and CREB4 appear to be larger than the non-transfected controls (~1.1 and ~1.2-fold changes respectively).

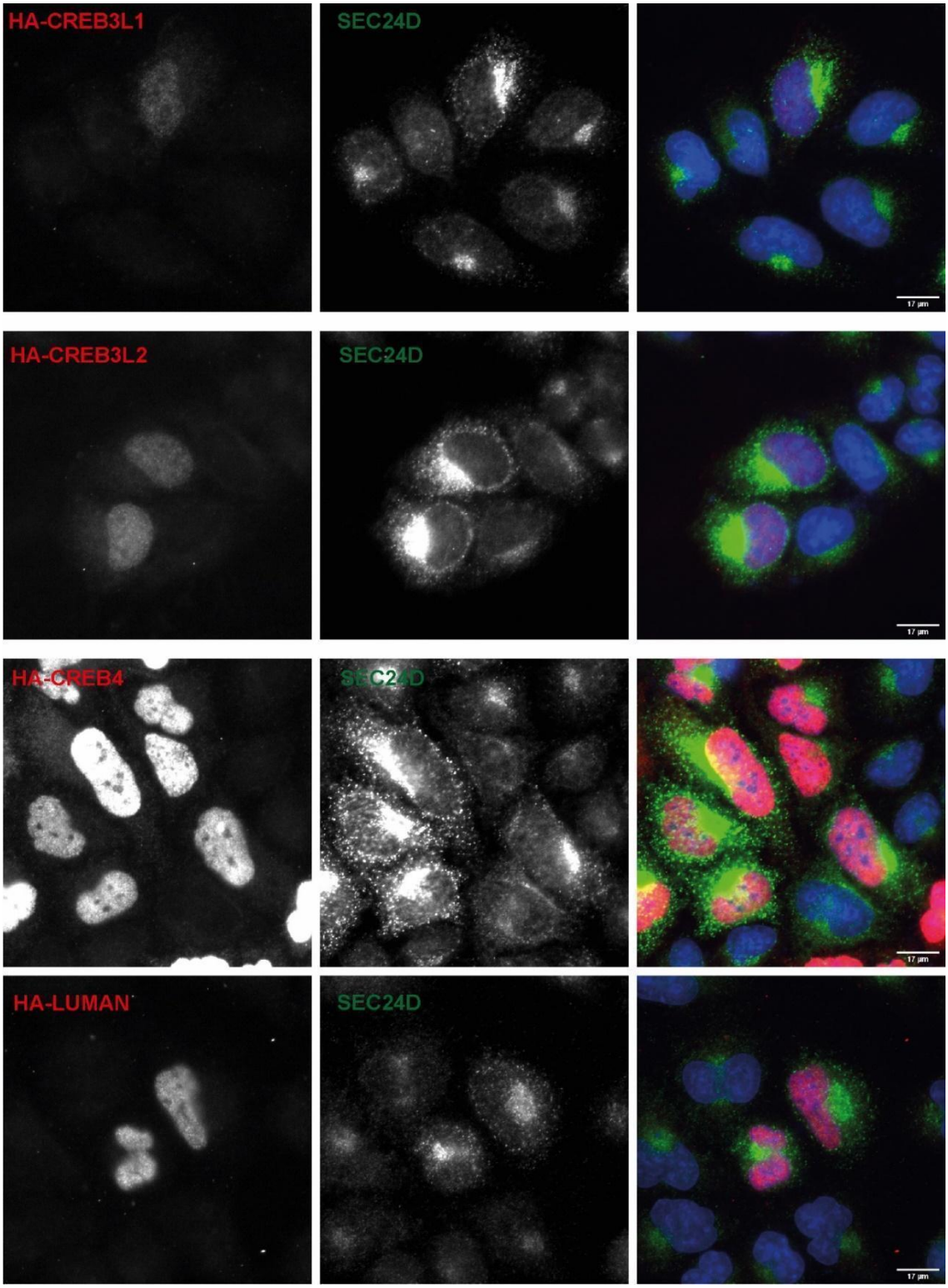

Figure 4.10: Transfection of active CREB3L1/2, CREB4 and Luman in HeLa cells increases SEC24D protein levels. Cells were transfected with the mentioned constructs and fixed one day post transfection with methanol for immunostaining using anti-HA and SEC24D antibodies. Results indicate a potential upregulation of SEC24D in response to all transfected proteins. CREB3L2 and CREB4 seem to have the most pronounced impact on SEC24D levels.

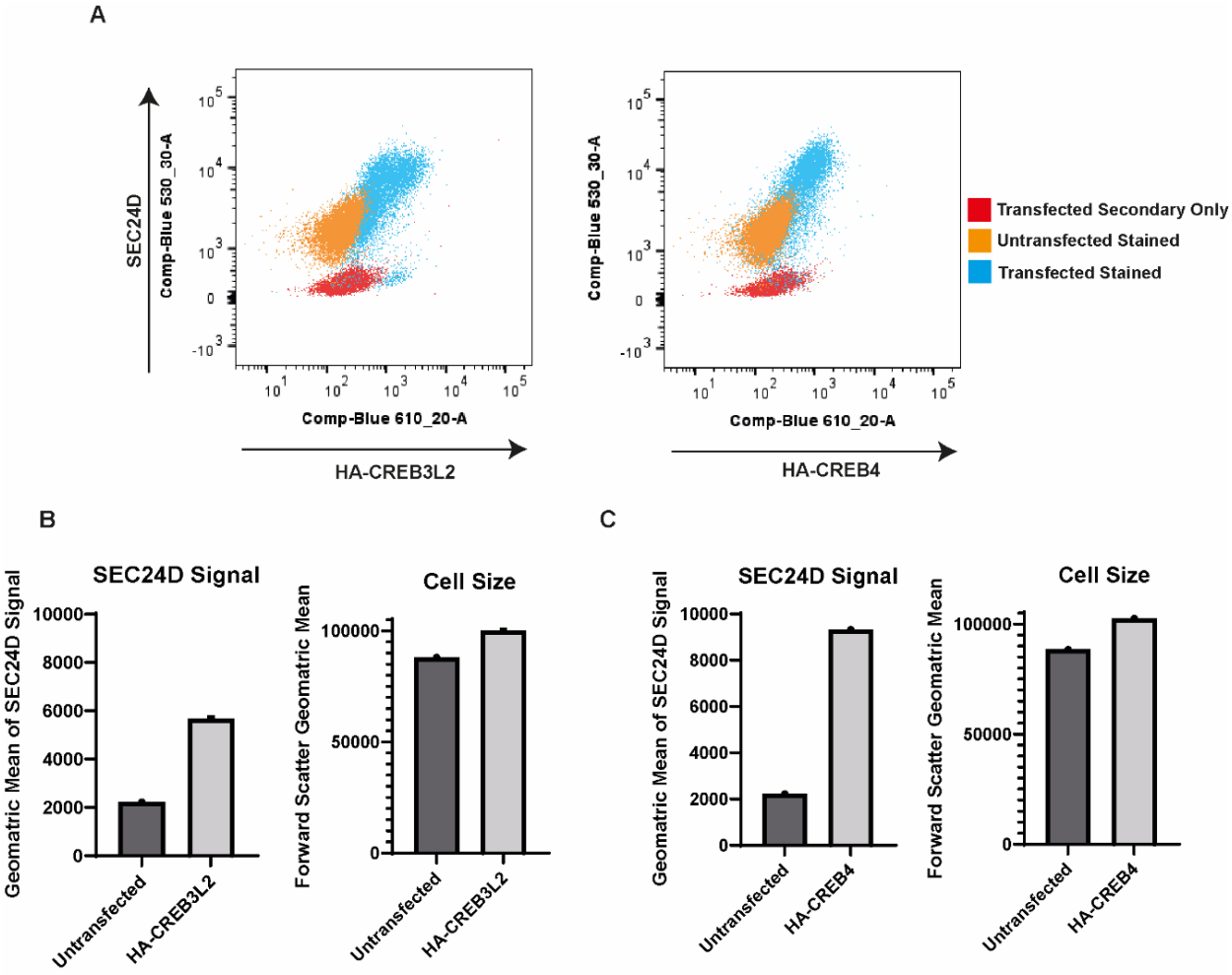

Figure 4.11: CREB3L2 and CREB4 increase cell size and expression of SEC24D. HeLa cells were transfected with HA-CREB3L2 and HA-CREB4 with ViaFect. 2 days post transfection, cells were fixed with methanol and stained with anti-HA and SEC24D antibodies. Cells were then run on the LRSII flow cytometer and live cells were gated using forward and side scatter to analyse fluorescence intensities of stained cells**. A)** Dot plot showing SEC24D expression in response to the expression of activated CREB3L2 and CREB4. **B)** HA-positive and negative cells were gated in the transfected population to quantify the fluorescence signal of SEC24D, and the geometric mean of the forward scatter of the cells (indicating size) in the transfected and untransfected cells **(C)** (**n=1**).

4.2.11 Investigating Impact of SEC24D's Loss on I.29 Differentiation and ER Markers

We have shown that perturbations in CREB3L2 alone does not result in reduction in SEC24D indicating a potential redundancy with other OASIS family members in the I.29s. We next wondered whether SEC24D itself is required for proper CREB3L2 trafficking for its activation. Unfortunately, we have struggled to see the activated form of CREB3L2 in the I.29s with the antibodies we had at the time. As an alternative way to explore this hypothesis, we moved to characterise the effect of SEC24D's loss in the I.29 cells by profiling the expression levels of protein markers of ASCs, most of which are also regulated by CREB3L2. Proteins predicted to be regulated by CREB3L2 include FNDC3B, SEC31A and SEC23A. C41 which has significantly reduced levels of SEC24D was induced to differentiate by LPS and collected for processing for immunoblotting two days post induction for the following proteins.

Assessing Regulation of Transcription Factors in C41

We first looked at the spliced form of the well characterised transcription factor XBP1 as an indicator of differentiation and the membrane bound transcription factors ATF6 and CREB3L2. We observed no significant difference in the protein levels of the mentioned factors (**Figure 4.12**). The band shown for CREB3L2 is the unprocessed form, therefore does not provide information on whether there is an effect on CREB3L2's processing in C41.

Assessing Regulation of COPII Subunits

As SEC24D exists in a complex of other coat proteins, we next looked at the protein levels of the other COPII components in the absence of SEC24D. SEC31A and SEC23 are both predicted to be regulated by CREB3L2. We noted a significant reduction in both SEC31A and SEC23 (**Figure 4.13**) in C41.

ER Proteins and SNAREs

Moving from the COPII subunits, we looked at ER proteins upregulated during differentiation (**4.14A**). BIP, a protein chaperone and marker of ER stress, showed no significant difference in C41. Interestingly, we observed a significant reduction in FNDC3B, a poorly characterised transmembrane protein which we previously identified as highly co-expressed with CREB3L2 (Rahman, 2019). We also look at FNDC3A, its homologue, which we also previously identified to be consistently upregulated in ASCs but to a lesser extent to FNDC3B and find a small and insignificant reduction. We finally look at the levels of the SNAREs SEC22B and YKT6 which are upregulated in ASCs (**Figures 4.14B**) and observe no significant differences in C41.

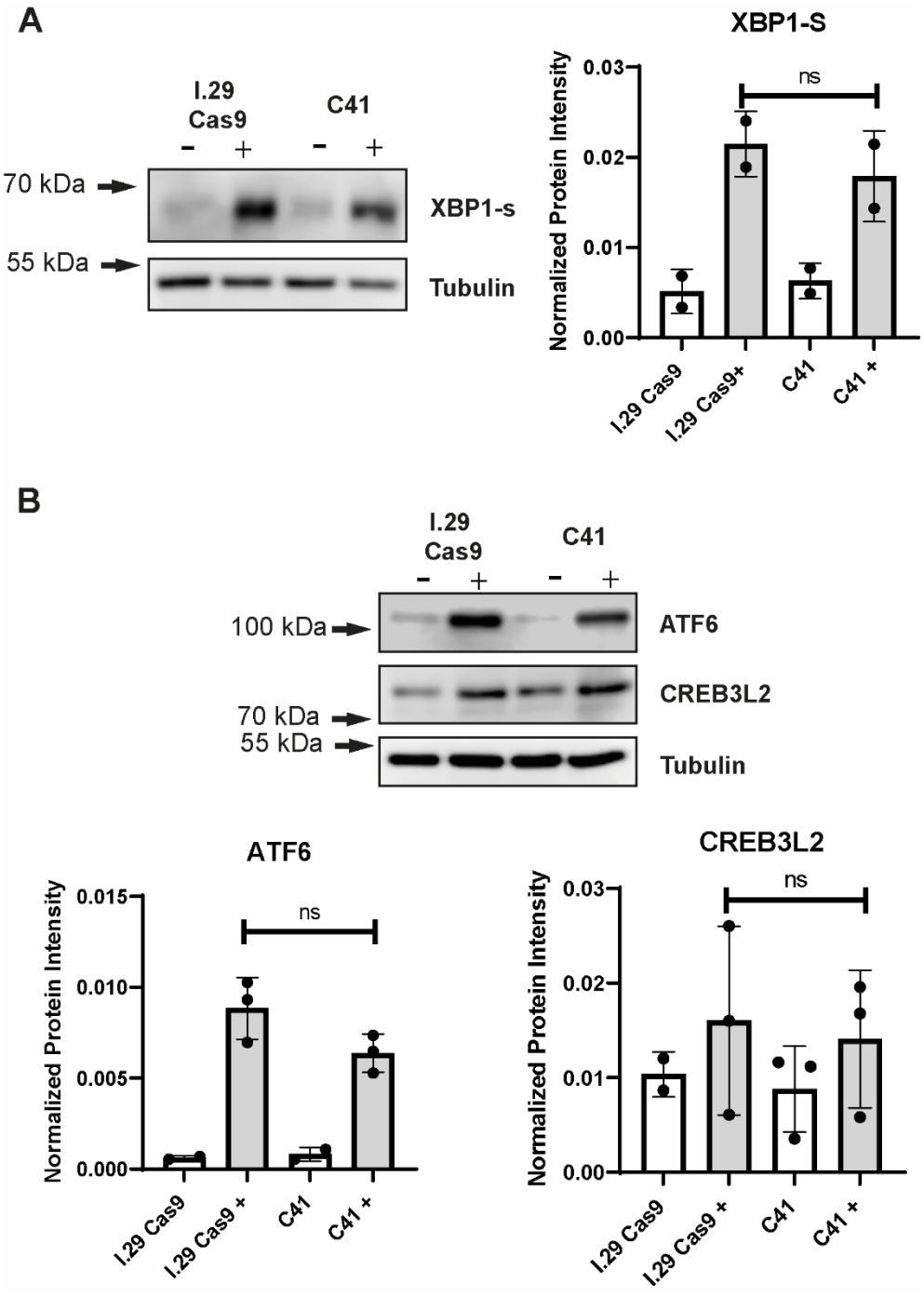

Figure 4.12: SEC24D deficient I.29 cells (C41) have normal protein levels of XBP1-s, ATF6 and CREB3L2. I.29 cells differentiated with 20µg/ml of LPS (+) were collected two days post induction for immunoblot analysis of spliced XBP1 **(A)** and ATF6 and CREB3L2 **(B).** Quantification was performed by normalising protein intensities against tubulin. **Unpaired t-test performed on data from three biological replicates (n=3). ns; not significant. Error bar indicates standard deviation of the mean.**

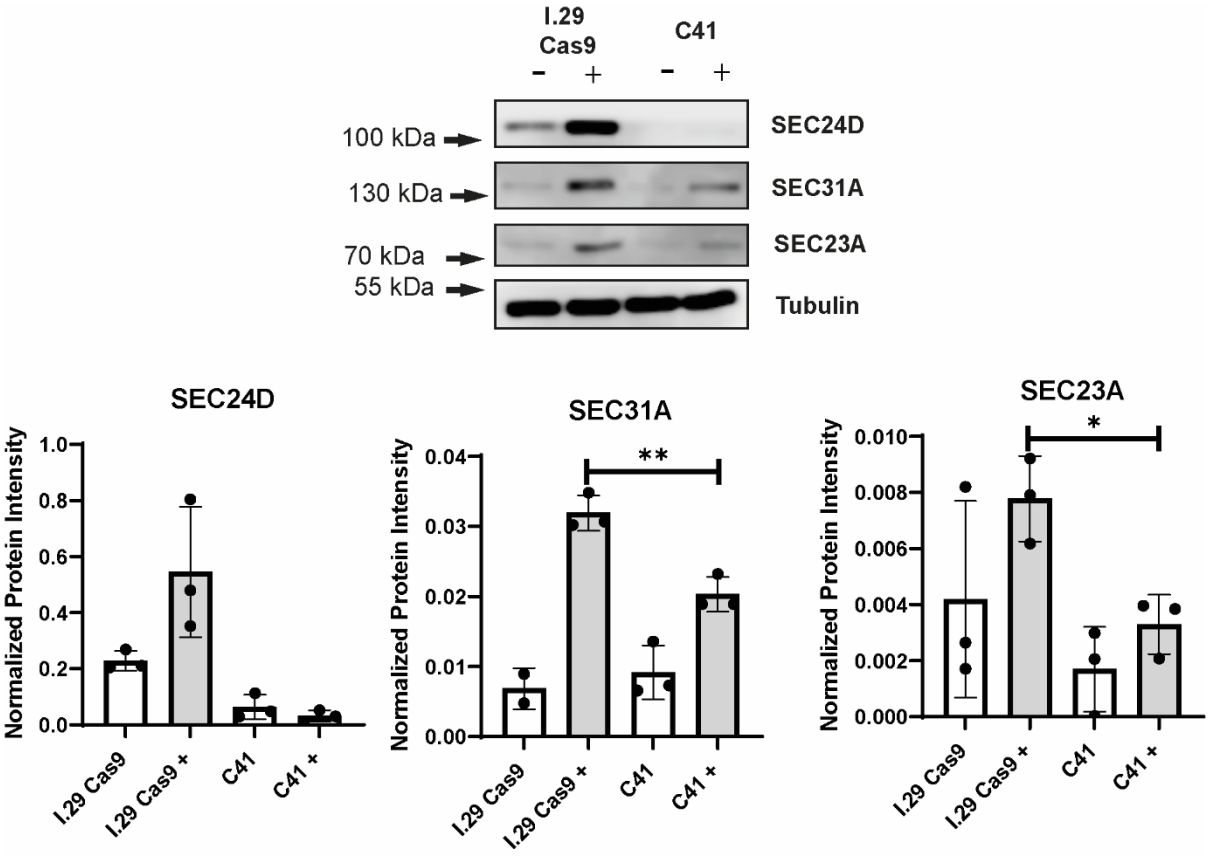

Figure 4.13: SEC24D deficient differentiated I.29 cells (C41) have reduced levels of SEC31A and SEC23. I.29 cells differentiated with 20µg/ml of LPS (+) were collected two days post induction for immunoblot analysis of SEC24D, SEC31A and SEC23. Quantification was performed by normalising protein intensities against tubulin. **Unpaired t-test performed on data from three biological replicates (n=3). *; p-value ≤ 0.05. **; p-value ≤ 0.01. Error bar indicates standard deviation of the mean.**

Note: Quantification of SEC24D levels in C41/+ is an artefact due to background levels around expected bands' locations.

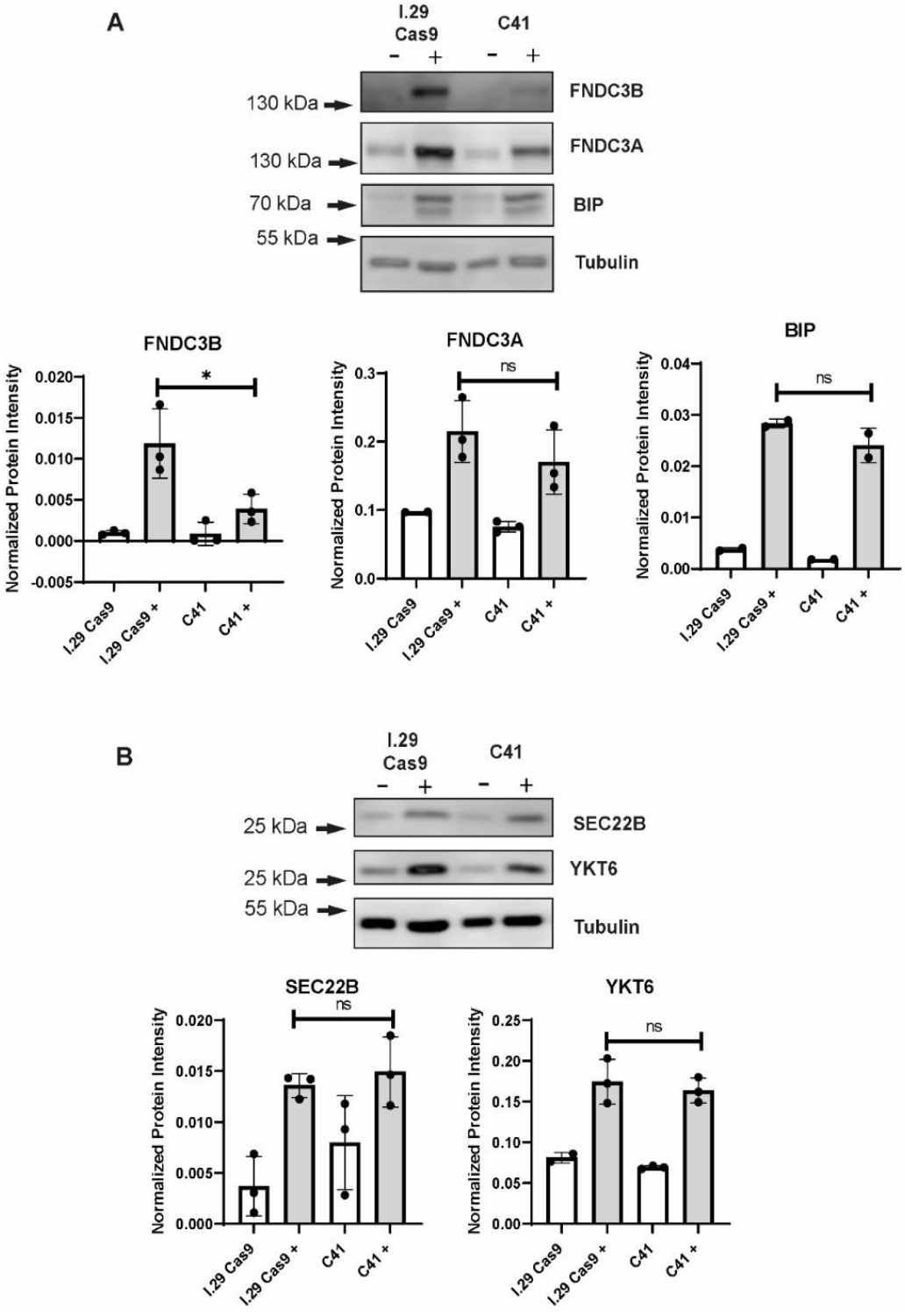

Figure 4.14: SEC24D deficient differentiated I.29 cells (C41) have reduced levels of FNDC3B. I.29 cells differentiated with 20µg/ml of LPS (+) were collected two days post induction for western blot analysis of FNDC3B, FNDC3A and BIP (**A**) and the SNAREs SEC22B and YKT6 (**B**). Quantification was performed by normalising protein intensities against tubulin. **Unpaired t-test performed on data from three biological replicates (n=3). ns; not significant. *; p-value ≤ 0.05. Error bar indicates standard deviation of the mean.**

The data described so far suggests that loss of SEC24D on its own does not impact the secretion of IgM possibly due to redundancy with other SEC24 paralogues. Its loss also does not impact the general differentiation process of the cells as shown by normal levels of transcription factors in response to induction. Differentiated cells also seem to have normal levels of BIP and the upregulated SNAREs SEC22B and YKT6. However, we observed a significant reduction in the other COPII vesicle components SEC31A and SEC23A, and in FNDC3B. To confirm that this phenotype is caused by the loss of SEC24D and not a clone specific phenotype, we next aim to rescue C41 cells by reintroducing SEC24D and seeing whether the impacted proteins return to normal levels. Importantly, we also aim to profile more proteins to better dissect the potential role of SEC24D.

4.2.12 SEC24D Rescue in C41 Cells - Creating a SEC24D construct resistant to Cas9

To confirm that the observed reductions in SEC31A, SEC23 and FNDC3B were specific to the loss out of SEC24D, we proceeded to re-introduce SEC24D into the C41 cells. To create the SEC24D construct for viral transduction we obtained a plasmid (SinoBiological, Cat #: MG5A4182-U) which encodes the cDNA of mouse SEC24D. As C41 cells stably express Cas9 and the guide against SEC24D, we used site directed mutagenesis to generate a construct which was resistant to the guide (**Figure 4.15**). The SEC24D sequence in the successfully mutated construct was then cloned into a lentiviral PLVX-IRES plasmid, which was used to transduce the C41 line.

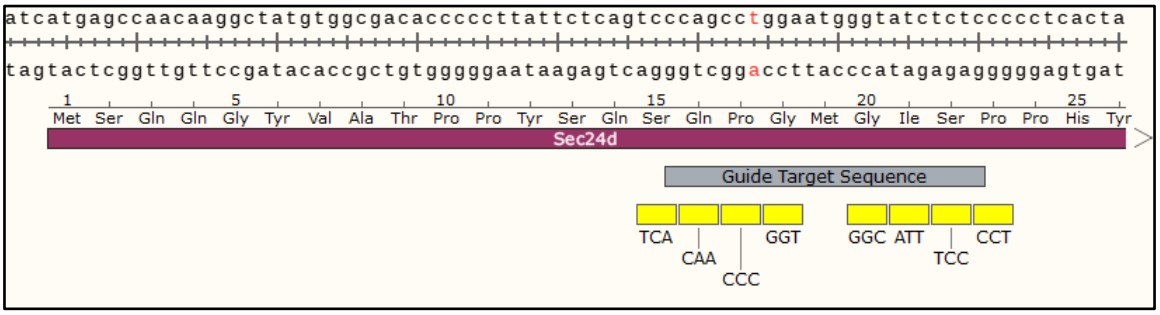

Figure 4.15: Mutating SEC24D's sequence for resistance against the guide. Figure showing part of SEC24D's sequence with the RefSeq NM_027135.2 (used in plasmid #MG5A4182-U) visualised using SnapGene viewer. Highlighted in grey is the sequence targeted by the guide stably expressed by C41 and coloured in red is the nucleotides predicted to be cut by the Cas9 endonuclease. Primers (**Table 2.2**) were designed to be used with the Q5 polymerase to introduce the base pair substitutions shown in yellow to prevent the guide's recognition of the sequence while conserving the amino acids.

4.2.13 Reintroducing SEC24D in C41 Cells

SEC24D was reintroduced into C41 cells by viral transduction and a stable population of cells were selected using the appropriate antibiotic. The cells were assayed for SEC24D protein expression using immunofluorescence (IF) microscopy and immunoblotting (**Figure 4.16**). As predicted the population of cells expressed SEC24D. Surprisingly, the levels of the SEC24D were regulated by LPS induction even though SEC24D expression is driven by the exogenous CMV promoter. We have previously observed a similar phenotype for the Cas9, TurboID and ApexID expression cassettes in I.29 cells. This may be caused by the cells changing their transcriptional program during differentiation (**see 3.2.2.8**). As this upregulation is what would normally happen in response to LPS treatment this result is potentially beneficial. However, the expression level of the SEC24D construct was weaker compared to endogenous SEC24D expression in the parental population (**Figure 4.16A**). To determine how uniform the SEC24D expression was within the population of cells we utilised immunofluorescence microscopy. The levels of SEC24D within the population were heterogeneous and most cells exhibited lower SEC24D levels than the parental control (**Figure 4.16B**).

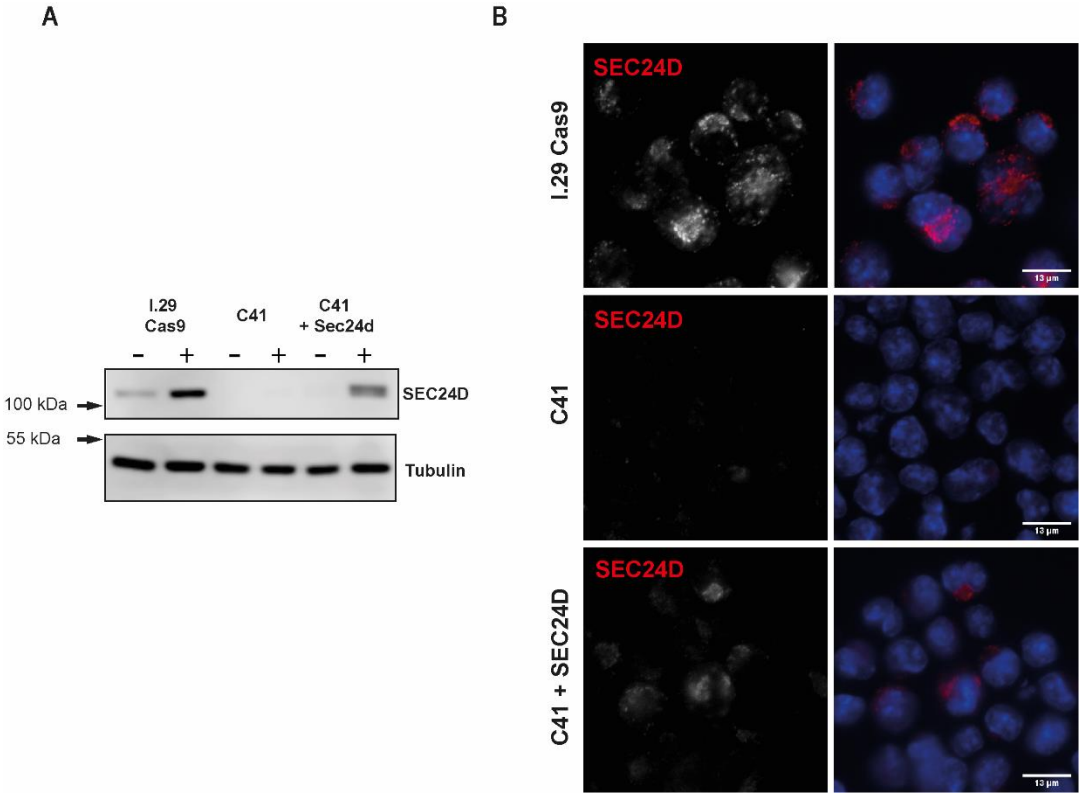

Figure 4.16: The level of SEC24D expression in C41 rescue population is heterogeneous. A) Cells were differentiated using LPS (+) and collected two days post induction. Collected pellets were processed for immunoblotting and blots probed with anti-SEC24D antibody. Blots show that the rescue population expresses less SEC24D than the parent when induced with LPS. **B)** 2 days post differentiation cells were collected, centrifuged on fibronectin coated coverslips and immunofluorescence microscopy performed to stain for SEC24D. C41 rescue population showed heterogeneous SEC24D expression with most cells exhibiting low expression compared to the parent.

4.2.14 Single-Cell Cloning to Generate a Clonal Line with Higher Levels of SEC24D

In the previous experiment, it was clear that there was significant heterogeneity of SEC24D expression in the transduced C41 population. To mitigate this problem, we performed single cell cloning of the transduced population to select clones which express SEC24D at comparable level to the parental population. To measure the levels of SEC24D in the reconstituted clones immunoblotting was performed on cells differentiated with LPS post 2 days of induction. **Figure 4.17** shows a representative blot of the clones (C1, C4, C7 and C9). Clone 4 (C4) has the highest levels of SEC24D expression. We also determined the levels of FNDC3B in the clones and observed that its expression was higher than the C41 cells suggesting a possible link between SEC24D and FNDC3B. Therefore, to continue our characterisation, we moved forward with C4 as a reconstituted clone to investigate whether the previously observed phenotypes could be rescued.

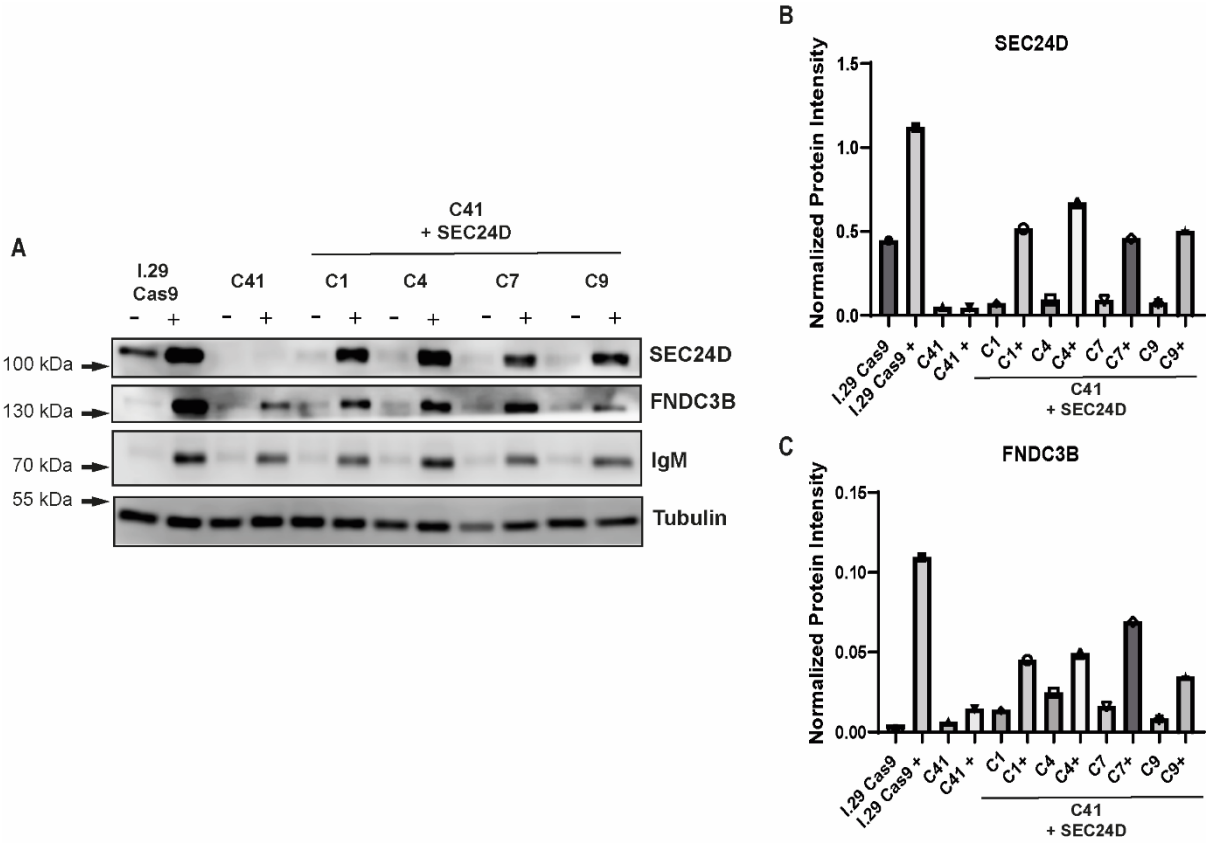

Figure 4.17: SEC24D may regulate the levels of FNDC3B. Cells were differentiated using 20µg/ml of LPS and collected 2 days post LPS induction (+). Cell lysates were processed for immunoblotting. Results showed C4 as having the highest SEC24D expression level among the rescued clones **(A) (B)** and that all rescued clones had higher expression of FNDC3CB than C41 which significantly lacks SEC24D **(C).** Quantification is from one biological replicate (**n=1**)

4.2.15 Profiling Differentiation Markers in C41 and SEC24D Reconstituted cells

To determine the role of SEC24D in remodelling the biosynthetic pathway and whether the previously observed phenotypes are SEC24D specific, we used immunoblotting to examine the level of key factors in the SEC24D mutant and reconstituted cells. All immunoblots performed to this point of the thesis were done using chemiluminescence (ECL). For this set of characterization experiments, we moved to using fluorescent secondary antibodies in an effort to yield more robust quantification of protein levels. The cells were induced to differentiate by LPS treatment and collected for processing for immunoblotting two days post induction for the following proteins.

ATF6, COPII Proteins and SNAREs

We look again at the transcription factor ATF6 in this set of experiments and note no significant differences between all three cell lines indicating that the reconstituted clone is responding as expected in response to differentiation (**Figure 4.18A**). We next look at the COPII components and as previously seen, there is a significant reduction in SEC23 levels in C41 (**Figure 4.18B**). In the rescue clone, SEC23 levels increase suggesting that loss of SEC24D may be responsible for this phenotype in C41 cells. The same trend is observed for SEC31A. The reduction in SEC31A in this set of experiments is not significant as we have seen previously (**Figure 4.13**).

In addition to the SNAREs SEC22B and YKT6 which we previously looked at and found to be unchanged in C41, we also look at Syntaxin5 and Vamp3 (**Figure 4.19**). All tested SNAREs show no significant differences between cell lines.

ER Proteins

We have previously seen a significant reduction in FNDC3B in C41 cells. In this set of experiments, this is also observed, and the significant reduction is diminished with the re-introduction of SEC24D (**Figure 4.20**). As before, we also saw an insignificant reduction in FNDC3A, which is also reversed here with the reintroduction of SEC24D. To investigate whether this effect is specific to FNDCB/A and not a general effect in ER localised proteins, we look at another 3 ASCs markers which reside in the ER (IRE1alpha, ERp72 and CRELD2) and note no significant differences. We also utilised immunofluorescence (IF) microscopy to stain for FNDC3B in the 3 cell lines (**Figure 4.21**). C41 cells show reduced staining of FNDC3B compared to the parent line. The rescued clone (C4) shows more FNDC3B staining compared to C41 albeit still less than the parent. C41 cells also seem smaller in size compared to the parent. At least 30 cells of each condition were quantified (**Figure 4.21B**), however this is only from one biological replicate so the significance of any observed phenotype cannot be drawn from the IF data.

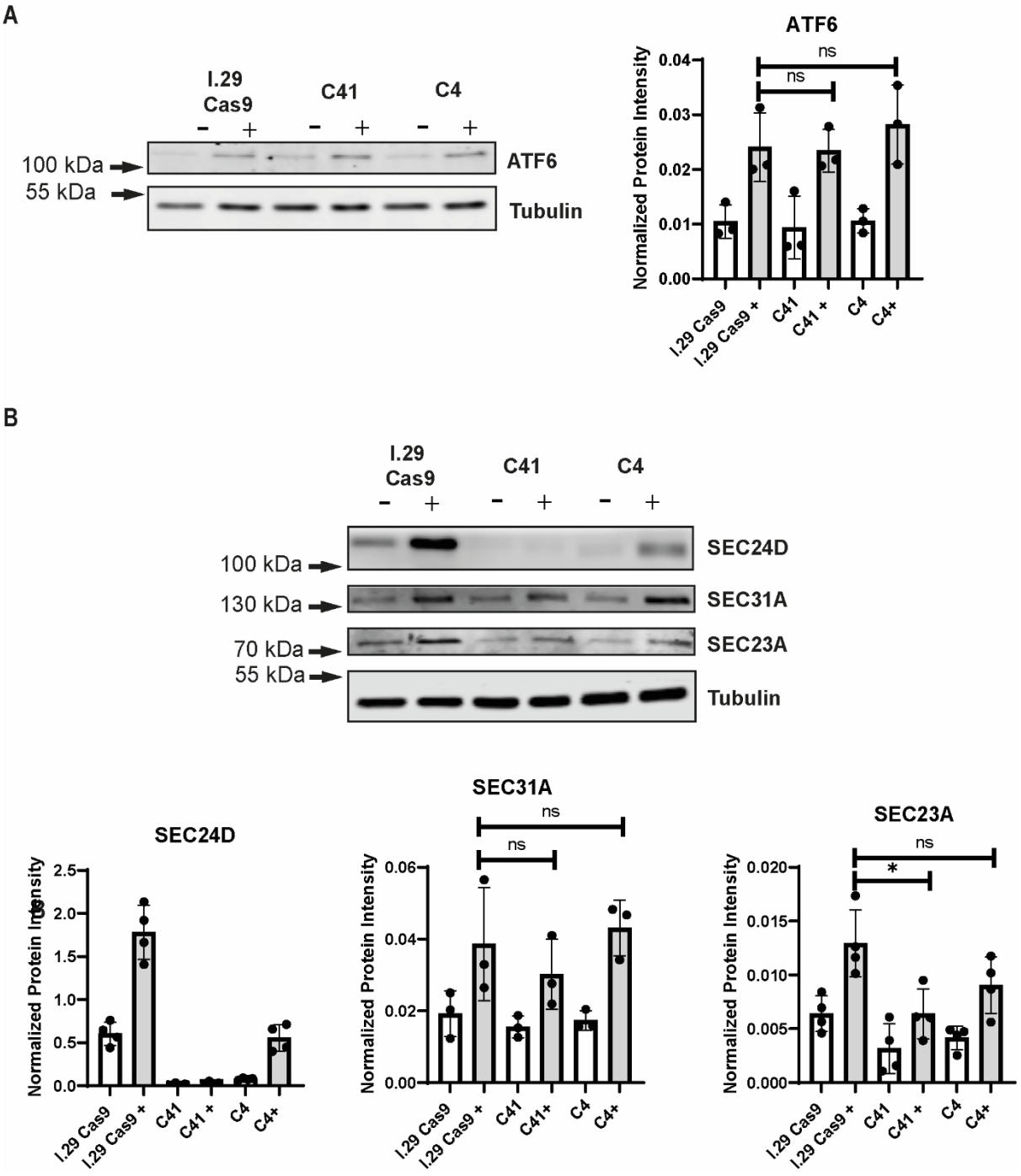

Figure 4.18: SEC24D deficient I.29 cells have normal levels of ATF6 and reduced levels of SEC23. I.29 cells differentiated with 20µg/ml of LPS (+) were collected two days post induction for immunoblotting of the transcription factor ATF6 **(A)** and the COPII components SEC24D, SEC31A and SEC23 **(B).** Quantification was performed by normalising protein intensities against tubulin. **Unpaired t-test performed on data from three biological replicates (n=3). ns; not significant. *; p-value ≤ 0.05. Error bar indicates standard deviation of the mean.**

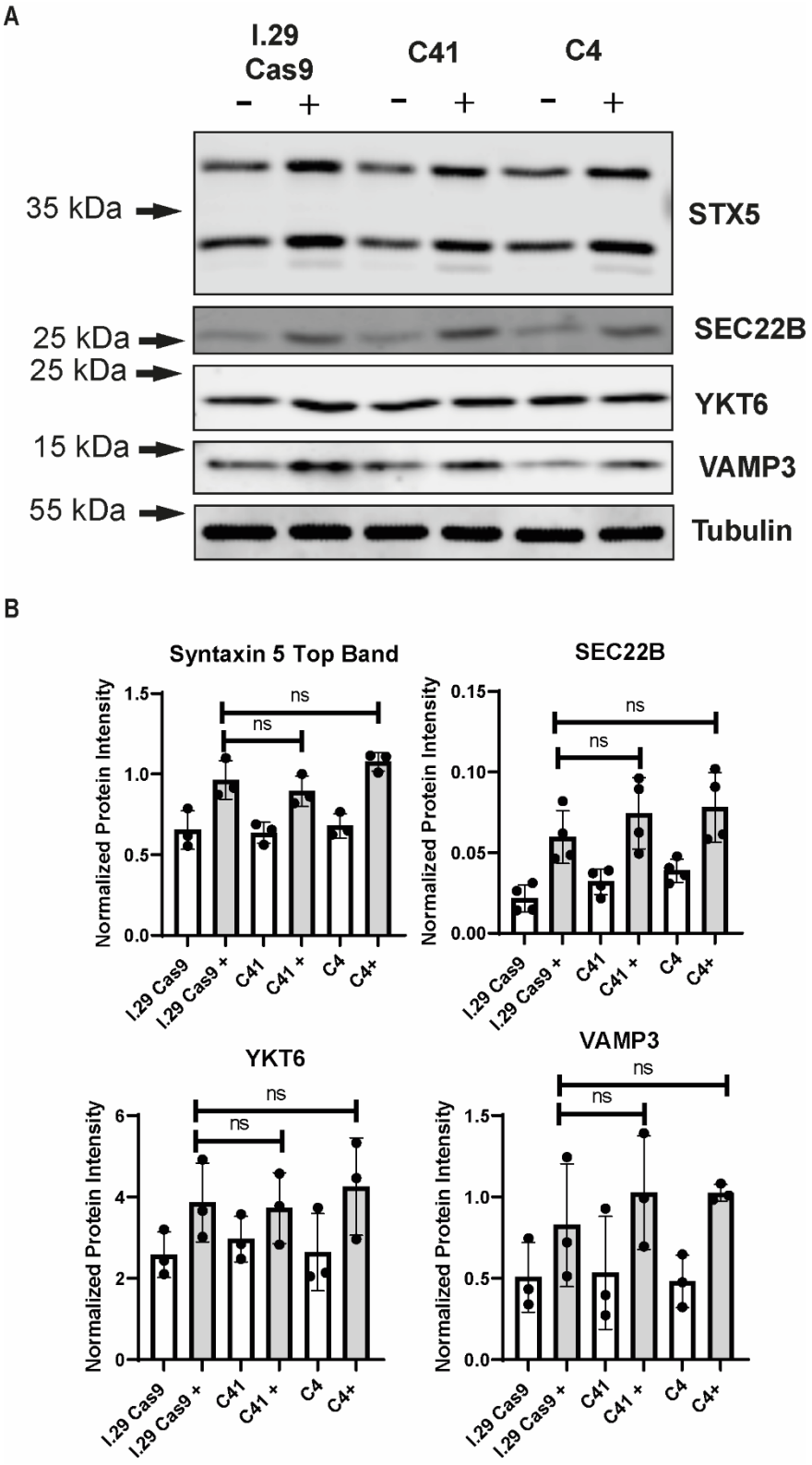

Figure 4.19: SEC24D deficient I.29 cells have normal levels of the SNAREs STX5, SEC22B, YKT6 and VAMP3. I.29 cells differentiated with 20µg/ml of LPS (+) were collected two days post induction for immunoblotting **(A).** Quantification was performed by normalising protein intensities against tubulin **(B)**. **Unpaired t-test performed on data from three biological replicates (n=3). *; p-value ≤ 0.05. Error bar indicates standard deviation of the mean.**

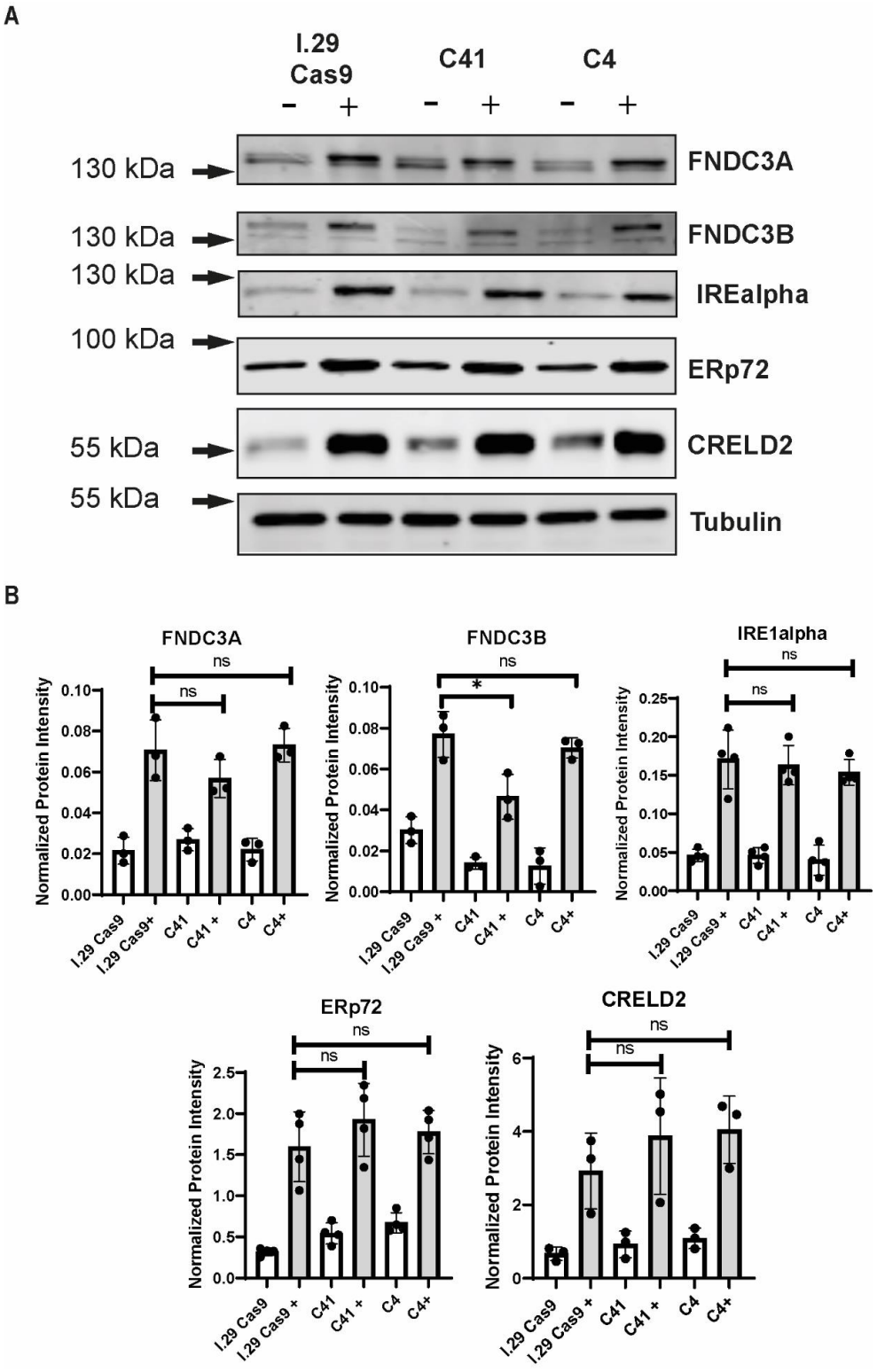

Figure 4.20: SEC24D deficient I.29 cells have reduced levels of FNDC3B and normal levels for other ER proteins. I.29 cells differentiated with 20µg/ml of LPS (+) were collected two days post induction for immunoblotting of FNDC3B, FNDC3A, IRE1alpha, ERp72 and CRELD2 **(A)** Quantification was performed by normalising protein intensities against tubulin **(B). Unpaired t-test performed on data from three biological replicates (n=3). ns; not significant. *; p-value ≤ 0.05. Error bar indicates standard deviation of the mean.**

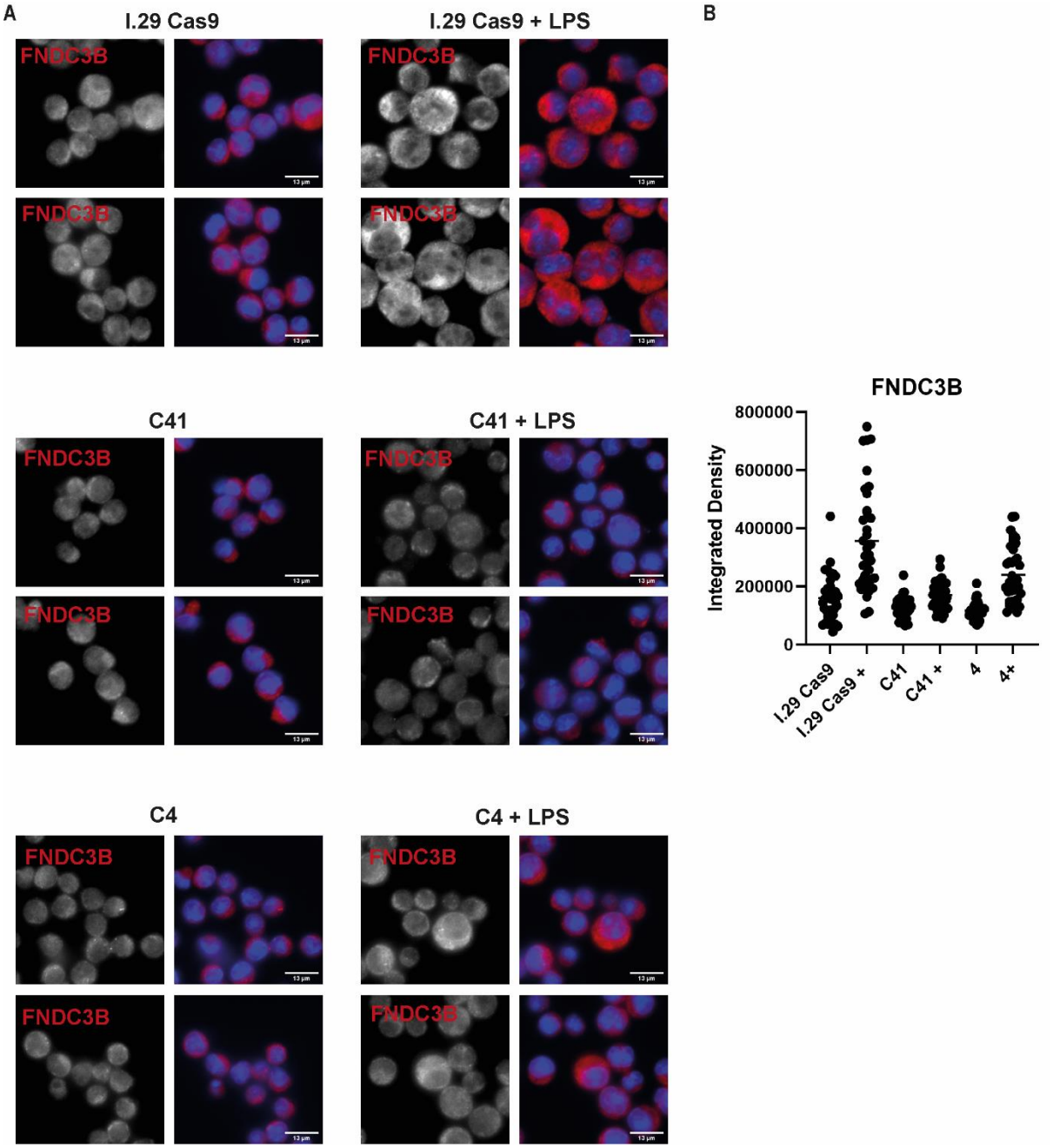

Figure 4.21: C41 shows reduced FNDC3B levels using immunofluorescence microscopy. 2 days post differentiation with 20µg/ml of LPS, cells were collected, centrifuged on fibronectin coated coverslips. Cells were fixed using methanol and immunofluorescence performed to stain for FNDC3B **(A)**. **B)** FNDC3B signal was quantified from at least 30 cells from each condition using ImageJ and integrated density plotted. The quantification is from one biological replicate **(n=1)**. **Scale bar = 13µm**

4.2.16 C41 Cells have Enhanced Viability Four Days Post LPS Induction

Differentiated I.29 cells typically exhibit significant cell death four days post LPS induction due to proteostatic stress. During our experimental work, we noted that the SEC24D mutant clone (C41) line generally exhibited better fitness in culture and retained higher viability post induction. To directly test this, the cell lines were induced to differentiate by LPS and collected four days post induction. The cells were stained using propidium iodide (PI) as a viability dye which labels the DNA inside permeable cells, and the cells were analysed using flow cytometry (**Figure 4.22**). On average ~34%, 24% and 25% of cells at day 4 were stained by PI for the parent line, C41 and the rescue clone (C4) respectively. Surprisingly, the reconstituted clone still showed enhanced viability at day 4. This result potentially suggests that this phenotype is not SEC24D specific or that the SEC24D levels in these cells is not sufficient to rescue this phenotype. SEC24D's expression level in the rescue clone (C4) is around ~30% of the level expressed in the parent at day two post induction (**Figure 4.18**).

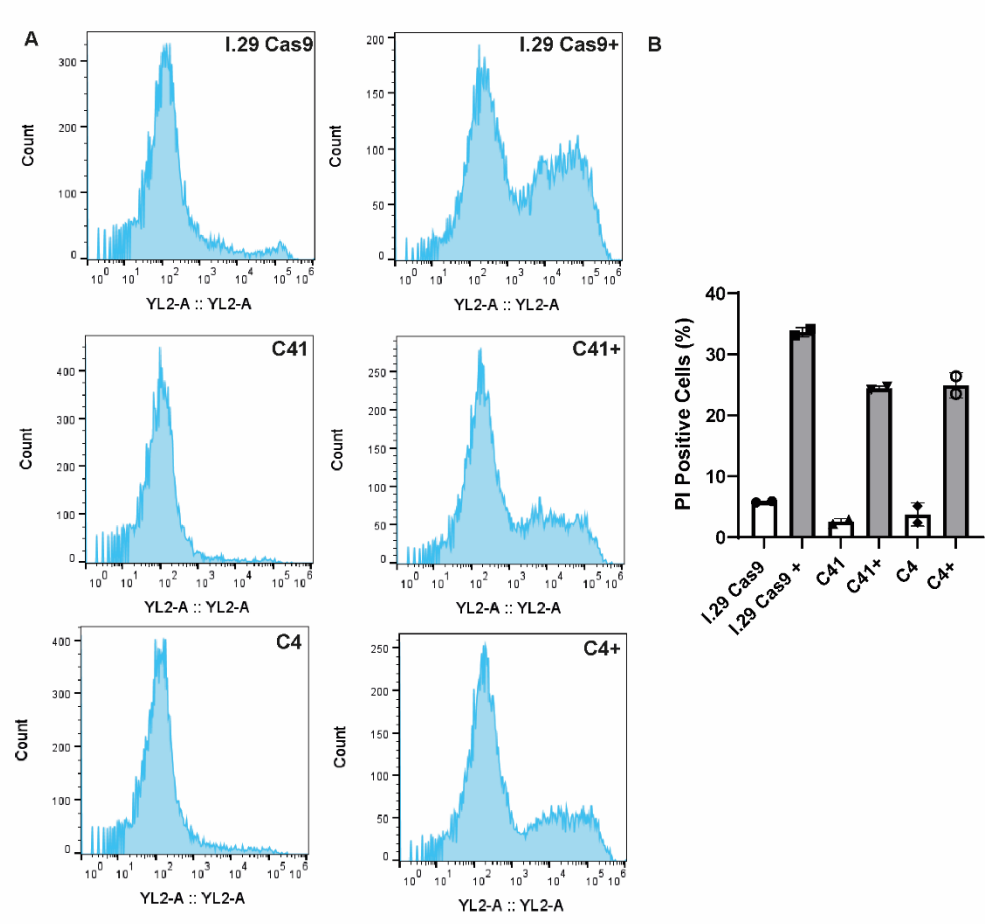

Figure 4.22: SEC24D deficient cells exhibit enhanced viability at day 4 post LPS induction. I.29 cells were induced to differentiate using 20µg/ml of LPS (+). Four days post induction, around $1x10^6$ cells were collected and resuspended in 300µl of fresh media. PI were then added to the cells, and they were mixed by gently inverting the tube for ~20 to 30 seconds. They were then run on the Attune flow cytometer to measure PI incorporation into dead cells by looking at the YL2 channel and the data is presented as histograms. Cell lines tested are the I.29 parent cell line (expressing Cas9), SEC24D mutant I.29 clonal line (C41) and SEC24D rescued C41 clonal line (C4) **(A). B)** PI positive cells were quantified as a percentage of total cell population.

4.3 Chapter Discussion & Summary

The main aims of this chapter were to investigate the role of SEC24D in antibody secretion. To achieve this, we generated a SEC24D deficient I.29 cell line and determined whether the loss of SEC24D impacted antibody secretion and ER proteostasis. We also investigated the regulation of SEC24D by CREB3L2, and whether loss of SEC24D impacted other proteins potentially regulated by CREB3L2. Finally, we explored whether other OASIS family proteins can regulate SEC24D levels.

4.3.1 SEC24D is not Required for IgM Secretion

According to our previous proteogenomic data, SEC24D is highly upregulated in ASCs (**Figure 1.4**). Our first hypothesis to test was whether it was required for IgM synthesis and secretion, and we have shown that the absence of SEC24D two days post induction does not impact either (**Figure 4.6**). We have previously noted a potential link between collagen and antibody secretion based on the upregulation of several genes in ASCs implicated in collagen secretion such as NBAS, SEC24D and CREB3L2 (Rahman, 2019). To further draw from this link, we look at the requirement for different SEC24 paralogues for collagen export. Even though mutations of SEC24D have been reported with severe skeletal phenotypes, mouse fibroblasts lacking SEC24D or depleted from any individual SEC24 paralogue show no accumulation of collagen (Lu et al., 2022). Accumulation of collagen only occurred with the double depletion of SEC24A or D with any other paralogue which was suggested to occur due to a modest block in ER export of procollagen. Knocking down three paralogues also resulted in modest phenotypes, while knocking down all four paralogues resulted in a considerable block in collagen secretion. Therefore, the authors propose that the consequence of SEC24D KO depends on the presence of other paralogues in the tissue and that they can cooperate to facilitate ER export of some proteins, in this case procollagen or its adaptors. They propose a model where a threshold level of any SEC24 paralogue is required for efficient export of procollagen in which its export signal is shared among the paralogues. This redundancy can be demonstrated by other cargo proteins in addition to collagen, such as CD59 and fibronectin which are preferentially exported with SEC24C and SEC24D (Bonnon et al., 2010) (Lu et al., 2022).

Relating this potential redundancy between SEC24 paralogues for cargo secretion, it is also likely that the secretion of immunoglobulins (Ig) does not rely on only one paralogue. It would be interesting to perform protein depletions of other SEC24 paralogues in the SEC24D KO cells and assess which combination of depletions leads to a significant reduction to assess whether there might be preferential selection of the Ig. **Figure 1.4** shows the PlasmacytOMICs plots of the COPII components in ASCs. SEC24A is the second next highly upregulated SEC24 protein making it likely to be a key paralogue in ASCs. This does not rule out possible contributions to Ig trafficking by the other

paralogues, SEC24C and SEC24B. SEC24C is mildly upregulated, whilst SEC24B is downregulated. However, as this data does not indicate actual protein expression levels, more experiments investigating all paralogues need to be performed.

4.3.2 CREB3L2 is not Required for SEC24D's Upregulation

In ASCs, our previous proteogenomic project's data showed that CREB3L2 was co-expressed with the highest number of markers which were involved in trafficking. Similarly, in Drosophila, more than half the genes targeted by CrebA which is most similar to the mammalian orthologues CREB3L1/2 are involved in the secretory pathway (Fox et al., 2010)(Johnson et al., 2020). Even though Luman and CREB3L1 are also potentially upregulated in ASCs (**Figure 4.23**), the upregulation of CREB3L2 was most significant and has also been reported to be induced in PCs in other independent studies (Cocco et al., 2012) (Shi et al., 2015). CREB3L2 has also been shown to regulate SEC24D (Tomoishi et al., 2017), so we were particularly interested to test whether it was required for the upregulation of SEC24D in ASCs. Loss of CREB3L2 in I.29s had no impact on protein levels of SEC24D (**Figure 4.7**), suggesting potential redundancy with other OASIS family members. In a recent study, both CREB3L1 and CREB3L2 were reported to be required for enhancing the secretory pathway during the differentiation of endometrial stromal cells and collagen secretion (Pittari et al., 2022). Importantly suppression of CREB3L2 resulted in reduced expression of SEC24D which becomes even more significant with depleting CREB3L1. The data suggests that both paralogues contribute to the expression of SEC24D in these cells. We have also utilised constructs expressing the activated form of multiple OASIS family proteins and our preliminary data suggests that they may all be able to upregulate SEC24D in HeLa cells with varying degrees (**Figures 4.10-4.11**)

The next steps ideally would be assessing which OASIS family proteins are expressed in the I.29 cells and attempting their perturbations to identify which predominantly/preferentially regulate SEC24D in ASCs. Importantly this kind of work can help identify whether the OASIS transcription factors are required for normal differentiation of ASCs, which is a question that remains to be answered. Previous work has shown that utilising S1 protease (activator of OASIS TFs, ATF6 and SREBP proteins) inhibitor has shown significant reduction in plasmablasts differentiating from B-cells and IgG secretion, and results in changes in gene expression (Al-Maskari et al., 2018). These results suggest that S1P-regulated processes could play a role in early ASC development, however, does not delineate CREB3L2 from ATF6 and/or SREBPs (sterol regulatory element-binding proteins).

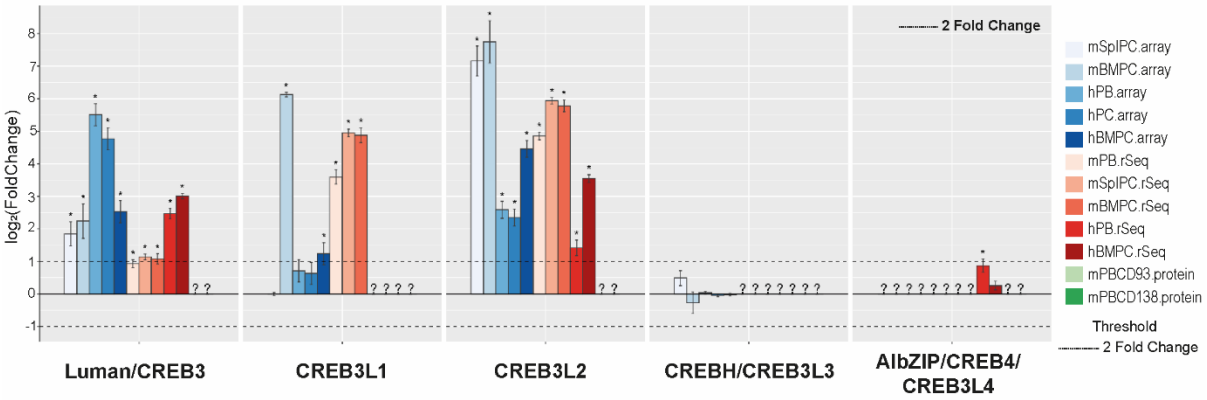

Figure 4.23: Differential regulation of OASIS proteins in ASCs. Fold change in mRNA and protein expression were plotted using the PlasmacytOMICs web resource which shows differential regulation of indicated markers between naïve B cells and ASCs. **Error bars indicate standard error of mean.**

4.3.3 Expression of OASIS Family Members May Enhance Secretory Abilities in Non-professional Secretory Cells

We have shown that HeLa cells transfected with CREB3L1, CREB3L2, CREB4 and Luman show enhanced SEC24D expression (**Figures 4.10-4.11**). Interestingly, transfected cells (notably with CREB3L2 and CREB4) appear to increase in size and have a larger nucleus. They also exhibit increased levels of SEC24D which appears to be more widely distributed throughout the cell. At present it is unclear what these additional structures are, and additional co-staining experiments will need to be performed. Interestingly, the spliced form of XBP1, which is highly expressed in ASCs, can result in a similar phenotype (Shaffer et al., 2004). Expression of spliced XBP1 not only drives an increased cell volume and nuclear size but also causes an upregulation of ER/secretory pathway genes, ER and mitochondrial mass, lysosomal content, and total protein synthesis. These results suggest that the increase in cell size may be reflecting multiple organelles, and so it would be something that we would be interested in testing for the OASIS proteins. Expression of CREB3L1 in HeLa cells has indeed been shown to upregulate the secretory pathway including COPII components such as SEC24D and SEC24A (Fox et al., 2010). However, to the best of our knowledge, the effect of overexpression of other OASIS family proteins on the secretory pathway in HeLa cells has not been investigated.

The levels of CREB3L1 and CREB3L2 are tightly regulated through ubiquitination (Shinichi Kondo et al., 2007)(S. Kondo et al., 2012). Surprisingly, CREB4 does not appear to be regulated as tightly as the other OASIS family members in HeLa cells (**Figure 4.10**). Direct comparison between CREB3L2 and Luman in response to different chemical treatments has indicated that the full-length proteins are partially regulated by different mechanisms (Oh-Hashi et al., 2021). It may be that the cleaved forms of these transcription factors also exhibit differential regulation as suggested by our data. It is possible that the ubiquitin ligase which would normally target CREB4 is not expressed in Hela cells. In the future,

it will be of interest to determine whether these factors can directly upregulate the production and secretion of biologically important molecules in CHO cells. We have previously developed a flow cytometry-based assay to measure constitutive secretion which can greatly complement this work (Gordon et al., 2021). Moreover, measuring the protein levels of other biosynthetic proteins (i.e., not only SEC24D) can also provide insight into the effect of these transcription factors on the biosynthetic pathway.

4.3.4 Is SEC24D Required for CREB3L2's Activation?

During ER stress, CREB3L2 is trafficked to the Golgi for processing where it's proteolytically cleaved. This cleaved form then translocates to the nucleus where it acts as a transcription factor. At present it is unclear whether SEC24D has a role in this process. One could imagine a scenario where SEC24D traffics CREB3L2 from the ER to the Golgi for its processing. Unfortunately, at the time of performing this work we had not optimised the antibody staining conditions to visualise the processed form of CREB3L2. As an indirect way of testing this, we looked at the expression of other proteins predicted to be regulated by CREB3L2 which are SEC31A, SEC23A and FNDC3B. The three proteins showed significant reduction in SEC24D deficient I.29 cells at day 2 post differentiation (**Figures 4.13-4.14)**. Importantly their reduction was reversed with the reintroduction of SEC24D (**Figure 4.17-4.18,4.20**). Taken together, the data suggests that there might be a reduction in CREB3L2's target genes in the absence of SEC24D but more target proteins need to be tested to support this hypothesis. This was previously directly tested by depleting SEC24D, and no impact on the activation of CREB3L2 was reported suggesting that CREB3L2's activation at the Golgi may not depend on SEC24D (Tomoishi et al., 2017). However, this data is based on partial depletions (not a complete knockout) and also used a different cell line (LX-2 cells). Thus, it will be important to retest this hypothesis in our antibody secretion model. It will also be important to assess the mRNA levels of these proteins to determine whether their downregulation is due to reduced transcription or whether this reduction is due to post-translational changes.

4.3.5 Destabilisation of Other COPII Components in Absence of SEC24D

Loss of SEC24D reduces the levels of SEC23 and to a lesser extent SEC31A (**Figure 4.13,4.18**). It is possible that the loss of SEC24D reduces stability of SEC23 which is in the same structural layer of the coat. Destabilisation of COPII components has previously been reported. For example, depletion of SEC13 results in the destabilisation and reduction in levels of SEC31A (both present in the outer COPII layer) (Townley et al., 2008). This destabilisation was predicted to occur due to the close interactions between the SEC13 and SEC31 subunits (Fath et al., 2007). It is also likely that this will be true for SEC23 and SEC24 as these proteins interact in the pre-budding complex (Bi et al., 2002). Moreover, it

is possible that the loss of SEC24D will also be impacting the levels of SEC31 as it has previously been shown that SEC23A mutant impacts recruitment of the SEC13-31 outer complex (Fromme et al., 2007).

As it is very likely that that there are other SEC24 paralogues in the I.29s, it is interesting that the paralogues were not able to compensate fully for this phenotype. It may suggest that the presence of different paralogues is required for efficient coat formation. In this sense, perhaps, the presence of SEC24D may be required for efficient COPII formation. This has been previously proposed for SEC23A, where it has been suggested to enable effective coupling of the COPII layers which collagen export relies on, instead of having a cargo specific role (Townley et al., 2008). We were not able to look at other SEC24 paralogues in the I.29s as we currently lack antibodies that work on mouse cells.

4.3.6 What is the link between SEC24D and FNDC3B? Background Into FNDC3B

FNDC3B was initially proposed to be a positive regulator of adipocyte differentiation (Tominaga et al., 2004). Loss of FNDC3B in mice results in neonatal death suggesting it plays an important role for survival post birth (Nishizuka et al., 2009). Embryonic fibroblasts generated from the mice showed defects in cell proliferation, adhesion, spreading and migration in addition to adipocyte differentiation. FNDC3B has also been described as a negative regulator of osteoblast differentiation (Kishimoto et al., 2010). To the best of our knowledge, the first link between FNDC3B and ER stress was made in this paper. Given that CREB3L1 which is an ER stress transducer, was reported to play a role in osteoblast differentiation and FNDC3B is ER localised, the authors propose that FNDC3B may be part of this ER stress response.

Abnormal expression of FNDC3B was reported in several types of cancers (C. F. Chen et al., 2010) (Cai et al., 2012) (Lin et al., 2016) (Cheng et al., 2017) (Li et al., 2020) (Han et al., 2020) and most recently in gliomas (X. Wang et al., 2022). Despite these associations, the function of FNDC3B remains largely uncharacterized. The co-expression network of FNDC3B in cervical cancer was analysed using Gene Ontology and KEGG (Han et al., 2020). Results indicated a potential association of FNDC3B in cell migration and invasion, in addition to ER stress responses and the UPR which have both been reported to be implicated in different types of cancers (M. Wang & Kaufman, 2014)(Cubillos-Ruiz et al., 2017). The co-expression network also identified SEC24D to be co-expressed with FNDC3B, which is interesting as we show that loss of SEC24D results in reduction of FNDC3B levels.

4.3.7 FNDC3B is Required for the Function of FAM46C

FNDC3B has recently been implicated as an interactor with the multiple myeloma tumour suppressor FAM46C (Fucci et al., 2020). This gene is commonly mutated in multiple myeloma whose loss results in enhancement of pathogenesis, myeloma cell survival (Zhu et al., 2017) and migration (Herrero et al., 2020). Its upregulation in ASCs has also been reported (Shi et al., 2015)(Rahman, 2019). Functionally, FAM46C is a non-canonical poly(A)polymerase which polyadenylates mRNAs in the cytoplasm enhancing their stability and translational efficiency (Mroczek et al., 2017) (Bilska et al., 2020). The activity of FAM46C has been shown to be strongly specific to mRNAs which encode ER-proteins. Multiple myeloma cells are sensitive to ER stress due to high proteostatic stress, therefore FAM46C's ER specific function may explain why it behaves as a tumour suppressor. The mRNAs encoding immunoglobulins have been shown to be targets of FAM46C. Therefore, FAM46C KO ASCs produce fewer antibodies and exhibit reduced ER expansion and ER stress, which is reflected in their faster proliferation and differentiation rates (Bilska et al., 2020). FAM46C has also been shown to regulate the levels of ER and ERGIC proteins, and results in close to doubling of the ER area (Fucci et al., 2020). Finally, overexpression of FAM46C triggers multiple myeloma cell death with increased oxidative stress and reduced ATP levels, and overexpression of FAM46C/D in non-professional secretory cells such as HeLa and HEK293T results in the expansion of ER size.

The ER expanding activity of FAM46C has been demonstrated to require its interaction with FNDC3 proteins (FNDC3A and FNDC3B) (Fucci et al., 2020). This ER enhancing ability requires the presence of at least one FNDC3 indicating potential redundancy between both proteins. Even though uncharacterised, this dependency could be due to the FNDC3 proteins enabling FAM46C's ER localization, as knocking out FNDC3 proteins resulted in significant reduction of FAM46C in membrane associated fractions. Despite FNDC3B and FNDC3A showing redundancy in terms of enabling FAM46C's function, FNDC3B silencing results in a more significant decrease in expression of ER proteins compared to FNDC3A which may indicate that they have partial different functions. Moreover, FNDC3B's effect on ER proteins still occurs in FAM46C mutated cells which may suggest that it has functions related to ER homeostasis independent of FAM46C.

4.3.8 Why is FNDC3B Reduced with Loss of SEC24D?

At present, it is unclear why the loss of SEC24D results in reduction in the levels of FNDC3B. It is possible that SEC24D has a role important for maintaining the stability of FNDC3B. Colocalization and biochemical binding experiments for FNDC3B and SEC24D will provide some insight into this.

FAM46C has been shown to be expressed at the late stages of B-cell differentiation (Bilska et al., 2020). Thus, in the context of our work it may be better to perform characterisation experiments at later

time points in the differentiation process as this may yield bigger phenotypic differences. Interestingly, C41 cells appear to have enhanced viability at day 4 post induction (**Figure 4.22**). This observation would fit a model where the loss of SEC24D is impacting the levels of FNDC3B/A and FAM46C which then resulted in a reduction of ER expansion. Reduction of FNDC3A has previously been reported to increase the fitness of myeloma cells which express FAM46C which may support this hypothesis (Manfrini et al., 2020). We have generally avoided carrying out characterisation experiments four days post LPS induction due to the significant cell death that occurs at that time. In an effort to mitigate this, we have optimised the use of a dead cell removal kit that could be beneficial for future experiments (**Figure 4.24**).

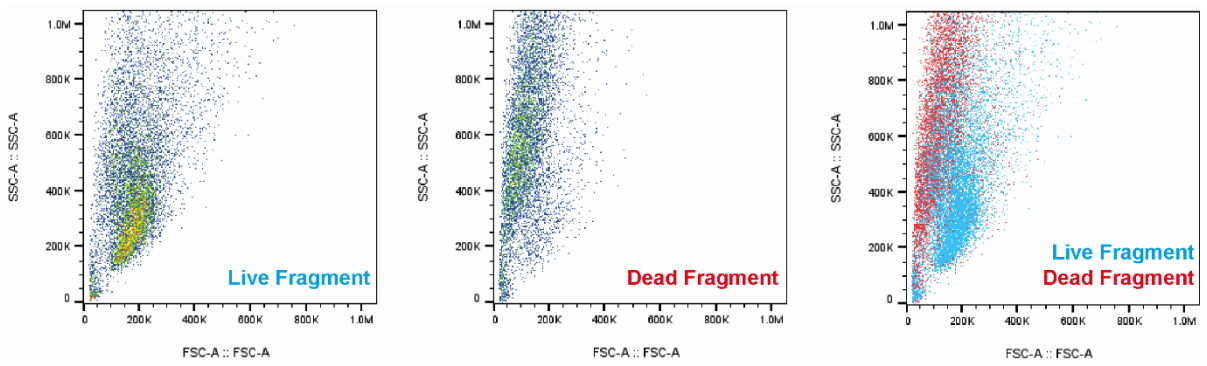

Figure 4.24: Successful segregation of live and dead Cells from differentiated I.29 cells day 4 post induction. I.29 cells were induced to differentiate using 20µg/ml of LPS. Four days post induction, the differentiated population was collected to deplete the dead cells following the manufacturer's protocol (Dead Cell Removal Kit (Miltenyi Biotech, 130-090-101)), using the MS column and the MiniMACS separator. Post separation, the live and dead cell fractions were collected and run on the Attune flow cytometer to check the forward and side scatter profiles of both fractions. The plots show the expected behaviour where dead cells typically exhibit smaller size and more side scatter.

In response to proteasome inhibition by bortezomib, FAM46C rapidly accumulates and interacts with the autophagic receptor P62. When the proteasome is not inhibited, no aggregation of FAM46C occurs when cells are treated with bafilomycin A1 (blocks autophagy). However, when both autophagy and the ubiquitin proteasome system (UPS) are inhibited, further accumulation of FAM46C occurs. These results suggest that FAM46C is tightly regulated and normally degraded by the UPS; however, this control is also synchronised with autophagy and interactions with p62, and that autophagy compensates for proteasome insufficiencies. It would be interesting in the future to assess whether SEC24D results in any relevant phenotype in these regulatory processes through the reduction of FNDCB or independently. We performed a proof of principle experiment to test some antibodies we could use in the future for these experiments (**Figure 4.25**). We observed that SEC24D may itself be a target of the proteasome however more repeats and further experiments are needed to confirm any phenotypes.

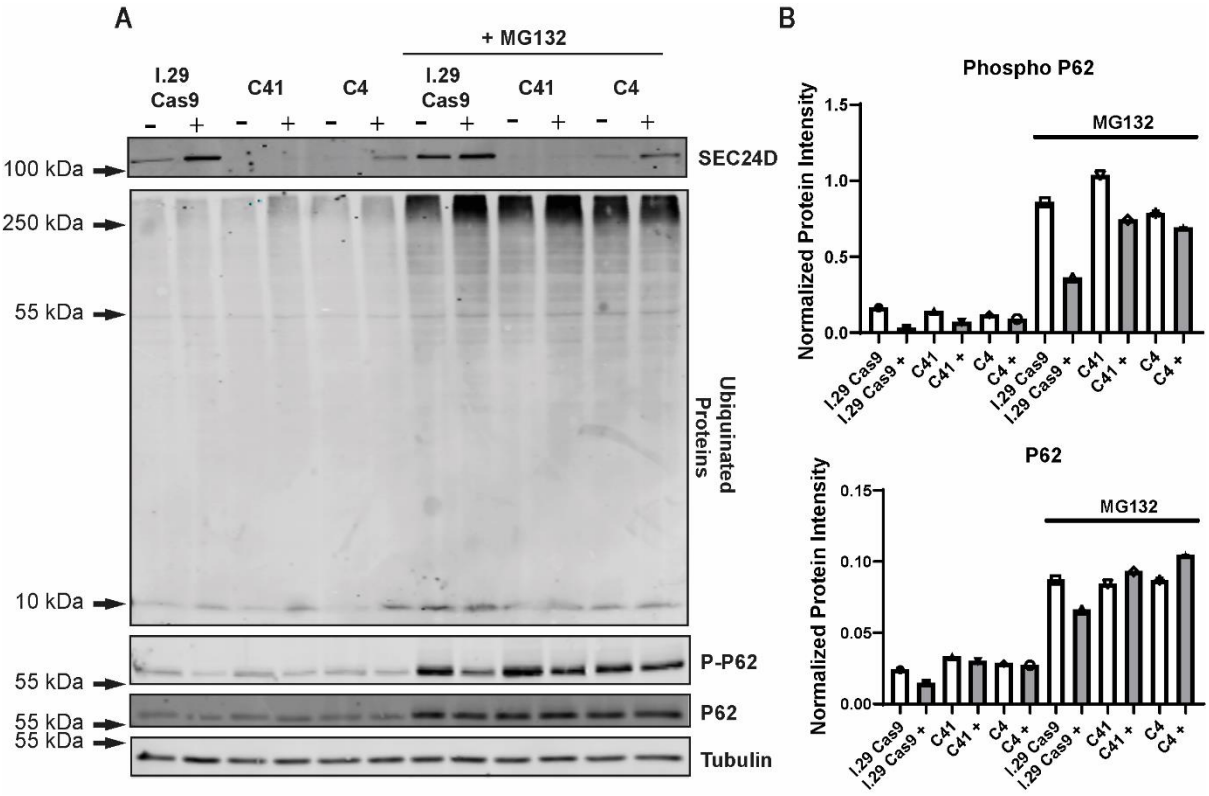

Figure 4.25: Pilot experiment to test P62 antibodies in the I.29s. I.29 cells were induced to differentiate using 20µg/ml of LPS. The I.29 cell lines used are the I.29 expressing Cas9, the C41 clone (SEC24D mutant clone) and the C4 clone (a clone of C41 rescued with SEC24D). Cells were collected two days post LPS induction. ~16 hours before collection, cells were treated with 1µM of the proteasome inhibitor MG132. Immunoblots showing SEC24D, ubiquitinated proteins, phosphorylated P62 and P62 (**A**). Levels of proteins were quantified and normalised against tubulin **n=1** (**B**)

Interestingly, loss of TECPR2, a positive regulator of autophagy, has been shown to result in destabilisation of SEC24D and its degradation which is likely by the proteasome (Stadel et al., 2015). Even though TECPR2 does not bind SEC23A, its levels were reported to decrease, implying that reduction of SEC24D impacts the coat assembly. This is in line with what we have seen in I.29 cells lacking SEC24D. The stabilising role of TECPR2 of SEC24D is described to maintain ERES. This prompts us to wonder for future experiments whether loss of SEC24D would impact TECPR2, ERES and autophagy.

In parallel to the immunoblotting studies, we have generated ER-APEX cell lines as a tool for measuring changes in the proteome of the ER. These reporter cell lines will be very useful for determining how loss of SEC24D and reduction of FNDC3B impact the secretory capacity of the ER in antibody secreting cells (**Figure 4.26**). Unfortunately, the Orbitrap mass analyser in our mass spectrometry facility was broken during this time so the prepared samples could not be run and analysed in time for this thesis.

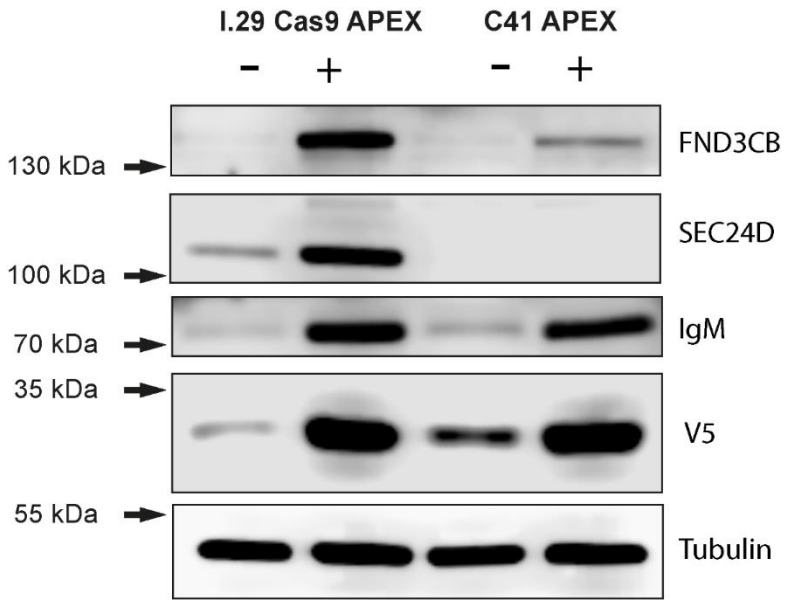

Figure 4.26: V5-APEX2 expressing I.29 Cas9 cells and C41. I.29 Cas9 and C41 cells were transduced with the V5-APEX2 construct localised to the ER membrane. Post selection, cells were induced to differentiate using 20µg/ml of LPS (+) and collected for immunoblotting two days post differentiation. FNDC3B is upregulated during differentiation, however C41 cells exhibit a large reduction in its protein levels post differentiation. The APEX2 construct is also upregulated as seen by V5 immunoblotting.

4.3.9 Technical Challenges

In our efforts to achieve a SEC24D knocked out line and re-express it for rescue experiments, we have faced some technical challenges described below.

The heterogeneity of exogenous protein expression in transduced populations is a major challenge which we faced when attempting to knockout and to re-introduce SEC24D (**Figures 4.2-3, 4.16**). To try and mitigate this issue, we used single cell cloning. Use of single cell cloning in I.29 cells post introduction of exogenous proteins has been independently reported which may suggest that this problem has been experienced by other researchers (Qiu & Stavnezer, 1998)(Van Anken et al., 2009).

Due to time constraints, we were unable to screen a large number of SEC24D reconstituted clones to select one with comparable expression levels to the parent line. However, the tested clones were showing rescue in terms of FNDC3B levels despite lower levels of SEC24D expression (**Figure 4.17**), therefore we decided to proceed with C4 at the time which had the highest expression level of SEC24D among the screened clones.

Interestingly, we observed upregulation of SEC24D expression in response to LPS induction despite the use of a constitutive promoter (**Figure 4.16**), which we have previously observed and discussed for other proteins (**Figure 3.12-3.13, 3.15**). We also note that there could be potential post transcription/translation regulation of SEC24D to maintain it at low levels in the B-cell stages, which could be investigated by RT-qPCR, however this is outside the scope of this thesis. In addition to screening a larger number of clones for better protein expression levels, we aim to also explore the use of different promoters, including tet-inducible, in the I.29s in the future.

4.3.10 Summary

In this chapter, we have utilised a CRISPR/Cas9 based approach to disrupt the function of SEC24D in the I.29 model. We have shown that loss of SEC24D does not impact IgM secretion at two days post differentiation. However, we have observed a significant reduction in the levels of FNDC3B and SEC23 that can be rescued by re-introduction of SEC24D. The levels of FNDC3A and SEC31A were also reduced but to a lesser extent. At present it is unclear whether these changes in protein expression are directly due to the loss of SEC24D or changes in gene transcription caused by a defect in the activation of CREB3L2 or other OASIS family members. It is plausible that SEC24D may be required for the stabilisation of COPII subunits, and/or interact with FNDC3B at the ER to stabilise it.

We have also shown that the expression of SEC24D is not fully controlled by CREB3L2 in I.29 cells, despite being the most consistent and highly upregulated OASIS family members in ASCs. Expression of OASIS family members in HeLa cells increases the expression of SEC24D, expands/alters its compact perinuclear staining and increases cell size. Taken together these preliminary results suggest that OASIS family members may be interesting targets for engineering the secretory pathway.

Chapter 5: General Discussion

Antibody secreting cells (ASCs) are the cells solely responsible for synthesising and secreting protective antibodies in the body. As professional secretors, their constitutive secretory pathway is highly upregulated which enables them to secrete thousands of antibodies per second. Due to their specialty, ASCs represent a unique physiological model for studying constitutive secretion.

To gain better understanding on how these cells reach such impressive biosynthetic feat, we have previously carried out proteogenomic analysis to identify consistently differentially expressed genes between ASCs and precursor naïve B-cells. Our working hypothesis being that proteins that are significantly and consistently upregulated were likely directly involved in the process required for antibody secretion and/or proteostasis. As a membrane trafficking lab, we were particularly interested in components of vesicular transport, specifically COPII for this project. The SEC24 paralogue, SEC24D, stood out to us as being the highest and most consistently upregulated COPII component. As SEC24 proteins are responsible for cargo selection at the ER during transport, our initial hypothesis was that SEC24D may enable efficient immunoglobulin secretion. In our effort to characterise SEC24D's role in the I.29 cells, we have uncovered that its upregulation potentially reflects roles beyond cargo selection in ASCs.

Proposed SEC24D Roles in ASCs

Through CRISPR/Cas9 we were able to create clone 41 (C41) which has significantly reduced levels of SEC24D and IgM synthesis and secretion did not seem to be significantly impacted with loss of SEC24D two days post induction. However, the protein levels of FNDC3B and SEC23A were significantly reduced in its absence. This reduction could be compensated by the reintroduction of SEC24D suggesting that SEC24D or COPII plays some role in regulating the levels of these proteins. Interestingly, the protein levels of SEC31A and FNDC3A were also decreased in C41, albeit insignificantly. FNDC3B, SEC23A and SEC31A are all proteins predicted to be regulated by CREB3L2, a transcription factor which also regulates SEC24D (Rahman, 2019)(Saito et al., 2009)(Tomoishi et al., 2017). Therefore, it seems that there could potentially be a positive regulation loop between SEC24D and CREB3L2 in the I.29 cells. It has previously been reported that depletion of SEC24D in a hepatic cell line did not impact the activation of CREB3L2 (Tomoishi et al., 2017). However, this is yet to be tested in our system. Thus, in the future it will be important to look at the processing of CREB3L2 in the SEC24D deficient cells and at the mRNA levels of its downstream targets.

It is possible that the phenotypes we are observing are independent of CREB3L2. In terms of the reduction in COPII components, it may be due to a requirement of SEC24D to stabilise the formation

of the COPII complex. A similar phenomenon was reported previously for SEC13 whose depletion resulted in reduction of SEC31A levels (Townley et al., 2008). Interactions between SEC23 and SEC24 have been previously described (Bi et al., 2002), therefore loss of SEC24D potentially may destabilise the pre-budding complex. This consequently may reduce the stability of the recruited COPII outer layer, as SEC23 is known to directly interact with SEC31. Mutations in SEC23 have been reported to result in impaired SEC13-SEC31 assembly (Boyadjiev et al., 2006)(Fromme et al., 2007)(Fromme et al., 2008). Immunofluorescence (IF) microscopy previously revealed diffusive cytoplasmic mislocalisation of SEC31 due to a mutation in SEC23 indicative of abnormal COPII formation (Boyadjiev et al., 2006). Thus, performing IF to stain COPII components in our SEC24D KO line can help us further elucidate the described phenotypes.

At present, it is unclear why the loss of SEC24D is causing a reduction in the level of FNDC3B. FNDC3B has a hydrophobic transmembrane domain at its C-terminus which resembles tail anchored proteins. It may be that SEC24D acts as a preferred cargo selector for FNDC3B and enables its trafficking or enables the trafficking of one of the chaperones that allows its correct targeting to the ER (e.g., GET complex components) (Jiang, 2021). Extensive quality control mechanisms for mis-localised tail anchored protein may suggest that a defect in its proper trafficking/localisation would lead to its degradation.

In addition, it is also feasible that SEC24D may be part of a complex with FNDC3B at the ER. FNDC3A has been previously shown to exist in a complex with other ER (trafficking and resident) proteins at the cytoplasmic side of the ER with FAM46C, however SEC24D was not identified (Manfrini et al., 2020). FNDC3B, in addition to FNDC3A, has also been shown to enable FAM46C's localisation to the ER (Fucci et al., 2020). Therefore, it is possible that a complex containing FNDC3B/FNDC3A/FAM46C is binding SEC24D at the ER and thus, disrupting SEC24D may be destabilising these proteins and impacting their stability. To address this, it will be informative to perform immunoprecipitation and colocalization experiments with these proteins in I.29 cells. Importantly, these experiments may help us understand whether SEC24D has a moonlighting role separate from its role in cargo selection. Some of the proposed potential mechanisms outlined here are briefly illustrated in **Figure 5.1**.

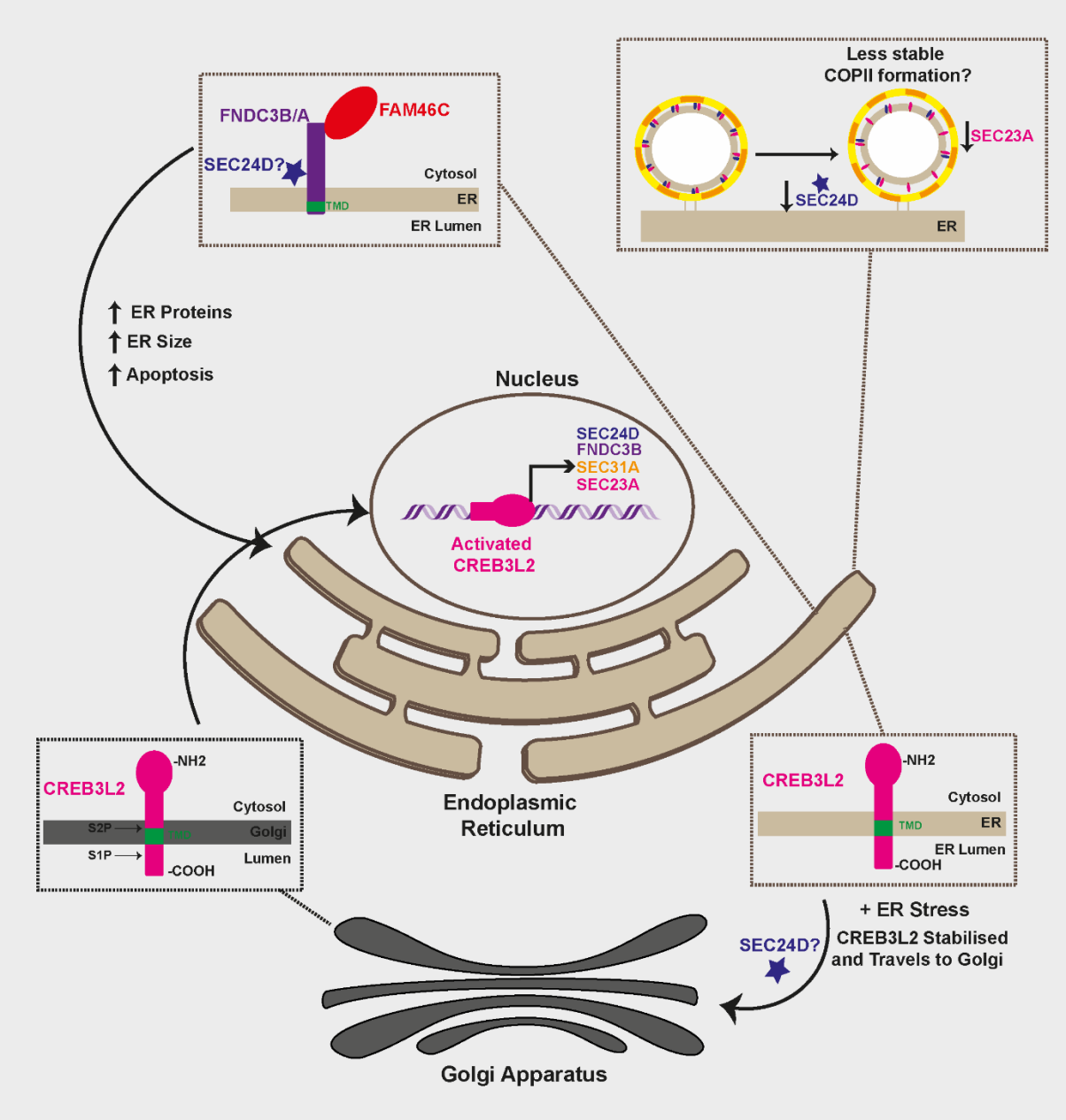

Figure 5.1: Model of potential roles of SEC24D in ASCs. SEC24D is activated by the transcriptional factor CREB3L2. In response to ER stress, CREB3L2 is trafficked to the Golgi apparatus (possibly via a SEC24D dependent COPII pathway?). At the Golgi, CREB3L2 is cleaved by the Golgi resident S1P and S2P. The released N-terminus fragment then translocates to the nucleus where it binds and activates cAMP elements. In the absence of SEC24D, the level of SEC23A was reduced then increased with SEC24D's reintroduction. This may indicate that SEC24D's presence may be required for stabilising other COPII components. FNDC3B is another protein which was significantly reduced in the absence of SEC24D. Reintroducing SEC24D increased its level. Both FNDC3B and FNDC3A have been previously shown to interact with FAM46C at the cytoplasmic side of the ER. As FNDC3A's interaction with FAM46C has been reported to occur with a network of other ER proteins, it may be possible that SEC24D is a part of this network.

Membrane Trafficking and Proteostasis

We have previously identified the SNARE, SEC22B, as an upregulated protein in ASCs (Rahman, 2019). Conventionally SNAREs are involved in vesicular transport, however SEC22B has recently been shown to play a key role in the homeostasis of ASCs (Bonaud et al., 2023). In ASCs lacking SEC22B, the PERK branch of the unfolded protein response, which is normally suppressed in ASCs, was upregulated, likely causing apoptosis in these cells. The cells also exhibited a less mature transcriptional profile, reduced ER expansion and ER/mitochondrial contact site compared to the WT cells. Therefore, in addition to its vesicular transport role, SEC22B seems to carry out different cellular functions which could likely partly occur via interactions with other proteins. Therefore, it is possible that the upregulation of SEC24D in ASCs reflects a broader role than initially anticipated and that it may be involved in proteostasis of the ER.

COPII has been implicated in pathways beyond just trafficking between the ER and the Golgi. For example, COPII components have been shown to be required for the formation of ER whorls, a new ER stress response proposed to separate translocons from ribosomes to relieve ER stress by lowering protein translation in a PERK dependent mechanism (Xu et al., 2020). COPII has also been shown to contribute to the initiation of autophagy by budding from the ERGIC in response to autophagic signals to provide membrane precursors for the lipidation of LC3 (Ge et al., 2016)(Ge et al., 2017). In both these processes, COPII does not participate in a completely conventional manner. SAR1 which typically dissociates shortly after COPII vesicle formation stays attached to ER whorls precursors. They also contain ER resident proteins which are typically not sorted into COPII such as Sec61 and PERK. With autophagy, COPII vesicles budding from the ERGIC is unconventional in the sense that it is normally thought that COPII bud only from the ER. In response to starvation which induces autophagy, the expansion of ERES and relocation of SEC12 from the ER to the ERGIC is thought to trigger COPII assembly at the ERGIC. Taken together, COPII and components of COPII are involved in processes on top of ER to Golgi trafficking.

Interestingly, TECPR2 which is a positive regulator of autophagy has been shown to interact with SEC24D and is required for SEC24D's stabilisation (Stadel et al., 2015). We have previously observed that HeLa cells overexpressing OASIS proteins and expressing high levels of SEC24D exhibit brighter and enlarged SEC24D staining. Taking into consideration that autophagy has been previously reported to cause expansion and relocation of SEC12 to the ERGIC (Ge et al., 2017), we wonder whether the observed phenotype in HeLa cells is autophagy related.

Our data suggests that SEC24D is not required for the trafficking of IgM but may be required for the maintenance of other proteins which are localised to the ER. Thus, it is possible that SEC24D may have an important role in regulating ER proteostasis during antibody synthesis and secretion. We have observed that C41 exhibits higher fitness in culture and higher viability four days post differentiation. We reason that a potential cause for this is the reduction of FNDC3B/A with SEC24D's loss. Limiting ER expansion can be generally beneficial for ASCs' survival due to reduced proteostatic stress. This can be exemplified by the enhanced viability of multiple myeloma cells with FAM46C's mutations. Following from this, reduction of FNDC3A has previously been reported to increase the fitness of myeloma cells which express FAM46C (Manfrini et al., 2020). FNDC3B may also result in the expansion of the ER independently from FAM46C (Fucci et al., 2020). Taken together, the reduction of FNDC3B/A in cells lacking SEC24D may be resulting in the enhancement of the fitness of the cells by reducing ER expansion during differentiation (in/dependently of FAM46C). However, this phenotype is yet to be confirmed by reintroduction of comparable levels of SEC24D in C41. For future studies, we also aim to characterise the levels of these proteins four days post differentiation as this is when the effect of loss of SEC24D was clearest in terms of enhanced viability.

The I.29 Cell Model – Evaluation

We have validated the I.29 cell line as a useful ASC model. We have shown that in response to differentiation by LPS, the cells increase in size, secrete IgM and increase its synthesis. Furthermore, we confirmed the expression of important ASC markers in the I.29s. These include transcription factors including the ASCs identity marker, XBP1. We investigated levels of proteins involved in the biosynthetic pathway to assess whether they were upregulated in response to differentiation as one would expect of an ASC. These showed upregulation and included protein chaperones (e.g., BIP, ERp72), COPII components (e.g., SEC31A, SEC24D) and SNAREs (e.g., SEC22B, YKT6). We also utilised our own previous analysis of ASCs and the literature to validate the expression of specific ER proteins such as RRBP1, TMEM214, CRELD2 and FNDC3B (Rahman, 2019). This shows that the proteins upregulated in primary ASCs are also appropriately upregulated in the I.29s. Taken together, the I.29 cell model seems to respond and behave in an expected manner as plasmablasts in response to LPS stimulation.

To the best of our knowledge, we are first to successfully utilise CRISPR/Cas9 in these cells to generate a platform for studying the role of genes in antibody secretion. On further evaluation of the experimental work done for this thesis using the I.29 cells, we describe below a few considerations for future work.

Days Post Differentiation

During the differentiation process, reduction in viability is expected to occur due to proteostatic stress. For example, LPS differentiated splenic mouse B-cells were ~40% viable on day 4 post differentiation (Aragon et al., 2012). C41 exhibited similar dynamics to the parent line, however at days 3 and 4 post induction it typically showed enhanced viability which may indicate that the cell line was experiencing reduced biosynthetic stress. Characterising the effect of SEC24D loss later in the differentiation process as opposed to just at day 2 may have revealed stronger phenotypes possibly implicated with the protein's loss and the reduction of potentially associated proteins such as FNDC3B. Therefore, in addition to assaying for IgM secretion on days 3/4, looking at the differentiation markers as we have previously done at day 2 could indicate whether the absence of SEC24D results in delayed/reduced differentiation. Further investigations into this would involve characterising whether the associated phenotype is FNDC3B and/or FAM46C specific, the latter previously shown to be expressed in later stages of differentiation (Bilska et al., 2020).

B-cells derived from SEC22B knockout mice seem to differentiate normally till day 2 post differentiation, however, start to die shortly after (Bonaud et al., 2023). Therefore, even though SEC22B is upregulated early on in differentiation, it is not required for ACS differentiation but required for their maintenance. This example shows how a function of a protein may not manifest an obvious phenotype due to its absence in the early stages of differentiation, further pointing us to carry more characterization work of the effect of perturbing SEC24D at later differentiation time points.

Importance of In Vivo Validation

Despite I.29 cells typically showing behaviours of ASCs, future validation of observed phenotypes is necessary in primary cells and in vivo models. MIST1 is a specific ASCs marker, and up until recently studies have suggested that it is not required for ASCs functions with its loss resulting in minimal effects (Bhattacharya et al., 2007)(Capoccia et al., 2011) (Yeung et al., 2012). However, in a recent paper, MIST1 was investigated in vivo under normal and immunised conditions (Wöhner et al., 2022). Results indicated that MIST1 may be playing a regulatory role in ASCs. MIST1 deficient plasma cells exhibited reduced number, increased IgM production and secretion per PC, and increased expression of BLIMP1. Taken together, the authors suggest that MIST1 negatively regulates BLIMP1 expression therefore limiting antibody secretion and aiding in the maintenance of cells' viability. Importantly, the authors investigated these phenotypes in in vitro differentiated B-cells and noted that the loss of MIST1 did not result in reduced number of ASCs and produced normal antibody levels. These results highlighted that in vitro differentiation did not reflect the phenotypes otherwise observed in in vivo differentiated PCs lacking MIST1.

HeLa Cells May be a Useful Parallel Platform

I.29 cells are a useful model for studying the cellular processes involved in antibody secretion. However, their culturing and manipulation are more challenging compared to other generic cell lines. An exciting observation made during this thesis is that some cellular processes that occur in ASC can be modelled in non-professional secretory cells such as HeLa cells. We have shown that overexpression of OASIS family proteins (e.g. CREB3L2) in HeLa cells can result in increase in their size and upregulate expression of SEC24D. Optimisation and use of these transcription factors in nonprofessional secretory cells may help push and enhance a secretory phenotype. Importantly, this might allow for validation work of some phenotypes in an easier to modulate cell model while introducing a layer of the biological context of ASCs. One example of a possible phenotype to validate in HeLa cells is the possible functional interaction between SEC24D and FNDC3B.

Engineering non-professional secretory cells using insights obtained from the biology of ASCs has been previously carried out. For example, co-overexpression of BLIMP1 and XBP1 in Chinese Hamster Ovary (CHO) cells, which are commonly used to produce biologics, resulted in an increase in their productivity (Torres & Dickson, 2022). Recent studies have also been performed by directly investigating ASCs in relation to CHOs to gain insights for rational engineering. For example, spatial proteomics of both cell types and profiling their miRNomes to identify engineering targets (Kretz et al., 2022)(Raab et al., 2022). Therefore, the OASIS protein family work which we have presented may be of industrial interest and we plan to expand it in other cell types such as CHOs.

Closing Remarks & Future Direction

Uncovering the mechanistic and molecular aspects that are important for the function of ASCs may aid, in the long term, the development of new therapeutics to target diseases caused by their dysregulation. For example, a better understanding on how ASCs manage their proteostasis can provide therapeutic insights for multiple myeloma. In addition to being a unique model for studying constitutive secretion, we have shown that ASCs can be useful for studying proteostatic regulation which may provide new links between proteostasis and secretion. A big part of this project was dedicated to establishing the systems and tools in an ASC model, which we have worked to validate, that can enable these important studies. To the best of our knowledge, we are the first to successfully implement the CRISPR/Cas9 based approach in I.29 cells and through this work, we have uncovered a potential role for SEC24D for stabilising COPII. SEC24D may also be required to maintain normal protein levels of FNDC3B, whose loss may disturb the homeostasis of ASCs specifically in the later stages of differentiation. More studies are required to confirm and elucidate these potential mechanisms; however, these observations possibly implicate SEC24D in the proteostasis of ASCs.

For future studies, we are specifically interested in investigating and confirming the potential link between SEC24D and the stabilisation of FNDC3B. The creation of a parallel SEC24D knocked out HeLa line may be experimentally useful and enabling, especially with the added “ASC” layer achieved by transfecting HeLa cells with TFs such as CREB3L2. Performing immunofluorescence imaging of FNDC3B with other compartment markers in HeLa cells lacking SEC24D could provide insight on whether FNDC3B is mis-localised in its absence. Treating SEC24D deficient cells with autophagy and UPS inhibitors will also help dissect which pathways are responsible for FNDC3B’s degradation in the absence of SEC24D. It would be insightful to further characterise the effect of the reduction of FNDC3B, as a result of SEC24D’s loss, by looking at aspects such as ER expansion and survival in response to proteostatic stresses (while reintroducing FNDC3B). These experiments can help further our understanding of the function of SEC24D and why it is highly upregulated in ASCs. Finally, due to the presence of links between COPII and autophagy components, it would be interesting to explore whether loss of SEC24D impacts ER-phagy, a process shown to be important for the homeostasis of ASCs.

References

Adams, E. J., Chen, X. W., O'Shea, K. S., & Ginsburg, D. (2014). Mammalian COPII coat component SEC24C is required for embryonic development in mice. The Journal of Biological Chemistry, 289(30), 20858–20870. https://doi.org/10.1074/JBC.M114.566687

Adams, E. J., Khoriaty, R., Kiseleva, A., Cleuren, A. C. A., Tomberg, K., van der Ent, M. A., Gergics, P., Tang, V. T., Zhu, G., Hoenerhoff, M. J., O'Shea, K. S., Saunders, T. L., & Ginsburg, D. (2021). Murine SEC24D can substitute functionally for SEC24C during embryonic development. Scientific Reports 2021 11:1, 11(1), 1–12. https://doi.org/10.1038/s41598-021-00579-x

Adolf, F., Rhiel, M., Hessling, B., Gao, Q., Hellwig, A., Béthune, J., & Wieland, F. T. (2019). Proteomic Profiling of Mammalian COPII and COPI Vesicles. Cell Reports, 26(1), 250-265.e5. https://doi.org/10.1016/j.celrep.2018.12.041

Adolf, F., Rhiel, M., Reckmann, I., & Wieland, F. T. (2016). Sec24c/D-isoform-specific sorting of the preassembled ER-Golgi Q-SNARE complex. Molecular Biology of the Cell, 27(17), 2697–2707. https://doi.org/10.1091/mbc.E16-04-0229

Alberini, C., Biassoni, R., Deambrosis, S., Vismara, D., & Sitia, R. (1987). Differentiation in the murine B cell lymphoma I.29: individual μ+ clones may be induced by lipopolysaccharide to both IgM secretion and isotype switching. European Journal of Immunology, 17(4), 555–562. https://doi.org/10.1002/EJI.1830170419

Allman, D., & Pillai, S. (2008). Peripheral B cell subsets. In Current Opinion in Immunology (Vol. 20, Issue 2, pp. 149–157). https://doi.org/10.1016/j.coi.2008.03.014

Al-Maskari, M., Care, M. A., Robinson, E., Cocco, M., Tooze, R. M., & Doody, G. M. (2018). Site-1 protease function is essential for the generation of antibody secreting cells and reprogramming for secretory activity. Scientific Reports 2018 8:1, 8(1), 1–11. https://doi.org/10.1038/s41598-018-32705-7

Aragon, I. V., Barrington, R. A., Jackowski, S., Mori, K., & Brewer, J. W. (2012). The specialized unfolded protein response of B lymphocytes: ATF6α-independent development of antibody-secreting B cells. Molecular Immunology, 51(3–4), 347–355. https://doi.org/10.1016/J.MOLIMM.2012.04.001

Ayala, M. V., Bonaud, A., Bender, S., Lambert, J.-M., Lechouane, F., Carrion, C., Cogné, M., Pascal, V., & Sirac, C. (2020). New models to study plasma cells in mouse based on the restriction of IgJ expression to antibody secreting cells. BioRxiv. https://doi.org/10.1101/2020.08.13.249441

Baines, A. C., & Zhang, B. (2007). Receptor-mediated protein transport in the early secretory pathway. In Trends in Biochemical Sciences (Vol. 32, Issue 8, pp. 381–388). https://doi.org/10.1016/j.tibs.2007.06.006

Baines, A. C., Adams, E. J., Zhang, B., & Ginsburg, D. (2013). Disruption of the Sec24d Gene Results in Early Embryonic Lethality in the Mouse. PLOS ONE, 8(4), e61114. https://doi.org/10.1371/JOURNAL.PONE.0061114

Balasubramanian, M., Hurst, J., Brown, S., Bishop, N. J., Arundel, P., DeVile, C., Pollitt, R. C., Crooks, L., Longman, D., Caceres, J. F., Shackley, F., Connolly, S., Payne, J. H., Offiah, A. C., Hughes, D., Parker, M. J., Hide, W., & Skerry, T. M. (2017). Compound heterozygous variants in NBAS as a cause of atypical osteogenesis imperfecta. Bone, 94, 65–74. https://doi.org/10.1016/J.BONE.2016.10.023

Bannard, O., & Cyster, J. G. (2017). Germinal centers: programmed for affinity maturation and antibody diversification. In Current Opinion in Immunology (Vol. 45, pp. 21–30). Elsevier Ltd. https://doi.org/10.1016/j.coi.2016.12.004

Barlowe, C., Orci, L., Yeung, T., Hosobuchi, M., Hamamoto, S., Salama, N., Rexach, M. F., Ravazzola, M., Amherdt, M., & Schekman, R. (1994). COPII: A membrane coat formed by Sec proteins that drive vesicle budding from the endoplasmic reticulum. Cell, 77(6), 895–907. https://doi.org/10.1016/0092-8674(94)90138-4

Baumgarth, N. (2010). The double life of a B-1 cell: self-reactivity selects for protective effector functions. Nature Reviews Immunology 2011 11:1, 11(1), 34–46. https://doi.org/10.1038/nri2901

Benhamron, S., Hadar, R., Iwawaky, T., So, J. S., Lee, A. H., & Tirosh, B. (2014). Regulated IRE1-dependent decay participates in curtailing immunoglobulin secretion from plasma cells. European Journal of Immunology, 44(3), 867–876. https://doi.org/10.1002/eji.201343953

Benhamron, S., Pattanayak, S. P., Berger, M., & Tirosh, B. (2015). mTOR activation promotes plasma cell differentiation and bypasses XBP-1 for immunoglobulin secretion. Molecular and Cellular Biology, 35(1), 153–166. https://doi.org/10.1128/MCB.01187-14

Benson, M. J., Äijö, T., Chang, X., Gagnon, J., Pape, U. J., Anantharaman, V., Aravind, L., Pursiheimo, J. P., Oberdoerffer, S., Liu, X. S., Lahesmaa, R., Lähdesmäki, H., & Rao, A. (2012). Heterogeneous nuclear ribonucleoprotein L-like (hnRNPLL) and elongation factor, RNA polymerase II, 2(ELL2) are regulators of mRNA processing in plasma cells. Proceedings of the National Academy of Sciences of the United States of America, 109(40), 16252–16257. https://doi.org/10.1073/PNAS.1214414109/SUPPL_FILE/SD01.XLSX

Bergman, L. W., & Kuehl, W. M. (1979). Co-translational modification of nascent immunoglobulin heavy and light chains. Journal of Supramolecular Structure, 11(1), 9–24. https://doi.org/10.1002/jss.400110103

Bertolotti, A., Zhang, Y., Hendershot, L. M., Harding, H. P., & Ron, D. (2000). Dynamic interaction of BiP and ER stress transducers in the unfolded-protein response. Nature Cell Biology 2000 2:6, 2(6), 326–332. https://doi.org/10.1038/35014014

Bhattacharya, D., Cheah, M. T., Franco, C. B., Hosen, N., Pin, C. L., Sha, W. C., & Weissman, I. L. (2007). Transcriptional Profiling of Antigen-Dependent Murine B Cell Differentiation and Memory Formation. Journal of Immunology (Baltimore, Md. : 1950), 179(10), 6808. https://doi.org/10.4049/JIMMUNOL.179.10.6808

Bi, X., Corpina, R. A., & Goldberg, J. (2002). Structure of the Sec23/24-Sar1 pre-budding complex of the COPII vesicle coat. Nature, 419(6904), 271–277. https://doi.org/10.1038/nature01040

Bi, X., Mancias, J. D., & Goldberg, J. (2007). Insights into COPII Coat Nucleation from the Structure of Sec23•Sar1 Complexed with the Active Fragment of Sec31. Developmental Cell, 13(5), 635–645. https://doi.org/10.1016/j.devcel.2007.10.006

Bianchi, P., Fermo, E., Vercellati, C., Boschetti, C., Barcellini, W., Iurlo, A., Marcello, A. P., Righetti, P. G., & Zanella, A. (2009). Congenital dyserythropoietic anemia type II (CDAII) is caused by mutations in the SEC23B gene. Human Mutation, 30(9), 1292–1298. https://doi.org/10.1002/HUMU.21077

Bilska, A., Kusio-Kobiałka, M., Krawczyk, P. S., Gewartowska, O., Tarkowski, B., Kobyłecki, K., Nowis, D., Golab, J., Gruchota, J., Borsuk, E., Dziembowski, A., & Mroczek, S. (2020). Immunoglobulin expression and the humoral immune response is regulated by the non-canonical poly(A) polymerase TENT5C. Nature Communications, 11(1). https://doi.org/10.1038/S41467-020-15835-3

Bjørkøy, G., Lamark, T., Pankiv, S., Øvervatn, A., Brech, A., & Johansen, T. (2009). Chapter 12 Monitoring Autophagic Degradation of p62/SQSTM1. Methods in Enzymology, 452(C), 181–197. https://doi.org/10.1016/S0076-6879(08)03612-4

Bommiasamy, H., Back, S. H., Fagone, P., Lee, K., Meshinchi, S., Vink, E., Sriburi, R., Frank, M., Jackowski, S., Kaufman, R. J., & Brewer, J. W. (2009). ATF6alpha induces XBP1-independent expansion of the endoplasmic reticulum. Journal of Cell Science, 122(Pt 10), 1626–1636. https://doi.org/10.1242/JCS.045625

Bonaud, A., Gargowitsch, L., Gilbert, S. M., Rajan, E., Canales-Herrerias, P., Stockholm, D., Rahman, N. F., Collins, M. O., Taskiran, H., Hill, D. L., Alloatti, A., Alouche, N., Balor, S., Soldan, V., Gillet, D., Barbier, J., Bachelerie, F., Smith, K. G. C., Jellusova, J., … Espéli, M. (2023). Sec22b is a critical and nonredundant regulator of plasma cell maintenance. Proceedings of the National Academy of Sciences of the United States of America, 120(2). https://doi.org/10.1073/PNAS.2213056120

Bonnon, C., Wendeler, M. W., Paccaud, J. P., & Hauri, H. P. (2010). Selective export of human GPI-anchored proteins from the endoplasmic reticulum. Journal of Cell Science, 123(10), 1705–1715. https://doi.org/10.1242/JCS.062950

Boyadjiev, S. A., Fromme, J. C., Ben, J., Chong, S. S., Nauta, C., Hur, D. J., Zhang, G., Hamamoto, S., Schekman, R., Ravazzola, M., Orci, L., & Eyaid, W. (2006). Cranio-lenticulo-sutural dysplasia is caused by a SEC23A mutation leading to abnormal endoplasmic-reticulum-to-Golgi trafficking. Nature Genetics 2006 38:10, 38(10), 1192–1197. https://doi.org/10.1038/ng1876

Branon, T. C., Bosch, J. A., Sanchez, A. D., Udeshi, N. D., Svinkina, T., Carr, S. A., Feldman, J. L., Perrimon, N., & Ting, A. Y. (2018). Efficient proximity labeling in living cells and organisms with TurboID. Nature Biotechnology, 36(9), 880. https://doi.org/10.1038/NBT.4201

Briney, B., Inderbitzin, A., Joyce, C., & Burton, D. R. (2019). Commonality despite exceptional diversity in the baseline human antibody repertoire. Nature 2019 566:7744, 566(7744), 393–397. https://doi.org/10.1038/s41586-019-0879-y

Bromage, E., Stephens, R., & Hassoun, L. (2009). The third dimension of ELISPOTs: quantifying antibody secretion from individual plasma cells. Journal of Immunological Methods, 346(1–2), 75–79. https://doi.org/10.1016/J.JIM.2009.05.005

Cai, C., Rajaram, M., Zhou, X., Liu, Q., Marchica, J., Li, J., & Powers, R. S. (2012). Activation of multiple cancer pathways and tumor maintenance function of the 3q amplified oncogene FNDC3B. Cell Cycle, 11(9), 1773. https://doi.org/10.4161/CC.20121

Capoccia, B. J., Lennerz, J. K. M., Bredemeyer, A. J., Klco, J. M., Frater, J. L., & Mills, J. C. (2011). Transcription factor MIST1 in terminal differentiation of mouse and human plasma cells. Physiological Genomics, 43(3), 174. https://doi.org/10.1152/PHYSIOLGENOMICS.00084.2010

Carlezon, W. A., Duman, R. S., & Nestler, E. J. (2005). The many faces of CREB. https://doi.org/10.1016/j.tins.2005.06.005

Castro-Mondragon, J. A., Riudavets-Puig, R., Rauluseviciute, I., Berhanu Lemma, R., Turchi, L., Blanc-Mathieu, R., Lucas, J., Boddie, P., Khan, A., Perez, N. M., Fornes, O., Leung, T. Y., Aguirre, A., Hammal, F., Schmelter, D., Baranasic, D., Ballester, B., Sandelin, A., Lenhard, B., … Mathelier, A. (2022). JASPAR 2022: the 9th release of the open-access database of transcription factor binding profiles. Nucleic Acids Research, 50(D1), D165. https://doi.org/10.1093/NAR/GKAB1113

Chatterjee, S., Choi, A. J., & Frankel, G. (2021). A systematic review of Sec24 cargo interactome. Traffic, 22(12), 412–424. https://doi.org/10.1111/TRA.12817

Chen, C. F., Hsu, E. C., Lin, K. T., Tu, P. H., Chang, H. W., Lin, C. H., Chen, Y. J., Gu, D. L., Lin, C. H., Wu, J. Y., Chen, Y. T., Hsu, M. T., & Jou, Y. S. (2010). Overlapping high-resolution copy number alterations in cancer genomes identified putative cancer genes in hepatocellular carcinoma. Hepatology (Baltimore, Md.), 52(5), 1690–1701. https://doi.org/10.1002/HEP.23847

Chen, X. W., Wang, H., Bajaj, K., Zhang, P., Meng, Z. X., Ma, D., Bai, Y., Liu, H. H., Adams, E., Baines, A., Yu, G., Sartor, M. A., Zhang, B., Yi, Z., Lin, J., Young, S. G., Schekman, R., & Ginsburg, D. (2013). SEC24A deficiency lowers plasma cholesterol through reduced PCSK9 secretion. ELife, 2013(2). https://doi.org/10.7554/ELIFE.00444

Chen, X., Shen, J., & Prywes, R. (2002). The luminal domain of ATF6 senses endoplasmic reticulum (ER) stress and causes translocation of ATF6 from the er to the Golgi. Journal of Biological Chemistry, 277(15), 13045–13052. https://doi.org/10.1074/jbc.M110636200

Chen, Y., & Brandizzi, F. (2013). IRE1: ER stress sensor and cell fate executor. Trends in Cell Biology, 23(11), 547–555. https://doi.org/10.1016/J.TCB.2013.06.005

Cheng, C. K., Wang, A. Z., Wong, T. H. Y., Wan, T. S. K., Cheung, J. S., Raghupathy, R., Chan, N. P. H., & Ng, M. H. L. (2017). FNDC3B is another novel partner fused to RARA in the t(3;17)(q26;q21) variant of acute promyelocytic leukemia. Blood, 129(19), 2705–2709. https://doi.org/10.1182/BLOOD-2017-02-767707

Chu, V. T., Graf, R., Wirtz, T., Weber, T., Favret, J., Li, X., Petsch, K., Tran, N. T., Sieweke, M. H., Berek, C., Kühn, R., & Rajewsky, K. (2016). Efficient CRISPR-mediated mutagenesis in primary immune cells using CrispRGold and a C57BL/6 Cas9 transgenic mouse line. Proceedings of the National

Academy of Sciences of the United States of America, 113(44), 12514–12519. https://doi.org/10.1073/PNAS.1613884113/SUPPL_FILE/PNAS.201613884SI.PDF

Cocco, M., Stephenson, S., Care, M. A., Newton, D., Barnes, N. A., Davison, A., Rawstron, A., Westhead, D. R., Doody, G. M., & Tooze, R. M. (2012). In Vitro Generation of Long-lived Human Plasma Cells. The Journal of Immunology, 189(12), 5773–5785. https://doi.org/10.4049/JIMMUNOL.1103720

Cornejo, V. H., Pihán, P., Vidal, R. L., & Hetz, C. (2013). Role of the unfolded protein response in organ physiology: Lessons from mouse models. IUBMB Life, 65(12), 962–975. https://doi.org/10.1002/IUB.1224

Cubillos-Ruiz, J. R., Bettigole, S. E., & Glimcher, L. H. (2017). Tumorigenic and Immunosuppressive Effects of Endoplasmic Reticulum Stress in Cancer. Cell, 168(4), 692–706. https://doi.org/10.1016/J.CELL.2016.12.004

Daste, F., Galli, T., & Tareste, D. (2015). Structure and function of longin SNAREs. Journal of Cell Science, 128(23), 4263–4272. https://doi.org/10.1242/JCS.178574/259974/AM/STRUCTURE-AND-FUNCTION-OF-LONGIN-SNARES

Deng, S. jun, Shen, Y., Gu, H. mei, Guo, S., Wu, S. R., & Zhang, D. wei. (2020). The role of the C-terminal domain of PCSK9 and SEC24 isoforms in PCSK9 secretion. Biochimica et Biophysica Acta (BBA) - Molecular and Cell Biology of Lipids, 1865(6), 158660. https://doi.org/10.1016/J.BBALIP.2020.158660

Dennis, E. P., Edwards, S. M., Jackson, R. M., Hartley, C. L., Tsompani, D., Capulli, M., Teti, A., Boot-Handford, R. P., Young, D. A., Piróg, K. A., & Briggs, M. D. (2020). CRELD2 Is a Novel LRP1 Chaperone That Regulates Noncanonical WNT Signaling in Skeletal Development. Journal of Bone and Mineral Research, 35(8), 1452–1469. https://doi.org/10.1002/jbmr.4010

Dossou, A. S., & Basu, A. (2019). The Emerging Roles of mTORC1 in Macromanaging Autophagy. Cancers, 11(10). https://doi.org/10.3390/CANCERS11101422

Eaton, S. L., Hurtado, M. L., Oldknow, K. J., Graham, L. C., Marchant, T. W., Gillingwater, T. H., Farquharson, C., & Wishart, T. M. (2014). A Guide to Modern Quantitative Fluorescent Western Blotting with Troubleshooting Strategies. Journal of Visualized Experiments : JoVE, 93, e52099. https://doi.org/10.3791/52099

Ehrenstein, M. R., & Notley, C. A. (2010). The importance of natural IgM: scavenger, protector and regulator. Nature Publishing Group. https://doi.org/10.1038/nri2849

Fairfax, K. A., Corcoran, L. M., Pridans, C., Huntington, N. D., Kallies, A., Nutt, S. L., & Tarlinton, D. M. (2007). Different kinetics of blimp-1 induction in B cell subsets revealed by reporter gene. Journal of Immunology (Baltimore, Md. : 1950), 178(7), 4104–4111. https://doi.org/10.4049/JIMMUNOL.178.7.4104

Enninga, J., Levay, A., & Fontoura, B. M. (2003). Sec13 shuttles between the nucleus and the cytoplasm and stably interacts with nup96 at the Nuclear Pore Complex. Molecular and Cellular Biology, 23(20), 7271–7284. https://doi.org/10.1128/mcb.23.20.7271-7284.2003

Fairfax, K. A., Kallies, A., Nutt, S. L., & Tarlinton, D. M. (2008). Plasma cell development: From B-cell subsets to long-term survival niches. Seminars in Immunology, 20, 49–58. https://doi.org/10.1016/j.smim.2007.12.002

Farhan, H., Reiterer, V., Korkhov, V. M., Schmid, J. A., Freissmuth, M., & Sitte, H. H. (2007). Concentrative export from the endoplasmic reticulum of the γ-aminobutyric acid transporter 1 requires binding to SEC24D. Journal of Biological Chemistry, 282(10), 7679–7689. https://doi.org/10.1074/jbc.M609720200

Farhana, A., & Khan, Y. S. (2022). Biochemistry, Lipopolysaccharide. StatPearls. https://www.ncbi.nlm.nih.gov/books/NBK554414/

Feige, M. J., Hendershot, L. M., & Buchner, J. (2010). How antibodies fold. Trends in Biochemical Sciences, 35(4), 189. https://doi.org/10.1016/J.TIBS.2009.11.005

Ferrara, C., Grau, S., Jaǧer, C., Sondermann, P., Bruñker, P., Waldhauer, I., Hennig, M., Ruf, A., Rufer, A. C., Stihle, M., Umanã, P., & Benz, J. (2011). Unique carbohydrate-carbohydrate interactions are required for high affinity binding between FcγRIII and antibodies lacking core fucose.

Proceedings of the National Academy of Sciences of the United States of America, 108(31), 12669–12674. https://doi.org/10.1073/PNAS.1108455108/-/DCSUPPLEMENTAL

Fischer, S., Handrick, R., & Otte, K. (2015). The art of CHO cell engineering: A comprehensive retrospect and future perspectives. Biotechnology Advances, 33(8), 1878–1896. https://doi.org/10.1016/J.BIOTECHADV.2015.10.015

Forthal, D. N. (2015). Functions of Antibodies. Microbiology Spectrum, 2(4), 1. https://doi.org/10.1128/9781555817411.ch2

Fox, R. M., Hanlon, C. D., & Andrew, D. J. (2010). The CrebA/Creb3-like transcription factors are major and direct regulators of secretory capacity. The Journal of Cell Biology, 191(3), 479. https://doi.org/10.1083/JCB.201004062

Fromme, J. C., Orci, L., & Schekman, R. (2008). Coordination of COPII vesicle trafficking by Sec23. Trends in Cell Biology, 18(7), 330–336. https://doi.org/10.1016/J.TCB.2008.04.006

Fromme, J. C., Ravazzola, M., Hamamoto, S., Al-Balwi, M., Eyaid, W., Boyadjiev, S. A., Cosson, P., Schekman, R., & Orci, L. (2007). The genetic basis of a craniofacial disease provides insight into COPII coat assembly. Developmental Cell, 13(5), 623. https://doi.org/10.1016/J.DEVCEL.2007.10.005

Fucci, C., Resnati, M., Riva, E., Perini, T., Ruggieri, E., Orfanelli, U., Paradiso, F., Cremasco, F., Raimondi, A., Pasqualetto, E., Nuvolone, M., Rampoldi, L., Cenci, S., & Milan, E. (2020). The Interaction of the Tumor Suppressor FAM46C with p62 and FNDC3 Proteins Integrates Protein and Secretory Homeostasis. Cell Reports, 32(12). https://doi.org/10.1016/j.celrep.2020.108162

Garbes, L., Kim, K., Rieß, A., Hoyer-Kuhn, H., Beleggia, F., Bevot, A., Kim, M. J., Huh, Y. H., Kweon, H. S., Savarirayan, R., Amor, D., Kakadia, P. M., Lindig, T., Kagan, K. O., Becker, J., Boyadjiev, S. A., Wollnik, B., Semler, O., Bohlander, S. K., … Netzer, C. (2015). Mutations in SEC24D, encoding a component of the COPII machinery, cause a syndromic form of osteogenesis imperfecta. American Journal of Human Genetics, 96(3), 432–439. https://doi.org/10.1016/j.ajhg.2015.01.002

Gass, J. N., Gifford, N. M., & Brewer, J. W. (2002). Activation of an unfolded protein response during differentiation of antibody-secreting B cells. Journal of Biological Chemistry, 277(50), 49047–49054. https://doi.org/10.1074/jbc.M205011200

Gaudette, B. T., Jones, D. D., Bortnick, A., Argon, Y., & Allman, D. (2020). mTORC1 coordinates an immediate unfolded protein response-related transcriptome in activated B cells preceding antibody secretion. Nature Communications 2020 11:1, 11(1), 1–16. https://doi.org/10.1038/s41467-019-14032-1

Ge, L., Wilz, L., & Schekman, R. (2016). Biogenesis of autophagosomal precursors for LC3 lipidation from the ER-Golgi intermediate compartment. Https://Doi.Org/10.1080/15548627.2015.1105422, 11(12), 2372–2374. https://doi.org/10.1080/15548627.2015.1105422

Ge, L., Zhang, M., Kenny, S. J., Liu, D., Maeda, M., Saito, K., Mathur, A., Xu, K., & Schekman, R. (2017). Remodeling of ER-exit sites initiates a membrane supply pathway for autophagosome biogenesis. EMBO Reports, 18(9), 1586–1603. https://doi.org/10.15252/EMBR.201744559

Gearing, L. J., Cumming, H. E., Chapman, R., Finkel, A. M., Woodhouse, I. B., Luu, K., Gould, J. A., Forster, S. C., & Hertzog, P. J. (2019). CiiiDER: A tool for predicting and analysing transcription factor binding sites. PLoS ONE, 14(9). https://doi.org/10.1371/JOURNAL.PONE.0215495

Geffroy-luseau, A., Jégo, G., Bataille, R., Campion, L., & Pellat-deceunynck, C. (2008). Osteoclasts support the survival of human plasma cells in vitro. International Immunology, 20(6), 775–782. https://doi.org/10.1093/INTIMM/DXN035

Genestier, L., Taillardet, M., Mondiere, P., Gheit, H., Bella, C., & Defrance, T. (2007). TLR agonists selectively promote terminal plasma cell differentiation of B cell subsets specialized in thymus-independent responses. Journal of Immunology (Baltimore, Md. : 1950), 178(12), 7779–7786. https://doi.org/10.4049/JIMMUNOL.178.12.7779

Ghosh, R., Wang, L., Wang, E. S., Perera, B. G. K., Igbaria, A., Morita, S., Prado, K., Thamsen, M., Caswell, D., Macias, H., Weiberth, K. F., Gliedt, M. J., Alavi, M. V., Hari, S. B., Mitra, A. K., Bhhatarai, B., Schürer, S. C., Snapp, E. L., Gould, D. B., … Papa, F. R. (2014). Allosteric inhibition of the IRE1α RNase preserves cell viability and function during endoplasmic reticulum stress. Cell, 158(3), 534–548. https://doi.org/10.1016/j.cell.2014.07.002

Godin, J. D., Creppe, C., Laguesse, S., & Nguyen, L. (2016). Emerging Roles for the Unfolded Protein Response in the Developing Nervous System. Trends in Neurosciences, 39(6), 394–404. https://doi.org/10.1016/J.TINS.2016.04.002

Goldfinger, M., Shmuel, M., Benhamron, S., & Tirosh, B. (2011). Protein synthesis in plasma cells is regulated by crosstalk between endoplasmic reticulum stress and mTOR signaling. European Journal of Immunology, 41(2), 491–502. https://doi.org/10.1002/EJI.201040677

Gordon, D. E., Bond, L. M., Sahlender, D. A., & Peden, A. A. (2010). A Targeted siRNA Screen to Identify SNAREs Required for Constitutive Secretion in Mammalian Cells. Traffic, 11(9), 1191–1204. https://doi.org/10.1111/j.1600-0854.2010.01087.x

Gorur, A., Yuan, L., Kenny, S. J., Baba, S., Xu, K., & Schekman, R. (2017). COPII-coated membranes function as transport carriers of intracellular procollagen I. Journal of Cell Biology, 216(6), 1745–1759. https://doi.org/10.1083/JCB.201702135/VIDEO-7

GSK announces further positive data from DREAMM-1 study of anti-BCMA antibody-drug conjugate in patients with relapsed/refractory multiple myeloma | GSK. (n.d.). Retrieved December 8, 2019, from https://www.gsk.com/en-gb/media/press-releases/gsk-announces-further-positive-data-from-dreamm-1-study-of-anti-bcma-antibody-drug-conjugate/

Han, B., Wang, H., Zhang, J., & Tian, J. (2020). FNDC3B is associated with ER stress and poor prognosis in cervical cancer. Oncology Letters, 19(1), 406. https://doi.org/10.3892/OL.2019.11098

Hanna, M. G., Block, S., Frankel, E. B., Hou, F., Johnson, A., Yuan, L., Knight, G., Moresco, J. J., Yates, J. R., Ashton, R., Schekman, R., Tong, Y., & Audhya, A. (2017). TFG facilitates outer coat disassembly on COPII transport carriers to promote tethering and fusion with ER–Golgi intermediate compartments. Proceedings of the National Academy of Sciences of the United States of America, 114(37), E7707–E7716. https://doi.org/10.1073/PNAS.1709120114/SUPPL_FILE/PNAS.201709120SI.PDF

Hanna, M. G., Mela, I., Wang, L., Henderson, R. M., Chapman, E. R., Edwardson, J. M., & Audhya, A. (2016). Sar1 GTPase activity is regulated by membrane curvature. Journal of Biological Chemistry, 291(3), 1014–1027. https://doi.org/10.1074/jbc.M115.672287

Hanna, M. G., Peotter, J. L., Frankel, E. B., & Audhya, A. (2018). Membrane Transport at an Organelle Interface in the Early Secretory Pathway: Take Your Coat Off and Stay a While. BioEssays, 40(7), 1800004. https://doi.org/10.1002/BIES.201800004

Harding, H. P., Novoa, I., Zhang, Y., Zeng, H., Wek, R., Schapira, M., & Ron, D. (2000). Regulated translation initiation controls stress-induced gene expression in mammalian cells. Molecular Cell, 6(5), 1099–1108. https://doi.org/10.1016/S1097-2765(00)00108-8

Hartley, C. L., Edwards, S., Mullan, L., Bell, P. A., Fresquet, M., Boot-Handford, R. P., & Briggs, M. D. (2013). Armet/Manf and Creld2 are components of a specialized ER stress response provoked by inappropriate formation of disulphide bonds: implications for genetic skeletal diseases. https://doi.org/10.1093/hmg/ddt383

Haze, K., Yoshida, H., Yanagi, H., Yura, T., & Mori, K. (1999). Mammalian Transcription Factor ATF6 Is Synthesized as a Transmembrane Protein and Activated by Proteolysis in Response to Endoplasmic Reticulum Stress. Molecular Biology of the Cell, 10(11), 3787. https://doi.org/10.1091/MBC.10.11.3787

Herbst, F., Ball, C. R., Tuorto, F., Nowrouzi, A., Wang, W., Zavidij, O., Dieter, S. M., Fessler, S., Van Der Hoeven, F., Kloz, U., Lyko, F., Schmidt, M., Von Kalle, C., & Glimm, H. (2012). Extensive Methylation of Promoter Sequences Silences Lentiviral Transgene Expression During Stem Cell Differentiation In Vivo. Molecular Therapy, 20(5), 1014. https://doi.org/10.1038/MT.2012.46

Herrero, A. B., Quwaider, D., Corchete, L. A., Mateos, M. V., García-Sanz, R., & Gutiérrez, N. C. (2020). FAM46C controls antibody production by the polyadenylation of immunoglobulin mRNAs and inhibits cell migration in multiple myeloma. Journal of Cellular and Molecular Medicine, 24(7), 4171–4182. https://doi.org/10.1111/JCMM.15078

Hibi, T., & Dosch, H.-M. (1986). Limiting dilution analysis of the B cell compartment in human bone marrow. European Journal of Immunology, 16(2), 139–145. https://doi.org/10.1002/eji.1830160206

Hideshima, T., Qi, J., Paranal, R. M., Tang, W., Greenberg, E., West, N., Colling, M. E., Estiu, G., Mazitschek, R., Perry, J. A., Ohguchi, H., Cottini, F., Mimura, N., Görgün, G., Tai, Y. T., Richardson, P. G., Carrasco, R. D., Wiest, O., Schreiber, S. L., … Bradner, J. E. (2016). Discovery of selective small-molecule HDAC6 inhibitor for overcoming proteasome inhibitor resistance in multiple myeloma. Proceedings of the National Academy of Sciences of the United States of America, 113(46), 13162–13167. https://doi.org/10.1073/PNAS.1608067113

Ho, M., Patel, A., Hanley, C., Murphy, A., McSweeney, T., Zhang, L., McCann, A., O Gorman, P., & Bianchi, G. (2019). Exploiting autophagy in multiple myeloma. Journal of Cancer Metastasis and Treatment, 5, 70. https://doi.org/10.20517/2394-4722.2019.25

Hollien, J., & Weissman, J. S. (2006). Decay of endoplasmic reticulum-localized mRNAs during the unfolded protein response. Science (New York, N.Y.), 313(5783), 104–107. https://doi.org/10.1126/SCIENCE.1129631

Hoshino, K., Takeuchi, O., Kawai, T., Sanjo, H., Ogawa, T., Takeda, Y., Takeda, K., & Akira, S. (1999). Cutting edge: Toll-like receptor 4 (TLR4)-deficient mice are hyporesponsive to lipopolysaccharide: evidence for TLR4 as the Lps gene product. Journal of Immunology, 162(7), 3749–3752. https://doi.org/10.4049/JIMMUNOL.162.7.3749

Huggins, J., Pellegrin, T., Felgar, R. E., Wei, C., Brown, M., Zheng, B., Milner, E. C. B., Bernstein, S. H., Sanz, I., & Zand, M. S. (2007). CpG DNA activation and plasma-cell differentiation of CD27- naive human B cells. Blood, 109(4), 1611–1619. https://doi.org/10.1182/BLOOD-2006-03-008441

Hung, V., Udeshi, N. D., Lam, S. S., Loh, K. H., Cox, K. J., Pedram, K., Carr, S. A., & Ting, A. Y. (2016). Spatially resolved proteomic mapping in living cells with the engineered peroxidase APEX2. Nature Protocols 2016 11:3, 11(3), 456–475. https://doi.org/10.1038/nprot.2016.018

Hutchings, J., & Zanetti, G. (2019). Coat flexibility in the secretory pathway: a role in transport of bulky cargoes. Current Opinion in Cell Biology, 59, 104. https://doi.org/10.1016/J.CEB.2019.04.002

Hutchings, J., Stancheva, V. G., Brown, N. R., Cheung, A. C. M., Miller, E. A., & Zanetti, G. (2021). Structure of the complete, membrane-assembled COPII coat reveals a complex interaction network. Nature Communications, 12(1). https://doi.org/10.1038/S41467-021-22110-6

Hutchings, J., Stancheva, V., Miller, E. A., & Zanetti, G. (2018). Subtomogram averaging of COPII assemblies reveals how coat organization dictates membrane shape. Nature Communications, 9(1). https://doi.org/10.1038/S41467-018-06577-4

Hwang, J., & Espenshade, P. J. (2016). Proximity-dependent biotin labelling in yeast using the engineered ascorbate peroxidase APEX2. Biochemical Journal, 473(16), 2463–2469. https://doi.org/10.1042/BCJ20160106

Ishikawa, T., Toyama, T., Nakamura, Y., Tamada, K., Shimizu, H., Ninagawa, S., Okada, T., Kamei, Y., Ishikawa-Fujiwara, T., Todo, T., Aoyama, E., Takigawa, M., Harada, A., & Mori, K. (2017). UPR transducer BBF2H7 allows export of type II collagen in a cargo- and developmental stage-specific manner. The Journal of Cell Biology, 216(6), 1761–1774. https://doi.org/10.1083/JCB.201609100

Ishikawa, Y., Ito, S., Nagata, K., Sakai, L. Y., & Bächinger, H. P. (2016). Intracellular mechanisms of molecular recognition and sorting for transport of large extracellular matrix molecules. Proceedings of the National Academy of Sciences of the United States of America, 113(41), E6036–E6044. https://doi.org/10.1073/PNAS.1609571113/ASSET/5FCECC05-3066-4BE4-8E13-4A1ABEB67B92/ASSETS/GRAPHIC/PNAS.1609571113FIG07.JPEG

Jennewein, M. F., & Alter, G. (2017). The Immunoregulatory Roles of Antibody Glycosylation. Trends in Immunology, 38(5), 358–372. https://doi.org/10.1016/J.IT.2017.02.004

Jiang, H. (2021). Quality control pathways of tail-anchored proteins. Biochimica et Biophysica Acta (BBA) - Molecular Cell Research, 1868(2), 118922. https://doi.org/10.1016/J.BBAMCR.2020.118922

Johnson, A., Bhattacharya, N., Hanna, M., Pennington, J. G., Schuh, A. L., Wang, L., Otegui, M. S., Stagg, S. M., & Audhya, A. (2015). TFG clusters COPII-coated transport carriers and promotes early secretory pathway organization. The EMBO Journal, 34(6), 811–827. https://doi.org/10.15252/EMBJ.201489032

Jones, D. D., Gaudette, B. T., Wilmore, J. R., Chernova, I., Bortnick, A., Weiss, B. M., & Allman, D. (2016). mTOR has distinct functions in generating versus sustaining humoral immunity. The Journal of Clinical Investigation, 126(11), 4250–4261. https://doi.org/10.1172/JCI86504

Jourdan, M., Caraux, A., Caron, G., Robert, N., Fiol, G., Rème, T., Bolloré, K., Vendrell, J.-P., Le Gallou, S., Mourcin, F., De Vos, J., Kassambara, A., Duperray, C., Hose, D., Fest, T., Tarte, K., & Klein, B. (2011). Characterization of a Transitional Preplasmablast Population in the Process of Human B Cell to Plasma Cell Differentiation. The Journal of Immunology, 187(8), 3931–3941. https://doi.org/10.4049/JIMMUNOL.1101230

Jung, J., Khan, M. M., Landry, J., Halavatyi, A., Machado, P., Reiss, M., & Pepperkok, R. (2021). A high throughput SEC23 functional interaction screen reveals a role for focal adhesion and extracellular matrix signalling in the regulation of COPII subunit SEC23A. BioRxiv, 2021.03.16.435679. https://doi.org/10.1101/2021.03.16.435679

Kaji, T., Ishige, A., Hikida, M., Taka, J., Hijikata, A., Kubo, M., Nagashima, T., Takahashi, Y., Kurosaki, T., Okada, M., Ohara, O., Rajewsky, K., & Takemori, T. (2012). Distinct cellular pathways select germline-encoded and somatically mutated antibodies into immunological memory. The Journal of Experimental Medicine, 209(11), 2079–2097. https://doi.org/10.1084/JEM.20120127

Kassambara, A., Rème, T., Jourdan, M., Fest, T., Hose, D., Tarte, K., & Klein, B. (2015). GenomicScape: An Easy-to-Use Web Tool for Gene Expression Data Analysis. Application to Investigate the Molecular Events in the Differentiation of B Cells into Plasma Cells. PLoS Computational Biology, 11(1). https://doi.org/10.1371/JOURNAL.PCBI.1004077

Khoriaty, R., Hesketh, G. G., Bernard, A., Weyand, A. C., Mellacheruvu, D., Zhu, G., Hoenerhoff, M. J., McGee, B., Everett, L., Adams, E. J., Zhang, B., Saunders, T. L., Nesvizhskii, A. I., Klionsky, D. J., Shavit, J. A., Gingras, A. C., & Ginsburg, D. (2018). Functions of the COPII gene paralogs SEC23A and SEC23B are interchangeable in vivo. Proceedings of the National Academy of Sciences of the United States of America, 115(33), E7748–E7757. https://doi.org/10.1073/PNAS.1805784115/-/DCSUPPLEMENTAL

Kim, B. W., Kwon, D. H., & Song, H. K. (2016). Structure biology of selective autophagy receptors. BMB Reports, 49(2), 73. https://doi.org/10.5483/BMBREP.2016.49.2.265

Kim, D. I., Jensen, S. C., Noble, K. A., Kc, B., Roux, K. H., Motamedchaboki, K., & Roux, K. J. (2016). An improved smaller biotin ligase for BioID proximity labeling. Molecular Biology of the Cell, 27(8), 1188–1196. https://doi.org/10.1091/MBC.E15-12-0844

King, R., Lin, Z., Balbin-Cuesta, G., Myers, G., Friedman, A., Zhu, G., McGee, B., Saunders, T. L., Kurita, R., Nakamura, Y., Engel, J. D., Reddy, P., & Khoriaty, R. (2021). SEC23A rescues SEC23B-deficient congenital dyserythropoietic anemia type II. Science Advances, 7(48). https://doi.org/10.1126/SCIADV.ABJ5293/SUPPL_FILE/SCIADV.ABJ5293_SM.PDF

Kirk, S. J., Cliff, J. M., Thomas, J. A., & Ward, T. H. (2010). Biogenesis of secretory organelles during B cell differentiation. Journal of Leukocyte Biology, 87(2), 245–255. https://doi.org/10.1189/JLB.1208774

Kishimoto, K., Kato, A., Osada, S., Nishizuka, M., & Imagawa, M. (2010). Fad104, a positive regulator of adipogenesis, negatively regulates osteoblast differentiation. Biochemical and Biophysical Research Communications, 397(2), 187–191. https://doi.org/10.1016/J.BBRC.2010.05.077

Kondo, S., Hino, S. I., Saito, A., Kanemoto, S., Kawasaki, N., Asada, R., Izumi, S., Iwamoto, H., Oki, M., Miyagi, H., Kaneko, M., Nomura, Y., Urano, F., & Imaizumi, K. (2012). Activation of OASIS family,

ER stress transducers, is dependent on its stabilization. Cell Death & Differentiation 2012 19:12, 19(12), 1939–1949. https://doi.org/10.1038/cdd.2012.77

Kondo, Shinichi, Murakami, T., Tatsumi, K., Ogata, M., Kanemoto, S., Otori, K., Iseki, K., Wanaka, A., & Imaizumi, K. (2005). OASIS, a CREB/ATF-family member, modulates UPR signalling in astrocytes. Nature Cell Biology, 7(2), 186–194. https://doi.org/10.1038/NCB1213

Kondo, Shinichi, Saito, A., Asada, R., Kanemoto, S., & Imaizumi, K. (2011). Physiological unfolded protein response regulated by OASIS family members, transmembrane bZIP transcription factors. IUBMB Life, 63(4), 233–239. https://doi.org/10.1002/IUB.433

Kondo, Shinichi, Saito, A., Hino, S., Murakami, T., Ogata, M., Kanemoto, S., Nara, S., Yamashita, A., Yoshinaga, K., Hara, H., & Imaizumi, K. (2007). BBF2H7, a Novel Transmembrane bZIP Transcription Factor, Is a New Type of Endoplasmic Reticulum Stress Transducer. Molecular and Cellular Biology, 27(5), 1716. https://doi.org/10.1128/MCB.01552-06

Koskela, E. V., Gonzalez Salcedo, A., Piirainen, M. A., Iivonen, H. A., Salminen, H., & Frey, A. D. (2020). Mining Data From Plasma Cell Differentiation Identified Novel Genes for Engineering of a Yeast Antibody Factory. Frontiers in Bioengineering and Biotechnology, 8. https://doi.org/10.3389/fbioe.2020.00255

Kretz, R., Walter, L., Raab, N., Zeh, N., Gauges, R., Otte, K., Fischer, S., & Stoll, D. (2022). Spatial Proteomics Reveals Differences in the Cellular Architecture of Antibody-Producing CHO and Plasma Cell-Derived Cells. Molecular and Cellular Proteomics, 21(10). https://doi.org/10.1016/J.MCPRO.2022.100278/ATTACHMENT/38002CE6-7CA2-4F93-92CE-5D672FEB2383/MMC9.XLSX

Lam, S. S., Martell, J. D., Kamer, K. J., Deerinck, T. J., Ellisman, M. H., Mootha, V. K., & Ting, A. Y. (2014). Directed evolution of APEX2 for electron microscopy and proximity labeling. Nature Methods 2014 12:1, 12(1), 51–54. https://doi.org/10.1038/nmeth.3179

Lam, W. Y., Becker, A. M., Kennerly, K. M., Wong, R., Curtis, J. D., Llufrio, E. M., McCommis, K. S., Fahrmann, J., Pizzato, H. A., Nunley, R. M., Lee, J., Wolfgang, M. J., Patti, G. J., Finck, B. N., Pearce, E. L., & Bhattacharya, D. (2016). Mitochondrial pyruvate import promotes long-term survival of antibody-secreting plasma cells. Immunity, 45(1), 60. https://doi.org/10.1016/J.IMMUNI.2016.06.011

Lang, M. R., Lapierre, L. A., Frotscher, M., Goldenring, J. R., & Knapik, E. W. (2006). Secretory COPII coat component Sec23a is essential for craniofacial chondrocyte maturation. Nature Genetics 2006 38:10, 38(10), 1198–1203. https://doi.org/10.1038/ng1880

Lee, M. C. S., Orci, L., Hamamoto, S., Futai, E., Ravazzola, M., & Schekman, R. (2005). Sar1p N-terminal helix initiates membrane curvature and completes the fission of a COPII vesicle. Cell, 122(4), 605–617. https://doi.org/10.1016/J.CELL.2005.07.025

Lee, S. Y., Kang, M. G., Park, J. S., Lee, G., Ting, A. Y., & Rhee, H. W. (2016). APEX Fingerprinting Reveals the Subcellular Localization of Proteins of Interest. Cell Reports, 15(8), 1837–1847. https://doi.org/10.1016/J.CELREP.2016.04.064

Lee, Y. K., Brewer, J. W., Hellman, R., & Hendershot, L. M. (1999). BiP and Immunoglobulin Light Chain Cooperate to Control the Folding of Heavy Chain and Ensure the Fidelity of Immunoglobulin Assembly. Molecular Biology of the Cell, 10(7), 2209. https://doi.org/10.1091/MBC.10.7.2209

Li, P., Li, J., Wang, L., & Di, L. J. (2017). Proximity Labeling of Interacting Proteins: Application of BioID as a Discovery Tool. PROTEOMICS, 17(20), 1700002. https://doi.org/10.1002/PMIC.201700002

Li, Y., Yang, J., Wang, H., Qiao, W., Guo, Y., Zhang, S., & Guo, Y. (2020). FNDC3B, Targeted by miR-125a-5p and miR-217, Promotes the Proliferation and Invasion of Colorectal Cancer Cells via PI3K/mTOR Signaling. OncoTargets and Therapy, 13, 3501–3510. https://doi.org/10.2147/OTT.S226520

Lin, C. H., Lin, Y. W., Chen, Y. C., Liao, C. C., Jou, Y. S., Hsu, M. T., & Chen, C. F. (2016). FNDC3B promotes cell migration and tumor metastasis in hepatocellular carcinoma. Oncotarget, 7(31), 49498. https://doi.org/10.18632/ONCOTARGET.10374

Lin, K.-I., Angelin-Duclos, C., Kuo, T. C., & Calame, K. (2002). Blimp-1-dependent repression of Pax-5 is required for differentiation of B cells to immunoglobulin M-secreting plasma cells. Molecular and Cellular Biology, 22(13), 4771–4780. https://doi.org/10.1128/MCB.22.13.4771-4780.2002

Luckey, C. J., Bhattacharya, D., Goldrath, A. W., Weissman, I. L., Benoist, C., & Mathis, D. (2006). Memory T and memory B cells share a transcriptional program of self-renewal with long-term hematopoietic stem cells. Proceedings of the National Academy of Sciences of the United States of America, 103(9), 3304–3309. https://doi.org/10.1073/PNAS.0511137103

Lyu, L., Wang, B., Xiong, C., Zhang, X., Zhang, X., & Zhang, J. (2017). Selective export of autotaxin from the endoplasmic reticulum. The Journal of Biological Chemistry, 292(17), 7011–7022. https://doi.org/10.1074/JBC.M116.774356

Ma, W., & Goldberg, J. (2016). TANGO1/cTAGE5 receptor as a polyvalent template for assembly of large COPII coats. Proceedings of the National Academy of Sciences of the United States of America, 113(36), 10061–10066. https://doi.org/10.1073/PNAS.1605916113/SUPPL_FILE/PNAS.201605916SI.PDF

Ma, Y., Shimizu, Y., Mann, M. J., Jin, Y., & Hendershot, L. M. (2010). Plasma cell differentiation initiates a limited ER stress response by specifically suppressing the PERK-dependent branch of the unfolded protein response. Cell Stress & Chaperones, 15(3), 281–293. https://doi.org/10.1007/S12192-009-0142-9

Maiuolo, J., Bulotta, S., Verderio, C., Benfante, R., & Borgese, N. (2011). Selective activation of the transcription factor ATF6 mediates endoplasmic reticulum proliferation triggered by a membrane protein. Proceedings of the National Academy of Sciences of the United States of America, 108(19), 7832–7837. https://doi.org/10.1073/PNAS.1101379108

Mancias, J. D., & Goldberg, J. (2007). The Transport Signal on Sec22 for Packaging into COPII-Coated Vesicles Is a Conformational Epitope. Molecular Cell, 26(3), 403–414. https://doi.org/10.1016/J.MOLCEL.2007.03.017

Mancias, J. D., & Goldberg, J. (2008). Structural basis of cargo membrane protein discrimination by the human COPII coat machinery. The EMBO Journal, 27(21), 2918. https://doi.org/10.1038/EMBOJ.2008.208

Manfrini, N., Mancino, M., Miluzio, A., Oliveto, S., Balestra, M., Calamita, P., Alfieri, R., Rossi, R. L., Sassoe-Pognetto, M., Salio, C., Cuomo, A., Bonaldi, T., Manfredi, M., Marengo, E., Ranzato, E., Martinotti, S., Cittaro, D., Tonon, G., & Biffo, S. (2020). FAM46C and FNDC3A are multiple myeloma tumor suppressors that act in concert to impair clearing of protein aggregates and autophagy. Cancer Research, 80(21), 4693–4706. https://doi.org/10.1158/0008-5472.CAN-20-1357/654588/AM/FAM46C-AND-FNDC3A-ARE-MULTIPLE-MYELOMA-TUMOR

Mannix, K. M., Starble, R. M., Kaufman, R. S., & Cooley, L. (2019). Proximity labeling reveals novel interactomes in live Drosophila tissue. Development (Cambridge), 146(14). https://doi.org/10.1242/DEV.176644/264921/AM/PROXIMITY-LABELING-REVEALS-NOVEL-INTERACTOMES-IN

Marino, S., Petrusca, D. N., Simpson, E., Anderson, J. L., Xie, X.-Q., Liu, Y., Chirgwin, J., & Roodman, G. D. (2019). Targeting the p62-ZZ/N-End Rule Pathway in Multiple Myeloma Overcomes Proteasome Inhibitor-Resistance Via Induction of Necroptosis and Enhances the Bone Anabolic Effects of Proteasome Inhibitors. Blood, 134(Supplement_1), 4391–4391. https://doi.org/10.1182/BLOOD-2019-131865

Martell, J. D., Deerinck, T. J., Sancak, Y., Poulos, T. L., Mootha, V. K., Sosinsky, G. E., Ellisman, M. H., & Ting, A. Y. (2012). Engineered ascorbate peroxidase as a genetically encoded reporter for electron microscopy. Nature Biotechnology 2012 30:11, 30(11), 1143–1148. https://doi.org/10.1038/nbt.2375

Martin, F., Oliver, A. M., & Kearney, J. F. (2001). Marginal zone and B1 B cells unite in the early response against T-independent blood-borne particulate antigens. Immunity, 14(5), 617–629. https://doi.org/10.1016/S1074-7613(01)00129-7

Martinon, F., Chen, X., Lee, A. H., & Glimcher, L. H. (2010). TLR activation of the transcription factor XBP1 regulates innate immune responses in macrophages. Nature Immunology, 11(5), 411–418. https://doi.org/10.1038/NI.1857

Mazzarella, R. A., Srinivasan, M., Haugejorden, S. M., & Green, M. (1990). ERp72, an abundant luminal endoplasmic reticulum protein, contains three copies of the active site sequences of protein disulfide isomerase. Journal of Biological Chemistry, 265(2), 1094–1101. https://doi.org/10.1016/S0021-9258(19)40163-4

McCaughey, J., & Stephens, D. J. (2018). COPII-dependent ER export in animal cells: adaptation and control for diverse cargo. Histochemistry and Cell Biology 2018 150:2, 150(2), 119–131. https://doi.org/10.1007/S00418-018-1689-2

McCaughey, J., & Stephens, D. J. (2019). ER-to-Golgi Transport: A Sizeable Problem. Trends in Cell Biology, 29(12), 940–953. https://doi.org/10.1016/J.TCB.2019.08.007

Mccaughey, J., Stevenson, N. L., Cross, S., & Stephens, D. J. (2019). ER-to-Golgi trafficking of procollagen in the absence of large carriers. J. Cell Biol, 218(3), 929–948. https://doi.org/10.1083/jcb.201806035

Melville, D. B., Montero-Balaguer, M., Levic, D. S., Bradley, K., Smith, J. R., Hatzopoulos, A. K., & Knapik, E. W. (2011). The feelgood mutation in zebrafish dysregulates COPII-dependent secretion of select extracellular matrix proteins in skeletal morphogenesis. DMM Disease Models and Mechanisms, 4(6), 763–776. https://doi.org/10.1242/DMM.007625/-/DC1

Merte, J., Jensen, D., Wright, K., Sarsfield, S., Wang, Y., Schekman, R., & Ginty, D. D. (2010). Sec24b selectively sorts Vangl2 to regulate planar cell polarity during neural tube closure. Nature Cell Biology, 12(1), 41. https://doi.org/10.1038/NCB2002

Milan, E., Fabbri, M., & Cenci, S. (2016). Autophagy in Plasma Cell Ontogeny and Malignancy. Journal of Clinical Immunology, 36 Suppl 1, 18–24. https://doi.org/10.1007/S10875-016-0254-9

Milan, E., Perini, T., Resnati, M., Orfanelli, U., Oliva, L., Raimondi, A., Cascio, P., Bachi, A., Marcatti, M., Ciceri, F., & Cenci, S. (2015). A plastic SQSTM1/p62-dependent autophagic reserve maintains proteostasis and determines proteasome inhibitor susceptibility in multiple myeloma cells. Autophagy, 11(7), 1161–1178. https://doi.org/10.1080/15548627.2015.1052928

Minnich, M., Tagoh, H., Bönelt, P., Axelsson, E., Fischer, M., Cebolla, B., Tarakhovsky, A., Nutt, S. L., Jaritz, M., & Busslinger, M. (2016). Multifunctional role of the transcription factor Blimp-1 in coordinating plasma cell differentiation. Nature Immunology, 17(3), 331–343. https://doi.org/10.1038/ni.3349

Montegna, E. A., Bhave, M., Liu, Y., Bhattacharyya, D., & Glick, B. S. (2012). Sec12 Binds to Sec16 at Transitional ER Sites. PLoS ONE, 7(2). https://doi.org/10.1371/JOURNAL.PONE.0031156

Mroczek, S., Chlebowska, J., Kuliński, T. M., Gewartowska, O., Gruchota, J., Cysewski, D., Liudkovska, V., Borsuk, E., Nowis, D., & Dziembowski, A. (2017). The non-canonical poly(A) polymerase FAM46C acts as an onco-suppressor in multiple myeloma. Nature Communications, 8(1). https://doi.org/10.1038/S41467-017-00578-5

Murakami, T., Kondo, S., Ogata, M., Kanemoto, S., Saito, A., Wanaka, A., & Imaizumi, K. (2006). Cleavage of the membrane-bound transcription factor OASIS in response to endoplasmic reticulum stress. Journal of Neurochemistry, 96(4), 1090–1100. https://doi.org/10.1111/J.1471-4159.2005.03596.X

Murakami, T., Saito, A., Hino, S. I., Kondo, S., Kanemoto, S., Chihara, K., Sekiya, H., Tsumagari, K., Ochiai, K., Yoshinaga, K., Saitoh, M., Nishimura, R., Yoneda, T., Kou, I., Furuichi, T., Ikegawa, S., Ikawa, M., Okabe, M., Wanaka, A., & Imaizumi, K. (2009). Signalling mediated by the endoplasmic reticulum stress transducer OASIS is involved in bone formation. Nature Cell Biology, 11(10), 1205–1211. https://doi.org/10.1038/NCB1963

Nigro, C. Lo, Macagno, M., Sangiolo, D., Bertolaccini, L., Aglietta, M., & Merlano, M. C. (2019). NK-mediated antibody-dependent cell-mediated cytotoxicity in solid tumors: biological evidence and clinical perspectives. Annals of Translational Medicine, 7(5), 105–105. https://doi.org/10.21037/ATM.2019.01.42

Ninagawa, S., George, G., & Mori, K. (2021). Mechanisms of productive folding and endoplasmic reticulum-associated degradation of glycoproteins and non-glycoproteins. Biochimica et Biophysica Acta. General Subjects, 1865(3). https://doi.org/10.1016/J.BBAGEN.2020.129812

Ninagawa, S., Okada, T., Sumitomo, Y., Horimoto, S., Sugimoto, T., Ishikawa, T., Takeda, S., Yamamoto, T., Suzuki, T., Kamiya, Y., Kato, K., & Mori, K. (2015). Forcible destruction of severely misfolded mammalian glycoproteins by the non-glycoprotein ERAD pathway. The Journal of Cell Biology, 211(4), 775. https://doi.org/10.1083/JCB.201504109

Nishizuka, M., Kishimoto, K., Kato, A., Ikawa, M., Okabe, M., Sato, R., Niida, H., Nakanishi, M., Osada, S., & Imagawa, M. (2009). Disruption of the novel gene fad104 causes rapid postnatal death and attenuation of cell proliferation, adhesion, spreading and migration. Experimental Cell Research, 315(5), 809–819. https://doi.org/10.1016/J.YEXCR.2008.12.013

Nutt, S. L., & Tarlinton, D. M. (2011). Germinal center B and follicular helper T cells: siblings, cousins or just good friends? Nature Immunology 2011 12:6, 12(6), 472–477. https://doi.org/10.1038/ni.2019

O'Connor, B. P., Raman, V. S., Erickson, L. D., Cook, W. J., Weaver, L. K., Ahonen, C., Lin, L. L., Mantchev, G. T., Bram, R. J., & Noelle, R. J. (2004). BCMA is essential for the survival of long-lived bone marrow plasma cells. The Journal of Experimental Medicine, 199(1), 91–97. https://doi.org/10.1084/JEM.20031330

Ochiai, K., Maienschein-Cline, M., Simonetti, G., Chen, J., Rosenthal, R., Brink, R., Chong, A. S., Klein, U., Dinner, A. R., Singh, H., & Sciammas, R. (2013). Transcriptional Regulation of Germinal Center B and Plasma Cell Fates by Dynamical Control of IRF4. Immunity, 38(5), 918–929. https://doi.org/10.1016/j.immuni.2013.04.009

Oh-hashi, K., Koga, H., Ikeda, S., Shimada, K., Hirata, Y., & Kiuchi, K. (2009). CRELD2 is a novel endoplasmic reticulum stress-inducible gene. Biochemical and Biophysical Research Communications, 387(3), 504–510. https://doi.org/10.1016/j.bbrc.2009.07.047

Ohisa, S., Inohaya, K., Takano, Y., & Kudo, A. (2010). sec24d encoding a component of COPII is essential for vertebra formation, revealed by the analysis of the medaka mutant, vbi. Developmental Biology, 342(1), 85–95. https://doi.org/10.1016/J.YDBIO.2010.03.016

Omori, Y., Imai, J. I., Watanabe, M., Komatsu, T., Suzuki, Y., Kataoka, K., Watanabe, S., Tanigami, A., & Sugano, S. (2001). CREB-H: a novel mammalian transcription factor belonging to the CREB/ATF family and functioning via the box-B element with a liver-specific expression. Nucleic Acids Research, 29(10), 2154–2162. https://doi.org/10.1093/NAR/29.10.2154

Pengo, N., Scolari, M., Oliva, L., Milan, E., Mainoldi, F., Raimondi, A., Fagioli, C., Merlini, A., Mariani, E., Pasqualetto, E., Orfanelli, U., Ponzoni, M., Sitia, R., Casola, S., & Cenci, S. (2013). Plasma cells require autophagy for sustainable immunoglobulin production. Nature Immunology, 14(3), 298–305. https://doi.org/10.1038/ni.2524

Peotter, J., Kasberg, W., Pustova, I., & Audhya, A. (2019). COPII-mediated trafficking at the ER/ERGIC interface. Traffic (Copenhagen, Denmark), 20(7), 491. https://doi.org/10.1111/TRA.12654

Peperzak, V., Vikström, I., Walker, J., Glaser, S. P., Lepage, M., Coquery, C. M., Erickson, L. D., Fairfax, K., MacKay, F., Strasser, A., Nutt, S. L., & Tarlinton, D. M. (2013). Mcl-1 is essential for the survival of plasma cells. Nature Immunology, 14(3), 290–297. https://doi.org/10.1038/ni.2527

Pinter, T., Fischer, M., Schäfer, M., Fellner, M., Jude, J., Zuber, J., Busslinger, M., & Wöhner, M. (2022). Comprehensive CRISPR-Cas9 screen identifies factors which are important for plasmablast development. Frontiers in Immunology, 13, 979606. https://doi.org/10.3389/FIMMU.2022.979606/BIBTEX

Pioli, P. D. (2019). Plasma Cells, the Next Generation: Beyond Antibody Secretion. Frontiers in Immunology, 10, 2768. https://doi.org/10.3389/FIMMU.2019.02768

Pittari, D., Dalla Torre, M., Borini, E., Hummel, B., Sawarkar, R., Semino, C., van Anken, E., Panina-Bordignon, P., Sitia, R., & Anelli, T. (2022). CREB3L1 and CREB3L2 control Golgi remodelling during decidualization of endometrial stromal cells. *Frontiers in Cell and Developmental Biology*, *10*, 2015. https://doi.org/10.3389/FCELL.2022.986997/BIBTEX

Poltorak, A., He, X., Smirnova, I., Liu, M. Y., Van Huffel, C., Du, X., Birdwell, D., Alejos, E., Silva, M., Galanos, C., Freudenberg, M., Ricciardi-Castagnoli, P., Layton, B., & Beutler, B. (1998). Defective LPS signaling in C3H/HeJ and C57BL/10ScCr mice: mutations in Tlr4 gene. Science (New York, N.Y.), 282(5396), 2085–2088. https://doi.org/10.1126/SCIENCE.282.5396.2085

Qi, L., Tsai, B., & Arvan, P. (2017). New insights into the physiological role of ERAD. Trends in Cell Biology, 27(6), 430. https://doi.org/10.1016/J.TCB.2016.12.002

Qiu, G., & Stavnezer, J. (1998). Overexpression of BSAP/Pax-5 inhibits switching to IgA and enhances switching to IgE in the I.29 mu B cell line. Journal of Immunology (Baltimore, Md. : 1950), 161(6), 2906–2918. http://www.ncbi.nlm.nih.gov/pubmed/9743352

Raab, N., Zeh, N., Schlossbauer, P., Mathias, S., Lindner, B., Stadermann, A., Gamer, M., Fischer, S., Holzmann, K., Handrick, R., & Otte, K. (2022). A blueprint from nature: miRNome comparison of plasma cells and CHO cells to optimize therapeutic antibody production. New Biotechnology, 66, 79–88. https://doi.org/10.1016/J.NBT.2021.10.005

Rahman, N. F. (2019). Proteogenomic Identification of Membrane Trafficking Components affecting Antibody Secretion in Plasma Cells.

Raote, I., Ortega-Bellido, M., Santos, A. J. M., Foresti, O., Zhang, C., Garcia-Parajo, M. F., Campelo, F., & Malhotra, V. (2018). TANGO1 builds a machine for collagen export by recruiting and spatially organizing COPII, tethers and membranes. ELife, 7. https://doi.org/10.7554/eLife.32723

Reimold, A. M., Etkin, A., Clauss, I., Perkins, A., Friend, D. S., Zhang, J., Horton, H. F., Scott, A., Orkin, S. H., Byrne, M. C., Grusby, M. J., & Glimcher, L. H. (2000). An essential role in liver development for transcription factor XBP-1. Genes & Development, 14(2), 152. https://doi.org/10.1101/gad.14.2.152

Rhee, H. W., Zou, P., Udeshi, N. D., Martell, J. D., Mootha, V. K., Carr, S. A., & Ting, A. Y. (2013). Proteomic mapping of mitochondria in living cells via spatially restricted enzymatic tagging. Science, 339(6125), 1328–1331. https://doi.org/10.1126/SCIENCE.1230593/SUPPL_FILE/RHEE_SUPPSS2.REVISION.1.XLSX

Ricci, D., Gidalevitz, T., & Argon, Y. (2021). The special unfolded protein response in plasma cells. Immunological Reviews, 303(1), 35–51. https://doi.org/10.1111/IMR.13012

Rickert, R. C., Roes, J., & Rajewsky, K. (1997). B Lymphocyte-Specific, Cre-mediated Mutagenesis in Mice. Nucleic Acids Research, 25(6), 1317–1318. https://doi.org/10.1093/NAR/25.6.1317

Romijn, E. P., Christis, C., Wieffer, M., Gouw, J. W., Fullaondo, A., van der Sluijs, P., Braakman, I., & Heck, A. J. R. (2005). Expression clustering reveals detailed co-expression patterns of functionally related proteins during B cell differentiation: a proteomic study using a combination of one-dimensional gel electrophoresis, LC-MS/MS, and stable isotope labeling by amino acids in cell culture (SILAC). Molecular & Cellular Proteomics : MCP, 4(9), 1297–1310. https://doi.org/10.1074/MCP.M500123-MCP200

Rosenbaum, M., Andreani, V., Kapoor, T., Herp, S., Flach, H., Duchniewicz, M., & Grosschedl, R. (2014). MZB1 is a GRP94 cochaperone that enables proper immunoglobulin heavy chain biosynthesis upon ER stress. Genes & Development, 28(11), 1165–1178. https://doi.org/10.1101/GAD.240762.114

Roux, K. J., Kim, D. I., Raida, M., & Burke, B. (2012). A promiscuous biotin ligase fusion protein identifies proximal and interacting proteins in mammalian cells. The Journal of Cell Biology, 196(6), 801. https://doi.org/10.1083/JCB.201112098

Rutkowski, D. T., & Hegde, R. S. (2010). Regulation of basal cellular physiology by the homeostatic unfolded protein response. Journal of Cell Biology, 189(5), 783–794. https://doi.org/10.1083/JCB.201003138

Saito, A., Hino, S. I., Murakami, T., Kanemoto, S., Kondo, S., Saitoh, M., Nishimura, R., Yoneda, T., Furuichi, T., Ikegawa, S., Ikawa, M., Okabe, M., & Imaizumi, K. (2009). Regulation of endoplasmic reticulum stress response by a BBF2H7-mediated Sec23a pathway is essential for

chondrogenesis. Nature Cell Biology 2009 11:10, 11(10), 1197–1204. https://doi.org/10.1038/ncb1962

Saito, K., Chen, M., Bard, F., Chen, S., Zhou, H., Woodley, D., Polischuk, R., Schekman, R., & Malhotra, V. (2009). TANGO1 Facilitates Cargo Loading at Endoplasmic Reticulum Exit Sites. Cell, 136(5), 891–902. https://doi.org/10.1016/j.cell.2008.12.025

Sarmah, S., Barrallo-Gimeno, A., Melville, D. B., Topczewski, J., Solnica-Krezel, L., & Knapik, E. W. (2010). Sec24D-dependent transport of extracellular matrix proteins is required for zebrafish skeletal morphogenesis. PloS One, 5(4). https://doi.org/10.1371/JOURNAL.PONE.0010367

Sato, K., & Nakano, A. (2005). Dissection of COPII subunit-cargo assembly and disassembly kinetics during Sar1p-GTP hydrolysis. Nature Structural and Molecular Biology, 12(2), 167–174. https://doi.org/10.1038/nsmb893

Schallus, T., Jaeckh, C., Fehér, K., Palma, A. S., Liu, Y., Simpson, J. C., Mackeen, M., Stier, G., Gibson, T. J., Feizi, T., Pieler, T., & Muhle-Goll, C. (2008). Malectin: a novel carbohydrate-binding protein of the endoplasmic reticulum and a candidate player in the early steps of protein N-glycosylation. Molecular Biology of the Cell, 19(8), 3404–3414. https://doi.org/10.1091/MBC.E08-04-0354

Scharaw, S., Iskar, M., Ori, A., Boncompain, G., Laketa, V., Poser, I., Lundberg, E., Perez, F., Beck, M., Bork, P., & Pepperkok, R. (2016). The endosomal transcriptional regulator RNF11 integrates degradation and transport of EGFR. Journal of Cell Biology, 215(4), 543–558. https://doi.org/10.1083/JCB.201601090

Schubert, U., Antón, L. C., Gibbs, J., Norbury, C. C., Yewdell, J. W., & Bennink, J. R. (2000). Rapid degradation of a large fraction of newly synthesized proteins by proteasomes. Nature 2000 404:6779, 404(6779), 770–774. https://doi.org/10.1038/35008096

Sciammas, R., Shaffer, A. L., Schatz, J. H., Zhao, H., Staudt, L. M., & Singh, H. (2006). Graded Expression of Interferon Regulatory Factor-4 Coordinates Isotype Switching with Plasma Cell Differentiation. Immunity, 25(2), 225–236. https://doi.org/10.1016/j.immuni.2006.07.009

Shaffer, A. L., Lin, K. I., Kuo, T. C., Yu, X., Hurt, E. M., Rosenwald, A., Giltnane, J. M., Yang, L., Zhao, H., Calame, K., & Staudt, L. M. (2002). Blimp-1 orchestrates plasma cell differentiation by extinguishing the mature B cell gene expression program. Immunity, 17(1), 51–62. https://doi.org/10.1016/S1074-7613(02)00335-7

Shaffer, A. L., Shapiro-Shelef, M., Iwakoshi, N. N., Lee, A. H., Qian, S. B., Zhao, H., Yu, X., Yang, L., Tan, B. K., Rosenwald, A., Hurt, E. M., Petroulakis, E., Sonenberg, N., Yewdell, J. W., Calame, K., Glimcher, L. H., & Staudt, L. M. (2004). XBP1, downstream of Blimp-1, expands the secretory apparatus and other organelles, and increases protein synthesis in plasma cell differentiation. Immunity, 21(1), 81–93. https://doi.org/10.1016/j.immuni.2004.06.010

Sharma, R. B., Darko, C., & Alonso, L. C. (2020). Intersection of the ATF6 and XBP1 ER stress pathways in mouse islet cells. The Journal of Biological Chemistry, 295(41), 14164–14177. https://doi.org/10.1074/JBC.RA120.014173

Shen, J., Chen, X., Hendershot, L., & Prywes, R. (2002). ER Stress Regulation of ATF6 Localization by Dissociation of BiP/GRP78 Binding and Unmasking of Golgi Localization Signals. Developmental Cell, 3(1), 99–111. https://doi.org/10.1016/S1534-5807(02)00203-4

Shenkman, M., & Lederkremer, G. Z. (2019). Compartmentalization and Selective Tagging for Disposal of Misfolded Glycoproteins. Trends in Biochemical Sciences, 44(10), 827–836. https://doi.org/10.1016/j.tibs.2019.04.012

Shi, M. J., & Stavnezer, J. (1998). CBF alpha3 (AML2) is induced by TGF-beta1 to bind and activate the mouse germline Ig alpha promoter - PubMed. Journal of Immunology . https://pubmed.ncbi.nlm.nih.gov/9862705/

Shi, W., Liao, Y., Willis, S. N., Taubenheim, N., Inouye, M., Tarlinton, D. M., Smyth, G. K., Hodgkin, P. D., Nutt, S. L., & Corcoran, L. M. (2015). Transcriptional profiling of mouse B cell terminal differentiation defines a signature for antibody-secreting plasma cells. Nature Immunology, 16(6), 663–673. https://doi.org/10.1038/ni.3154

Sönnichsen, B., Lowe, M., Levine, T., Jämsä, E., Dirac-Svejstrup, B., & Warren, G. (1998). A Role for Giantin in Docking COPI Vesicles to Golgi Membranes. The Journal of Cell Biology, 140(5), 1013. https://doi.org/10.1083/JCB.140.5.1013

Sriburi, R., Bommiasamy, H., Buldak, G. L., Robbins, G. R., Frank, M., Jackowski, S., & Brewer, J. W. (2007). Coordinate Regulation of Phospholipid Biosynthesis and Secretory Pathway Gene Expression in XBP-1(S)-induced Endoplasmic Reticulum Biogenesis. Journal of Biological Chemistry, 282(10), 7024–7034. https://doi.org/10.1074/JBC.M609490200

Stadel, D., Millarte, V., Tillmann, K. D., Huber, J., Tamin-Yecheskel, B. C., Akutsu, M., Demishtein, A., Ben-Zeev, B., Anikster, Y., Perez, F., Dötsch, V., Elazar, Z., Rogov, V., Farhan, H., & Behrends, C. (2015). TECPR2 Cooperates with LC3C to Regulate COPII-Dependent ER Export. Molecular Cell, 60(1), 89–104. https://doi.org/10.1016/j.molcel.2015.09.010

Staufner, C., Peters, B., Wagner, M., Alameer, S., Barić, I., Broué, P., Bulut, D., Church, J. A., Crushell, E., Dalgıç, B., Das, A. M., Dick, A., Dikow, N., Dionisi-Vici, C., Distelmaier, F., Bozbulut, N. E., Feillet, F., Gonzales, E., Hadzic, N., … Lenz, D. (2020). Defining clinical subgroups and genotype–phenotype correlations in NBAS-associated disease across 110 patients. Genetics in Medicine, 22(3), 610–621. https://doi.org/10.1038/s41436-019-0698-4

Stavnezer, J, Bradley, S., Rousseau, N., Pearson, T., Shanmugam, A., Waite, D., Rogers, P., & Kenter, A. (1999). Switch recombination in a transfected plasmid occurs preferentially in a B cell line that undergoes switch recombination of its chromosomal Ig heavy chain genes-Web of Science Core Collection. Journal of Immunology. https://www.webofscience.com/wos/woscc/full-record/WOS:000081900200044

Stavnezer, J, Marcu, K. B., Sirlin, S., Alhadeff, B., & Hammerling, U. (1982). Rearrangements and deletions of immunoglobulin heavy chain genes in the double-producing B cell lymphoma I.29. Molecular and Cellular Biology, 2(8), 1002–1013. https://doi.org/10.1128/MCB.2.8.1002-1013.1982

Stavnezer, Janet, Sirlin, S., & Abbott, J. (1985). Induction of immunoglobulin isotype switching in cultured I.29 B lymphoma cells. Characterization of the accompanying rearrangements of heavy chain genes. The Journal of Experimental Medicine, 161(3), 577–601. https://doi.org/10.1084/JEM.161.3.577

Tagaya, M., Arasaki, K., Inoue, H., & Kimura, H. (2014). Moonlighting functions of the NRZ (mammalian Dsl1) complex. In Frontiers in Cell and Developmental Biology (Vol. 2, Issue JUN). Frontiers Media S.A. https://doi.org/10.3389/fcell.2014.00025

Tan, B., Peng, S., Yatim, S. M. J. M., Gunaratne, J., Hunziker, W., & Ludwig, A. (2020). An Optimized Protocol for Proximity Biotinylation in Confluent Epithelial Cell Cultures Using the Peroxidase APEX2. STAR Protocols, 1(2), 100074. https://doi.org/10.1016/J.XPRO.2020.100074

Tang, B. L., Kausalya, J., Low, D. Y. H., Lock, M. L., & Hong, W. (1999). A family of mammalian proteins homologous to yeast Sec24p. Biochemical and Biophysical Research Communications, 258(3), 679–684. https://doi.org/10.1006/BBRC.1999.0574

Tannous, A., Pisoni, G. B., Hebert, D. N., & Molinari, M. (2015). N-linked sugar-regulated protein folding and quality control in the ER. Seminars in Cell & Developmental Biology, 41, 79. https://doi.org/10.1016/J.SEMCDB.2014.12.001

Tao, J., Zhu, M., Wang, H., Afelik, S., Vasievich, M. P., Chen, X. W., Zhu, G., Jensen, J., Ginsburg, D., & Zhang, B. (2012). SEC23B is required for the maintenance of murine professional secretory tissues. Proceedings of the National Academy of Sciences of the United States of America, 109(29). https://doi.org/10.1073/PNAS.1209207109/-/DCSUPPLEMENTAL/PNAS.201209207SI.PDF

Taubenheim, N., Tarlinton, D. M., Crawford, S., Corcoran, L. M., Hodgkin, P. D., & Nutt, S. L. (2012). High Rate of Antibody Secretion Is not Integral to Plasma Cell Differentiation as Revealed by XBP-1 Deficiency. The Journal of Immunology, 189(7), 3328–3338. https://doi.org/10.4049/jimmunol.1201042

Tellier, J., Shi, W., Minnich, M., Liao, Y., Crawford, S., Smyth, G. K., Kallies, A., Busslinger, M., & Nutt, S. L. (2016). Blimp-1 controls plasma cell function through the regulation of immunoglobulin secretion and the unfolded protein response. Nature Immunology, 17(3), 323–330. https://doi.org/10.1038/ni.3348

Gass, J. N., Jiang, H. Y., Wek, R. C., & Brewer, J. W. (2008). The unfolded protein response of B-lymphocytes: PERK-independent development of antibody-secreting cells. *Molecular Immunology*, *45*(4), 1035–1043. https://doi.org/10.1016/J.MOLIMM.2007.07.029

King, R., Lin, Z., Balbin-Cuesta, G., Myers, G., Friedman, A., Zhu, G., McGee, B., Saunders, T. L., Kurita, R., Nakamura, Y., Engel, J. D., Reddy, P., & Khoriaty, R. (2021). SEC23A rescues SEC23B-deficient congenital dyserythropoietic anemia type II. *Science Advances*, *7*(48). https://doi.org/10.1126/SCIADV.ABJ5293/SUPPL_FILE/SCIADV.ABJ5293_SM.PDF

Kretz, R., Walter, L., Raab, N., Zeh, N., Gauges, R., Otte, K., Fischer, S., & Stoll, D. (2022). Spatial Proteomics Reveals Differences in the Cellular Architecture of Antibody-Producing CHO and Plasma Cell-Derived Cells. *Molecular and Cellular Proteomics*, *21*(10). https://doi.org/10.1016/J.MCPRO.2022.100278/ATTACHMENT/38002CE6-7CA2-4F93-92CE-5D672FEB2383/MMC9.XLSX

Ma, Y., Shimizu, Y., Mann, M. J., Jin, Y., & Hendershot, L. M. (2010). Plasma cell differentiation initiates a limited ER stress response by specifically suppressing the PERK-dependent branch of the unfolded protein response. *Cell Stress and Chaperones*, *15*(3), 281–293. https://doi.org/10.1007/s12192-009-0142-9

Raab, N., Zeh, N., Schlossbauer, P., Mathias, S., Lindner, B., Stadermann, A., Gamer, M., Fischer, S., Holzmann, K., Handrick, R., & Otte, K. (2022). A blueprint from nature: miRNome comparison of plasma cells and CHO cells to optimize therapeutic antibody production. *New Biotechnology*, *66*, 79–88. https://doi.org/10.1016/J.NBT.2021.10.005

Rahman, N. F. (2019). *Proteogenomic Identification of Membrane Trafficking Components affecting Antibody Secretion in Plasma Cells*.

Stadel, D., Millarte, V., Tillmann, K. D., Huber, J., Tamin-Yecheskel, B. C., Akutsu, M., Demishtein, A., Ben-Zeev, B., Anikster, Y., Perez, F., Dötsch, V., Elazar, Z., Rogov, V., Farhan, H., & Behrends, C. (2015). TECPR2 Cooperates with LC3C to Regulate COPII-Dependent ER Export. *Molecular Cell*, *60*(1), 89–104. https://doi.org/10.1016/j.molcel.2015.09.010

Zhu, H., Bhatt, B., Sivaprakasam, S., Cai, Y., Liu, S., Kodeboyina, S. K., Patel, N., Savage, N. M., Sharma, A., Kaufman, R. J., Li, H., & Singh, N. (2019). Ufbp1 promotes plasma cell development and ER expansion by modulating distinct branches of UPR. *Nature Communications*, *10*(1). https://doi.org/10.1038/s41467-019-08908-5

Zhu, M., Tao, J., Vasievich, M. P., Wei, W., Zhu, G., Khoriaty, R. N., & Zhang, B. (2015). Neural tube opening and abnormal extraembryonic membrane development in SEC23A deficient mice. *Scientific Reports 2015 5:1*, *5*(1), 1–15. https://doi.org/10.1038/srep15471

Thor, F., Gautschi, M., Geiger, R., & Helenius, A. (2009). Bulk flow revisited: Transport of a soluble protein in the secretory pathway. Traffic, 10(12), 1819–1830. https://doi.org/10.1111/j.1600-0854.2009.00989.x

Tominaga, K., Kondo, C., Johmura, Y., Nishizuka, M., & Imagawa, M. (2004). The novel gene fad104, containing a fibronectin type III domain, has a significant role in adipogenesis. FEBS Letters, 577(1–2), 49–54. https://doi.org/10.1016/J.FEBSLET.2004.09.062

Tomoishi, S., Fukushima, S., Shinohara, K., Katada, T., & Saito, K. (2017). CREB3L2-mediated expression of Sec23A/Sec24D is involved in hepatic stellate cell activation through ER-Golgi transport. Scientific Reports 2017 7:1, 7(1), 1–11. https://doi.org/10.1038/s41598-017-08703-6

Torres, M., & Dickson, A. J. (2022). Reprogramming of Chinese hamster ovary cells towards enhanced protein secretion. Metabolic Engineering, 69, 249–261. https://doi.org/10.1016/J.YMBEN.2021.12.004

Townley, A. K., Feng, Y., Schmidt, K., Carter, D. A., Porter, R., Verkade, P., & Stephens, D. J. (2008). Efficient coupling of Sec23-Sec24 to Sec13-Sec31 drives COPII-dependent collagen secretion and

is essential for normal craniofacial development. Journal of Cell Science, 121(18), 3025–3034. https://doi.org/10.1242/JCS.031070

Trezise, S., & Nutt, S. L. (2021). The gene regulatory network controlling plasma cell function. Immunological Reviews, 303(1), 23–34. https://doi.org/10.1111/IMR.12988

Trudel, S., Lendvai, N., Popat, R., Voorhees, P. M., Reeves, B., Libby, E. N., Richardson, P. G., Hoos, A., Gupta, I., Bragulat, V., He, Z., Opalinska, J. B., & Cohen, A. D. (2019). Antibody–drug conjugate, GSK2857916, in relapsed/refractory multiple myeloma: an update on safety and efficacy from dose expansion phase I study. Blood Cancer Journal 2019 9:4, 9(4), 1–10. https://doi.org/10.1038/s41408-019-0196-6

Ueno, T., Kaneko, K., Sata, T., Hattori, S., & Ogawa-Goto, K. (2011). Regulation of polysome assembly on the endoplasmic reticulum by a coiled-coil protein, p180. https://www.ncbi.nlm.nih.gov/pmc/articles/PMC3326322/?report=classic

Ueno, T., Tanaka, K., Kaneko, K., Taga, Y., Sata, T., Irie, S., Hattori, S., & Ogawa-Goto, K. (2010). Enhancement of procollagen biosynthesis by p180 through augmented ribosome association on the endoplasmic reticulum in response to stimulated secretion. Journal of Biological Chemistry, 285(39), 29941–29950. https://doi.org/10.1074/jbc.M109.094607

Urano, F., Wang, X. Z., Bertolotti, A., Zhang, Y., Chung, P., Harding, H. P., & Ron, D. (2000). Coupling of stress in the ER to activation of JNK protein kinases by transmembrane protein kinase IRE1. Science (New York, N.Y.), 287(5453), 664–666. https://doi.org/10.1126/SCIENCE.287.5453.664

Ushioda, R., Hoseki, J., & Nagata, K. (2013). Glycosylation-independent ERAD pathway serves as a backup system under ER stress. Molecular Biology of the Cell, 24(20), 3155. https://doi.org/10.1091/MBC.E13-03-0138

Van Anken, E., Pena, F., Hafkemeijer, N., Christis, C., Romijn, E. P., Grauschopf, U., Oorschot, V. M. J., Pertel, T., Engels, S., Ora, A., Lástun, V., Glockshuber, R., Klumperman, J., Heck, A. J. R., Luban, J., & Braakman, I. (2009). Efficient IgM assembly and secretion require the plasma cell induced endoplasmic reticulum protein pERp1. Proceedings of the National Academy of Sciences of the United States of America, 106(40), 17019–17024. https://doi.org/10.1073/PNAS.0903036106/SUPPL_FILE/0903036106SI.PDF

Van Anken, E., Romijn, E. P., Maggioni, C., Mezghrani, A., Sitia, R., Braakman, I., & Heck, A. J. R. (2003). Sequential waves of functionally related proteins are expressed when B cells prepare for antibody secretion. Immunity, 18(2), 243–253. https://doi.org/10.1016/S1074-7613(03)00024-4

Vanhove, M., Usherwood, Y. K., & Hendershot, L. M. (2001). Unassembled Ig heavy chains do not cycle from BiP in vivo but require light chains to trigger their release. Immunity, 15(1), 105–114. https://doi.org/10.1016/S1074-7613(01)00163-7

Walter, P., & Ron, D. (2011). The Unfolded Protein Response: From Stress Pathway to Homeostatic Regulation. Science, 334(6059), 1081–1086. https://doi.org/10.1126/SCIENCE.1209038

Wang, H., Gonzalez-Garcia, I., Traba, J., Jain, S., Conteh, S., Shin, D. M., Qi, C., Gao, Y., Sun, J., Kang, S., Abbasi, S., Naghashfar, Z., Yoon, J., Dubois, W., Kovalchuk, A. L., Sack, M. N., Duffy, P., & Morse, H. C. (2017). ATP-degrading ENPP1 is required for survival (or persistence) of long-lived plasma cells. Scientific Reports, 7(1). https://doi.org/10.1038/S41598-017-18028-Z

Wang, M., & Kaufman, R. J. (2014). The impact of the endoplasmic reticulum protein-folding environment on cancer development. Nature Reviews. Cancer, 14(9), 581–597. https://doi.org/10.1038/NRC3800

Wang, T., Li, L., & Hong, W. (2017). SNARE proteins in membrane trafficking. Traffic, 18(12), 767–775. https://doi.org/10.1111/tra.12524

Wang, X., Huang, Y., Li, S., & Zhang, H. (2022). Integrated machine learning methods identify FNDC3B as a potential prognostic biomarker and correlated with immune infiltrates in glioma. Frontiers in Immunology, 13, 1027154. https://doi.org/10.3389/FIMMU.2022.1027154/FULL

Wang, Z. V., Deng, Y., Gao, N., Pedrozo, Z., Li, D. L., Morales, C. R., Criollo, A., Luo, X., Tan, W., Jiang, N., Lehrman, M. A., Rothermel, B. A., Lee, A. H., Lavandero, S., Mammen, P. P. A., Ferdous, A., Gillette, T. G., Scherer, P. E., & Hill, J. A. (2014). Spliced X-box binding protein 1 couples the

unfolded protein response to hexosamine biosynthetic pathway. Cell, 156(6), 1179–1192. https://doi.org/10.1016/J.CELL.2014.01.014

Watson, P., Townley, A. K., Koka, P., Palmer, K. J., & Stephens, D. J. (2006). Sec16 defines endoplasmic reticulum exit sites and is required for secretory cargo export in mammalian cells. Traffic (Copenhagen, Denmark), 7(12), 1678–1687. https://doi.org/10.1111/J.1600-0854.2006.00493.X

Weissman, J. T., Plutner, H., & Balch, W. E. (2001). The mammalian guanine nucleotide exchange factor mSec12 is essential for activation of the Sar1 GTPase directing endoplasmic reticulum export. Traffic, 2(7), 465–475. https://doi.org/10.1034/j.1600-0854.2001.20704.x

Widmera, C., Gebauerb, J. M., Brunsteinb, E., Rosenbaumc, S., Zauckec, F., Drogemüllerd, C., Leebd, T., & Baumannb, U. (2012). Molecular basis for the action of the collagen-specific chaperone Hsp47/SERPINH1 and its structure-specific client recognition. Proceedings of the National Academy of Sciences of the United States of America, 109(33), 13243–13247. https://doi.org/10.1073/PNAS.1208072109/SUPPL_FILE/PNAS.201208072SI.PDF

Wiest, D. L., Burkhardt, J. K., Hester, S., Hortsch, M., Meyer, D. I., & Argon, Y. (1990). Membrane biogenesis during B cell differentiation: most endoplasmic reticulum proteins are expressed coordinately. Journal of Cell Biology, 110(5), 1501–1511. https://doi.org/10.1083/JCB.110.5.1501

Wilmore, J. R., & Allman, D. (2017). Here, There, and Anywhere? Arguments for and against the Physical Plasma Cell Survival Niche. The Journal of Immunology, 199(3), 839–845. https://doi.org/10.4049/JIMMUNOL.1700461

Witte, K., Schuh, A. L., Hegermann, J., Sarkeshik, A., Mayers, J. R., Schwarze, K., Yates, J. R., Eimer, S., & Audhya, A. (2011). TFG-1 function in protein secretion and oncogenesis. Nature Cell Biology 2011 13:5, 13(5), 550–558. https://doi.org/10.1038/ncb2225

Wöhner, M., Pinter, T., Bönelt, P., Hagelkruys, A., Kostanova-Poliakova, D., Stadlmann, J., Konieczny, S. F., Fischer, M., Jaritz, M., & Busslinger, M. (2022). The Xbp1-regulated transcription factor Mist1 restricts antibody secretion by restraining Blimp1 expression in plasma cells. Frontiers in Immunology, 13, 7286. https://doi.org/10.3389/FIMMU.2022.859598/BIBTEX

Wong, L.-Y., Brulois, K., Toth, Z., Inn, K.-S., Lee, S.-H., O'Brien, K., Lee, H., Gao, S.-J., Cesarman, E., Ensser, A., & Jung, J. U. (2013). The Product of Kaposi's Sarcoma-Associated Herpesvirus Immediate Early Gene K4.2 Regulates Immunoglobulin Secretion and Calcium Homeostasis by Interacting with and Inhibiting pERP1. Journal of Virology, 87(22), 12069–12079. https://doi.org/10.1128/JVI.01900-13

Xia, X., Zhang, Y., Zieth, C. R., & Zhang, S. C. (2007). Transgenes Delivered by Lentiviral Vector Are Suppressed in Human Embryonic Stem Cells in a Promoter-Dependent Manner. Stem Cells and Development, 16(1), 167. https://doi.org/10.1089/SCD.2006.0057

Xiong, E., Popp, O., Salomon, C., Mertins, P., Kocks, C., Rajewsky, K., & Chu, V. T. (2023). A CRISPR/Cas9-mediated screen identifies determinants of early plasma cell differentiation. Frontiers in Immunology, 13, 7891. https://doi.org/10.3389/FIMMU.2022.1083119/BIBTEX

Xu, A. Q., Barbosa, R. R., & Calado, D. P. (2020). Genetic timestamping of plasma cells in vivo reveals tissue-specific homeostatic population turnover. ELife, 9, 1–18. https://doi.org/10.7554/ELIFE.59850

Xu, F., Du, W., Zou, Q., Wang, Y., Zhang, X., Xing, X., Li, Y., Zhang, D., Wang, H., Zhang, W., Hu, X., Liu, X., Liu, X., Zhang, S., Yu, J., Fang, J., Li, F., Zhou, Y., Yue, T., … Yu, L. (2020). COPII mitigates ER stress by promoting formation of ER whorls. Cell Research 2020 31:2, 31(2), 141–156. https://doi.org/10.1038/s41422-020-00416-2

Yamamoto, K., Sato, T., Matsui, T., Sato, M., Okada, T., Yoshida, H., Harada, A., & Mori, K. (2007). Transcriptional Induction of Mammalian ER Quality Control Proteins Is Mediated by Single or Combined Action of ATF6α and XBP1. Developmental Cell, 13(3), 365–376. https://doi.org/10.1016/j.devcel.2007.07.018

Yasuda, T., Wirtz, T., Zhang, B., Wunderlich, T., Schmidt-Supprian, M., Sommermann, T., & Rajewsky, K. (2013). Studying Epstein–Barr Virus Pathologies and Immune Surveillance by Reconstructing

EBV Infection in Mice. Cold Spring Harbor Symposia on Quantitative Biology, 78(1), 259–263. https://doi.org/10.1101/SQB.2013.78.020222

Yeung, C. C. S., Mills, J. C., Hassan, A., Kreisel, F. H., Nguyen, T. T., & Frater, J. L. (2012). MIST1-a novel marker of plasmacytic differentiation. Applied Immunohistochemistry and Molecular Morphology, 20(6), 561–565. https://doi.org/10.1097/PAI.0B013E31824E93F2

Yoshida, H., Matsui, T., Yamamoto, A., Okada, T., & Mori, K. (2001). XBP1 mRNA is induced by ATF6 and spliced by IRE1 in response to ER stress to produce a highly active transcription factor. Cell, 107(7), 881–891. https://doi.org/10.1016/S0092-8674(01)00611-0

Zagury, D., Uhr, J. W., Jamieson, J. D., & Palade, G. E. (1970). Immunoglobulin synthesis and secretion. II. Radioautographic studies of sites of addition of carbohydrate moieties and intracellular transport. The Journal of Cell Biology, 46(1), 52–63. https://doi.org/10.1083/JCB.46.1.52

Zanetti, G., Pahuja, K. B., Studer, S., Shim, S., & Schekman, R. (2012). COPII and the regulation of protein sorting in mammals. In Nature Cell Biology (Vol. 14, Issue 1, pp. 20–28). Nature Publishing Group. https://doi.org/10.1038/ncb2390

Zanetti, G., Prinz, S., Daum, S., Meister, A., Schekman, R., Bacia, K., & Briggs, J. A. G. (2013). The structure of the COPII transport-vesicle coat assembled on membranes. ELife, 2(2). https://doi.org/10.7554/ELIFE.00951

Zellner, M., Babeluk, R., Diestinger, M., Pirchegger, P., Skeledzic, S., & Oehler, R. (2008). Fluorescence-based Western blotting for quantitation of protein biomarkers in clinical samples. Electrophoresis, 29(17), 3621–3627. https://doi.org/10.1002/ELPS.200700935

Zhu, M., Tao, J., Vasievich, M. P., Wei, W., Zhu, G., Khoriaty, R. N., & Zhang, B. (2015). Neural tube opening and abnormal extraembryonic membrane development in SEC23A deficient mice. Scientific Reports 2015 5:1, 5(1), 1–15. https://doi.org/10.1038/srep15471

Zhu, Y. X., Shi, C. X., Bruins, L. A., Jedlowski, P., Wang, X., Kortüm, K. M., Luo, M., Ahmann, J. M., Braggio, E., & Stewart, A. K. (2017). Loss of FAM46C Promotes Cell Survival in Myeloma. Cancer Research, 77(16), 4317–4327. https://doi.org/10.1158/0008-5472.CAN-16-3011

Zinkernagel, R. M., & Hengartner, H. (2006). Protective 'immunity' by pre-existent neutralizing antibody titers and preactivated T cells but not by so-called 'immunological memory.' Immunological Reviews, 211(1), 310–319. https://doi.org/10.1111/J.0105-2896.2006.00402.X